THEORETICAL INVESTIGATION OF TAUTOMERIC EQUILIBRIA IN CERTAIN EXPLOSIVE MATERIALS

A THESIS SUBMITTED TO
THE GRADUATE SCHOOL OF NATURAL AND APPLIED SCIENCES
OF
MIDDLE EAST TECHNICAL UNIVERSITY

BY

ÇAĞLAR ÇELİK BAYAR

IN PARTIAL FULFILLMENT OF THE REQUIREMENTS
FOR
THE DEGREE OF DOCTOR OF PHILOSOPHY
IN
CHEMISTRY

DECEMBER 2012

Approval of the thesis:

THEORETICAL INVESTIGATION OF TAUTOMERIC EQUILIBRIA IN CERTAIN EXPLOSIVE MATERIALS

submitted by **ÇAĞLAR ÇELİK BAYAR** in partial fulfillment of the requirements for the degree of **Doctor of Philosophy in Chemistry Department, Middle East Technical University** by,

Prof. Dr. Canan Özgen _____
Dean, Graduate School of **Natural and Applied Sciences**

Prof. Dr. İlker Özkan _____
Head of Department, **Chemistry**

Prof. Dr. Lemi Türker _____
Supervisor, **Chemistry Dept., METU**

Examining Committee Members:

Prof. Dr. Şakir Erkoç _____
Physics Dept., METU

Prof. Dr. Lemi Türker _____
Chemistry Dept., METU

Prof. Dr. İlker Özkan _____
Chemistry Dept., METU

Prof. Dr. Canan Ünaleroğlu _____
Chemistry Dept., Hacettepe University

Prof. Dr. Fatma Sevin Düz _____
Chemistry Dept., Hacettepe University

Date: _____

I hereby declare that all information in this document has been obtained and presented in accordance with academic rules and ethical conduct. I also declare that, as required by these rules and conduct, I have fully cited and referenced all material and results that are not original to this work.

Name, Last name : ÇAĞLAR ÇELİK BAYAR

Signature :

ABSTRACT

THEORETICAL INVESTIGATION OF TAUTOMERIC EQUILIBRIA IN CERTAIN EXPLOSIVE MATERIALS

Çelik Bayar, Çağlar

Ph.D, Department of Chemistry

Supervisor: Prof. Dr. Lemi Türker

December 2012, 177 pages

Explosive materials have always been attracting the attention of scientists. Various explosives either in pure bulk form or as admixtures are synthesized and investigated from different points of view. However, because of dangerous character of these materials, their syntheses and properties have to be forecasted by theoretical studies.

The new research trends of explosive materials generally include the designs of novel derivatives of well–known explosives to improve their detonation performances (heats of explosion, detonation velocities and detonation pressures) and thermal stabilities and decrease their sensitivities towards friction, electric spark, shock and impact either experimentally or theoretically.

NTO (5–nitro–2,4–dihydro–3*H*–1,2,4–triazol–3–one) and PATO (3–picrylamino–1,2,4–triazole) are very important secondary explosives that take place in the literature for many years in terms of their explosive properties. In this thesis study, new species of these explosives have been designed to enhance their detonation performances (ballistic properties) and to lower their sensitivities and reactivities computationally. Additionally, aromatic nitration reactions and their mechanisms for unprotonated and protonated PATO species have been analyzed. The *ab initio* quantum chemistry methods, Hartree–Fock (HF) and Density Functional Theory (DFT), have been used in the calculations with Pople basis sets.

Novel NTO and PATO tautomeric species have been designed and investigated to enlighten the effects of tautomerism on their quantum chemical properties and detonation performances in the gas phase.

Various aromatic nitration mechanisms (carbon and nitrogen mono–nitration mechanisms) of unprotonated tautomeric PATO species as well as PATO have been designed in gas phase and the reaction states (pre–transition states, transition states, intermediates and nitration products) have been detected belonging to these mechanisms. Nitrations in solution phase have also been analyzed. The reaction states have been detected for carbon and nitrogen mono–nitrations of protonated PATO species in the gas phase. The detonation performances of unnitrated and nitrated PATO products have been presented.

Keywords: aromatic nitration, transition state, charge transfer, detonation performance, NTO (5–nitro–2,4–dihydro–3*H*–1,2,4–triazol–3–one), PATO (3–picrylamino–1,2,4–triazole), a*b initio*.

ÖZ

BAZI PATLAYICI MADDELERİN TOTOMERİK DENGELERİ ÜZERİNE TEORİK ARAŞTIRMALAR

Çelik Bayar, Çağlar
Doktora, Kimya Bölümü
Tez Yöneticisi: Prof. Dr. Lemi Türker

Aralık 2012, 177 sayfa

Patlayıcı madddeler her zaman bilim insanlarının ilgisini çekmiştir. Saf ya da karışım halinde birçok patlayıcı sentezlenmekte ve değişik açılardan araştırılmaktadır. Fakat bu maddelerin tehlikeli karakterlerinden dolayı, sentezlenebilirlikleri ve özellikleri önceden teorik olarak tahmin edilebilmelidir.

Günümüzde, daha çok, literatürde bilinen bazı patlayıcıların özellikleri, bunların yeni türevleri sentezlenerek geliştirilmeye çalışılmaktadır. Deneysel ya da teorik olarak yürütülen bu çalışmalarda bu materyallerin balistik özellikleri (patlama ısısı, patlama hızı ve patlama basıncı) ve termal kararlılıkları artırılmaya çalışılmakta, sürtünme hassasiyeti, elektrik kıvılcım hasasiyeti, şok ve etki hassasiyeti gibi özellikleri ise azaltılmaya çalışılmaktadır.

NTO (5–nitro–2,4–dihidro–3*H*–1,2,4–triazol–3–on) ve PATO (3–pikrilamino–1,2,4–triazol) patlayıcıları literatürde yer alan çok önemli ikincil patlayıcılardır ve balistik değerleri ile yıllardır yerlerini korumaktadırlar. Bu tez çalışmasında, teorik olarak, bu patlayıcıların değişik izomerleri ve totomerleri tasarlanmış, balistik özellikleri geliştirilmeye çalışılmış, hassasiyetleri ve reaktiflikleri ise azaltılmaya çalışılmıştır. Buna ilave olarak, PATO ve totomerlerinin protonlanmış ve protonlanmamış halde aromatik nitrolama reaksiyonları ve mekanizmaları kinetik yönden incelenmiştir.

Çalışmada Hartree–Fock (HF) ve Density Functional Theory (DFT) hesaplamalı kimya yöntemleri Pople basis setleri ile kullanılmıştır.

Totomerizmin, yeni tasarlanmış NTO ve PATO türevi patlayıcıların kuantum kimyasal ve balistik özellikleri üzerine olan etkileri gaz fazında aydınlatılmıştır.

Protonlanmamış PATO ve totomerik PATO türlerinin çeşitli aromatik karbon ve azot mono–nitrasyon mekanizmaları gaz fazında tasarlanmış ve bu mekanizmalara ait geçiş halleri, ara ürünler ve nitrolanmış ana ürünler tespit edilmiştir. Nitrolanmış PATO ana ürünlerine ait balistik değerler ayrıca hesaplanmıştır. Nitrolama reaksiyonları çözelti fazında da incelenmiştir. Ayrıca, protonlanmış PATO türlerinin aromatik karbon ve azot mono–nitrasyon reaksiyonlarına ait ara ürünleri ve nitrolanmış ana ürünleri gaz fazında çalışılmıştır.

Anahtar Kelimeler: aromatik nitrolama reaksiyonları, geçiş hali, yük transferi, balistik özellikler, NTO (5–nitro–2,4–dihidro–3*H*–1,2,4–triazol–3–on), PATO (3–pikrilamino–1,2,4–triazol), a*b initio*.

to my future

ACKNOWLEDGMENTS

First, I would like to express my sincere thanks to my supervisor, Prof. Dr. Lemi Türker, for his continuous interest, help, guidance, support and patience. I always believe that joining to his group was one of my best decisions in my life.

Thanks to Prof. Dr. Hyung J. Kim, from Chemistry Department of Carnegie Mellon University, for his supervision, friendship and kindness when I was in Pittsburgh, USA, for my collaborative research. He has provided me theoretical and technical support every time. He has mainly contributed to Chapter 5. He has also reviewed Chapter 4.

Thanks to my thesis progress committee members, Prof. Dr. İlker Özkan and Prof. Dr. Şakir Erkoç, for their guidance during my research.

My special thanks go to my husband, Gökhan Bayar, for his great support, trust, patience and love. This work couldn't be accomplished without him. He was always with me when I was in trouble. He is always very good at technical subjects as an engineer and used his intelligence and experience to solve my technical problems every time.

I'm grateful to my parents and my sister for their endless love, support, trust and encouragement. I was not lonely on this long way. They were always with me.

I also want to thank Gökhan's family for their help and support.

I would like to thank my previous lab–mates Selçuk Gümüş, Taner Atalar, Hamza Turhan and recent lab–mate Serhat Varış for their sincere support during my Ph.D study.

Thanks to my friend Eda Durkan for her helps during my research in USA. If she hadn't helped me, I wouldn't do my parallel work in Turkey and collect that much data.

Thanks to Sinan Umu from Middle East Technical University and Florin Manolache from Carnegie Mellon University for their technical (network) support.

I want to thank Prof. Dr. Hyung J. Kim's group members at Carnegie Mellon University; Hyunjin Kim, Nilesh Dhumal, Sang–Won Park and Andrew DeYoung; for their friendship, help and support.

Lastly, thanks to my other friends at Carnegie Mellon University; Hadi Abroshan, Lea Veras and Hose Flores; for their friendship and intimacy.

TABLE OF CONTENTS

ABSTRACT iv
ÖZ vi
ACKNOWLEDGMENTS ix
TABLE OF CONTENTS xi
LIST OF TABLES xv
LIST OF FIGURES xx

CHAPTERS

1 INTRODUCTION 1
1.1 DEFINITIONS 1
1.1.1 Isomers and Tautomers 1
1.1.2 Explosion 1
1.1.2.1 Atomic (Nuclear) Explosions 2
1.1.2.2 Physical Explosions 2
1.1.2.3 Chemical Explosions 2
1.1.2.3.1 Primary Explosives 3
1.1.2.3.2 Secondary Explosives 3
1.1.2.3.3 Propellants 4
1.1.3 Oxygen Balance (Ω (%)) 5
1.2 THE AIM OF THE THESIS STUDY 6

2 NTO–PICRYL CONSTITUTIONAL ISOMERS – A DFT STUDY
PART 1 8
2.1 INTRODUCTION 8
2.2 THEORETICAL METHODS 13
2.3 RESULTS AND DISCUSSION 14
2.3.1 Relative Total Energies 14
2.3.2 Bond Lengths and Bond Dissociation Energies 16

2.3.3 Frontier Molecular Orbitals 20
2.3.4 Detonation Performances 22
2.3.5 Isogyric Heats of Formation Calculations and Detonation Performance Analyses for A5 and B5 Isomers 25
2.4 CONCLUSION 29

3 NTO–PICRYL CONSTITUTIONAL ISOMERS – A DFT STUDY PART 2 30
3.1 INTRODUCTION 30
3.2 THEORETICAL METHODS 31
3.3 RESULTS AND DISCUSSION 31
3.3.1 Considered NTO–Picryl Structures and Relative Total Energies 31
3.3.2 Bond Dissociation Energies 32
3.3.3 The Frontier Molecular Orbitals 44
3.3.4 Detonation Performances 44
3.4 CONCLUSION 51

4 A COMPUTATIONAL VIEW OF PATO AND ITS TAUTOMERS 52
4.1 INTRODUCTION 52
4.2 THEORETICAL METHODS 54
4.3 RESULTS AND DISCUSSION 56
4.3.1 Relative Total Energies 56
4.3.2 NICS(0) Calculations and Bird Aromaticity Indexes (I_5 and I_6) 57
4.3.3 Bond Dissociation Energies 60
4.3.4 Frontier Molecular Orbitals 61
4.3.5 Heats of Formation Calculations and Detonation Performances 62
4.4 CONCLUSION 66

5 COMPUTATIONAL STUDIES OF AROMATIC NITRATION MECHANISMS OF 3–PICRYLAMINO–1,2,4–TRIAZOLE (PATO) AND ITS TAUTOMERS 67
5.1 INTRODUCTION 67
5.2 METHODS OF CALCULATION 68
5.3 RESULTS AND DISCUSSION 69
5.3.1 Thermodynamic Stabilities of the Starting Molecules 69
5.3.2 Atom Numberings 70
5.3.3 Nitration Mechanisms 71
5.3.4 C(N)–NO_2 Distances and NO_2 Angles Stand for NO_2 Moieties Involved in Nitration Process 79
5.3.5 Potential Energy Diagrams of Nitration Reactions 79
5.3.6 Discussion of Charge Transfers in Nitration Reactions 93
5.3.7 Nitrations in Solution Phase 94
5.3.8 Nitrations using Protonated PATO Species as Substrates 96
5.3.9 Thermodynamic Stabilities and Detonation Performances of the Nitration Products 102
5.4 CONCLUSION 105

6 CONCLUSIONS 106

REFERENCES 108

APPENDICES

APPENDIX A 123
APPENDIX B 141
APPENDIX C 144
APPENDIX D 168

APPENDIX E ……...…… 175

CURRICULUM VITAE

LIST OF TABLES

TABLES

Table 2.1 Calculated relative total energies of the A– and B–type isomers at B3LYP/6–31G(d,p) theoretical level 15

Table 2.2 Some of the selected bond lengths (Å) of the optimized A– and B–type isomers at the theoretical level of B3LYP/6–31G(d,p) 17

Table 2.3 The homolytic bond dissociation energies (BDEs) of C−NO_2 bonds of A– and B–type isomers calculated at UB3LYP/6–31G(d,p) theoretical level. Data in parentheses denote the computed BSSE values in kJ/mol calculated at the same theoretical level. BDEs include BSSE and ZPE corrections 19

Table 2.4 The HOMO, LUMO, Δε energies ($\Delta\varepsilon = \varepsilon_{LUMO} - \varepsilon_{HOMO}$), Mulliken electronegativities (χ_M) and chemical hardnesses (η) of all A– and B–type isomers calculated at HF/6–31G(d,p)//B3LYP/6–31G(d,p) theoretical level 21

Table 2.5 Stoichiometric relations key to calculations of the N, M_{ave}, and Q parameters of the $C_aH_bO_cN_d$ explosive [Qiu et al., 2006] 23

Table 2.6 Predicted densities and detonation properties of the A– and B–type isomers at the theoretical level of B3LYP/6–31G(d,p) 24

Table 2.7 The computed zero point energy corrected total energies, values of thermal correction (H_T) and experimental heats of formation (ΔH^o_f) in gas phase for the reference compounds used in the isogyric reactions (1) and (2) 27

Table 2.8 The computed zero point energy corrected total energies and values of thermal correction obtained from B3LYP/6–31G(d,p) calculations for A5 and B5 isomers 28
Table 2.9 Kamlet–Jacobs detonation performance values of A5 isomer using heats of formation calculated by both PM3 and isogyric methods 28
Table 2.10 Kamlet–Jacobs detonation performance values of B5 isomer using heats of formation calculated by both PM3 and isogyric methods 28

Table 3.1 The relative ZPE corrected total energies of all the considered isomers and tautomers calculated at B3LYP/6–31G(d,p) theoretical level 37
Table 3.2 The homolytic BDEs of all the considered isomers and tautomers at the theoretical level of UB3LYP/6–31G(d,p). The BDEs written in bold present the trigger bonds of the corresponding structures. Data in parentheses denote the BSSE values in kJ/mol computed at the same theoretical level. BDEs include BSSE and ZPE corrections 38
Table 3.3 The HOMO, LUMO, Δε energies ($\Delta\varepsilon = \varepsilon_{LUMO} - \varepsilon_{HOMO}$), Mulliken electronegativities (χ_M) and chemical hardnesses (η) of all the considered isomers and tautomers calculated at HF/6–31G(d,p)//B3LYP/6–31G(d,p) theoretical level 45
Table 3.4 Predicted densities and detonation properties of all isomers and their tautomers at the theoretical level of B3LYP/6–31G(d,p). Bold written values present the highest detonation performance values of structures having the same “i” number (i = 1 – 6) 47

Table 4.1 The relative total energies of PATO and its tautomers obtained at the theoretical level of B3LYP/6–31G(d,p) 56
Table 4.2 Values of a and b used in the calculation of bond orders [Gordy, 1947] 57

Table 4.3 The optimized bond lengths of the triazole and picryl rings at the theoretical level of B3LYP/6–31G(d,p). Bonds 1–5 belong to the triazole ring, 6–11 to the picryl ring of the related compound (see atom numberings in Figure 4.2) 59

Table 4.4 Aromaticities of the triazole and picryl moieties of the considered compounds (ordered in decreasing order of the aromaticities of the triazole rings). I_5 and I_6 (%) represent Bird aromaticity indexes calculated via B3LYP/6–31G(d,p) optimized bond lengths; NICS(0) (ppm) values represent aromaticities at the ring centers calculated at B3LYP/6–31G(d,p) theoretical level 59

Table 4.5 Homolytic bond dissociation energies (BDEs) of C−NO_2 bonds of PATO and its tautomers calculated at UB3LYP/6–31G(d,p) theoretical level. Data in parentheses denote the BSSE values in kJ/mol computed at the same theoretical level. BDEs include BSSE and ZPE corrections 61

Table 4.6 HOMO, LUMO, Δε energies ($\Delta\varepsilon = \varepsilon_{LUMO} - \varepsilon_{HOMO}$), Mulliken electronegativities (χ_M) and chemical hardnesses (η) of PATO and its tautomers calculated at HF/6–31G(d,p)//B3LYP/6–31G(d,p) theoretical level 62

Table 4.7 The zero point energy corrected total energies and values of thermal correction (H_T) of the isogyric reaction compounds at the theoretical level of B3LYP/6–31G(d,p). The last column presents the experimental heats of formation of the reference compounds in the gas phase 64

Table 4.8 Calculated Kamlet–Jacobs detonation performances of PATO using isogyric (B3LYP/6–31G(d,p)) and PM3 results for heats of formation (ΔH^o_f) 64

Table 4.9 Predicted densities and detonation properties of PATO and its tautomers at the theoretical level of B3LYP/6–31G(d,p) 65

Table 5.1 Relative total electronic energies of PATO and its tautomers in increasing order (HF/6–311++G(d,p) theoretical level) 69
Table 5.2 Equilibrium constants for the conversion of PATO to its tautomers (HF/6–311++G(d,p) theoretical level) 70
Table 5.3 C(N)–NO_2 distances and NO_2 angles stand for NO_2 moieties involved in nitration process (HF/6–311++G(d,p) theoretical level) 81
Table 5.4 The relative total electronic energies of the reaction states of PATO nitration mechanisms with respect to isolated (PATO + NO_2^+) (HF/6–311++G(d,p) theoretical level). See the associated graph in Figure 5.7 84
Table 5.5 Population of molecules with enough energy to create successful collisions for the pre–transition states associated with PATO nitration mechanisms (HF/6–311++G(d,p) theoretical level). See the associated graph in Figure 5.7 85
Table 5.6 The relative total electronic energies of the reaction states of 1,3–CCW–Tautomer nitration mechanisms with respect to isolated (PATO + NO_2^+) (HF/6–311++G(d,p) theoretical level). See the associated graph in Figure 5.8 87
Table 5.7 Population of molecules with enough energy to create successful collisions for the pre–transition states associated with 1,3–CCW–Tautomer nitration mechanisms (HF/6–311++G(d,p) theoretical level). See the associated graph in Figure 5.8 88
Table 5.8 The relative total electronic energies of the reaction states of 1,5–CCW–Tautomer nitration mechanisms with respect to isolated (PATO + NO_2^+) (HF/6–311++G(d,p) theoretical level). See the associated graph in Figure 5.9 90

Table 5.9 Population of molecules with enough energy to create successful collisions for the pre–transition states associated with 1,5–CCW–Tautomer nitration mechanisms (HF/6–311++G(d,p) theoretical level). See the associated graph in Figure 5.9 91

Table 5.10 Comparison of the NO_2 moiety of the pre–transition state of each nitration mechanism with isolated NO_2 radical and NO_2^+ ion in terms of electrostatic charges (q) calculated using Chelpg method at HF/6–311++G(d,p) level of theory 94

Table 5.11 The relative total electronic energy orders of protonated PATO species at the theoretical level of HF/6–311++G(d,p) 98

Table 5.12 The relative total electronic energy orders of intermediates of PATO–B and PATO–C species compiled in Figures 5.12 and 5.13 (HF/6–311++G(d,p)) 101

Table 5.13 The relative total electronic energy orders of nitration products of PATO–B and PATO–C species compiled in Figures 5.12 and 5.13 (HF/6–311++G(d,p)) 101

Table 5.14 The relative total electronic energy orders of nitration products presented in Figure 5.5 (HF/6–311++G(d,p)) 102

Table 5.15 The predicted densities and Kamlet–Jacobs detonation properties of unnitrated and nitrated PATO species 104

LIST OF FIGURES

FIGURES

Figure 1.1	The structural formulas of RDX, HMX and TATB	4
Figure 1.2	The structural formulas of NTO and PATO	6
Figure 2.1	The structural formulas of the A– and B–type isomers	11
Figure 2.2	The numbering of atoms in A–type (A1−A6) isomers	13
Figure 2.3	The numbering of atoms in B–type (B1–B6) isomers	13
Figure 2.4	The isogyric reactions used to derive heats of formation (ΔH^{o}_{f}) of A5 and B5 isomers, respectively	26
Figure 3.1	The structural formulas of all the considered isomers and tautomers	33
Figure 4.1	Schematic representation of the chemical structures of PATO and its possible clockwise (CW) and counterclockwise (CCW) 1,3– and 1,5– tautomers	53
Figure 4.2	Atom numberings of PATO and its tautomers. The representative structure in the figure is PATO	54
Figure 4.3	The isogyric reaction used to derive the standard heat of formation of PATO	63
Figure 5.1	The mono–nitration pathways of PATO	72
Figure 5.2	The mono–nitration pathways of 1,3–CCW–Tautomer	73
Figure 5.3	The mono–nitration pathways of 1,5–CCW–Tautomer	74
Figure 5.4	The representative Wheland intermediate structures of PATO–C(5)–(R) and PATO–C(5)–(S) nitrations	75
Figure 5.5	Nitration products of the reactions compiled in Figures 5.1–5.3	76

Figure 5.6 Single electron transfer (SET) mono–nitration mechanism of PATO 78
Figure 5.7 Energy profiles of nitration mechanisms of PATO at HF/6–311++G(d,p) theoretical level (The sum of absolute total electronic energies of isolated PATO and NO_2^+ is –1339.61564 au) 86
Figure 5.8 Energy profiles of nitration mechanisms of 1,3–CCW–Tautomer at HF/6–311++G(d,p) theoretical level (The sum of absolute total electronic energies of isolated PATO and NO_2^+ is –1339.61564 au) 89
Figure 5.9 Energy profiles of nitration mechanisms of 1,5–CCW–Tautomer at HF/6–311++G(d,p) theoretical level (The sum of absolute total electronic energies of isolated PATO and NO_2^+ is –1339.61564 au) 92
Figure 5.10 Solution phase single point energies performed over the most favored *1,3–CCW–Tautomer–N(1)–Nitration* mechanisms' gas phase nitration states' fixed optimized structures at the theoretical level of HF/6–311++G(d,p). The polarizable continuum model (PCM) using the integral equation formalism variant (IEFPCM) [Frisch et al., 2009] has been used in the calculations 95
Figure 5.11 The chemical structures of the considered protonated PATO species 97
Figure 5.12 Various nitration mechanisms for PATO–B 99
Figure 5.13 Various nitration mechanisms for PATO–C 100

CHAPTER 1

INTRODUCTION

1.1 DEFINITIONS

1.1.1 Isomers and Tautomers

Isomers are compounds having the same molecular formula but different structures. There are two forms of isomers: constitutional (structural) isomers and stereoisomers (spatial isomers). Constitutional isomers are the structures that have the same molecular formula but different connectivities. Stereoisomers have the same molecular formula and connectivities but different three dimensional orientations of atoms in space [Solomons and Fryhle, 2000].

Tautomers are special types of constitutional isomers formed by tautomerization reactions. In these reactions a hydrogen atom or proton migrates accompanied by a switch of a single bond and adjacent double bond.

1.1.2 Explosion

An explosion occurs when a large amount of energy is suddenly released. There are three kinds of explosions [Akhavan, 2004]:

a. Atomic (Nuclear) Explosions

b. Physical Explosions

c. Chemical Explosions

1.1.2.1 Atomic (Nuclear) Explosions

They occur by heavy flux of neutrons and emit gamma and intense infrared and ultra–violet radiation and some particles. They are fatal [Akhavan, 2004].

1.1.2.2 Physical Explosions

They are seen when a substance is compressed and undergoes a physical transformation. At the end of the explosion, potential energy turns into kinetic energy and temperature rises rapidly. Shockwave production is observed in the surrounding [Akhavan, 2004].

1.1.2.3 Chemical Explosions

They are the results of chemical reactions that end up with short space of time (~ one–hundredth of a second), large amount of heat (several thousands of kJ/g), large quantity of gas (moles of gas per gram of explosive), high temperature (several thousands of degrees), very high pressure (several hundreds or thousands of atmospheres) and blast wave that breaks the walls of the container and causes damage to the surrounding objects [Akhavan, 2004].

Chemical explosives generally contain oxygen, nitrogen and oxidizable elements (fuels) such as carbon and hydrogen. Oxygen is generally attached to nitrogen as in NO, NO_2 and NO_3. Some of the exceptions are azides (PbN_6), nitrogen triiodide (NI_3) and azoimide (NH_3NI_3).

The molecular groups that have the explosive properties are nitro compounds, nitric esters, nitramines, chloric and perchloric acid derivatives, azides and various compounds capable of producing an explosion, for example, fulminates, acetylides, nitrogen rich compounds such as tetrazene, peroxides and ozonides, etc.

Mainly, there are two types of explosives; chemical explosives and commercial chemical products sold for non–explosive purposes. Chemical explosives are three types; primary explosives, secondary explosives and propellants. Secondary explosives are grouped into two; commercial explosives and military explosives. Propellants are classified as gun propellants and rocket propellants.

1.1.2.3.1 Primary Explosives

Primary explosives have high degree of sensitivity to initiation through shock, friction, electric spark or high temperatures and explode whether they are confined or unconfined. They produce tremendous amount of heat or shock when they dissociate. Their detonation velocities are between 3500–5500 m/s. They have ability to transmit the detonation to less sensitive (more stable) explosives and are generally used in initiating devices. Some of the examples of primary explosives are mercury fulminate, lead azide, lead styphnate, silver azide and tetrazene [Akhavan, 2004].

1.1.2.3.2 Secondary Explosives

Secondary explosives are less sensitive than primary explosives and can only be initiated to detonation by the shock produced by the explosion of a primary explosive. After dissociation, more stable products are produced. They have detonation velocities between 5500–9000 m/s. Some of the examples are nitroglycerine, nitrocellulose, picric acid, tetryl, nitroguanidine, pentaerythritol tetranitrate (PETN), 1,3,3–trinitroazetidine (TNAZ), hexanitrostilbene (HNS), trinitrotoluene (TNT), 1,3,5–trinitroperhydro–1,3,5–triazine (RDX), octahydro–

1,3,5,7–tetranitro–1,3,5,7–tetrazocine (HMX), 1,3,5–triamino–2,4,6–trinitrobenzene (TATB), 5–nitro–2,4–dihydro–3*H*–1,2,4–triazol–3–one (NTO) and 3–picrylamino–1,2,4–triazole (PATO) [Akhavan, 2004].

The structural formulas of RDX, HMX and TATB which have been used as reference materials to compare the detonation properties of the considered novel structures existing in the thesis are presented in Figure 1.1.

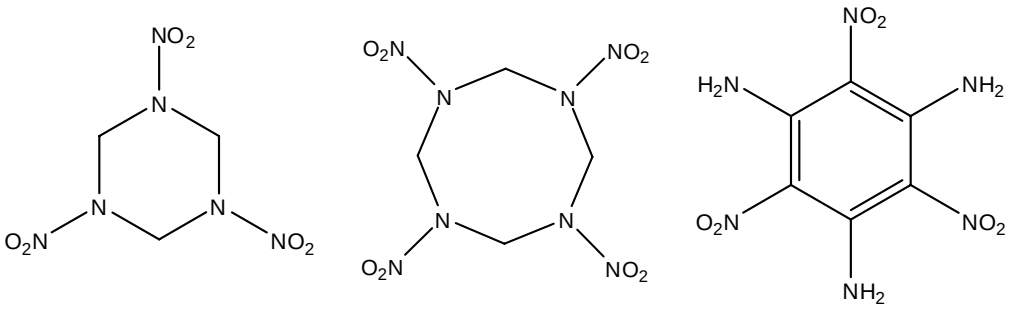

Figure 1.1: The structural formulas of RDX, HMX and TATB.

1.1.2.3.3 Propellants

Propellants are oxygen–rich compounds that only burn and do not explode. Burning usually proceeds rather violently with a flame or spark and a crackling sound. They can be initiated by a flame and spark, change from a solid to a gaseous state relatively slowly, in milliseconds. Some of the examples are black powder, smokeless propellants, blasting propellants and ammonium nitrate propellants [Akhavan, 2004].

1.1.3 Oxygen Balance (Ω (%))

Oxygen balance (Ω (%)) of an explosive is a highly important parameter to decide its performance and is defined as the percentage excess/deficiency of oxygen in the explosive. It is observed that the heat of explosion reaches a maximum for an oxygen balance of zero, since this corresponds to the stoichiometric oxidation of carbon to CO_2, hydrogen to H_2O and metal to metal oxide. Ω (%) can therefore be used to optimize the composition of the explosive to give as close to zero as possible [Akhavan, 2004].

Ω (%) provides information about the types of gases liberated during explosion. If it is large and negative then there is not enough oxygen for CO_2 to be formed. Consequently, toxic gases such as CO will be liberated. This is very important for commercial explosives as the amount of toxic gases liberated must be kept to a minimum. The molecule is said to have a positive Ω (%) if it contains more oxygen than is needed. An explosive with excess oxygen produces toxic NO and NO_2. Commercial explosives are usually close to oxygen–balanced, so that the main detonation products are H_2O, CO_2 and N_2.

The Ω (%) is calculated from the empirical formula of a compound in percentage of oxygen required for complete conversion of carbon to CO_2, hydrogen to H_2O and metal to metal oxide. The procedure for calculating Ω (%) in terms of 100 g of the explosive material is to determine the number of gram atoms of oxygen that are excess or deficient for 100 g of a compound. A quantitative measure of Ω (%) can be defined as:

$$\Omega\ (\%) = [-100 \times AW(O) \times (2C + H / 2 + M - O)] / MW(explosive)$$

where C, H, M and O are the number of carbon, hydrogen, metal and oxygen in a molecule, AW(O) is the atomic weight of oxygen (16 g/mol) and MW(explosive) is the molecular weight of explosive. Note that in a full combustion of an explosive nitrogen atoms are all converted to N_2 gas; the toxic NO and NO_2 gases are not liberated. That is why the oxygen balance formula above does not contain nitrogen.

1.2 THE AIM OF THE THESIS STUDY

The new research trends of explosive materials generally include the designs of novel derivatives of well–known explosives to improve their detonation performances (heats of explosion, detonation velocities and detonation pressures) and thermal stabilities and decrease their sensitivities towards friction, electric spark, shock and impact either experimentally or theoretically.

NTO (5–nitro–2,4–dihydro–3*H*–1,2,4–triazol–3–one) and PATO (3–picrylamino–1,2,4–triazole) (Figure 1.2) are very important secondary explosives that take place in the literature for many years in terms of their explosive properties. In this thesis study, new species of these explosives have been designed to enhance their detonation performances (ballistic properties) and to lower their sensitivities and reactivities computationally. Additionally, aromatic nitration reactions and their mechanisms for unprotonated and protonated PATO species have been analyzed.

The thesis contains 4 chapters prepared in this perspective. Every chapter has its own literature survey, methodology and results and conclusions. The *ab initio* quantum chemistry methods, Hartree–Fock (HF) and Density Functional Theory (DFT), have been used in the calculations with Pople basis sets.

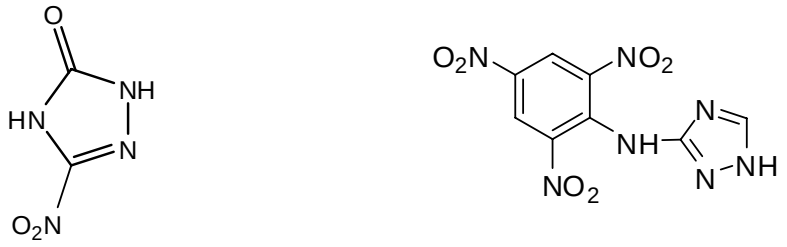

NTO PATO

Figure 1.2: The structural formulas of NTO and PATO.

Chapter 2 is about novel NTO–picryl constitutional isomers. Different constitutional structures of picryl ring (which increases the detonation properties of NTO) have been attached to NTO itself. Consequently, 12 different constitutional NTO–picryl isomers have been constructed and analyzed in the gas phase.

Chapter 3 is the enlarged form of Chapter 2. The possible tautomers of previously studied 12 NTO–picryl constitutional isomers have been taken into account. The tautomerizations have been performed over NTO rings. Totally, 36 different tautomers have been obtained and studied in the gas phase.

The triazole ring of PATO is an aromatic heterocyclic ring that can tautomerize by the shift of electron pair of nitrogen with its hydrogen in both clockwise (CW) and counterclockwise (CCW) directions. There are 4 different tautomers of PATO that are possible, at least theoretically, considering these two different directions. PATO and its possible CW and CCW 1,3– and 1,5– tautomers have been considered in Chapter 4. In the literature there has been neither a comprehensive computational analysis of PATO nor its tautomers to the best of our knowledge. We have reported the electronic and detonation properties of these structures computationally in the gas phase. The effect of triazole ring aromaticities on the stabilities of these species have also been investigated.

In Chapter 5, possible nitration positions of triazole rings of PATO and that of its possible tautomers (carbon and nitrogen mono–nitrations) and their nitration mechanisms have been investigated in the gas phase. In all these mechanisms PATO and its tautomers behave like free (uncharged) Lewis bases towards nitronium ion (Lewis acid). In another section, the solution–phase energetics for the most favored mechanism has been briefly analyzed using the reaction field method. Also, possible intermediates and nitration products have been analyzed in case of using protonated PATO species as substrates (Lewis bases) in their gas phase. The detonation performances of all possible nitration products have been calculated in last part of the chapter. This chapter has been constructed by the help of the collaborative study performed between the Middle East Technical University and Carnegie Mellon University (under the supervisions of Prof. Dr. Lemi Türker and Prof. Dr. Hyung J. Kim). The overall conclusions of the thesis are presented in Chapter 6.

CHAPTER 2

NTO–PICRYL CONSTITUTIONAL ISOMERS – A DFT STUDY
PART 1

2.1 INTRODUCTION

NTO (5–nitro–2,4–dihydro–3*H*–1,2,4–triazol–3–one) is prepared from 1,2,4–triazol–3–one under a variety of conditions; the latter has been prepared from the condensation of semicarbazide hydrochloride with formic acid [Lee et al., 1987], [Spear et al., 1989], [Langlet, 1990], [Le Campion et al., 1997]. The facile synthesis of NTO from readily available starting materials is its beneficial property. Its high performance (D (velocity of detonation)$_{unconfined}$ = 7860 m/s at ρ = 1.80 g/cm^3, $D_{confined}$ = 7940 m/s at ρ = 1.77 g/cm^3) [Meyer et al., 2007], and safe properties lets one to classify it as an insensitive high energy density explosive material so that, NTO is a very attractive explosive for use in insensitive munitions, as pressed or in a plastic bonded matrix.

NTO is less sensitive to impact (impact sensitivity ≥ 120 J) than the most commonly used military explosives HMX (octahydro–1,3,5,7–tetranitro–1,3,5,7–tetrazocine) and RDX (1,3,5–trinitroperhydro–1,3,5–triazine) (impact sensitivities of HMX and RDX are about 7.5 J) [Meyer et al., 2007]. NTO and HMX mixture was firstly used in France in plastic bonded explosives [Becuwe, 1987]. To prepare insensitive explosive munitions, NTO itself or its combinations with HMX and RDX are widely used today [Lee and Coburn, 1985], [Lee et al., 1987]. AFX644 is a typical example of combination containing NTO (40%), TNT (30%), Wax (10%) and Al powder (20%) and it is classified as an extremely insensitive detonating substance. It is prepared for filling bombs which has recently been used by the United States Air Force.

Monopicryl and dipicryl derivatives of NTO (5–nitro–2–picryl–2,4–dihydro–3*H*–1,2,4–triazol–3–one and 5–nitro–2,4–dipicryl–2,4–dihydro–3*H*–1,2,4–triazol–3–one) have been synthesized by the treatment of NTO with picryl fluoride in 1–methyl–2–pyrrolidinone (NMP) at room temperature [Coburn and Lee, 1990]. The synthetic routes to ^{15}N labeled (with N(1), N(2), N(4) and N(6) atom labeling) NTO isomers have been reported and identified by spectroscopic measurements [Oxley et al., 1995]. Theoretical and experimental studies on the structure and vibrational spectra of NTO have been done [Sorescu et al., 1996]. Ciezak and Trevino studied β–5–nitro–2,4–dihydro–3*H*–1,2,4–triazol–3–one (β–NTO) experimentally and theoretically considering inelastic neutron scattering spectra [Ciezak and Trevino, 2005]. Their data also include results of vibrational as well as solid state calculations. Quantum chemical studies on NTO, its constitutional isomers and tautomers have been performed at RHF/6–311G(d,p) level and by using Density Functional Theory (DFT) calculations at B3LYP/6–31G(d,p) and ROB3P86/6–311G(d,p) levels [Türker and Atalar, 2006].

Various experimental and theoretical studies on NTO exist in the literature such as crystal structure [Harris and Lammertsma, 1996], [Sorescu and Thompson, 1997], [Zhurova and Pinkerton, 2001], [Bolotina et al., 2003], [Zhurova et al., 2004], [Bolotina et al., 2005], [Ciezak and Trevino, 2005], preparation and characterization of metal salts [Singh and Felix, 2002], [Singh and Felix, 2003], [Kulkarni et al., 2005] and ^{15}N–NMR studies [Fan et al., 1996], [Oxley et al., 1997]. Rapid heating condition experiments of NTO have shown that the first observed decomposition product has been CO_2 [Botcher et al., 1996]. The decomposition mechanism of NTO has been investigated using restricted Hartree–Fock self–consistent field (SCF) and post SCF methods theoretically [Meredith et al., 1998]. Mechanism in unimolecular decomposition of NTO has been investigated by combining the *ab initio* molecular dynamics and a*b initio* molecular orbital methods [Yim and Liu, 2001]. The C–NO_2 homolysis is dominant at high temperature while HNO_2 formation mechanisms take place at low temperature. Thermogravimetric analyses and differential scanning calorimetry results have shown that the heating of NTO leads to competitive sublimation and condensed–phase exothermic decomposition with an autocatalytic behavior [Long et al., 2002]. It has been suggested that C–NO_2 bond homolysis is the most probable initial step for unimolecular decomposition of NTO. Also the initial

decomposition process of the NTO dimer has been investigated using DFT calculations at B3LYP/6–31G(d,p) level of theory [Kohno et al., 2001]. It has been concluded that a reaction path to produce CO_2 occurs in the gas phase beside the evolution of 5–nitroso–2,4–dihydro–3*H*–1,2,4–triazol–3–one, N_2, HNO_2 and HCN.

Spear et al. [Spear et al., 1989] have reviewed the history of NTO and its structural, chemical, explosive and thermal properties, together with its synthesis. The review of the chemistry and thermolysis of NTO and plausible decomposition pathways have been performed by Singh et al. [Singh et al., 2001]. Agrawal has also reviewed the advantage of using NTO in munitions and explosive formulations [Agrawal, 2005].

In this study, the theoretical investigations of two classes of NTO–picryl derivatives including twelve constitutional isomers have been performed. These two derivatives are 5–nitro–4–picryl–2,4–dihydro–3*H*–1,2,4–triazol–3–one (A5 in Figure 2.1) and 5–nitro–2–picryl–2,4–dihydro–3*H*–1,2,4–triazol–3–one (B5 in Figure 2.1). In the literature there have been no theoretical studies about neither of these NTO derivatives nor their constitutional isomers to the best of our knowledge. The oxygen balance (Ω (%)) values of NTO, NTO–picryl derivatives and TNT are –24.60 %, –39.86 % and –73.98 %, respectively, according to our calculations using the formula in section 1.1.3. The NTO–picryl structures presently considered have been thought to be the novel structures in between NTO and TNT in terms of Ω (%) and that is why their detonation properties have been noteworthy to be investigated.

In this sense, the constitutional isomers have been designed by changing the positions of nitro groups in the six–membered rings of both A5 and B5 NTO–picryl derivatives. As a result, twelve different isomeric structures have been constructed and the A–type isomers have been named as A1–A6 whereas the B–type isomers as B1–B6. The structural formulas of the A– and B– type isomers (A1–A6 and B1–B6) are presented in Figure 2.1. The numberings of atoms in the A– and B–type isomers are shown in Figures 2.2 and 2.3, respectively.

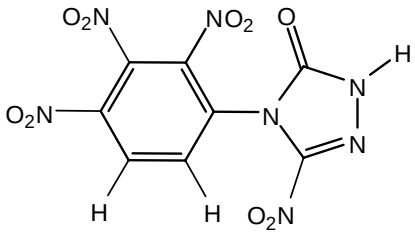

A1

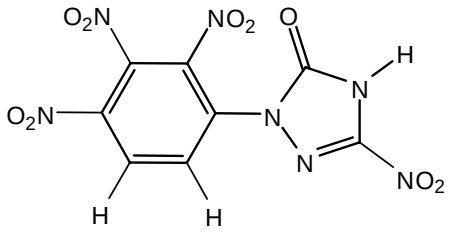

B1

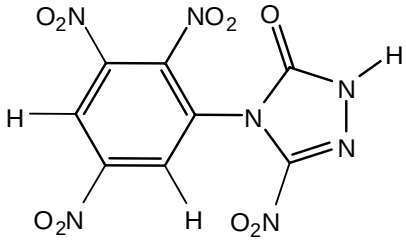

A2

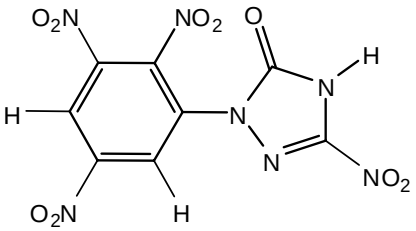

B2

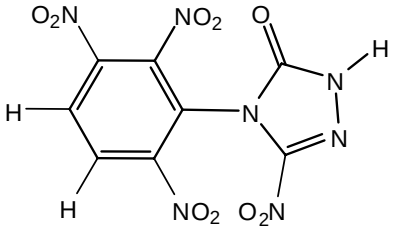

A3

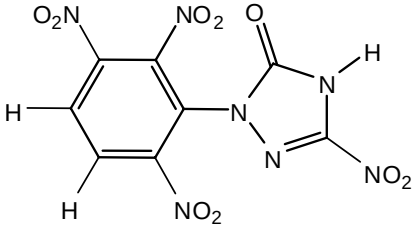

B3

Figure 2.1: The structural formulas of the A– and B–type isomers.

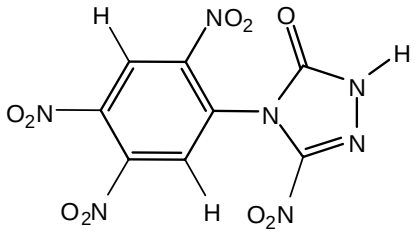

A4

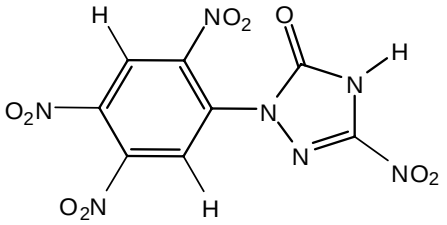

B4

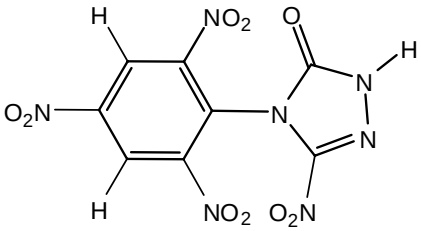

A5

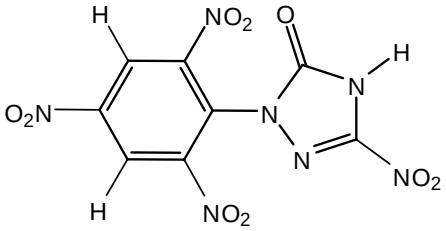

B5

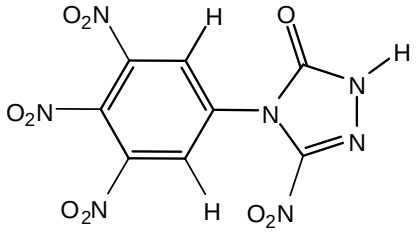

A6

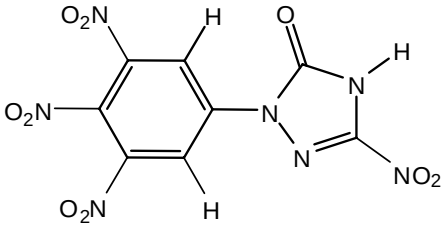

B6

Figure 2.1: The structural formulas of the A– and B–type isomers (cont'd).

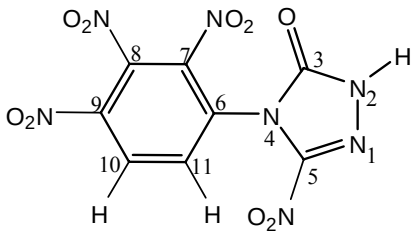

Figure 2.2: The numbering of atoms in A–type (A1−A6) isomers.

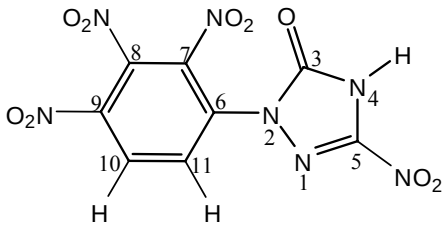

Figure 2.3: The numbering of atoms in B–type (B1–B6) isomers.

2.2 THEORETICAL METHODS

The initial structure optimizations leading to energy minima were achieved by using the molecular mechanics (MM2) method followed by semi–empirical PM3 and Hartree–Fock (HF) self–consistent field molecular orbital (SCF–MO) methods [Stewart, 1989a], [Stewart, 1989b], [Leach, 2001] at the restricted level [Fletcher, 1987], [Stewart, 1989a], [Stewart, 1989b], [Leach, 2001]. Then, the final structure optimizations were achieved within the framework of Density Functional Theory (DFT, B3LYP) [Kohn and Sham, 1965], [Parr and Yang, 1989] at the restricted level [Leach, 2001] using the 6–31G(d,p) basis set.

Vibrational analyses and the calculation of total electronic energies were performed using B3LYP/6–31G(d,p) method for closed–shell systems. In order to get frontier molecular orbital energies HF/6–31G(d,p)//B3LYP/6–31G(d,p) method was applied. The normal mode analysis for each compound yielded no imaginary frequencies

which indicate each compound had at least a local minimum on the potential energy surface. The total electronic energies were corrected for zero point vibrational energies (ZPE). Heats of formation of the molecules were calculated by both isogyric method (B3LYP/6–31G(d,p)) and semi–empirical approach (PM3) based on DFT (B3LYP/6–31G(d,p)) optimized structures. Additionally, the structure optimizations and single point calculations of all the structures were performed at UB3LYP/6–31G(d,p) theoretical level for bond dissociation energy (BDE) calculations. Note that in bond dissociation process open–shell systems are generated by the elimination of $–NO_2$ group via homolytic bond dissociation (radical dissociation process). The basis set superposition error (BSSE) analyses for bond dissociations were carried out with the counterpoise method, introduced by Boys and Bernardi [Boys and Bernardi, 1970], at the same level of theory (the BSSE results were taken into account in the calculations of bond dissociation energies in the studies of [Hou et al., 2012], [Wang et al., 2012] and [Wei et al., 2013]). All the computations were performed at 0 K using Gaussian 03 software package [Frisch et al., 2004].

2.3 RESULTS AND DISCUSSION

2.3.1 Relative Total Energies

Table 2.1 presents the relative total energies (total electronic energies corrected for ZPE) of the considered isomers calculated at the theoretical level of B3LYP/6–31G(d,p) (the Cartesian coordinates of the optimized structures are presented in APPENDIX A). The relative total energy order is found to be: A1 > B1 > A6 = B6 > A3 > B3 >A4 > A2 > B4 > A5 > B2 > B5. The most energetic (thermodynamically the most unstable) isomers are A1 and B1 with the relative total energies of 341 and 328 kJ/mol, respectively. Then, there is a sudden decrease in the values with A6 and B6 isomers (45 kJ/mol). The least energetic (thermodynamically the most stable) isomer is B5 with 0 kJ/mol (with absolute total energy of –3587331.76 kJ/mol). The presence of $–NO_2$ substituents at C(7), C(8) and C(9) positions produced structures having the highest relative total energies (A1 and B1 isomers) whereas that of C(7), C(9) and C(11) positions yielded the lowest energy having isomer B5. In the relative

total energy order, Ai–type isomers have higher energies than Bi–type isomers having the same "i" value (except for A6 and B6; their relative total energies are equal). Since, in Ai structures nitro groups substituted at C(5) positions are close to the six membered rings while they are away from in Bi structures. The other results mentioned above are also expected. In A1 and B1, neighboring $–NO_2$ groups at C(7), C(8) and C(9) positions have high steric hindrance and repulsion (repulsion arises from their electron withdrawing properties) and are close to their NTO moieties. A6 and B6 are less energetic than A1 and B1 since their $–NO_2$ groups substituted at C(8), C(9) and C(10) positions are away from their NTO moieties. The minimum steric hindrance and repulsion of $–NO_2$ groups are observed in A5 and B5. As a result they appear to be less energetic species. Table 2.1 also gives the relative heats of formation (ΔH^o_f) of the considered structures at DFT level. The present structures are constitutional isomers of each other. Therefore, they can be separately synthesized and investigated for their explosive properties. Note that the present calculations are for gaseous state of each single molecule. Obviously, in solid state, situation might be different. Of the various conformers of the molecule only one will be the realistic form. The others may only exist as defects or hot points.

Table 2.1: Calculated relative total energies of the A– and B–type isomers at B3LYP/6–31G(d,p) theoretical level.

Compound	E_{rel} (kJ/mol)
B5	0
B2	11
A5	12
B4	17
A2	27
A4	34
B3	36
A3	44
A6	45
B6	45
B1	328
A1	341

2.3.2 Bond Lengths and Bond Dissociation Energies

Table 2.2 illustrates some of the selected bond lengths of the optimized A– and B–type isomers at the theoretical level of B3LYP/6–31G(d,p). Also theoretical and experimental bond lengths of NTO [Bolotina et al., 2003], [Ciezak and Trevino, 2005], [Türker and Atalar, 2006] are presented in the same table in order to compare the bond lengths with those of NTO. The longest bonds of A– and B–type isomers stand for the C–NO_2 linkages in which the bond lengths change between 1.45–1.49 Å. Note that the –NO_2 groups have electron withdrawing property and both A1 and B1 isomers have neighboring –NO_2 groups close to the NTO moiety of the molecules and substituted at C(7), C(8) and C(9) positions of the six–membered rings. C(7)–NO_2 and C(8)–NO_2 bonds have been found to be shorter (1.33 Å) than C(9)–NO_2 bonds (1.47 Å) in these isomers. The reason may arise from the fact that all these isomeric structures have different topologies which affect the electron distribution as well as the steric hindrances developed between the substituents. Consequently, certain bond lengths may be different than the others while some others may be the same or comparable.

Behavior of explosives under heat treatment and impact conditions may exhibit variations. In our study, the *sensitivity* term implies the *impact sensitivitiy* of a considered energetic material. Impact sensitivities of energetic compounds can be determined with physical tests (drop height tests). However, differently from the physical test decomposition products, thermal effects at different temperatures may produce different decomposition products that can be produced by chemical reactions between the energetic molecules.

Although some other mechanisms rather than the cleavage trigger linkages (the most sensitive bonds to rupture) may be related to sensitivity [Murray et al., 2009], [Pospisil et al., 2010], Murray et al. [Murray et al., 2009] have indicated that there is a relationship between the bond dissociation energies (BDEs) of the N–NO_2 and C–NO_2 trigger linkages and the electrostatic potentials on the molecular surfaces of some energetic molecules. The most sensitive molecules have high levels of imbalance between the strong positive and weaker negative surface potentials. In the study of Pospisil et al. [Pospisil et al., 2010], a possible crystal volume factor (a free

Table 2.2: Some of the selected bond lengths (Å) of the optimized A– and B–type isomers at the theoretical level of B3LYP/6–31G(d,p).

	A1	B1	A2	B2	A3	B3	A4	B4	A5	B5	A6	B6	NTO[a]	NTO[b]	NTO[c]
N(1)–N(2)	1.36	1.37	1.36	1.37	1.36	1.37	1.36	1.37	1.36	1.37	1.36	1.37	1.36	1.37	1.37
N(2)–C(3)	1.38	1.42	1.39	1.42	1.39	1.42	1.38	1.42	1.39	1.42	1.39	1.42	1.40	1.37	1.37
C(3)–N(4)	1.43	1.39	1.43	1.39	1.42	1.39	1.43	1.39	1.42	1.39	1.43	1.40	1.40	1.37	1.38
N(4)–C(5)	1.38	1.37	1.38	1.36	1.38	1.37	1.38	1.36	1.38	1.37	1.39	1.36	1.37	1.35	1.35
C(5)–N(1)	1.29	1.29	1.29	1.29	1.29	1.29	1.29	1.29	1.29	1.29	1.30	1.29	1.30	1.29	1.30
N(2)–H	1.01		1.01		1.01		1.01		1.01		1.01		1.01		
N(2)–C(6)		1.41		1.41		1.41		1.40		1.40		1.41			
C(3)–O	1.21	1.21	1.21	1.21	1.21	1.21	1.21	1.21	1.21	1.21	1.21	1.21	1.21	1.23	1.24
N(4)–H		1.01		1.01		1.01		1.01		1.01		1.01	1.01		
N(4)–C(6)	1.42		1.42		1.42		1.42		1.41		1.42				
C(5)–NO_2	1.45	1.45	1.45	1.45	1.45	1.45	1.45	1.45	1.45	1.45	1.46	1.45	1.45	1.44	1.44
C(7)–NO_2	1.33	1.33	1.48	1.48	1.48	1.48	1.48	1.48	1.48	1.48					
C(8)–NO_2	1.33	1.33	1.48	1.48	1.48	1.48					1.48	1.48			
C(9)–NO_2	1.47	1.47					1.48	1.48	1.48	1.48	1.49	1.49			
C(10)–NO_2			1.48	1.48			1.48	1.48			1.48	1.48			
C(11)–NO_2					1.48	1.48			1.48	1.48					

[a]Values reported in [Türker and Atalar, 2006] at the theoretical level of B3LYP/6–31G(d,p).
[b]Experimental values at 298 K reported in [Ciezak and Trevino, 2005].
[c]Experimental values at 100 K reported in [Bolotina et al., 2003].

space in the molecule) has been thought to be effective in the impact sensitivities of some energetic compounds.

Additionally, previous studies in the literature [Owens, 1996], [Politzer and Lane, 1996], [Politzer and Murray, 1996], [Harris and Lammertsma, 1997], [Rice et al., 2002] on the homolytic BDE for the nitro compounds such as nitroaromatic and nitramine molecules have shown that there is a parallel relationship between the BDE for the weakest R–NO_2 bond scission in the molecule and its sensitivity. Usually the larger the homolytic BDE value for scission of R–NO_2 bond is, the lower the sensitivity. This is only applied to the molecules in which the R–NO_2 bond is the weakest one. For example, the C–C bond of the nitrocubane is weaker than the C–NO_2 bond and the initial step in decomposition is rupture of the C–C bond [Owens, 1999]. Thus, in such molecules, the R–NO_2 scission should not be used as an index of sensitivity.

In this sense, C–NO_2 bonds of all isomers should be considered as sensitive bonds to rupture. In this study, to calculate the relative sensitivities of the title compounds, the homolytic BDE calculations were performed with the removal of $-NO_2$ moiety from the structures. The homolytic BDE is defined as BDE = E(NO_2.) + E(R.) – E(R$-NO_2$) [Rice et al., 2002], [Shao et al., 2005], [Qiu et al., 2006], where E stands for the respective total electronic energy corrected for the ZPE for each parent structure and the fragments of the low–energy –NO_2 scission reaction. Furthermore, the BSSE analyses were carried out with the counterpoise method, introduced by Boys and Bernardi [Boys and Bernardi, 1970], at the same theoretical level (the BSSE results were taken into account in the calculations of bond dissociation energies in the studies of [Hou et al., 2012], [Wang et al., 2012] and [Wei et al., 2013]).

Additionally, the stabilities of the (R.) radicals after bond dissociations are important in determining the BDE values (for more stable R$^{\cdot}$ radicals the BDE values get lower). In the case of NTO–picryl isomers the secondary R$^{\cdot}$ radicals are formed after bond dissociations and the stabilities of these radicals are affected from the positions of the electron withdrawing –NO_2 groups surrounding them. Table 2.3 presents the BDE values for the selected bonds of all isomers. They vary with the positions of the

Table 2.3: The homolytic bond dissociation energies (BDEs) of C−NO_2 bonds of A– and B–type isomers calculated at UB3LYP/6–31G(d,p) theoretical level. Data in parentheses denote the computed BSSE values in kJ/mol calculated at the same theoretical level. BDEs include BSSE and ZPE corrections.

	BDE (kJ/mol)					
Compound	C(5)–NO_2	C(7)–NO_2	C(8)–NO_2	C(9)–NO_2	C(10)–NO_2	C(11)–NO_2
A1	227.6 (18.7)	203.7 (22.0)	**188.8** (18.7)	220.8 (17.4)		
B1	246.9 (14.8)	**192.8** (20.9)	194.5 (18.7)	227.1 (18.4)		
A2	231.5 (18.5)	**201.7** (19.9)	217.0 (17.2)		251.8 (14.8)	
B2	247.0 (14.8)	**185.0** (20.6)	216.9 (17.2)		251.3 (14.9)	
A3	239.7 (19.4)	**204.5** (19.7)	219.0 (17.0)			232.7 (20.0)
B3	248.8 (14.9)	**196.5** (20.2)	217.5 (17.0)			227.8 (17.5)
A4	230.1 (18.5)	229.3 (19.2)		216.8 (17.2)	**214.7** (16.5)	
B4	246.4 (14.7)	**212.9** (19.6)		218.1 (16.8)	213.7 (17.1)	
A5	242.3 (19.2)	230.2 (18.9)		250.5 (14.9)		**228.5** (17.1)
B5	248.1 (14.9)	**221.5** (19.3)		252.0 (15.0)		222.8 (18.5)
A6	221.8 (17.0)		226.9 (17.8)	**196.1** (18.3)	227.0 (17.8)	
B6	246.0 (14.5)		224.7 (17.6)	**197.6** (18.3)	225.3 (17.5)	
NTO[a] (C–NO_2)	276.00					
TNT (C–NO_2)	(276.10)					
RDX[b] (N–NO_2)	153.80 (152.09)					
HMX[b] (N–NO_2)	166.48					

[a]Value reported in [Türker and Atalar, 2006] at the theoretical level of ROB3P86/6–311G(d,p).
[b]Values reported in [Qiu et al., 2006] at the theoretical level of UB3LYP/6–31G(d,p).
Values in parenthesis are: a theoretical value corrected for ZPE using scaled UHF/6–31G(d) frequencies for RDX and an experimental value for TNT taken from [Harris and Lammertsma, 1997] and [Luo, 2003], respectively.

broken –NO_2 bonds however most of the C–NO_2 bond lengths are similar. In this sense we cannot conclude that there is a one to one correlation between the BDE

values and the bond lengths. When the trigger linkage BDEs of the considered isomers which are written in bold in Table 2.3 are compared with that of NTO [Türker and Atalar, 2006] and TNT [Luo, 2003] (276.00 and 276.10 kJ/mol, respectively), it is possible to say that all of the A– and B–type isomers are more sensitive than NTO and TNT. However, they all are less sensitive than RDX and HMX (BDEs of 153.80 and 166.48 kJ/mol, respectively) [Qiu et al., 2006].

According to the suggestion of Chung et al. [Chung et al., 2000], a molecule should have more than 20 kcal/mol (~ 80 kJ/mol) barrier to dissociate in order to be considered as a viable candidate for high energy density material. In the study of Wang et al. [Wang et al., 2009], this statement is verified and additionally it is mentioned that this barrier should be more than 30 kcal/mol (~ 120 kJ/mol) for an exploitable high energy density material. Thus, we can conclude that all of the considered A– and B–type isomers are viable candidates for exploitable high energy density materials (Table 2.3).

2.3.3 Frontier Molecular Orbitals

Mulliken electronegativity (χ_M) and absolute or chemical hardness (η) are important properties in reflecting chemical reactivity of the compounds. The χ_M and η values are calculated according to formulas given:

$$\chi_M = (I + A) / 2$$
$$\eta = (I - A) / 2$$

where I and A are the ionization potential and electron affinity, respectively [Pearson, 1997]. Note that $I = -\varepsilon_{HOMO}$ and $A = -\varepsilon_{LUMO}$ within the validity of the Koopmans' theorem [Koopmans, 1934], [Cramer, 2004].

The HOMO, LUMO, $\Delta\varepsilon$ energies ($\Delta\varepsilon = \varepsilon_{LUMO} - \varepsilon_{HOMO}$), Mulliken electronegativities and chemical hardnesses of all A– and B–type isomers calculated at HF/6–31G(d,p)//B3LYP/6–31G(d,p) theoretical level are shown in Table 2.4. When we

consider all Ai and Bi isomers (i = 1 – 6) in Table 2.4 and compare χ_M values, A4 isomer appears to be the most electronegative one (6.0 eV). Therefore, A4 appears to be less susceptible species to oxidation. Thermodynamically the most unstable isomers A1 and B1 (Table 2.1) have the lowest χ_M values (5.3 and 5.1 eV, respectively). They are more susceptible species to oxidation. Kinetic stability is dependent on chemical hardness [Hess and Schaad, 1971], [Pearson, 1973], [Haddon and Fukunaga, 1980], [Schmalz et al., 1988], [Zhou et al., 1988], [Zhou and Parr, 1989], [Zhou and Parr, 1990], [Manolopoulos et al., 1991], [Liu et al., 1992], [Parr and Zhou, 1993], [Aihara et al., 1996] and it is known that the harder the compound the higher the kinetic stability [Manolopoulos et al., 1991]. Thermodynamically the most unstable isomers A1 and B1 (Table 2.1) have also the lowest η values and are the softest (kinetically the most unstable) species of all (3.9 and 3.8 eV, respectively). Thermodynamically the most stable B5 isomer (Table 2.1) is the member of the kinetically stable compounds (5.2 eV). A6 stands for kinetically the most stable isomer (5.4 eV).

Table 2.4: The HOMO, LUMO, Δε energies ($\Delta\varepsilon = \varepsilon_{LUMO} - \varepsilon_{HOMO}$), Mulliken electronegativities (χ_M) and chemical hardnesses (η) of all A– and B–type isomers calculated at HF/6–31G(d,p)//B3LYP/6–31G(d,p) theoretical level.

Energy (eV)					
Compound	HOMO	LUMO	Δε	χ_M (eV)	η (eV)
A1	–9.1	–1.4	7.7	5.3	3.9
B1	–8.9	–1.3	7.6	5.1	3.8
A2	–11.1	–0.7	10.4	5.9	5.2
B2	–10.8	–0.6	10.2	5.7	5.1
A3	–11.0	–0.8	10.2	5.9	5.1
B3	–10.8	–0.6	10.2	5.7	5.1
A4	–11.0	–1.0	10.0	6.0	5.0
B4	–10.9	–0.7	10.2	5.8	5.1
A5	–11.0	–0.6	10.4	5.8	5.2
B5	–10.9	–0.6	10.3	5.8	5.2
A6	–11.1	–0.3	10.8	5.7	5.4
B6	–10.7	–0.5	10.2	5.6	5.1

2.3.4 Detonation Performances

Density (ρ), detonation velocity (D), and detonation pressure (P) are important parameters to evaluate the explosive performances of energetic materials and can be predicted by the Kamlet–Jacobs equations [Kamlet and Jacobs, 1968] based on the calculated mass densities and heats of formation. Kamlet–Jacobs equations are as follows:

$$D = 1.01\ (N\ M_{ave}^{1/2}\ Q^{1/2}\ )^{1/2}\ (1 + 1.30\rho)$$

$$P = 1.558\ \rho^2\ N\ (M_{ave})^{1/2}\ Q^{1/2}$$

where each term in equations is defined as follows: D, detonation velocity (km/s); P, detonation pressure (GPa); ρ, mass density of a compound (g/cm^3); N, moles of gaseous detonation products per gram of explosive (mol/g); M_{ave}, average molecular weight of gaseous products (g/mol); Q, chemical energy of detonation (cal/g). Here, the parameters N, M_{ave} and Q were calculated according to the chemical composition of each explosive as listed in the second column of Table 2.5 [Qiu et al., 2006]. In the table, M is the molecular weight of the compound in g/mol; ΔH^o_f is the standard heat of formation of the compound in kJ/mol. The density of each compound is defined as the molecular weight divided by the molar volume. Note that the densities and related detonation characteristics of explosives are solid state properties. However, the studies have indicated that, when the gas phase average molar volume (V) estimated by Monte–Carlo method based on 0.001 electrons/bohr^3 density space proposed by Bader et al. [Bader et al., 1987] is used at B3LYP/6–31G(d,p) theoretical level, theoretical densities become much close to the experimental ones [Qiu et al., 2006], [Wang et al., 2009]. The predicted densities and detonation properties of all A– and B–type isomers are listed in Table 2.6. The standard heats of formation (ΔH^o_f) obtained using PM3 method over DFT B3LYP/6–31G(d,p) optimized structures of all A– and B–type isomers were used in the calculation of chemical energies of detonation (Q). Previous studies [Akutsu et al., 1991], [Dorsett and White, 2000], [Sikder et al., 2001] have reported and proven that the standard heat of formation (ΔH^o_f) of an isolated gas phase molecule calculated at the PM3 level could replace the experimental data reasonably in just evaluating the detonation velocity (D) and detonation pressure (P) of the energetic compounds, because they

are not sensitive to the ΔH^o_f but are quite sensitive to the density (ρ) (D and P are directly proportional to $Q^{1/4}$ and $Q^{1/2}$ according to the Kamlet–Jacobs equations presented above). The other reason is that PM3 method uses parameters derived from experimental data to simplify the computations [Foresman and Frisch, 1996]. Table 2.6 also includes experimental and theoretical performance values of NTO [Türker and Atalar, 2006], [Meyer et al., 2007], TNT [Dong and Zhou, 1989], RDX [Lowe–Ma, 1990], [Mader, 1998], [Sikder et al., 2001], [Qiu et al., 2006], [Meyer et al., 2007] and HMX [Mader, 1998], [Qiu et al., 2006], [Meyer et al., 2007] taken from the literature.

According to the data in Table 2.6, A1 and B1 isomers have the highest Q, D and P values of all the considered isomers. Also all of the considered A– and B–type isomers have higher ρ, D and P values than that of NTO [Türker and Atalar, 2006] and TNT [Dong and Zhou, 1989] and also higher Q values than that of NTO [Türker and Atalar, 2006]. A1 and B1 isomers with the best detonation performances of all the considered isomers have higher Q values but lower D values than RDX and HMX [Qiu et al., 2006]. Additionally they have explosion pressures higher than RDX but lower than HMX [Qiu et al., 2006].

Table 2.5: Stoichiometric relations key to calculations of the N, M_{ave}, and Q parameters of the $C_aH_bO_cN_d$ explosive [Qiu et al., 2006].

Stoichiometric Relations			
Parameter	$c \geq 2a + b/2$	$2a + b/2 > c \geq b/2$	$b/2 > c$
N	$(b + 2c + 2d)/4M$	$(b + 2c + 2d)/4M$	$(b + d)/2M$
M_{ave}	$4M/(b + 2c + 2d)$	$(56d + 88c – 8b)/(b + 2c + 2d)$	$(2b + 28d + 32c)/(b + d)$
$Q \times 10^{-3}$	$(28.9b + 94.05a + 0.239\Delta H^o_f)/M$	$[28.9b + 94.05(c/2 – b/4) + 0.239\Delta H^o_f]/M$	$(57.8c + 0.239\Delta H^o_f)/M$

Table 2.6: Predicted densities and detonation properties of the A– and B–type isomers at the theoretical level of B3LYP/6–31G(d,p).

Compound	Ω (%)	ΔH^o_f [a] (kJ/mol)	Q (cal/g)	V[b] (cm^3/mol)	ρ (g/cm^3)	D (km/s)	P (GPa)
A1	–39.86	593.32	1703.62	177.93	1.92	8.71	34.91
B1	–39.86	576.28	1691.68	176.21	1.94	8.75	35.47
A2	–39.86	200.43	1428.40	182.31	1.87	8.19	30.45
B2	–39.86	199.40	1427.68	181.27	1.88	8.22	30.79
A3	–39.86	215.99	1439.30	178.96	1.91	8.31	31.72
B3	–39.86	211.72	1436.31	182.39	1.87	8.20	30.51
A4	–39.86	209.12	1434.49	176.23	1.94	8.40	32.66
B4	–39.86	193.53	1423.57	180.35	1.89	8.25	31.06
A5	–39.86	189.04	1420.42	177.68	1.92	8.33	31.97
B5	–39.86	181.21	1414.94	182.87	1.87	8.15	30.12
A6	–39.86	210.50	1435.45	182.54	1.87	8.19	30.45
B6	–39.86	198.42	1427.00	183.05	1.86	8.17	30.19
NTO[c]	–24.60	35.30	1232.24	75.21	1.73 (1.77)	7.95 (7.94)	27.38
TNT	–73.98				(1.64)	(6.95)	(19.00)
RDX[d]	–21.61	168.90	1597.39	124.92	1.78 (1.81)	8.88 (8.75)	34.75 (34.70)
HMX[d]	–21.61	270.41	1633.88	157.53	1.88 (1.90)	9.28 (9.10)	39.21 (39.30)

[a]Standard heats of formation obtained from the PM3 single point calculations [Akutsu et al., 1991], [Dorsett and White, 2000], [Sikder et al., 2001] over B3LYP/6–31G(d,p) optimized structures.

[b]Average molar volumes from 100 single point calculations at the B3LYP/6–31G(d,p) theoretical level [Qiu et al., 2006].

[c]Values reported in [Türker and Atalar, 2006] at the theoretical level of B3LYP/6–31G(d,p) (ΔH^o_f of NTO was calculated using PM3//B3LYP/6–31G(d,p) method in this reference).

[d]Values reported in [Qiu et al., 2006] at the theoretical level of B3LYP/6–31G(d,p) (ΔH^o_f of RDX and HMX were calculated using PM3//B3LYP/6–31G(d,p) method in this reference).

Data in parentheses are the experimental values taken from [Meyer et al., 2007] for NTO, [Dong and Zhou, 1989] for TNT, [Lowe–Ma, 1990], [Mader, 1998], [Sikder et al., 2001], [Meyer et al., 2007] for RDX and [Mader, 1998], [Meyer et al., 2007] for HMX.

2.3.5 Isogyric Heats of Formation Calculations and Detonation Performance Analyses for A5 and B5 Isomers

In addition to the studies above, the isogyric heats of formation calculations for A5 and B5 isomers have been performed by DFT B3LYP/6–31G(d,p) method in order to testify the validity of the usage of PM3 heats of formation in detonation performance calculations. In isogyric reactions, the total number of electron pairs is conserved both in the reactants and products [Jensen, 2007]. Note that only experimental gas phase heat of formation value of 2,4,6–trinitrobenzene is available in the literature among all trinitrobenzene constitutional isomers. That is why the isogyric reactions can just be designed for A5 and B5 NTO–picryl isomers. The isogyric reactions used to derive ΔH^{o}_{f} of A5 and B5 isomers are designed in Figure 2.4.

For the isogyric reaction, heat of reaction (ΔH_{298}) can be calculated from the following equation:

$$\Delta H_{(298)} = \sum \Delta H_{f,P} - \sum \Delta H_{f,R}$$

where $\sum \Delta H_{f,R}$ and $\sum \Delta H_{f,P}$ are the heats of formation of reactants and products at 298 K, respectively. The heats of formation of A5 and B5 can be figured out when $\Delta H_{(298)}$ values are known. Therefore, one of the most important thing is to compute the $\Delta H_{(298)}$ and it can be calculated using the following expression:

$$\begin{aligned} \Delta H_{(298)} &= \Delta E_{298} + \Delta(PV) \\ &= \Delta E_0 + \Delta ZPE + \Delta H_T + \Delta nRT \end{aligned}$$

where ΔE_0 is the change in total energy between the products and reactants at 0 K; ΔZPE is the difference between the zero–point energies (ZPE) of the products and reactants at 0 K; ΔH_T is thermal correction from 0 to 298 K. The $\Delta(PV)$ in equation is the PV work term. It equals to ΔnRT for the reactions in gas phase. For the isogyric reactions (1) and (2), $\Delta n = 0$, so $\Delta(PV) = 0$. We note that the ring moieties of NTO–picryl derivatives (NTO and TNB (trinitrobenzene)) were preserved in the isogyric reaction schemes to avoid large calculation errors involved in decomposition of these structures [Zhang et al., 2002], [Ju et al., 2005].

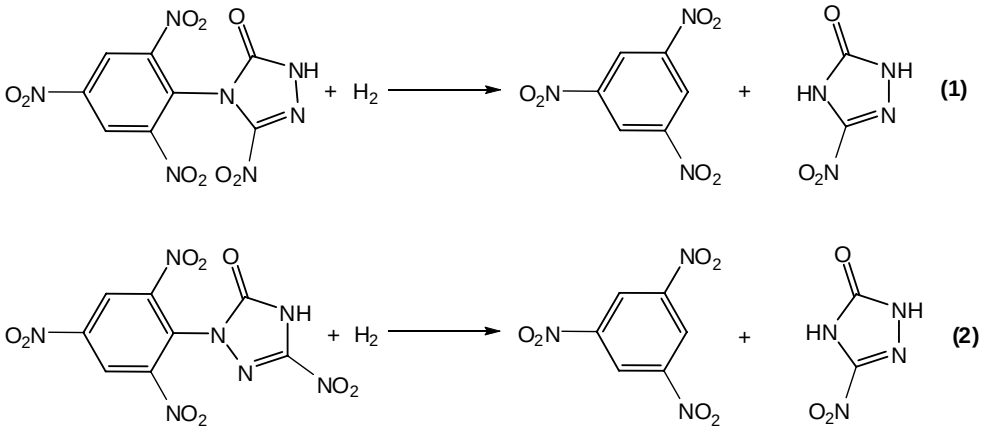

Figure 2.4: The isogyric reactions used to derive heats of formation (ΔH^{o}_{f}) of A5 and B5 isomers, respectively.

The experimental heat of formation of reference compound trinitrobenzene (TNB) is available in the literature [Politzer et al., 1997] (standard heat of formation of H_2 is 0 by definition [Silbey and Alberty, 2001]). As there has been no experimental ΔH^{o}_{f} value for NTO in gaseous state in the literature, a computed value at the theoretical level of B3LYP/6–31G(d,p) [Osmont et al., 2007] has been taken as a reference value in the calculations.

Heats of formation of A5 and B5 isomers using the reactions (1) and (2) can be calculated from the equations below:

$$\Delta H_{298\,(1)} = \Delta H^{o}_{f}\,(\text{TNB, exp}) + \Delta H^{o}_{f}(\text{NTO}) - \Delta H^{o}_{f}(\text{A5 isomer})$$

$$\Delta H_{298\,(2)} = \Delta H^{o}_{f}\,(\text{TNB, exp}) + \Delta H^{o}_{f}(\text{NTO}) - \Delta H^{o}_{f}(\text{B5 isomer})$$

Table 2.7 contains the computed zero point energy corrected total energies, values of thermal correction and experimental heats of formation in gas phase for reference compounds used in the isogyric reactions (1) and (2).

Table 2.8 lists the computed zero point energy corrected total energies and values of thermal correction obtained from B3LYP/6–31G(d,p) calculations for A5 and B5 isomers.

In Table 2.9, Kamlet–Jacobs detonation performance values of A5 isomer using heats of formation calculated by both PM3 and isogyric methods are shown.

Similarly, Table 2.10 presents the results for B5 isomer. As seen from both tables changes in heats of formation do not change the performance data significantly. Because D and P are not sensitive to the ΔH^{o}_{f} value as in the case of ρ (D is directly proportional to $Q^{1/4}$ and P to $Q^{1/2}$ in the Kamlet–Jacobs formula presented in section 2.3.4).

Table 2.7: The computed zero point energy corrected total energies, values of thermal correction (H_T) and experimental heats of formation (ΔH^{o}_{f}) in gas phase for the reference compounds used in the isogyric reactions (1) and (2).

Compound	$E_0 + ZPE$ (au)	H_T (au)	ΔH^{o}_{f}(exp) (kJ/mol)
H_2	–1.16837	0.01348	0.00
TNB	–845.63369	0.12070	62.34
NTO	–521.91547	0.07472	–3.77*
The experimental heat of formation of trinitrobenzene (TNB) is from [Politzer et al., 1997] (standard heat of formation of H_2 is 0 by definition [Silbey and Alberty, 2001]) and others are calculated at the B3LYP/6–31G(d,p) theoretical level. *A computed value at the theoretical level of B3LYP/6–31G(d,p) [Osmont et al., 2007]. The value has been calculated as: (absolute electronic energy + zero point energy (at 0 K)) + (thermal correction from 0 to 298 K) + (atomic corrections for each type of atom of NTO at 298 K). The atomic corrections present in the reference have been determined by least–square fitting of the 28 selected experimental gas–phase standard enthalpies of formation at 298 K.			

Table 2.8: The computed zero point energy corrected total energies and values of thermal correction obtained from B3LYP/6–31G(d,p) calculations for A5 and B5 isomers.

Compound	$E_0 + ZPE$ (au)	H_T (au)
A5 isomer	–1366.33789	0.17425
B5 isomer	–1366.34232	0.17417

Table 2.9: Kamlet–Jacobs detonation performance values of A5 isomer using heats of formation calculated by both PM3 and isogyric methods.

A5 isomer	ΔH^o_f (kJ/mol)	D (km/s)	P (GPa)
PM3 method	189.04	8.33	31.97
Isogyric method	151.01	8.29	31.67

Table 2.10: Kamlet–Jacobs detonation performance values of B5 isomer using heats of formation calculated by both PM3 and isogyric methods.

B5 isomer	ΔH^o_f (kJ/mol)	D (km/s)	P (GPa)
PM3 method	181.21	8.15	30.12
Isogyric method	139.17	8.11	29.81

2.4 CONCLUSION

Twelve A– and B–type constitutional isomers, A1–A6 and B1–B6, derived from two NTO–picryl derivatives (5–nitro–4–picryl–2,4–dihydro–3*H*–1,2,4–triazol–3–one and 5–nitro–2–picryl–2,4–dihydro–3*H*–1,2,4–triazol–3–one) have positive heats of formation. It is observed that all of the constitutional isomers are more sensitive than NTO and TNT but more insensitive than RDX and HMX (in terms of C–NO_2 homolytic bond dissociation energies). All of the constitutional isomers have higher detonation performances than NTO and TNT. However, except for A1 and B1 isomers, they have lower detonation performances than RDX and HMX. A1 and B1 isomers have comparable detonation performances to RDX and HMX.

P.S. The study presented in this chapter has been published in a SCI journal (Lemi Türker and Çağlar Çelik Bayar. (2012). NTO–Picryl Constitutional Isomers – A DFT Study. *Journal of Energetic Materials*, 30:72–96).

CHAPTER 3

NTO–PICRYL CONSTITUTIONAL ISOMERS – A DFT STUDY PART 2

3.1 INTRODUCTION

In the previous chapter of the thesis, the theoretical investigations of two classes of NTO–picryl derivatives including twelve constitutional isomers have been performed. These two derivatives have been 5–nitro–4–picryl–2,4–dihydro–3*H*–1,2,4–triazol–3–one (class A) and 5–nitro–2–picryl–2,4–dihydro–3*H*–1,2,4–triazol–3–one (class B). They all have signed new species between NTO (5–nitro–2,4–dihydro–3*H*–1,2,4–triazol–3–one) and TNT (trinitrotoluene) (Ω (%) values of NTO, NTO–picryl derivatives and TNT are –24.60 %, –39.86 % and –73.98 %, respectively, according to our calculations using the formula in section 1.1.3) and have been thought to be potential candidates for high energy density materials. The constitutional isomers have been designed by changing the positions of nitro groups in the six–membered rings of both A5 and B5 NTO–picryl derivatives. As a result, twelve different isomeric structures have been constructed and the A–type isomers have been named as A1–A6 whereas the B–type isomers as B1–B6.

In this chapter of the thesis the tautomeric equilibria of the A–type constitutional isomers (A1–A6) have been discussed. Each isomer has had an enol–tautomer named Ai–enol–tautomer and an aci–tautomer named Ai–aci–tautomer (i = 1 – 6). Similar calculations for the tautomeric equilibria of the B–type constitutional isomers (B1–B6) have been completed. Each isomer has had an enol–tautomer named Bi–enol–tautomer and a 1,3–tautomer named Bi–1,3–tautomer (i = 1 – 6). Finally, the quantum chemical and ballistic properties of these thirty six different types of NTO–picryl structures have been discussed together.

3.2 THEORETICAL METHODS

All theoretical methods used are the same as those of Section 2.2.

3.3 RESULTS AND DISCUSSION

3.3.1 Considered NTO–Picryl Structures and Relative Total Energies

The chemical structures of thirty six A– and B–type isomers and their tautomers are presented in Figure 3.1. Table 3.1 presents the relative total energies (total electronic energies corrected for ZPE) of the considered molecules calculated at B3LYP/6–31G(d,p) level at 0 K (the Cartesian coordinates of the optimized structures are presented in APPENDIX A).

Thermodynamically the most stable isomer is B5. Relative total energy has been defined as Ei – E(B5). As mentioned in Chapter 2, Bi isomers are more stable than Ai isomers having the same "i" value in the relative total energy order (except for A6 and B6, in which case relative total energies of A6 and B6 are equal). Similarly, Bi–enol–tautomers are less energetic than Ai–enol–tautomers. Another point is that Bi–1,3–tautomers are less energetic than Ai–aci–tautomers. However, 1,5–type tautomers are generally less energetic than 1,3–type tautomers, the case is different for 1,5–aci–tautomers. Ai isomers need more energy to convert to their Ai–aci–forms and to have a charge separation (formal charges) onto their N and O atoms. Therefore, Ai–aci–tautomers are more energetic than both Ai–enol–tautomers and Bi–1,3–tautomers (see Figure 3.1). The results are also consistent with those of literature obtained for NTO and its 1,3–enol– and 1,5–aci–tautomers [Harris and Lammertsma, 1996]. The total energy order in Ai series is observed as Ai < Ai–enol–tautomer < Ai–aci–tautomer for the same number of "i". In Bi series the trend is observed as Bi < Bi–enol–tautomer < Bi–1,3–tautomer except for i = 1. In Bi structures keto–enol tautomerizations occur between N, C and O atoms whereas 1,3–tautomerizations occur between N, C and N atoms (see Figure 3.1). As

electronegativity of an O atom is higher than N atom, it is more favored to produce less energetic enol tautomers than 1,3–tautomers.

3.3.2 Bond Dissociation Energies

To calculate the sensitivities of the title compounds, the homolytic bond dissociation energy (BDE) calculations have been performed with the removal of $–NO_2$,–OH and –O moieties from the structures (see section 2.3.2 for relation between BDE and sensitivity). Table 3.2 presents the homolytic BDEs of all the considered structures calculated at UB3LYP/6–31G(d,p) theoretical level (see Figures 2.2 and 2.3 for atom numberings). Furthermore, the basis set superposition error (BSSE) analyses have been carried out as described in section 2.3.2. In Table 3.2, the BDE value written in bold presents the trigger (the most sensitive) bond of each corresponding structure. When all these bold written values are compared with the BDEs of NTO and TNT (276.00 kJ/mol [Türker and Atalar, 2006] and 276.10 kJ/mol [Luo, 2003], respectively), it is possible to say that all of the considered structures are more sensitive than NTO and TNT. However, they all are less sensitive than RDX and HMX (BDEs of 153.80 and 166.48 kJ/mol, respectively [Qiu et al., 2006]). The negative BDEs belonging to A1–aci–tautomer and B1–enol–tautomer in Table 3.2 denote the formation of more stable products of ($R. + NO_2.$) after bond dissociations. The more stable radicalic product formations and consequently the negative homolytic BDEs are encountered in the literature [Lazzara et al., 1979], [Rule et al., 1982], [McKee, 1995].

We can conclude that all of the considered structures in Table 3.2 are viable candidates for exploitable high energy density compounds according to the suggestions of [Chung et al., 2000] and [Wang et al., 2009] (see section 2.3.2 for more details).

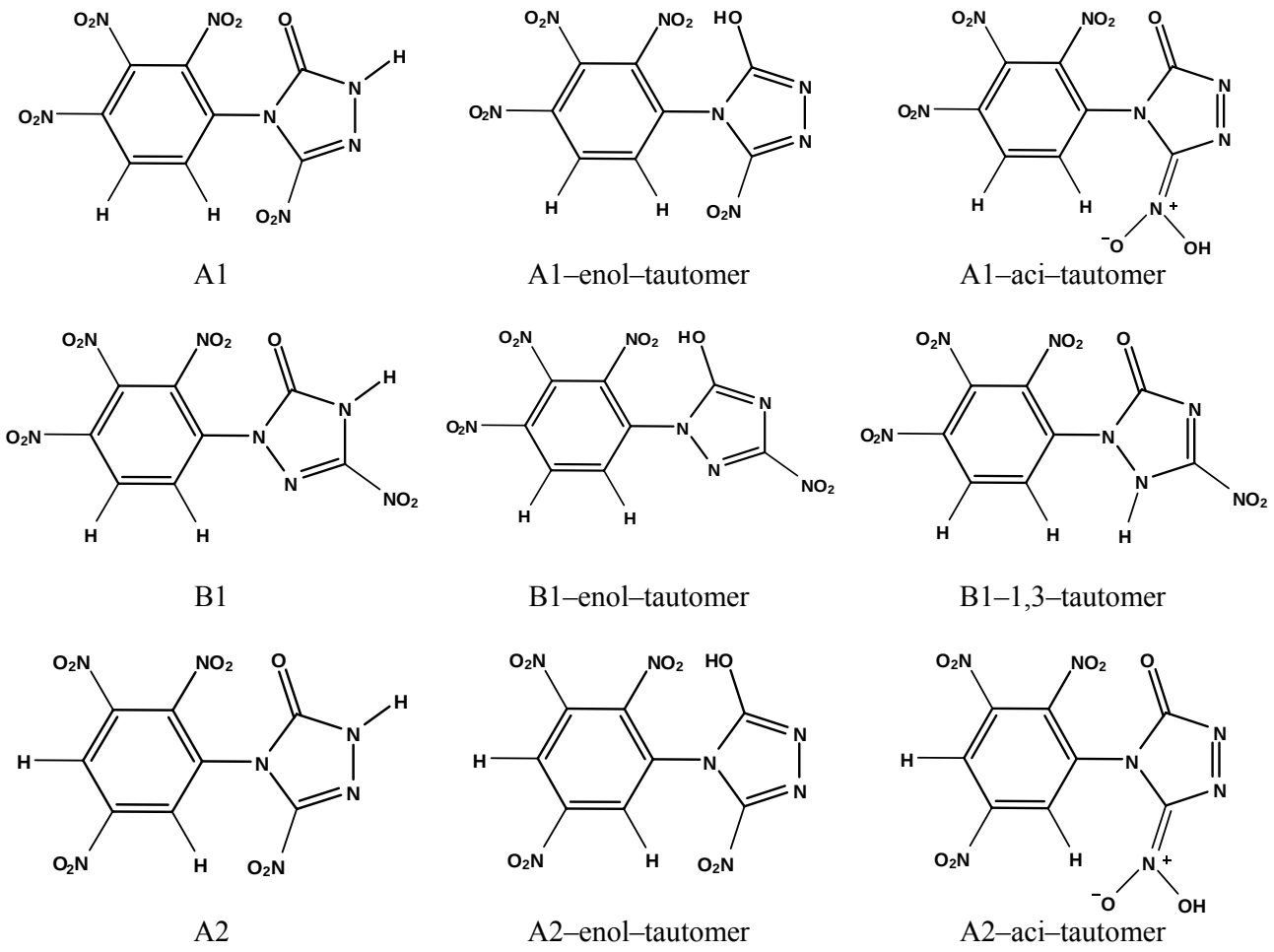

Figure 3.1: The structural formulas of all the considered isomers and tautomers.

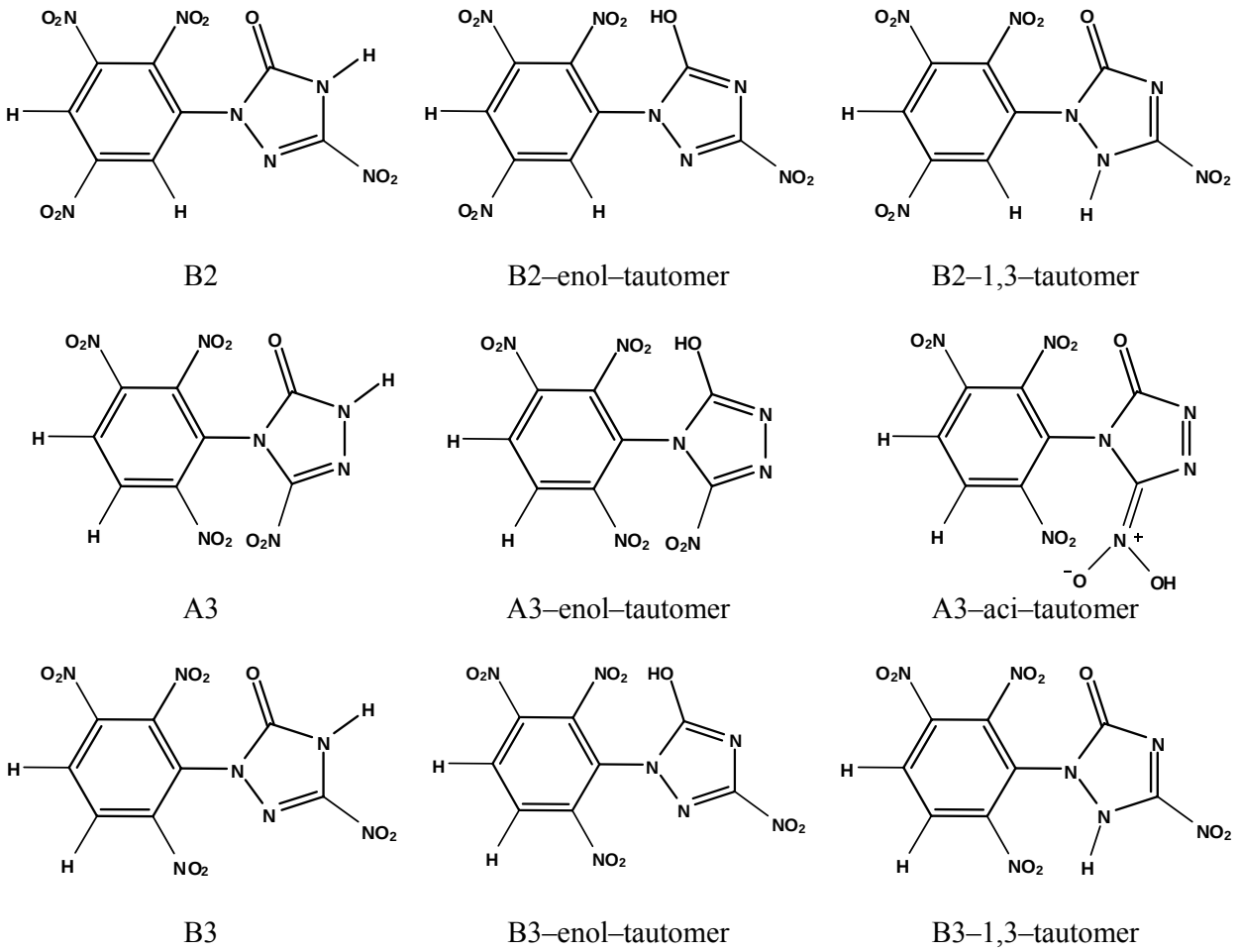

Figure 3.1: The structural formulas of all the considered isomers and tautomers (cont'd).

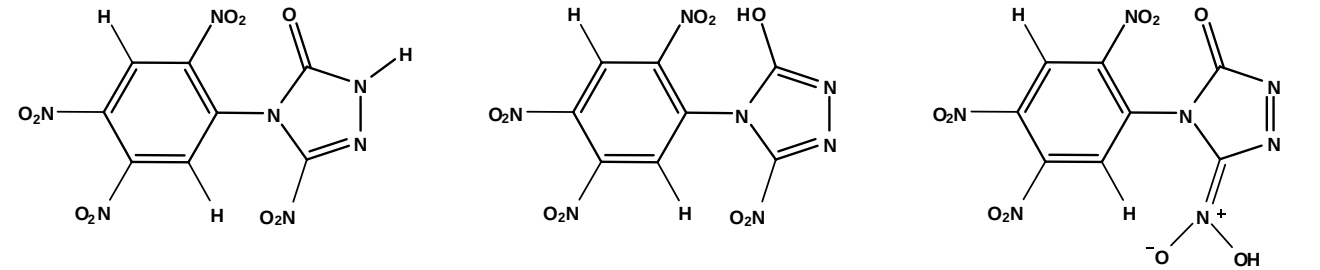

A4 A4–enol–tautomer A4–aci–tautomer

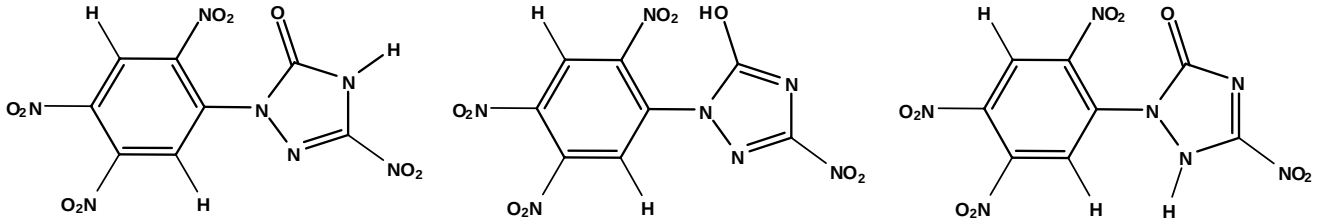

B4 B4–enol–tautomer B4–1,3–tautomer

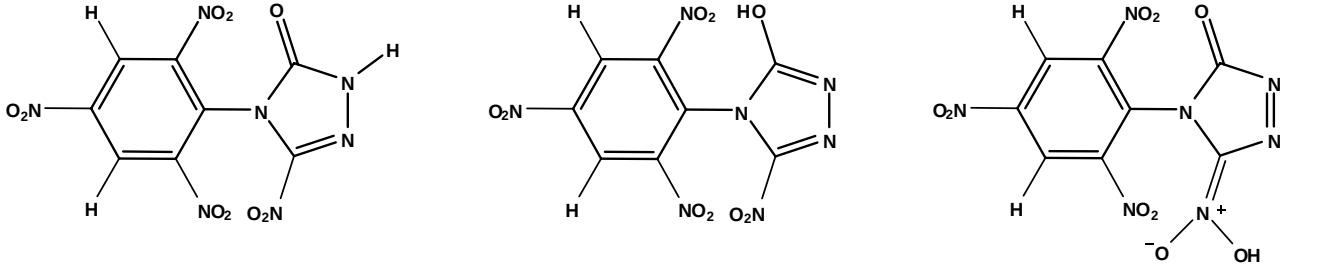

A5 A5–enol–tautomer A5–aci–tautomer

Figure 3.1: The structural formulas of all the considered isomers and tautomers (cont'd).

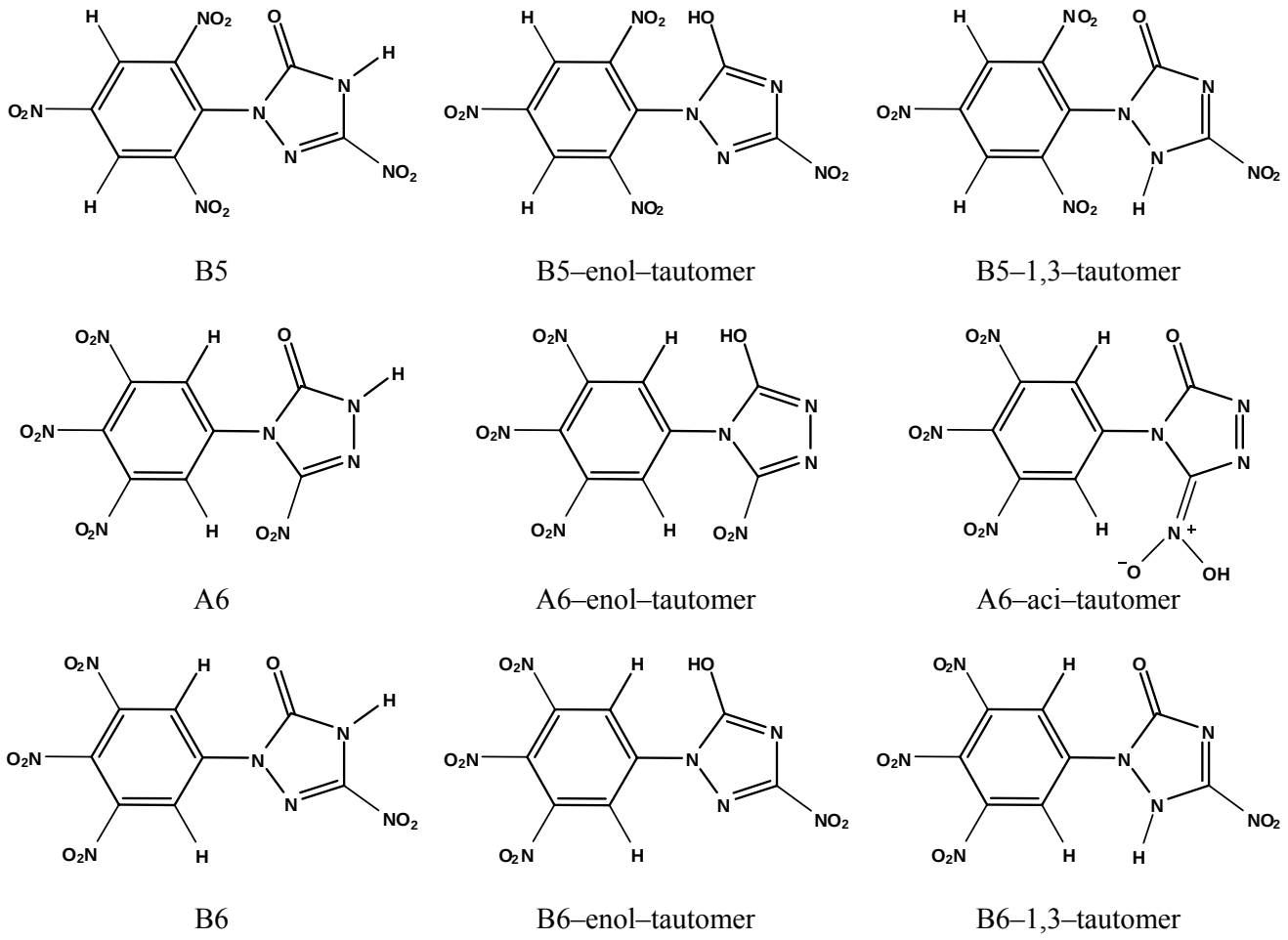

Figure 3.1: The structural formulas of all the considered isomers and tautomers (cont'd).

Table 3.1: The relative ZPE corrected total energies of all the considered isomers and tautomers calculated at B3LYP/6–31G(d,p) theoretical level.

Compound	E_{rel} (kJ/mol)
B5	0
B2	11
A5	12
B4	17
A2	27
A4	34
B3	36
B5–enol–tautomer	44
A3	44
B6	45
A6	45
B2–enol–tautomer	51
B6–enol–tautomer	54
B4–enol–tautomer	61
B3–enol–tautomer	76
A5–enol–tautomer	79
B4–1,3–tautomer	80
B5–1,3–tautomer	80
A2–enol–tautomer	89
B6–1,3–tautomer	91
B2–1,3–tautomer	98
B3–1,3–tautomer	98
A4–enol–tautomer	98
A6–enol–tautomer	107
A3–enol–tautomer	109
A5–aci–tautomer	110
B1–1,3–tautomer	115
A2–aci–tautomer	128
A4–aci–tautomer	131
A6–aci–tautomer	139
A3–aci–tautomer	146
B1	328
A1	341
B1–enol–tautomer	372
A1–enol–tautomer	406
A1–aci–tautomer	441

Table 3.2: The homolytic BDEs of all the considered isomers and tautomers at the theoretical level of UB3LYP/6–31G(d,p). The BDEs written in bold present the trigger bonds of the corresponding structures. Data in parentheses denote the BSSE values in kJ/mol computed at the same theoretical level. BDEs include BSSE and ZPE corrections.

	BDE (kJ/mol)								
Compound	C(5)–NO_2	C(7)–NO_2	C(8)–NO_2	C(9)–NO_2	C(10)–NO_2	C(11)–NO_2	C(3)–OH	N^+–OH	N^+–O^-
A1	227.6 (18.7)	203.7 (22.0)	**188.8** (18.7)	220.8 (17.4)					
A1–enol–tautomer	249.6 (17.7)	211.4 (20.3)	**191.9** (18.4)	219.8 (17.3)			486.8 (17.0)		
A1–aci–tautomer		–86.8 (27.8)	**–101.6** (26.2)	215.5 (17.2)				165.6 (12.6)	794.7 (123.2)
B1	246.9 (14.8)	**192.8** (20.9)	194.5 (18.7)	227.1 (18.4)					
B1–enol–tautomer	256.2 (13.9)	–93.7 (26.3)	**–99.0** (25.7)	212.2 (17.1)			481.2 (18.5)		
B1–1,3–tautomer	223.1 (14.9)	193.6 (19.4)	**176.1** (20.0)	216.6 (17.3)					

Table 3.2: The homolytic BDEs of all the considered isomers and tautomers at the theoretical level of UB3LYP/6–31G(d,p). The BDEs written in bold present the trigger bonds of the corresponding structures. Data in parentheses denote the BSSE values in kJ/mol computed at the same theoretical level. BDEs include BSSE and ZPE corrections (cont'd).

BDE (kJ/mol)									
Compound	C(5)–NO_2	C(7)–NO_2	C(8)–NO_2	C(9)–NO_2	C(10)–NO_2	C(11)–NO_2	C(3)–OH	N^+–OH	N^+–O^-
A2	231.5 (18.5)	**201.7** (19.9)	217.0 (17.2)		251.8 (14.8)				
A2–enol–tautomer	248.8 (18.2)	**205.9** (19.6)	218.3 (17.4)		251.9 (14.8)		487.1 (16.1)		
A2–aci–tautomer		197.1 (20.2)	214.4 (17.3)		251.6 (14.8)			**170.5** (12.7)	1081.7 (118.3)
B2	247.0 (14.8)	**185.0** (20.6)	216.9 (17.2)		251.3 (14.9)				
B2–enol–tautomer	253.8 (13.9)	**187.4** (20.3)	217.0 (17.2)		248.8 (14.9)		473.6 (20.7)		
B2–1,3–tautomer	222.8 (15.1)	**173.9** (20.7)	210.9 (17.1)		250.2 (14.9)				

Table 3.2: The homolytic BDEs of all the considered isomers and tautomers at the theoretical level of UB3LYP/6–31G(d,p). The BDEs written in bold present the trigger bonds of the corresponding structures. Data in parentheses denote the BSSE values in kJ/mol computed at the same theoretical level. BDEs include BSSE and ZPE corrections (cont'd).

	BDE (kJ/mol)								
Compound	C(5)–NO_2	C(7)–NO_2	C(8)–NO_2	C(9)–NO_2	C(10)–NO_2	C(11)–NO_2	C(3)–OH	N^+–OH	N^+–O^-
A3	239.7 (19.4)	**204.5** (19.7)	219.0 (17.0)			232.7 (20.0)			
A3–enol–tautomer	253.4 (19.4)	**202.7** (19.8)	219.5 (17.2)			230.9 (18.2)	484.0 (19.3)		
A3–aci–tautome		204.7 (19.8)	218.7 (17.1)			233.0 (19.1)		**166.2** (17.5)	1067.8 (119.3)
B3	248.8 (14.9)	**196.5** (20.2)	217.5 (17.0)			227.8 (17.5)			
B3–enol–tautomer	255.0 (14.1)	**200.2** (18.7)	218.4 (17.0)			227.2 (17.0)	481.0 (19.6)		
B3–1,3–tautomer	222.6 (15.1)	**205.6** (19.4)	221.2 (16.9)			219.6 (18.6)			

Table 3.2: The homolytic BDEs of all the considered isomers and tautomers at the theoretical level of UB3LYP/6–31G(d,p). The BDEs written in bold present the trigger bonds of the corresponding structures. Data in parentheses denote the BSSE values in kJ/mol computed at the same theoretical level. BDEs include BSSE and ZPE corrections (cont'd).

	BDE (kJ/mol)								
Compound	C(5)–NO_2	C(7)–NO_2	C(8)–NO_2	C(9)–NO_2	C(10)–NO_2	C(11)–NO_2	C(3)–OH	N^+–OH	N^+–O^-
A4	230.1 (18.5)	229.3 (19.2)		216.8 (17.2)	**214.7** (16.5)				
A4–enol–tautomer	249.8 (17.9)	232.3 (18.5)		214.0 (16.9)	**212.8** (16.8)		483.4 (18.7)		
A4–aci–tautomer		228.0 (18.0)		212.1 (16.0)	206.6 (17.0)			**164.3** (17.4)	1070.4 (119.6)
B4	246.4 (14.7)	**212.9** (19.6)		218.1 (16.8)	213.7 (17.1)				
B4–enol–tautomer	253.9 (13.8)	217.2 (16.9)		213.7 (17.0)	**212.9** (16.8)		483.7 (18.7)		
B4–1,3–tautomer	222.2 (14.9)	226.1 (18.9)		219.4 (17.1)	**211.3** (16.4)				

Table 3.2: The homolytic BDEs of all the considered isomers and tautomers at the theoretical level of UB3LYP/6–31G(d,p). The BDEs written in bold present the trigger bonds of the corresponding structures. Data in parentheses denote the BSSE values in kJ/mol computed at the same theoretical level. BDEs include BSSE and ZPE corrections (cont'd).

	BDE (kJ/mol)								
Compound	C(5)–NO_2	C(7)–NO_2	C(8)–NO_2	C(9)–NO_2	C(10)–NO_2	C(11)–NO_2	C(3)–OH	N^+–OH	N^+–O^-
A5	242.3 (19.2)	230.2 (18.9)		250.5 (14.9)		**228.5** (17.1)			
A5–enol–tautomer	255.3 (19.1)	**227.1** (17.4)		250.0 (14.9)		**227.1** (17.4)	484.5 (18.7)		
A5–aci–tautomer		228.9 (18.0)		250.5 (14.9)		222.3 (18.9)		**168.8** (19.6)	1091.0 (107.8)
B5	248.1 (14.9)	**221.5** (19.3)		252.0 (15.0)		222.8 (18.5)			
B5–enol–tautomer	254.3 (13.9)	224.5 (17.8)		249.7 (14.9)		**221.1** (17.3)	487.1 (19.6)		
B5–1,3–tautomer	223.0 (15.0)	**192.5** (17.3)		238.2 (15.0)		214.9 (17.9)			

Table 3.2: The homolytic BDEs of all the considered isomers and tautomers at the theoretical level of UB3LYP/6–31G(d,p). The BDEs written in bold present the trigger bonds of the corresponding structures. Data in parentheses denote the BSSE values in kJ/mol computed at the same theoretical level. BDEs include BSSE and ZPE corrections (cont'd).

	BDE (kJ/mol)								
Compound	C(5)–NO_2	C(7)–NO_2	C(8)–NO_2	C(9)–NO_2	C(10)–NO_2	C(11)–NO_2	C(3)–OH	N^+–OH	N^+–O^-
A6	221.8 (17.0)		226.9 (17.8)	**196.1** (18.3)	227.0 (17.8)				
A6–enol–tautomer	238.4 (16.9)		225.7 (17.7)	**193.8** (18.4)	225.4 (17.6)		482.4 (18.7)		
A6–aci–tautomer			226.6 (17.7)	196.2 (18.4)	225.9 (17.7)			**165.3** (19.7)	1090.7 (110.5)
B6	246.0 (14.5)		224.7 (17.6)	**197.6** (18.3)	225.3 (17.5)				
B6–enol–tautomer	253.2 (13.7)		225.9 (17.8)		**223.5** (17.5)		479.9 (19.9)		
B6–1,3–tautomer	222.7 (14.9)		221.9 (17.6)	**196.6** (18.3)	225.0 (17.7)				
NTO[a] (C–NO_2)	276.00								
TNT (C–NO_2)	(276.10)								
RDX[b] (N–NO_2)	153.80 (152.09)								
HMX[b] (N–NO_2)	166.48								

[a]Value reported in [Türker and Atalar, 2006] at the theoretical level of ROB3P86/6–311G(d,p).
[b]Values reported in [Qiu et al., 2006] at the theoretical level of UB3LYP/6–31G(d,p).
Values in parenthesis are: a theoretical value corrected for ZPE using scaled UHF/6–31G(d) frequencies for RDX and an experimental value for TNT taken from [Harris and Lammertsma, 1997] and [Luo, 2003], respectively.

3.3.3 The Frontier Molecular Orbitals

The HOMO, LUMO, Δε energies ($\Delta\varepsilon = \varepsilon_{LUMO} - \varepsilon_{HOMO}$), Mulliken electronegativities and chemical hardnesses of all the isomers and their tautomers calculated at HF/6–31G(d,p)//B3LYP/6–31G(d,p) theoretical level are shown in Table 3.3 (see section 2.3.3 for related definitions and theoretical information). The values written in bold present the highest values of χ_M and η of the structure which is in a group having the same number of "i". A compound having the largest χ_M in a group appears to be the most electronegative. It is less susceptible to oxidation. The compound having the largest η in a group is kinetically the most stable (the hardest) one.

3.3.4 Detonation Performances

The predicted densities and detonation properties of all Ai– and Bi–type compounds are listed in Table 3.4 (see sections 2.3.4 and 2.3.5 for related definitions and theoretical information). According to the data in table, the lowest D and P values belong to A2–enol–tautomer (8.13 km/s and 29.75 GPa) whereas that of the highest values belong to A1–enol–tautomer (8.79 km/s and 35.80 GPa). In the table, the D and P values written in bold present the highest performance values of the structures having the same number of "i". All of the considered Ai– and Bi–type isomers and tautomers have higher ρ, D and P values than that of NTO and TNT. A1–enol–tautomer with the best detonation performance of all has higher ρ value than that of RDX and HMX. Additionally, it has D and P values higher than RDX but lower than HMX.

Table 3.3: The HOMO, LUMO, Δε energies (Δε = $\varepsilon_{LUMO} - \varepsilon_{HOMO}$), Mulliken electronegativities (χ_M) and chemical hardnesses (η) of all the considered isomers and tautomers calculated at HF/6–31G(d,p)//B3LYP/6–31G(d,p) theoretical level.

	Energy (eV)				
Compound	HOMO	LUMO	Δε	χ_M (eV)	η (eV)
A1	–9.1	–1.4	7.7	5.3	3.9
A1–enol–tautomer	–9.2	–1.5	7.7	5.4	3.9
A1–aci–tautomer	–8.9	–1.3	7.6	5.1	3.8
B1	–8.9	–1.3	7.6	5.1	3.8
B1–enol–tautomer	–9.1	–1.4	7.7	5.3	3.9
B1–1,3–tautomer	–10.9	–0.7	10.2	**5.8**	**5.1**
A2	–11.1	–0.7	10.4	5.9	5.2
A2–enol–tautomer	–11.3	–0.7	10.6	6.0	5.3
A2–aci–tautomer	–10.1	–0.9	9.2	5.5	4.6
B2	–10.8	–0.6	10.2	5.7	5.1
B2–enol–tautomer	–11.3	–0.8	10.5	6.1	5.3
B2–1,3–tautomer	–11.6	–0.9	10.7	**6.3**	**5.4**
A3	–11.0	–0.8	10.2	5.9	5.1
A3–enol–tautomer	–11.0	–1.0	10.0	6.0	5.0
A3–aci–tautomer	–10.0	–0.8	9.2	5.4	4.6
B3	–10.8	–0.6	10.2	5.7	5.1
B3–enol–tautomer	–11.3	–0.9	10.4	6.1	5.2
B3–1,3–tautomer	–11.4	–0.9	10.5	**6.2**	**5.3**
A4	–11.0	–1.0	10.0	6.0	5.0
A4–enol–tautomer	–11.2	–1.1	10.1	6.2	5.1
A4–aci–tautomer	–10.2	–1.0	9.2	5.6	4.6
B4	–10.9	–0.7	10.2	5.8	5.1
B4–enol–tautomer	–11.4	–0.9	10.5	**6.2**	**5.3**
B4–1,3–tautomer	–11.0	–1.2	9.8	6.1	4.9

Table 3.3: The HOMO, LUMO, Δε energies (Δε = $\varepsilon_{LUMO} - \varepsilon_{HOMO}$), Mulliken electronegativities (χ_M) and chemical hardnesses (η) of all the considered isomers and tautomers calculated at HF/6–31G(d,p)//B3LYP/6–31G(d,p) theoretical level (cont'd).

	Energy (eV)				
Compound	HOMO	LUMO	Δε	χ_M (eV)	η (eV)
A5	–11.0	–0.6	10.4	5.8	5.2
A5–enol–tautomer	–11.1	–0.7	10.4	5.9	5.2
A5–aci–tautomer	–10.0	–1.0	9.0	5.5	4.5
B5	–10.9	–0.6	10.3	5.8	5.2
B5–enol–tautomer	–11.4	–0.8	10.6	6.1	5.3
B5–1,3–tautomer	–11.4	–0.7	10.7	**6.1**	**5.4**
A6	–11.1	–0.3	10.8	5.7	5.4
A6–enol–tautomer	–11.4	–0.4	11.0	**5.9**	**5.5**
A6–aci–tautomer	–10.3	–1.4	8.9	5.9	4.5
B6	–10.7	–0.5	10.2	5.6	5.1
B6–enol–tautomer	–11.1	–0.4	10.7	5.8	5.4
B6–1,3–tautomer	–10.9	–0.8	10.1	5.9	5.1

Table 3.4: Predicted densities and detonation properties of all isomers and their tautomers at the theoretical level of B3LYP/6–31G(d,p). Bold written values present the highest detonation performance values of structures having the same "i" number (i = 1 – 6).

Compound	Ω (%)	$\Delta H^{o\,a}_f$ (kJ/mol)	Q (cal/g)	V^b (cm^3/mol)	ρ (g/cm^3)	D (km/s)	P (GPa)
A1	–39.86	593.32	1703.62	177.93	1.92	8.71	34.91
A1–enol–tautomer	–39.86	614.82	1718.68	176.09	1.94	**8.79**	**35.80**
A1–aci–tautomer	–39.86	662.75	1752.26	179.75	1.90	8.71	34.70
B1	–39.86	576.28	1691.68	176.21	1.94	8.75	35.47
B1–enol–tautomer	–39.86	623.77	1724.95	178.60	1.91	8.71	34.87
B1–1,3–tautomer	–39.86	307.07	1503.10	182.34	1.87	8.29	31.23
A2	–39.86	200.43	1428.40	182.31	1.87	8.19	30.45
A2–enol–tautomer	–39.86	232.51	1450.87	185.17	1.84	8.13	29.75
A2–aci–tautomer	–39.86	270.33	1477.36	181.21	1.88	8.30	31.35
B2	–39.86	199.40	1427.68	181.27	1.88	8.22	30.79
B2–enol–tautomer	–39.86	251.39	1464.10	180.60	1.89	8.30	31.42
B2–1,3–tautomer	–39.86	271.18	1477.96	179.87	1.90	**8.34**	**31.82**

Table 3.4: Predicted densities and detonation properties of all isomers and their tautomers at the theoretical level of B3LYP/6–31G(d,p). Bold written values present the highest detonation performance values of structures having the same "i" number (i = 1 – 6) (cont'd).

Compound	Ω (%)	$\Delta H^{o\,a}_f$ (kJ/mol)	Q (cal/g)	V^b (cm^3/mol)	ρ (g/cm^3)	D (km/s)	P (GPa)
A3	–39.86	215.99	1439.30	178.96	1.91	8.31	31.72
A3–enol–tautomer	–39.86	254.98	1466.61	181.94	1.88	8.26	30.98
A3–aci–tautomer	–39.86	286.80	1488.90	177.33	1.92	**8.44**	**32.86**
B3	–39.86	211.72	1436.31	182.39	1.87	8.20	30.51
B3–enol–tautomer	–39.86	264.54	1473.31	181.46	1.88	8.28	31.22
B3–1,3–tautomer	–39.86	278.39	1483.01	181.12	1.88	8.31	31.44
A4	–39.86	209.12	1434.49	176.23	1.94	**8.40**	**32.66**
A4–enol–tautomer	–39.86	233.41	1451.50	183.88	1.86	8.17	30.18
A4–aci–tautomer	–39.86	281.00	1484.84	182.58	1.87	8.26	30.96
B4	–39.86	193.53	1423.57	180.35	1.89	8.25	31.06
B4–enol–tautomer	–39.86	244.84	1459.51	183.71	1.86	8.19	30.31
B4–1,3–tautomer	–39.86	271.16	1477.95	179.63	1.90	8.35	31.91

Table 3.4: Predicted densities and detonation properties of all isomers and their tautomers at the theoretical level of B3LYP/6–31G(d,p). Bold written values present the highest detonation performance values of structures having the same "i" number (i = 1 – 6) (cont'd).

Compound	Ω (%)	$\Delta H^{o\,a}_f$ (kJ/mol)	Q (cal/g)	V^b (cm^3/mol)	ρ (g/cm^3)	D (km/s)	P (GPa)
A5	–39.86	189.04	1420.42	177.68	1.92	**8.33**	**31.97**
A5–enol–tautomer	–39.86	226.38	1446.58	180.10	1.89	8.29	31.40
A5–aci–tautomer	–39.86	271.96	1478.51	182.16	1.87	8.27	31.03
B5	–39.86	181.21	1414.94	182.87	1.87	8.15	30.12
B5–enol–tautomer	–39.86	239.21	1455.56	182.57	1.87	8.22	30.65
B5–1,3–tautomer	–39.86	253.87	1465.84	183.65	1.86	8.20	30.40
A6	–39.86	210.50	1435.45	182.54	1.87	8.19	30.45
A6–enol–tautomer	–39.86	235.52	1452.98	179.57	1.90	8.31	31.66
A6–aci–tautomer	–39.86	287.14	1489.14	180.03	1.90	8.35	31.88
B6	–39.86	198.42	1427.00	183.05	1.86	8.17	30.19
B6–enol–tautomer	–39.86	250.78	1463.67	183.88	1.86	8.19	30.30
B6–1,3–tautomer	–39.86	273.70	1479.73	179.39	1.90	**8.36**	**32.01**

Table 3.4: Predicted densities and detonation properties of all isomers and their tautomers at the theoretical level of B3LYP/6–31G(d,p). Bold written values present the highest detonation performance values of structures having the same "i" number (i = 1 – 6) (cont'd).

Compound	Ω (%)	ΔH^{o}_{f} [a] (kJ/mol)	Q (cal/g)	V[b] (cm^3/mol)	ρ (g/cm^3)	D (km/s)	P (GPa)
NTO[c]	–24.60	35.30	1232.24	75.21	1.73 (1.77)	7.95 (7.94)	27.38
TNT	–73.98				(1.64)	(6.95)	(19.00)
RDX[d]	–21.61	168.90	1597.39	124.92	1.78 (1.81)	8.88 (8.75)	34.75 (34.70)
HMX[d]	–21.61	270.41	1633.88	157.53	1.88 (1.90)	9.28 (9.10)	39.21 (39.30)

[a]Standard heats of formation obtained from the PM3 single point calculations [Akutsu et al., 1991], [Dorsett and White, 2000], [Sikder et al., 2001] over B3LYP/6–31G(d,p) optimized structures.
[b]Average molar volumes from 100 single point calculations at the B3LYP/6–31G(d,p) level [Qiu et al., 2006].
[c]Values reported in [Türker and Atalar, 2006] at the theoretical level of B3LYP/6–31G(d,p) (ΔH^{o}_{f} of NTO was calculated using PM3//B3LYP/6–31G(d,p) method in this reference).
[d]Values reported in [Qiu et al., 2006] at the theoretical level of B3LYP/6–31G(d,p) (ΔH^{o}_{f} of RDX and HMX were calculated using PM3//B3LYP/6–31G(d,p) method in this reference).
Data in parentheses are the experimental values taken from [Meyer et al., 2007] for NTO, [Dong and Zhou, 1989] for TNT, [Lowe–Ma, 1990], [Mader, 1998], [Sikder et al., 2001], [Meyer et al., 2007] for RDX and [Mader, 1998], [Meyer et al., 2007] for HMX.

3.4 CONCLUSION

All of the isomeric and tautomeric compounds derived from two NTO–picryl derivatives (5–nitro–4–picryl–2,4–dihydro–3*H*–1,2,4–triazol–3–one and 5–nitro–2–picryl–2,4–dihydro–3*H*–1,2,4–triazol–3–one) are more sensitive than NTO and TNT whereas most of them are less sensitive than RDX and HMX. All of the structures have higher detonation performances than NTO and TNT. A1–enol–tautomer has the highest detonation performances competing with that of RDX and HMX.

CHAPTER 4

A COMPUTATIONAL VIEW OF PATO AND ITS TAUTOMERS

4.1 INTRODUCTION

Analyses of structures and properties of a large number of energetic materials reveal that the incorporation of a combination of amino and nitro groups into a molecule often leads to improved thermal stability, reduction in sensitivity to shock and impact and enhanced explosive performance because of an increase in mass density. Both intramolecular and intermolecular hydrogen bonding interactions between adjacent amino and nitro groups are thought to be effective in such observations. Some modern triazole–based energetic materials have been designed and synthesized in this manner [Agrawal and Hodgson, 2007].

1,2,4–Triazole and 3–amino–1,2,4–triazole are useful starting materials for synthesis of many 1,2,4–triazole–based explosives. Coburn and Jackson synthesized a number of picryl– and picrylamino–substituted 1,2,4–triazoles that were prepared by considering the appropriate 1,2,4–triazole or amino–1,2,4–triazole with a picryl halide and characterized their structures with infrared and proton nuclear magnetic resonance spectroscopies [Coburn and Jackson, 1968]. Among many similar structures considered in this reference, PATO (3–picrylamino–1,2,4–triazole), which offers a relatively inexpensive, insensitive and thermally stable explosive [Coburn and Jackson, 1968] (Figure 4.1), was first synthesized in which 3–amino–1,2,4–triazole and picryl chloride were dissolved in *N*,*N*–dimethylformamide at a temperature of 100 ^{o}C [Coburn and Jackson, 1968], [Coburn, 1969]. PATO was also synthesized by treating tetryl (*N*–methyl–*N*,2,4,6–tetranitroaniline) with 3–amino–1,2,4–triazole in methanol under reflux with sodium carbonate used as a catalyst [Li et al., 1999].

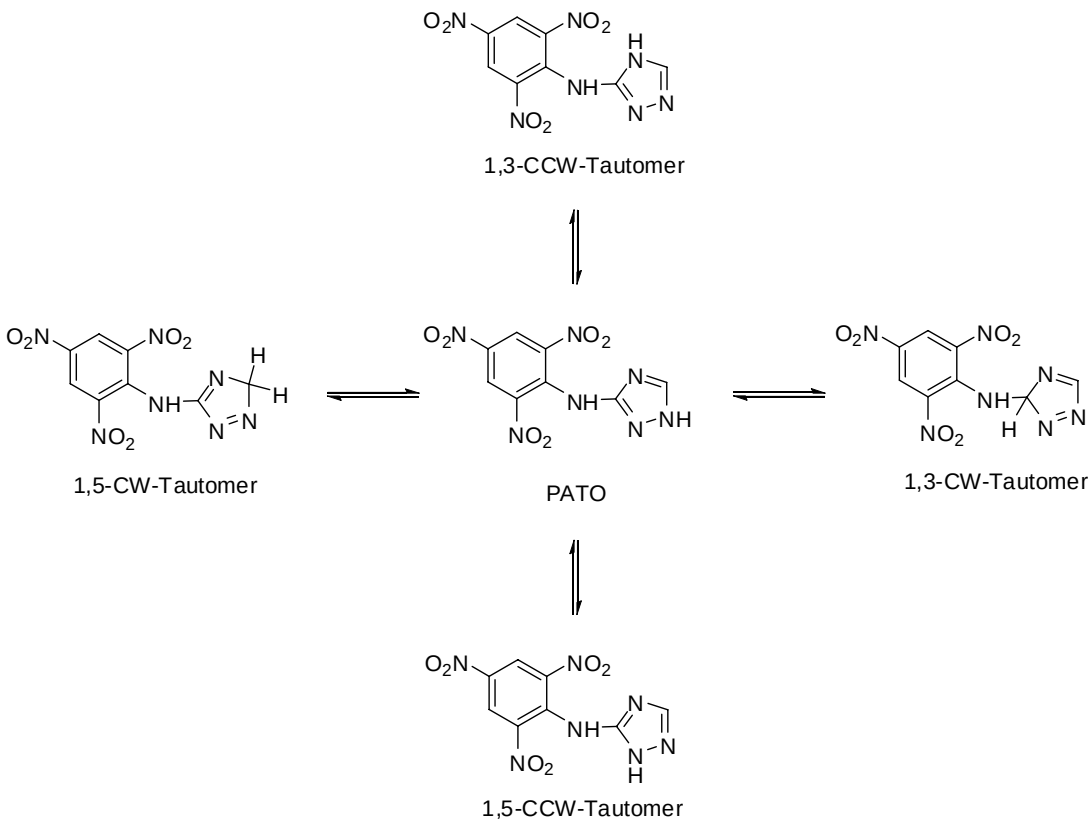

Figure 4.1: Schematic representation of the chemical structures of PATO and its possible clockwise (CW) and counterclockwise (CCW) 1,3– and 1,5– tautomers.

PATO, as an energetic material, creates interest in literature because of its resistance to heat. Differential thermal analyses and pyrolysis studies indicate that it is thermally stable up to 300 ^{o}C [Coburn and Jackson, 1968], [Coburn, 1969], [Coburn et al., 1986]. Its drop weight impact sensitivity (h_{50}) with a 2.5 kg weight is greater than 320 cm [Coburn and Jackson, 1968], [Coburn, 1969], [Coburn et al., 1986], while it is as insensitive as TATB (1,3,5–triamino–2,4,6–trinitrobenzene) ($h_{50\ (TATB)} \geq 320$ cm). Its detonation performance is lower than that of TATB. The detonation velocities (D) of TATB and PATO are 7.99 and 7.44 km/s and their detonation pressures (P) are 31.6 and 24.7 GPa, respectively [Coburn et al., 1986].

The triazole ring of PATO is an aromatic heterocyclic ring that can tautomerize by the shift of electron pair of nitrogen–1 with its hydrogen (see Figure 4.2) in both

clockwise (CW) and counterclockwise (CCW) directions. There are four different tautomers of PATO that are possible, at least theoretically, considering these two different directions. Since the triazole ring is free to rotate, the definition of clockwise or counterclockwise tautomerism is strictly restricted to Figure 4.1. 1,3–tautomerizations yield 1,3–CW and 1,3–CCW tautomers whereas that of 1,5–tautomerizations yield 1,5–CW and 1,5–CCW tautomers (Figure 4.1). In the literature, there has been neither a comprehensive computational analysis of PATO nor its tautomers to the best of our knowledge. In this chapter, we report the electronic and detonation properties of PATO and its tautomers obtained computationally. Atom numberings of PATO and its tautomers are shown in Figure 4.2.

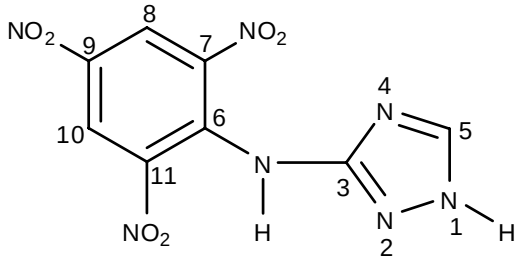

Figure 4.2: Atom numberings of PATO and its tautomers. The representative structure in the figure is PATO.

4.2 THEORETICAL METHODS

The initial structure optimizations leading to energy minima were achieved by using the molecular mechanics (MM2) method followed by semi–empirical PM3 and Hartree–Fock (HF) self–consistent field molecular orbital (SCF–MO) methods [Stewart, 1989a], [Stewart, 1989b], [Leach, 2001] at the restricted level [Fletcher, 1987], [Stewart, 1989a], [Stewart, 1989b], [Leach, 2001]. Then, the final structure optimizations were achieved within the framework of Density Functional Theory (DFT, B3LYP) [Kohn and Sham, 1965], [Parr and Yang, 1989] at the restricted level

[Leach, 2001] of 6–31G(d,p) basis set. Vibrational analyses and the calculation of total electronic energies were performed using B3LYP/6–31G(d,p) theory for closed–shell systems. The normal mode analysis for each compound yielded no imaginary frequencies, confirming its structure is for a local minimum on its potential energy surface. The total electronic energies were corrected for zero point vibrational energies (ZPE).

Aromaticities of the triazole and picryl moieties of the compounds considered here were calculated via Bird aromaticity indexes (% aromaticities) and Nucleus Independent Chemical Shift method, NICS (0) (ppm), within the B3LYP/6–31G(d,p) framework of theory.

For bond dissociation energy (BDE) calculations, the structure optimizations and the single point calculations of all the structures were performed at the UB3LYP/6–31G(d,p) level of theory. It should be noted that the elimination of $–NO_2$ group via homolytic bond cleavage (radical dissociation process) yields open–shell systems. The basis set superposition error (BSSE) analyses for bond dissociations were carried out with the counterpoise method, introduced by Boys and Bernardi [Boys and Bernardi, 1970], at the same level of theory (the BSSE results were taken into account in the calculations of bond dissociation energies in the studies of [Hou et al., 2012], [Wang et al., 2012] and [Wei et al., 2013]).

In order to obtain frontier molecular orbital energies HF/6–31G(d,p)//B3LYP/6–31G(d,p) method was applied. In calculation of heats of formation, isogyric (B3LYP/6–31G(d,p)) and semi–empirical methods (PM3 method based on B3LYP/6–31G(d,p) optimized structures) were used. The molar volume of an isolated gas phase molecule was calculated using a Monte Carlo integration technique (with the space enclosed by the 0.001 au (electrons/bohr^3) contour of the electron density of the molecule). All the computations were performed at 0 K using Gaussian 03 software package [Frisch et al., 2004].

4.3 RESULTS AND DISCUSSION

4.3.1 Relative Total Energies

PATO and its four different tautomers are thermodynamically stable with negative total energies. Most stable of these five structures is PATO with an absolute total energy of –1141.99001 au. The relative total energies of all the compounds calculated at the theoretical level of B3LYP/6–31G(d,p) are compiled in Table 4.1 (the Cartesian coordinates of the optimized structures are presented in APPENDIX B). The relative total energy increases in the order of PATO (0 kJ/mol) < 1,5–CCW–Tautomer (22 kJ/mol) < 1,3–CCW–Tautomer (37 kJ/mol) < 1,5–CW–Tautomer (106 kJ/mol) < 1,3–CW–Tautomer (153 kJ/mol). The CCW tautomers are found to be more stable than the CW tautomers. Additionally, the 1,5– tautomers are more stable than the 1,3– tautomers within the same electron shift direction, CW or CCW, for tautomerism introduced above. This energy ordering shows parallelism with the aromaticity order of the compounds. Picryl rings of all five structures have almost the same aromaticity however that of the heterocyclic triazole rings show differences because of tautomerization (for the methods and results of aromaticity calculation, see the next section). The most aromatic triazole ring belongs to PATO followed by the 1,5–CCW and 1,3–CCW tautomers. The triazole rings of 1,5–CW and 1,3–CW tautomers are not aromatic (see Table 4.4 below).

Table 4.1: The relative total energies of PATO and its tautomers obtained at the theoretical level of B3LYP/6–31G(d,p).

Compound	E_{rel} (kJ/mol)
PATO	0
1,5–CCW–Tautomer	22
1,3–CCW–Tautomer	37
1,5–CW–Tautomer	106
1,3–CW–Tautomer	153
Total energies were corrected for ZPE. The absolute total energy of PATO is –1141.99001 au.	

4.3.2 NICS(0) Calculations and Bird Aromaticity Indexes (I_5 and I_6)

The historical background of aromaticity and further development of its concept were discussed in detail by Balaban [Balaban, 1980]. Schleyer proposed the use of absolute magnetic shielding, computed at ring centers (non–weighted mean of heavy atom coordinates) as a new aromaticity/antiaromaticity criterion, which has gained popularity in recent years [Schleyer et al., 1996]. Specifically, NICS(y) is defined as the negative of Nucleus Independent Chemical Shift (NICS) computed at distance y from the center (in Ångströms). Negative and positive NICS values signify, respectively, aromaticity and antiaromaticity, while nonaromatic cases are characterized by values close to zero.

On the other hand, the Bird aromaticity index [Bird, 1985] is based on the statistical degree of uniformity of the bond orders of the ring periphery. The bond order, N, is calculated from the bond length, R, using Gordy relationship:

$$N = \frac{a}{R^2} + b$$

where the constants a and b change according to the bond type (Table 4.2) [Gordy, 1947].

Table 4.2: Values of a and b used in the calculation of bond orders [Gordy, 1947].

Bond	a	b
C−C	6.80	–1.71
C=C	6.80	–1.71
C−N	6.48	–2.00
C=N	6.48	–2.00
N−N	5.28	–1.41

The coefficient of variation for the bond orders of a particular ring is given by the expression:

$$V = \frac{100}{\overline{N}} \sqrt{\frac{\Sigma(N - \overline{N})^2}{n}}$$

where $\overline{N}$ is the arithmetic mean of the various bond orders, N, whereas n is the number of bonds. In the case of a fully delocalized ring V will have the value 0, whereas for a non–delocalized Kekulé form with alternating single and double bonds the value depends on the type of ring system. For a five–membered ring and for systems consisting of a five–membered and a six–membered ring fused together V_K = 35, while V_K = 33.3 for a six–membered ring (V_K is the value of V for the corresponding non–delocalized Kekulé form with alternating single and double bonds). In order to place the values of V on a more convenient scale than e.g. 0 to 35, the calculated V is substituted into the equation:

$$\text{Aromaticity index:} \qquad I = 100 \times (1 - \frac{V}{V_K})$$

The optimized bond lengths of both triazole and picryl moieties of all five compounds determined at the theoretical level of B3LYP/6–31G(d,p) are presented in Table 4.3 (the computed structure of PATO is not possible to be compared and contrasted with the experimental one since its X–ray crystallographic data are not available in the literature to the best of our knowledge). In Table 4.4, I_5 and I_6 represent the aromaticity indices of the five– and six–membered rings (triazole and picryl rings) of the considered structures, respectively. For a given type of ring, we notice that NICS(0) and the Bird index yield consistent results for aromaticity. NICS(0) aromaticities of the picryl moieties change between (–10.3)–(–10.5) ppm whereas their I_6 indexes are between 79–83 %. Thus, the aromaticities of the picryl rings remain almost the same in all the compounds. By contrast the aromaticity of triazole rings varies with structures. As mentioned above, PATO is characterized by the most aromatic triazole ring (I_5 = 82 %, NICS(0) = –12.9 ppm) followed by its 1,5– and 1,3–CCW tautomers (I_5 = 79 % and 68 %; NICS(0) = –12.5 ppm and –11.6 ppm, respectively). Triazole rings of 1,5–CW–Tautomer and 1,3–CW–Tautomer are

not aromatic (I_5 = 10 % and 0 %; NICS(0) = –2.4 ppm and –1.4 ppm, respectively). The aromaticity orders of all the compounds are consistent with their relative total energy orders as mentioned in the previous section.

Table 4.3: The optimized bond lengths of the triazole and picryl rings at the theoretical level of B3LYP/6–31G(d,p). Bonds 1–5 belong to the triazole ring, 6–11 to the picryl ring of the related compound (see atom numberings in Figure 4.2).

	Bond Length (Å)										
	1–2	2–3	3–4	4–5	5–1	6–7	7–8	8–9	9–10	10–11	11–6
PATO	1.36	1.33	1.36	1.32	1.35	1.44	1.39	1.38	1.39	1.38	1.43
1,3–CW–Tautomer	1.25	1.50	1.45	1.28	1.47	1.44	1.38	1.38	1.39	1.38	1.43
1,3–CCW–Tautomer	1.38	1.31	1.37	1.37	1.31	1.43	1.39	1.38	1.39	1.38	1.43
1,5–CW–Tautomer	1.25	1.45	1.28	1.44	1.48	1.43	1.39	1.38	1.39	1.39	1.43
1,5–CCW–Tautomer	1.36	1.36	1.32	1.36	1.32	1.44	1.39	1.39	1.39	1.38	1.43

Table 4.4: Aromaticities of the triazole and picryl moieties of the considered compounds (ordered in decreasing order of the aromaticities of the triazole rings). I_5 and I_6 (%) represent Bird aromaticity indexes calculated via B3LYP/6–31G(d,p) optimized bond lengths; NICS(0) (ppm) values represent aromaticities at the ring centers calculated at B3LYP/6–31G(d,p) theoretical level.

	Triazole Ring		Picryl Ring	
	I_5 (%)	NICS(0)	I_6 (%)	NICS(0)
PATO	82	–12.9	80	–10.3
1,5–CCW–Tautomer	79	–12.5	81	–10.4
1,3–CCW–Tautomer	68	–11.6	82	–10.4
1,5–CW–Tautomer	10	–2.4	83	–10.5
1,3–CW–Tautomer	0	–1.4	79	–10.3

4.3.3 Bond Dissociation Energies

To gain insight into the relative sensitivities of the compounds considered here, we analyzed the homolytic BDE associated with the removal of a $–NO_2$ moiety from the structures at the UB3LYP/6–31G(d,p) theoretical level (see section 2.3.2 for related definitions and theoretical information). The BSSE analyses were carried out with the counterpoise method, introduced by Boys and Bernardi [Boys and Bernardi, 1970], at the same theoretical level (the BSSE results were taken into account in the calculations of bond dissociation energies in the studies of [Hou et al., 2012], [Wang et al., 2012] and [Wei et al., 2013]).

The results for the homolytic BDE for $R–NO_2$ are compiled in Table 4.5. We notice that $C(11)–NO_2$ bonds can be regarded as trigger linkages in all compounds as their BDE values are the smallest. This indicates that sensitivities of 1,3–CCW and 1,5–CW tautomers are the same and lower than that of PATO; trigger linkage BDEs are 195.5 kJ/mol for these tautomers and 194.3 kJ/mol for PATO. Our results also suggest that 1,3–CW–Tautomer with trigger linkage BDE of 200.9 kJ/mol and 1,5–CCW–Tautomer with 185.3 kJ/mol are, respectively, less and more sensitive than PATO. It is interesting to note that these values are lower than the $C–NO_2$ bond dissociation energy of TATB (354.8 kJ/mol) [Li, 2010]. We thus conclude that PATO and all of its tautomeric structures are likely to be more sensitive than TATB. Additionally, they all are more sensitive than A5 and B5 structures presented in Chapter 2 when their trigger linkage BDEs are compared (Table 4.5).

PATO and its tautomers in Table 4.5 are viable candidates as exploitable high energy density materials according to the suggestions of [Chung et al., 2000] and [Wang et al., 2009] (see section 2.3.2 for more details).

Table 4.5: Homolytic bond dissociation energies (BDEs) of C−NO_2 bonds of PATO and its tautomers calculated at UB3LYP/6–31G(d,p) theoretical level. Data in parentheses denote the BSSE values in kJ/mol computed at the same theoretical level. BDEs include BSSE and ZPE corrections.

	BDE (kJ/mol)		
Compound	C(7)–NO_2	C(9)–NO_2	C(11)–NO_2
PATO	243.2 (17.6)	255.8 (15.3)	**194.3** (18.9)
1,3–CW–Tautomer	241.7 (17.7)	255.1 (15.1)	**200.9** (19.0)
1,3–CCW–Tautomer	245.6 (17.7)	252.8 (15.2)	**195.5** (18.8)
1,5–CW–Tautomer	238.4 (17.6)	250.5 (15.1)	**195.5** (18.9)
1,5–CCW–Tautomer	239.0 (17.7)	251.5 (15.1)	**185.3** (19.3)
A5 (Table 2.3)	230.2 (18.9)	250.5 (14.9)	**228.5** (17.1)
B5 (Table 2.3)	**221.5** (19.3)	252.0 (15.0)	222.8 (18.5)
TATB	354.8[a]		
[a]Value reported at the theoretical level of UB3LYP/6–31G(d,p) [Li, 2010].			

4.3.4 Frontier Molecular Orbitals

The HOMO, LUMO, Δε energies ($\Delta\varepsilon = \varepsilon_{LUMO} - \varepsilon_{HOMO}$), Mulliken electronegativities and chemical hardnesses of all the compounds calculated at HF/6–31G(d,p)//B3LYP/6–31G(d,p) theoretical level are shown in Table 4.6 (see section 2.3.3 for related definitions and theoretical information). The 1,3– and 1,5–CW tautomers are kinetically more stable (harder) (η = 5.1 eV) than PATO (η = 4.9 eV), while the 1,5–CCW–Tautomer (η = 4.8 eV) is less stable than PATO. The hardness of 1,3–CCW–Tautomer is the same as PATO (η = 4.9 eV).

All the tautomeric species have higher χ_M values than PATO ($\chi_{M(PATO)}$ = 4.7 eV) (Table 4.6); i.e., the former are more electronegative (less susceptible to oxidation) than the latter (converse statement holds for reduction). The most resistant species to oxidation is the 1,5–CW–Tautomer (χ_M = 5.3 eV). The inertness to oxidation decreases in the order of 1,3–CW–Tautomer (χ_M = 5.2 eV) > 1,5–CCW–Tautomer (χ_M = 5.1 eV) > 1,3–CCW–Tautomer (χ_M = 5.0 eV). It can be concluded that 1,3– and 1,5–CW tautomers (which are not aromatic) are kinetically more stable and less oxidizable than their more aromatic counterparts.

Table 4.6: HOMO, LUMO, Δε energies (Δε = ε_{LUMO} − ε_{HOMO}), Mulliken electronegativities (χ_M) and chemical hardnesses (η) of PATO and its tautomers calculated at HF/6–31G(d,p)//B3LYP/6–31G(d,p) theoretical level.

Energy (eV)					
Compound	HOMO	LUMO	Δε (eV)	χ_M (eV)	η (eV)
PATO	–9.6	0.2	9.8	4.7	4.9
1,3–CW–Tautomer	–10.2	–0.1	10.1	5.2	5.1
1,3–CCW–Tautomer	–9.8	–0.1	9.7	5.0	4.9
1,5–CW–Tautomer	–10.3	–0.2	10.1	5.3	5.1
1,5–CCW–Tautomer	–9.8	–0.3	9.5	5.1	4.8

4.3.5 Heats of Formation Calculations and Detonation Performances

(See sections 2.3.4 and 2.3.5 for related definitions and theoretical information). The experimental value for the heat of formation of PATO in the gas phase is not available in the literature to the best of our knowledge. The isogyric reaction scheme (Figure 4.3) has been constructed for PATO as the experimental information on heats of formation of reference compounds, trinitrobenzene (TNB) [Politzer et al., 1997], ammonia [Chase, Jr., 1998] and 1,2,4–triazole [Jimenez et al., 1989] is available in the gas phase (standard heat of formation of H_2 is 0 by definition [Silbey and Alberty, 2001]). We note that the ring moieties (picryl and triazole rings) of PATO have been

preserved in the isogyric reaction scheme to avoid large calculation errors involved in decomposition of these structures [Zhang et al., 2002], [Ju et al., 2005].

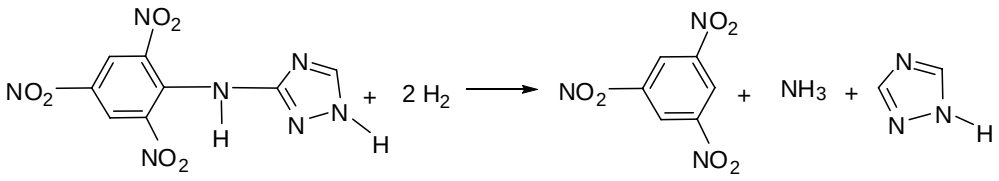

Figure 4.3: The isogyric reaction used to derive the standard heat of formation of PATO.

Table 4.7 presents the computed zero point energy corrected total energies and thermal correction (H_T) of PATO and the reference compounds at the theoretical level of B3LYP/6–31G(d,p). The experimental gas phase heats of formation (ΔH^o_f) of the reference compounds are also shown there. The isogyric ΔH^o_f value of PATO has been found to be 242.2 kJ/mol after calculation.

For the tautomers of PATO, standard heats of formation of the tautomerized 1,2,4–triazole rings are not available experimentally. According to previous studies, ΔH^o_f of an isolated gas phase molecule calculated at the PM3 level can be used in lieu of the experimental data in the evaluation of the detonation velocity (D) and detonation pressure (P) of the energetic compounds because these quantities are sensitive to the density (ρ) but not to ΔH^o_f [Akutsu et al., 1991], [Dorsett and White, 2000], [Sikder et al., 2001]. To test this, the results for Kamlet–Jacobs detonation performances of PATO determined using ΔH^o_f values obtained by isogyric (B3LYP/6–31G(d,p)) and PM3 treatments are compared in Table 4.8. The experimental results for mass density and detonation performance values of PATO [Coburn et al., 1986] are also presented there. Calculated Kamlet–Jacobs detonation performances of PATO using the isogyric and PM3 results for heats of formation are very similar and compare well with the experimental detonation values (Table 4.8). This confirms the earlier

Table 4.7: The zero point energy corrected total energies and values of thermal correction (H_T) of the isogyric reaction compounds at the theoretical level of B3LYP/6–31G(d,p). The last column presents the experimental heats of formation of the reference compounds in the gas phase.

Compound	E_0 + ZPE (au)	H_T (au)	ΔH^o_f(exp) (kJ/mol)
H_2	–1.16837	0.01348	0.0[a]
TNB	–845.63369	0.12070	62.3[b]
NH_3	–56.52334	0.03823	–45.9[c]
1,2,4–Triazole	–242.19587	0.06447	192.7[d]
PATO	–1141.98995	0.18282	

[a][Silbey and Alberty, 2001], [b][Politzer et al., 1997], [c][Chase, Jr., 1998], [d][Jimenez et al., 1989].

Table 4.8: Calculated Kamlet–Jacobs detonation performances of PATO using isogyric (B3LYP/6–31G(d,p)) and PM3 results for heats of formation (ΔH^o_f).

ΔH^o_f(kJ/mol)	Q (cal/g)	V^a (cm^3/mol)	ρ (g/cm^3)	D (km/s)	P (GPa)
242.2[b]	1243.2	166.8	1.8	7.4	24.1
350.3[c]	1330.8	166.8	1.8	7.5	24.9
			(1.82)	(7.44)	(24.7)

[a]Average molar volumes from 100 single point calculations at the B3LYP/6–31G(d,p) theoretical level [Qiu et al., 2006].
[b]Standard heat of formation value obtained from the isogyric reaction (Figure 4.3) at the theoretical level of B3LYP/6–31G(d,p).
[c]Standard heat of formation value obtained from the PM3 single point calculation [Akutsu et al., 1991], [Dorsett and White, 2000], [Sikder et al., 2001] over B3LYP/6–31G(d,p) optimized structure.
Data in parentheses are the experimental values for PATO [Coburn et al., 1986].

observations that PM3 method can replace isogyric method successfully [Akutsu et al., 1991], [Dorsett and White, 2000], [Sikder et al., 2001].

The predicted densities and detonation properties of PATO and its tautomers obtained via Kamlet–Jacobs equations with PM3 ΔH^{o}_{f} values are compiled in Table 4.9. For comparison, the experimental performance values of TATB [Coburn et al., 1986] are also shown there. Except for the 1,5–CCW–Tautomer, all the tautomers have higher D and P values than PATO. Their D values are all 7.6 km/s and P values change between 25.5–25.7 GPa (computed D_{PATO} = 7.5 km/s, P_{PATO} = 24.9 GPa). Because the 1,5–CCW–Tautomer has a lower mass density (1.7 g/cm^3) compared to the others (all 1.8 g/cm^3), it exhibits lower performance (D = 7.4 km/s, P = 23.9 GPa) than PATO and other tautomers. The other point is that TATB with mass density of 1.94 g/cm^3 shows higher detonation performance (D = 7.99 km/s, P = 31.6 GPa) than PATO and all its tautomeric structures. Finally, it can be concluded that detonation performances of the considered novel tautomeric structures lie between that of PATO and TATB (except for the 1,5–CCW–Tautomer).

Table 4.9: Predicted densities and detonation properties of PATO and its tautomers at the theoretical level of B3LYP/6–31G(d,p).

Compound	Ω (%)	ΔH^{o}_{f} [a] (kJ/mol)	Q (cal/g)	V[b] (cm^3/mol)	ρ (g/cm^3)	D (km/s)	P (GPa)
PATO	–67.76	350.3	1330.8	166.8	1.8 (1.82)	7.5 (7.44)	24.9 (24.7)
1,3–CW–Tautomer	–67.76	432.8	1397.6	166.4	1.8	7.6	25.6
1,3–CCW–Tautomer	–67.76	349.3	1330.0	164.1	1.8	7.6	25.7
1,5–CW–Tautomer	–67.76	405.9	1375.8	166.2	1.8	7.6	25.5
1,5–CCW–Tautomer	–67.76	391.0	1363.7	171.4	1.7	7.4	23.9
TATB	–55.78				(1.94)	(7.99)	(31.6)

[a]Standard heats of formation obtained from the PM3 single point calculations [Akutsu et al., 1991], [Dorsett and White, 2000], [Sikder et al., 2001] over B3LYP/6–31G(d,p) optimized structures.
[b]Average molar volumes from 100 single point calculations at the B3LYP/6–31G(d,p) theoretical level [Qiu et al., 2006].
Data in parentheses are the experimental values for PATO and TATB [Coburn et al., 1986].

4.4 CONCLUSION

Present study has revealed that various tautomers of PATO are possible and our analysis here indicates that the thermodynamic stabilities of PATO and its 1,3– and 1,5– tautomers depend mainly on the aromaticities of their triazole rings rather than that of their picryl rings. PATO tautomers which are not aromatic (1,3– and 1,5– CW Tautomers) were found to be kinetically more stable and less susceptible to oxidation than the others. Detonation performances of most of the PATO tautomers (1,5– CCW–Tautomer exception) lie between that of two thermally stable and insensitive explosives, PATO and TATB, the latter one is the best.

P.S. The study presented in this chapter has been published in a SCI journal (Lemi Türker and Çağlar Çelik Bayar. (2012). A Computational View of PATO and its Tautomers. *Zeitschrift für Anorganische und Allgemeine Chemie (ZAAC) (Journal of Inorganic and General Chemistry)*, 638:1316–1322).

CHAPTER 5

COMPUTATIONAL STUDIES OF AROMATIC NITRATION MECHANISMS OF 3–PICRYLAMINO–1,2,4–TRIAZOLE (PATO) AND ITS TAUTOMERS

5.1 INTRODUCTION

It is known that nitration of explosives leads to improved explosive performances such as heats of explosion, detonation velocities and detonation pressures [Agrawal and Hodgson, 2007]. Therefore, in this chapter of the thesis, various nitration mechanisms have been drawn up for PATO and its possible tautomers which have been presented in the previous chapter.

The triazole ring of PATO and those of its tautomers can be nitrated by a nitronium (NO_2^+) cation. In the literature, there has been no comprehensive experimental and computational analyses of their nitration to the best of our knowledge. The only study about PATO nitration is the synthesis of carbon mono–nitrated PATO performed by Li et al. [Li et al., 1991]. In our study, possible nitration positions of triazole rings of PATO and its possible tautomers (carbon and nitrogen mono–nitrations) and their nitration mechanisms have been investigated in the gas phase using the *ab initio* quantum chemistry methods. In all these mechanisms PATO and its tautomers behave like free (uncharged) Lewis bases towards nitronium cation (Lewis acid). In another section, the solution–phase energetics for the most favored mechanism has been briefly analyzed using the reaction field method [Frisch et al., 2009]. Additionally, possible intermediates and nitration products have been analyzed in case of using protonated PATO species as substrates (Lewis bases) in their gas phase. The detonation performances of all possible nitration products have been calculated in the last part of the study.

5.2 METHODS OF CALCULATION

Gas phase nitration mechanisms have been examined using the Linux version of Gaussian 09 program software [Frisch et al., 2009]. The initial structure optimizations leading to energy minima have been achieved by using the molecular mechanics (MM2) method followed by semi–empirical PM3 and Hartree–Fock (HF) self–consistent field molecular orbital (SCF–MO) methods [Stewart, 1989a], [Stewart, 1989b], [Leach, 2001] at the restricted level [Fletcher, 1987], [Stewart, 1989a], [Stewart, 1989b], [Leach, 2001]. Then, the final structure optimizations have been performed within the framework of restricted Hartree–Fock theory in the 6–311++G(d,p) basis set (Differently from the previous chapter, Hartree–Fock method has been used to study the kinetics of the nitration reactions because of the encountered convergence failures in some of the transition states computed at DFT level. To be able to compare all the reaction states as a complete set, Hartree–Fock method with a large basis set (6–311++G(d,p)) has been used for calculations). The normal mode analysis performed using the same basis set for each stationary point has yielded no imaginary frequencies, indicating that it is a local minimum on the potential energy surface. The basis set superposition error (BSSE) analyses for pre–transition states, [Hou et al., 2012], [Wang et al., 2012], [Wei et al., 2013], have been carried out with the counterpoise method, introduced by Boys and Bernardi [Boys and Bernardi, 1970], at the same level of theory. On the other hand, all transition states have had only one imaginary frequency. Furthermore, intrinsic reaction coordinate (IRC) analyses have been performed at the same theoretical level to ensure that the desired reactants and products have been connected to these transition states. The total electronic energies have been corrected for zero point vibrational energies (ZPE). The Gaussian 09 default SCRF method, the polarizable continuum model (PCM) using the integral equation formalism variant (IEFPCM), has been used in the solution phase calculations [Frisch et al., 2009]. The energy calculations of nitration states of protonated PATO species have been performed using HF/6–311++G(d,p) theoretical level. Finally, Kamlet–Jacobs detonation performances of the nitration products have been examined by using two types of calculations: PM3//B3LYP/6–31G(d,p) calculations to obtain their heats of formation and 100 single point calculations at the B3LYP/6–31G(d,p) theoretical level over B3LYP/6–31G(d,p) optimized structures to determine their average molar volumes [Qiu et al.,

2006] (see section 5.3.9 for more detailed information about methodology change in detonation performance calculations).

5.3 RESULTS AND DISCUSSION

5.3.1 Thermodynamic Stabilities of the Starting Molecules

Thermodynamic stabilities of PATO and its tautomers are compiled in terms of their relative total electronic energies in Table 5.1 (HF/6–311++G(d,p) theoretical level). The relative total electronic energy order is similar to that of compiled in Table 4.1 (B3LYP/6–31G(d,p) theoretical level). Additionally, equilibrium constants for the conversion of PATO to its tautomers are shown in Table 5.2.

Table 5.1: Relative total electronic energies of PATO and its tautomers in increasing order (HF/6–311++G(d,p) theoretical level).

	E_{rel} (kJ/mol)
PATO	0
1,5–CCW–Tautomer	9
1,3–CCW–Tautomer	38
1,5–CW–Tautomer	108
1,3–CW–Tautomer	153
Absolute total electronic energy of PATO is –1135.88758 au.	

Table 5.2: Equilibrium constants for the conversion of PATO to its tautomers (HF/6–311++G(d,p) theoretical level).

	ΔG^o (kJ/mol)	K
PATO $\rightleftharpoons$ 1,5–CCW–Tautomer	8	5×10^{-2}
PATO $\rightleftharpoons$ 1,3–CCW–Tautomer	37	3×10^{-7}
PATO $\rightleftharpoons$ 1,5–CW–Tautomer	108	8×10^{-20}
PATO $\rightleftharpoons$ 1,3–CW–Tautomer	152	3×10^{-27}
$\ln K=(-\Delta G^o/RT)$ G^o of PATO is –2982393 kJ/mol.		

Our results show that 1,3– and 1,5–CW tautomers (see Figure 4.1) are much higher in total electronic energies than PATO (Table 5.1); their K values are much lower than other tautomers (Table 5.2). Therefore, we drop 1,3– and 1,5–CW tautomers from our consideration and investigate nitration of only 1,3– and 1,5–CCW tautomers as well as PATO itself in other parts of this chapter.

5.3.2 Atom Numberings

The atom numberings of all the considered structures are shown in Figure 4.2 in the previous chapter. All the structures have tendencies to be nitrated at N(1), N(2) and N(4) nitrogen atoms. Since the triazole rings of PATO and its considered tautomers have sp^2 hybridized carbon atom (C(5)), the nitration is possible from both the upper and lower sides of C=N double bond (Figure 4.2). The upper and lower side C(5)–nitration mechanisms will be referred to as (R)– and (S)– nitrations, respectively. (R)– nitrations produce (R)– reaction states while (S)– nitrations produce (S)–reaction states on the potential energy profiles.

5.3.3 Nitration Mechanisms

The general nitration mechanism can be summarized as follows (Figures 5.1–5.3): the first step is the approach of a nitronium ion to a PATO species. The electrostatic interaction of the ion–dipole type between the two decreases their energy compared to the sum of the total electronic energies of the isolated PATO species and nitronium as they form a pre–transition state. This reaction state is also defined as a precursor complex, is formed as a result of a partial charge transfer between the donor (potentially nitratible molecule) and acceptor (NO_2^+) [Rosokha and Kochi, 2002], [Gwaltney et al., 2003]. As the separation between the nitronium ion and PATO species further decreases a σ–transition state is formed. In the third step, the reaction progresses past the transition state toward an intermediate complex and the system energy decreases accordingly. If the ring aromaticity is destroyed in the intermediate formation, this intermediate is called a Wheland intermediate. It is seen in the carbon mono–nitration reactions of PATO species at C(5) position and is a kind of nitration via π–skeleton (Figures 5.1–5.3). Figure 5.4 shows the representative Wheland intermediate structures of PATO–C(5)–(R) and PATO–C(5)–(S) nitrations. We note that the ring aromaticities are conserved in the intermediate formations of nitrogen mono–nitrations of PATO species (Figures 5.1–5.3) since these nitrations occur via σ–skeletons. The C(N)−NO_2 distance of the transition state is larger than that of the intermediate. The activation energy of the nitration reaction is calculated as the difference between the zero point energy (ZPE) corrected total electronic energies of the transition state and pre–transition state. This mechanism is known as a polar nitration mechanism [de Queiroz et al., 2006]. The intermediate thus formed is then deprotonated by a water molecule to form a nitrated product (see Figure 5.5 for the nitration products of reactions compiled in Figures 5.1–5.3) (the Cartesian coordinates of the optimized structures at HF/6–311++G(d,p) theoretical level are presented in APPENDIX C). Nitration steps are known as the rate determining steps as they have higher activation energies than deprotonation steps. Also note that nitrate (NO_3^-) ions act as counter ions in considered reactions.

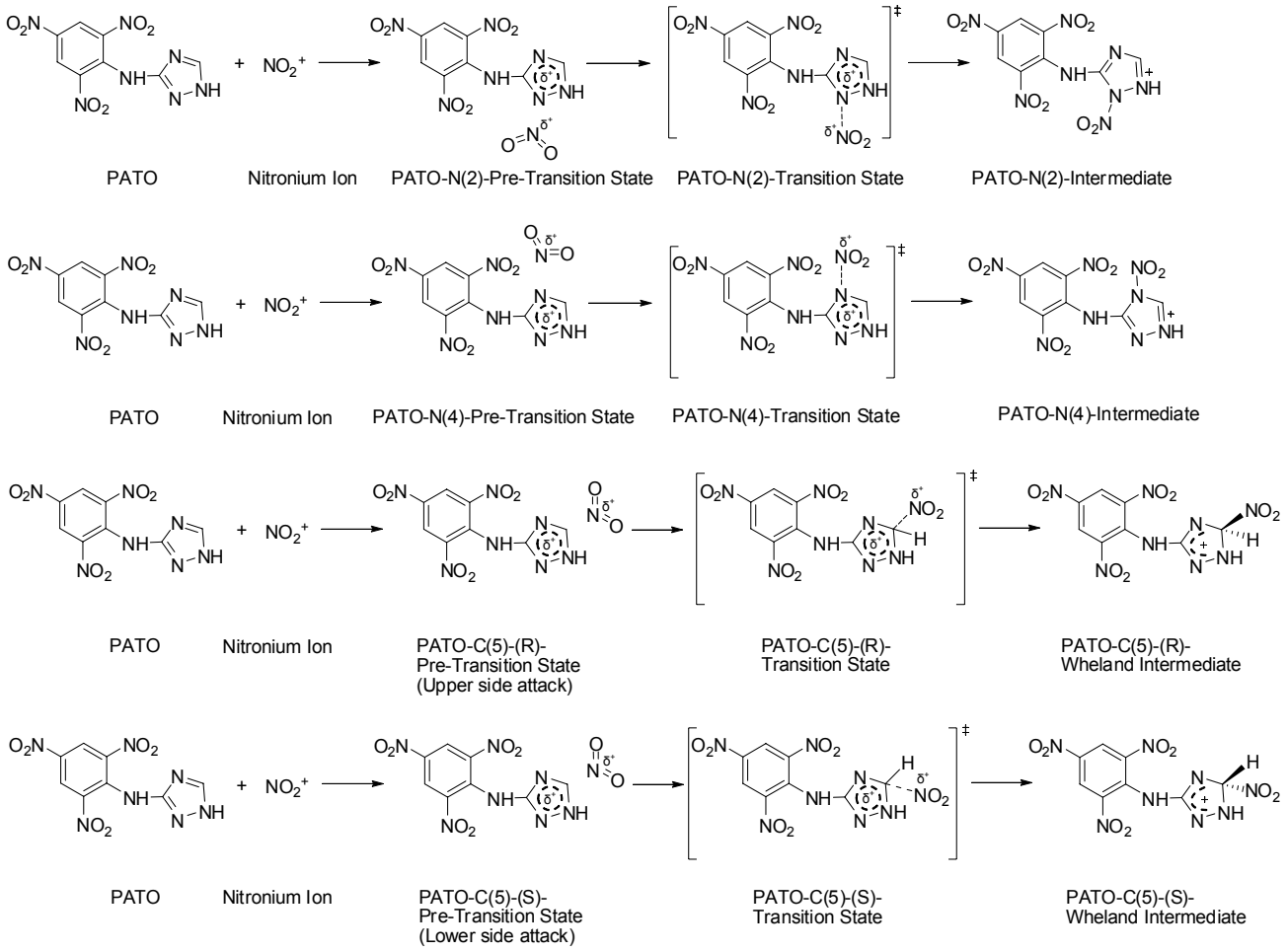

Figure 5.1: The mono–nitration pathways of PATO.

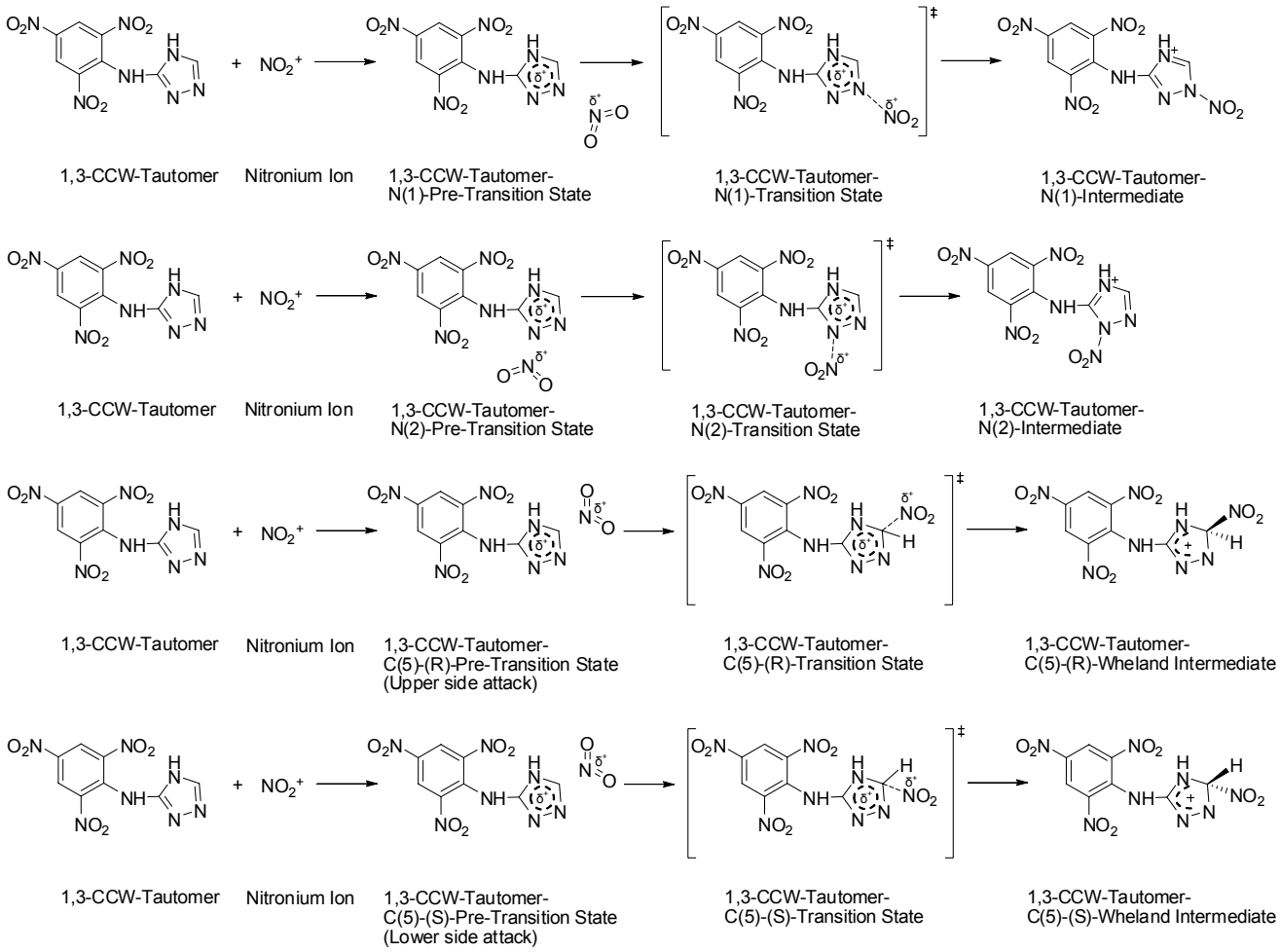

Figure 5.2: The mono–nitration pathways of 1,3–CCW–Tautomer.

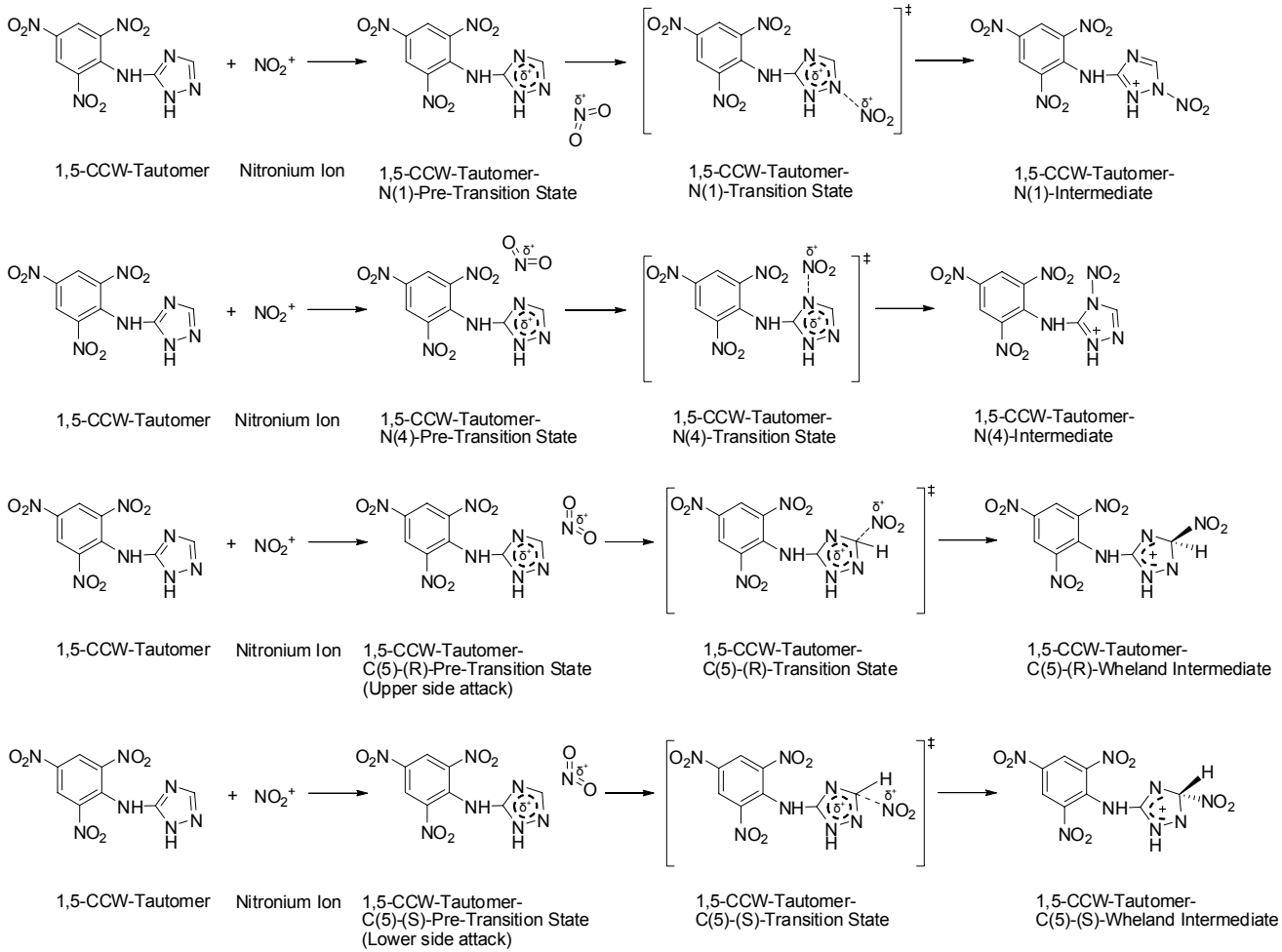

Figure 5.3: The mono–nitration pathways of 1,5–CCW–Tautomer.

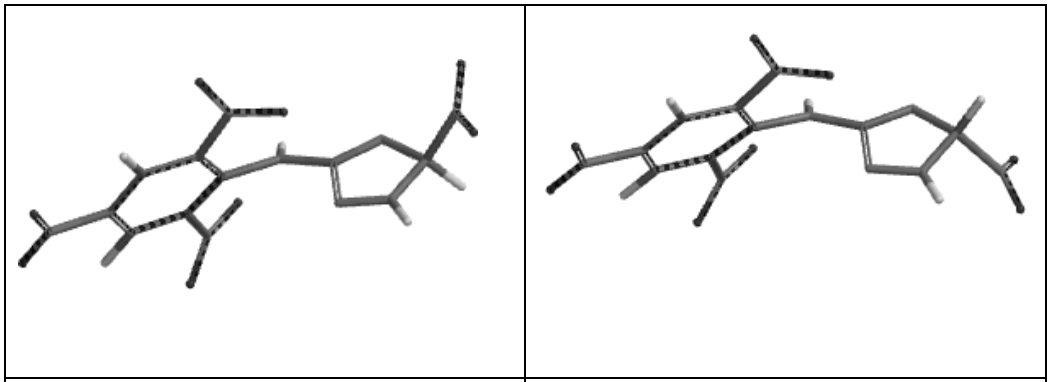

PATO–C(5)–(R)–Wheland Intermediate	PATO–C(5)–(S)–Wheland Intermediate

Figure 5.4: The representative Wheland intermediate structures of PATO–C(5)–(R) and PATO–C(5)–(S) nitrations.

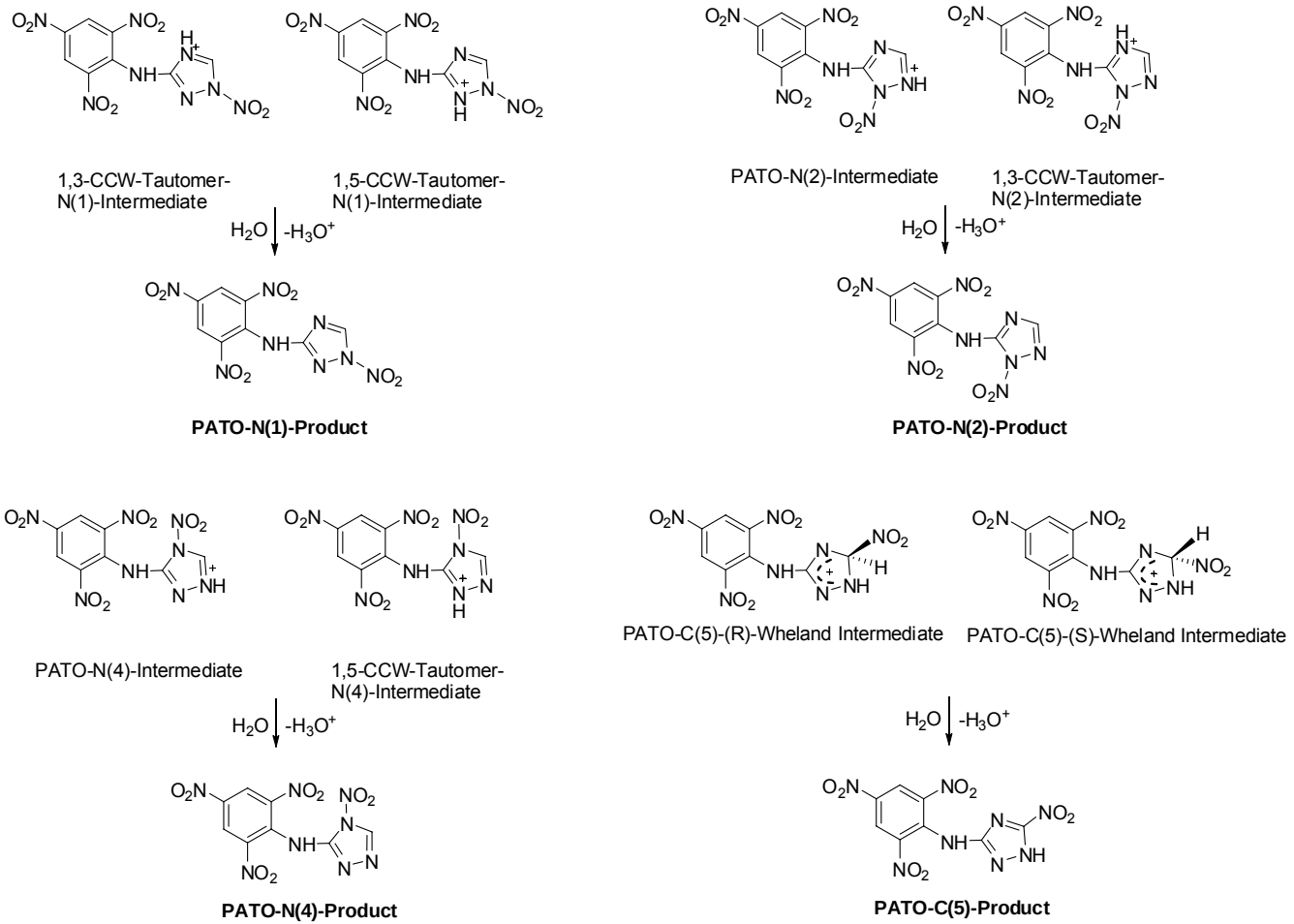

Figure 5.5: Nitration products of the reactions compiled in Figures 5.1–5.3.

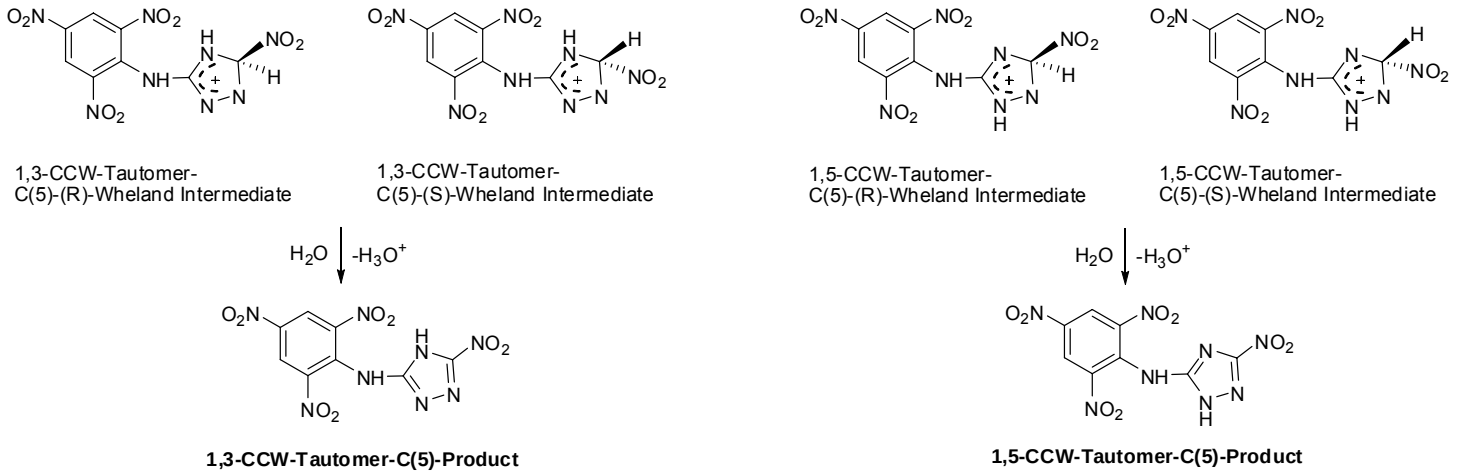

Figure 5.5: Nitration products of the reactions compiled in Figures 5.1–5.3 (cont'd).

If complete electron transfer occurs between the potentially nitratible molecule and nitronium ion prior to the transition state formation as shown in Figure 5.6, then the pre–transition state has a special name of *single electron transfer (SET) complex* [Esteves et al., 2003], [Sokolov, 2004], [de Queiroz et al., 2006]. We note that the SET complex is a biradical [Tanaka et al., 2000] (Figure 5.6). For further discussion see section 5.3.6.

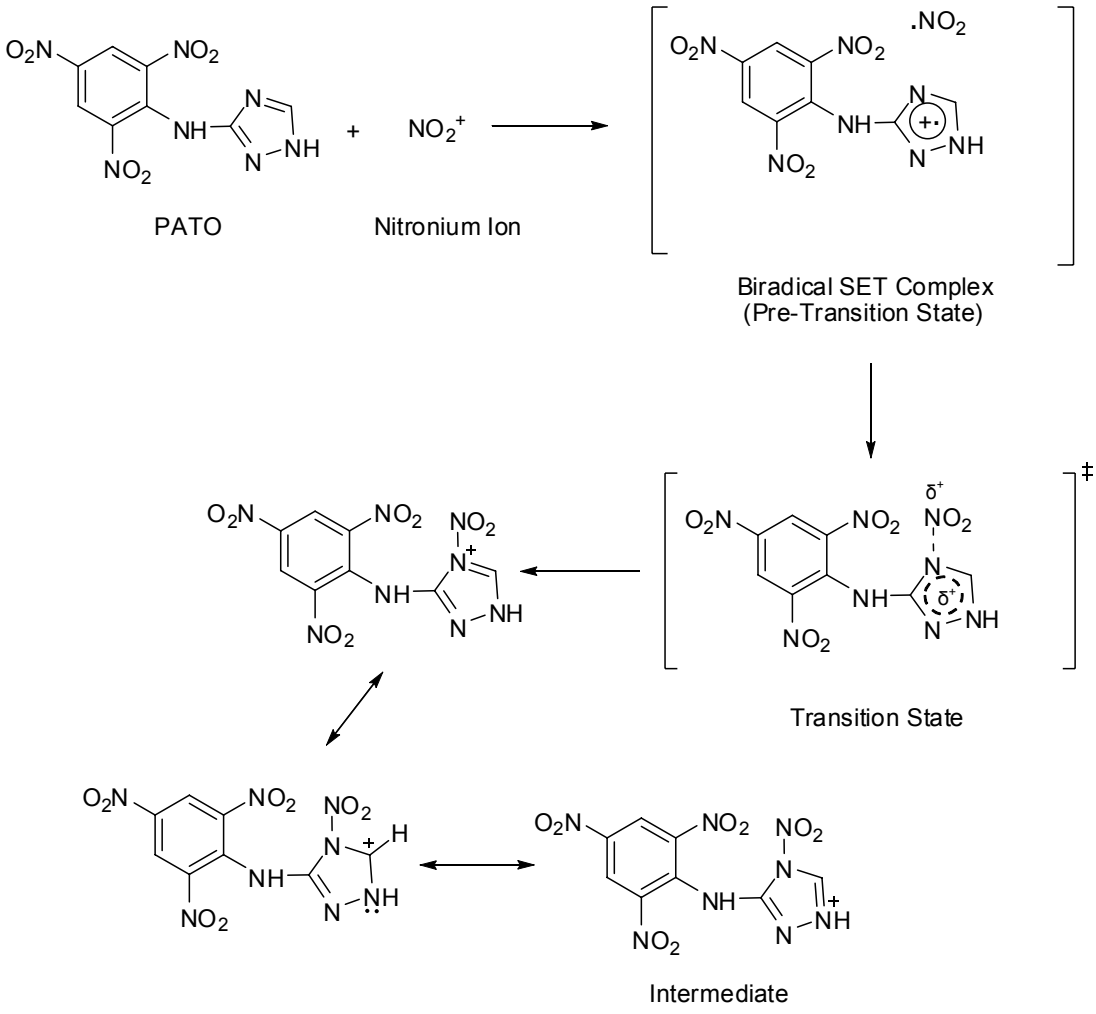

Figure 5.6: Single electron transfer (SET) mono–nitration mechanism of PATO.

5.3.4 C(N)–NO_2 Distances and NO_2 Angles Stand for NO_2 Moieties Involved in Nitration Process

Since we have three different substrates (PATO and its 1,3– and 1,5– CCW tautomers) that can be nitrated and four types of nitrations for each substrate (see Figures 5.1–5.3), a total of twelve different nitration mechanisms are taken into account. Each nitration mechanism has three different reaction states: pre–transition state, transition state and intermediate as mentioned earlier (there is no reaction mechanism having post–transition state). C(N)–NO_2 distances and NO_2 angles stand for NO_2 moieties involved in nitration process are presented in Table 5.3.

5.3.5 Potential Energy Diagrams of Nitration Reactions

The relative total electronic energies of the reaction states of PATO, 1,3–CCW–Tautomer and 1,5–CCW–Tautomer nitration mechanisms with respect to isolated (PATO + NO_2^+) are shown in Tables 5.4, 5.6 and 5.8, respectively. The related energy profiles are presented in Figures 5.7–5.9. All the N(1), N(2) and N(4) nitrations have negative ΔE values whereas the C(5) nitrations have positive ΔE values ($\Delta E = E_{intermediate} - E_{pre-transition\ state}$). For kinetics perspective, *1,3–CCW–Tautomer–N(1)–Nitration* mechanism is the most favored one among all since the population of molecules with enough energy to create a successful collision for its pre–transition state is the highest of all ($\alpha\ e^{78/RT}$; see Tables 5.5, 5.7 and 5.9). The competing nitration mechanism is *PATO–N(4)–Nitration* ($\alpha\ e^{70/RT}$) (Tables 5.5, 5.7 and 5.9).

It can also be concluded that carbon nitrations are much more difficult to perform than nitrogen nitrations (Tables 5.5, 5.7, 5.9 and Figures 5.7–5.9). However, the energy gaps between the pre–transition states of PATO nitration mechanisms are not so large (Figure 5.7), PATO–C(5)–(R/S) nitrations have higher activation energies (182 and 165 kJ/mol, respectively) than the other PATO nitrogen nitration mechanisms (E_a values are below 50 kJ/mol) (Table 5.5 and Figure 5.7). For 1,3–CCW–Tautomer–C(5)–(R/S) nitrations, pre–transition states are more stable and the

reactions have very high activation energies (E_a values are 346 kJ/mol for both) with respect to other 1,3–CCW–Tautomer nitrogen nitrations (E_a values are below 50 kJ/mol) (Table 5.7 and Figure 5.8). For 1,5–CCW–Tautomer–C(5)–(R/S) nitrations, the activation energies are 176 and 184 kJ/mol, respectively (Table 5.9). They also have more stable pre–transition states among the other nitrogen nitration mechanisms (Table 5.9 and Figure 5.9). The most unfavored nitration reactions belong to 1,3–CCW–Tautomer–C(5)–(R/S) mechanisms (compare Tables 5.5, 5.7 and 5.9). The other point is that all the considered C(5)–(R/S) nitrations have more energetic Wheland intermediates with respect to the intermediates of nitrogen nitrations (Figures 5.7–5.9).

Table 5.3: C(N)–NO_2 distances and NO_2 angles stand for NO_2 moieties involved in nitration process (HF/6–311++G(d,p) theoretical level).

	C(N)–NO_2 Distance (d) (Å)	NO_2 Angle (Θ) (Degree)
PATO–N(2)–NITRATION		
Pre–Transition State	2.71*	175.9**
Transition State	1.99	152.0
Intermediate	1.40	130.4
PATO–N(4)–NITRATION		
Pre–Transition State	2.67*	176.1**
Transition State	1.94	151.3
Intermediate	1.42	131.1
PATO–C(5)–(R)–NITRATION		
Pre–Transition State	3.63*	175.7**
Transition State	2.14	146.3
Wheland Intermediate	1.51	129.2
PATO–C(5)–(S)–NITRATION		
Pre–Transition State	5.65*	176.8**
Transition State	2.22	146.6
Wheland Intermediate	1.50	129.0

Table 5.3: C(N)–NO_2 distances and NO_2 angles stand for NO_2 moieties involved in nitration process (HF/6–311++G(d,p) theoretical level) (cont'd).

	C(N)–NO_2 Distance (d) (Å)	NO_2 Angle (Θ) (Degree)
1,3–CCW–TAUTOMER–N(1)–NITRATION		
Pre–Transition State	2.71*	176.9**
Transition State	2.01	155.2
Intermediate	1.43	132.4
1,3–CCW–TAUTOMER–N(2)–NITRATION		
Pre–Transition State	2.60*	176.5**
Transition State	2.02	154.8
Intermediate	1.41	130.5
1,3–CCW–TAUTOMER–C(5)–(R)–NITRATION		
Pre–Transition State	4.23*	105.0**
Transition State	2.51	119.4
Wheland Intermediate	1.52	127.9
1,3–CCW–TAUTOMER–C(5)–(S)–NITRATION		
Pre–Transition State	4.23*	105.0**
Transition State	2.51	119.4
Wheland Intermediate	1.52	127.9

Table 5.3: C(N)–NO_2 distances and NO_2 angles stand for NO_2 moieties involved in nitration process (HF/6–311++G(d,p) theoretical level) (cont'd).

	C(N)–NO_2 Distance (d) (Å)	NO_2 Angle (Θ) (Degree)
1,5–CCW–TAUTOMER–N(1)–NITRATION		
Pre–Transition State	2.51*	174.4**
Transition State	2.02	155.4
Intermediate	1.41	131.5
1,5–CCW–TAUTOMER–N(4)–NITRATION		
Pre–Transition State	2.65*	175.6**
Transition State	1.96	151.4
Intermediate	1.40	130.2
1,5–CCW–TAUTOMER–C(5)–(R)–NITRATION		
Pre–Transition State	2.45*	131.5**
Transition State	1.98	138.4
Wheland Intermediate	1.51	129.2
1,5–CCW–TAUTOMER–C(5)–(S)–NITRATION		
Pre–Transition State	2.45*	131.5**
Transition State	1.97	139.4
Wheland Intermediate	1.51	129.3

*Distance between the non–bonded atoms of pre–transition state.
**Angles between the non–bonded atoms of pre–transition state.

Table 5.4: The relative total electronic energies of the reaction states of PATO nitration mechanisms with respect to isolated (PATO + NO_2^+) (HF/6–311++G(d,p) theoretical level). See the associated graph in Figure 5.7.

	PATO–N(2)–Nitration	PATO–N(4)–Nitration	PATO–C(5)–(R)–Nitration	PATO–C(5)–(S)–Nitration
Pre–Transition State (kJ/mol)	–83 (8)	–116 (7)	–107 (7)	–94 (6)
Transition State (kJ/mol)	–41	–70	75	71
Intermediate (kJ/mol)	–127	–141	–50	–50
The relative total electronic energy of isolated (PATO + NO_2^+) is 0 kJ/mol. The absolute total electronic energy is –1339.61564 au. Data in parentheses denote the BSSE values in kJ/mol calculated at the same theoretical level. Pre–transition state energies include BSSE corrections.				

Table 5.5: Population of molecules with enough energy to create successful collisions for the pre–transition states associated with PATO nitration mechanisms (HF/6–311++G(d,p) theoretical level). See the associated graph in Figure 5.7.

	PATO–N(2)–Nitration	PATO–N(4)–Nitration	PATO–C(5)–(R)–Nitration	PATO–C(5)–(S)–Nitration
Relative Energy of Pre–Transition State (E_i) (kJ/mol)	–83	–116	–107	–94
Boltzmann Distribution of Pre–Transition State ($\alpha\ e^{-Ei/RT}$)	$e^{83/RT}$	$e^{116/RT}$	$e^{107/RT}$	$e^{94/RT}$
Activation Energy (E_a) (kJ/mol)	42	46	182	165
Nitration Rate ($\alpha\ e^{-Ea/RT}$)	$e^{-42/RT}$	$e^{-46/RT}$	$e^{-182/RT}$	$e^{-165/RT}$
Population of Molecules with Enough Energy to Create a Successful Collision $\alpha\ (e^{-Ei/RT})\ (e^{-Ea/RT})$	$e^{41/RT}$	$e^{70/RT}$	$e^{-75/RT}$	$e^{-71/RT}$
The relative total electronic energy of isolated (PATO + NO_2^+) is 0 kJ/mol. The absolute total electronic energy is –1339.61564 au.				

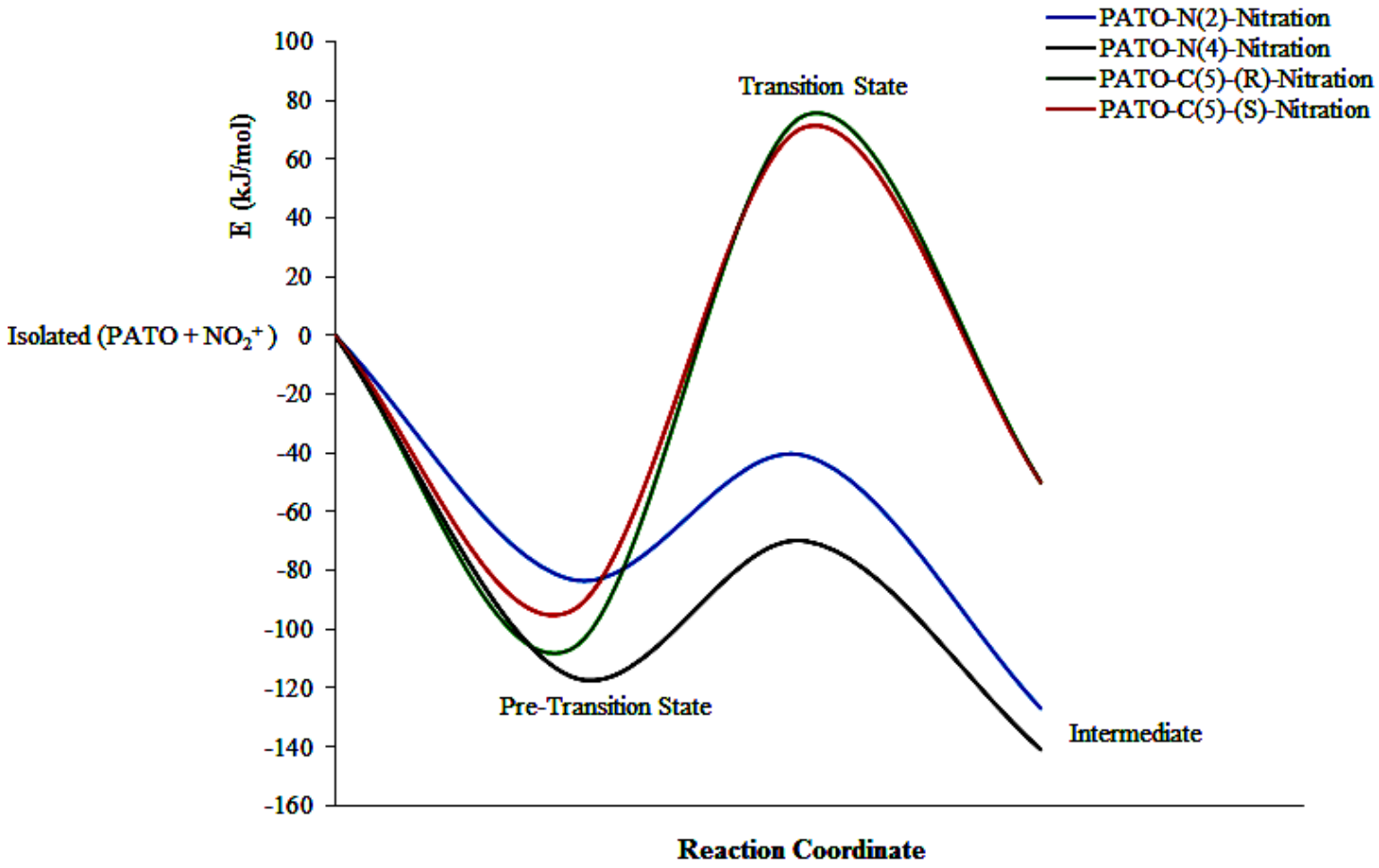

Figure 5.7: Energy profiles of nitration mechanisms of PATO at HF/6–311++G(d,p) theoretical level (The sum of absolute total electronic energies of isolated PATO and NO_2^+ is –1339.61564 au).

Table 5.6: The relative total electronic energies of the reaction states of 1,3–CCW–Tautomer nitration mechanisms with respect to isolated (PATO + NO_2^+) (HF/6–311++G(d,p) theoretical level). See the associated graph in Figure 5.8.

	1,3–CCW–Tautomer–N(1)–Nitration	1,3–CCW–Tautomer–N(2)–Nitration	1,3–CCW–Tautomer–C(5)–(R)–Nitration	1,3–CCW–Tautomer–C(5)–(S)–Nitration
Pre–Transition State (kJ/mol)	–115 (7)	–97 (7)	–187 (15)	–187 (15)
Transition State (kJ/mol)	–78	–49	159	159
Intermediate (kJ/mol)	–146	–140	–100	–100
The relative total electronic energy of isolated (PATO + NO_2^+) is 0 kJ/mol. The absolute total electronic energy is –1339.61564 au. Data in parentheses denote the BSSE values in kJ/mol calculated at the same theoretical level. Pre–transition state energies include BSSE corrections.				

Table 5.7: Population of molecules with enough energy to create successful collisions for the pre–transition states associated with 1,3–CCW–Tautomer nitration mechanisms (HF/6–311++G(d,p) theoretical level). See the associated graph in Figure 5.8.

	1,3–CCW–Tautomer–N(1)–Nitration	1,3–CCW–Tautomer–N(2)–Nitration	1,3–CCW–Tautomer–C(5)–(R)–Nitration	1,3–CCW–Tautomer–C(5)–(S)–Nitration
Relative Energy of Pre–Transition State (E_i) (kJ/mol)	–115	–97	–187	–187
Boltzmann Distribution of Pre–Transition State ($\alpha\, e^{-Ei/RT}$)	$e^{115/RT}$	$e^{97/RT}$	$e^{187/RT}$	$e^{187/RT}$
Activation Energy (E_a) (kJ/mol)	37	48	346	346
Nitration Rate ($\alpha\, e^{-Ea/RT}$)	$e^{-37/RT}$	$e^{-48/RT}$	$e^{-346/RT}$	$e^{-346/RT}$
Population of Molecules with Enough Energy to Create a Successful Collision α ($e^{-Ei/RT}$) ($e^{-Ea/RT}$)	$e^{78/RT}$	$e^{49/RT}$	$e^{-159/RT}$	$e^{-159/RT}$
The relative total electronic energy of isolated (PATO + NO_2^+) is 0 kJ/mol. The absolute total electronic energy is –1339.61564 au.				

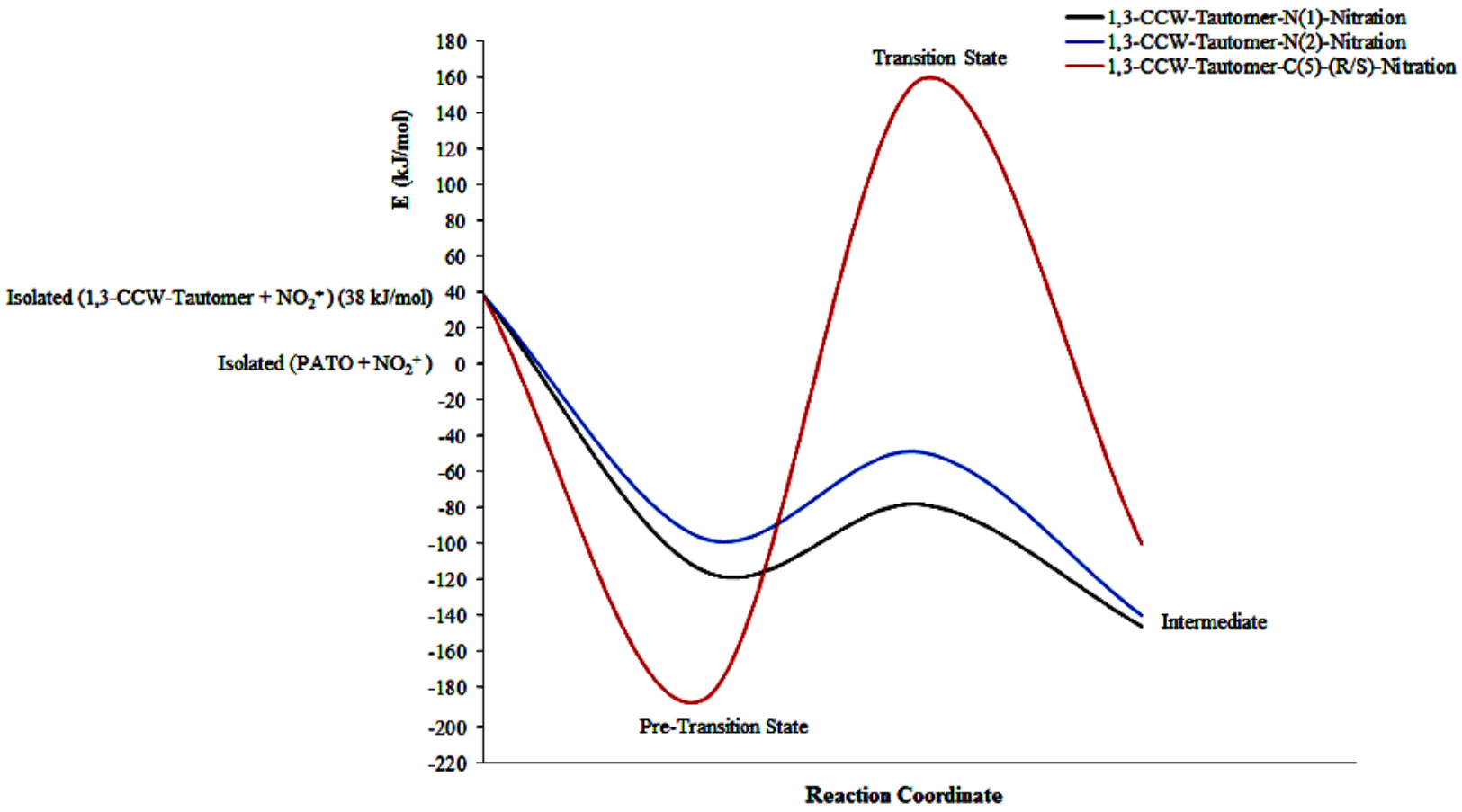

Figure 5.8: Energy profiles of nitration mechanisms of 1,3–CCW–Tautomer at HF/6–311++G(d,p) theoretical level (The sum of absolute total electronic energies of isolated PATO and NO_2^+ is –1339.61564 au).

Table 5.8: The relative total electronic energies of the reaction states of 1,5–CCW–Tautomer nitration mechanisms with respect to isolated (PATO + NO_2^+) (HF/6–311++G(d,p) theoretical level). See the associated graph in Figure 5.9.

	1,5–CCW–Tautomer–N(1)–Nitration	1,5–CCW–Tautomer–N(4)–Nitration	1,5 –CCW–Tautomer–C(5)–(R)–Nitration	1,5–CCW–Tautomer–C(5)–(S)–Nitration
Pre–Transition State (kJ/mol)	–72 (3)	–83 (8)	–155 (13)	–155 (13)
Transition State (kJ/mol)	–56	–40	21	29
Intermediate (kJ/mol)	–142	–137	–46	–38
The relative total electronic energy of isolated (PATO + NO_2^+) is 0 kJ/mol. The absolute total electronic energy is –1339.61564 au. Data in parentheses denote the BSSE values in kJ/mol calculated at the same theoretical level. Pre–transition state energies include BSSE corrections.				

Table 5.9: Population of molecules with enough energy to create successful collisions for the pre–transition states associated with 1,5–CCW–Tautomer nitration mechanisms (HF/6–311++G(d,p) theoretical level). See the associated graph in Figure 5.9.

	1,5–CCW–Tautomer–N(1)–Nitration	1,5–CCW–Tautomer–N(4)–Nitration	1,5 –CCW–Tautomer–C(5)–(R)–Nitration	1,5–CCW–Tautomer–C(5)–(S)–Nitration
Relative Energy of Pre–Transition State (E_i) (kJ/mol)	–72	–83	–155	–155
Boltzmann Distribution of Pre–Transition State ($\alpha\ e^{-Ei/RT}$)	$e^{72/RT}$	$e^{83/RT}$	$e^{155/RT}$	$e^{155/RT}$
Activation Energy (E_a) (kJ/mol)	16	43	176	184
Nitration Rate ($\alpha\ e^{-Ea/RT}$)	$e^{-16/RT}$	$e^{-43/RT}$	$e^{-176/RT}$	$e^{-184/RT}$
Population of Molecules with Enough Energy to Create a Successful Collision $\alpha\ (e^{-Ei/RT})\ (e^{-Ea/RT})$	$e^{56/RT}$	$e^{40/RT}$	$e^{-21/RT}$	$e^{-29/RT}$
The relative total electronic energy of isolated (PATO + NO_2^+) is 0 kJ/mol. The absolute total electronic energy is –1339.61564 au.				

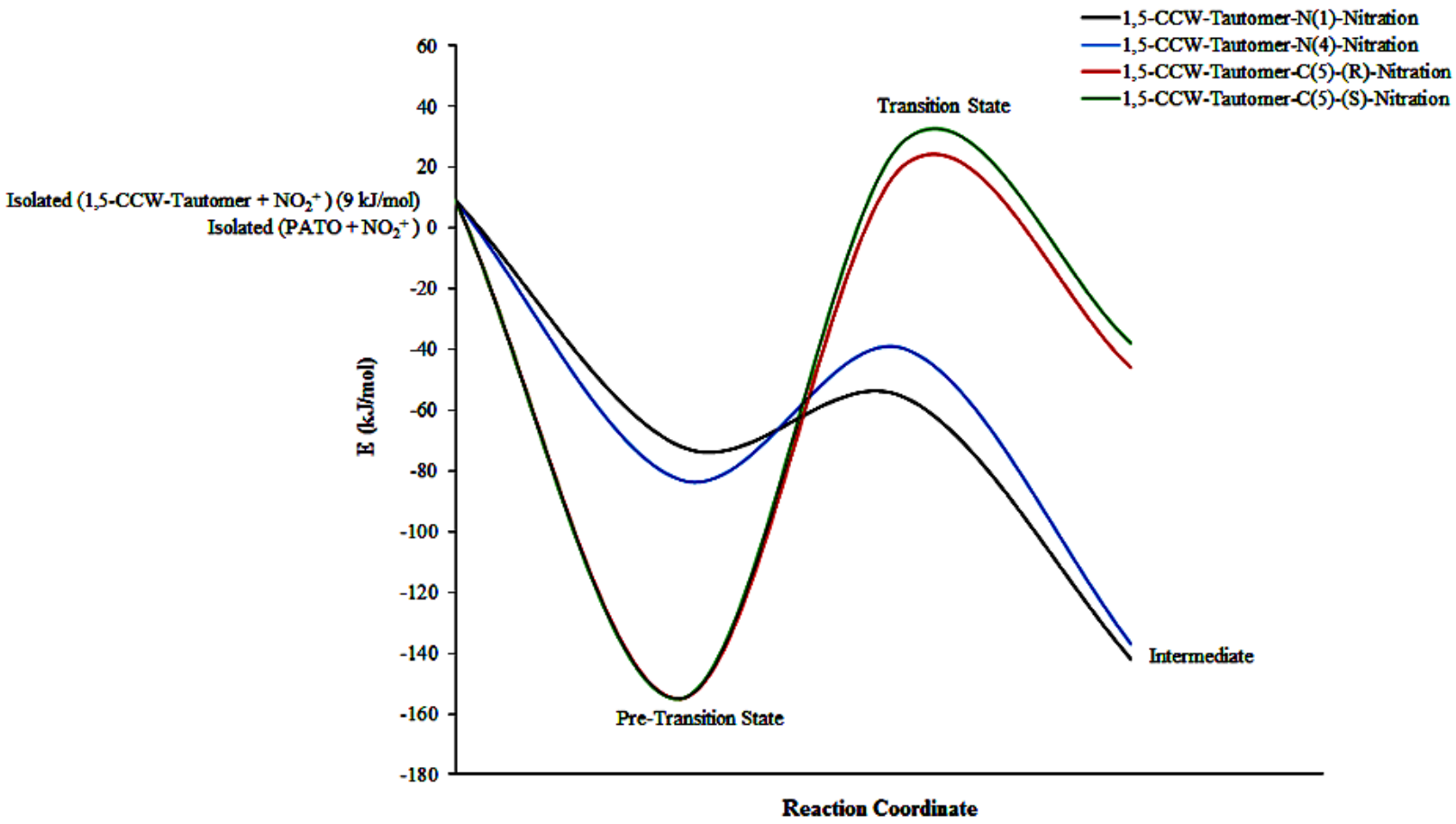

Figure 5.9: Energy profiles of nitration mechanisms of 1,5–CCW–Tautomer at HF/6–311++G(d,p) theoretical level (The sum of absolute total electronic energies of isolated PATO and NO_2^+ is –1339.61564 au).

5.3.6 Discussion of Charge Transfers in Nitration Reactions

In Table 5.10, the NO_2 moiety of the pre–transition state of each nitration pathway is compared with the isolated NO_2 radical and NO_2^+ ion to better understand the reaction mechanism, i.e., the polar versus SET. Specifically, their electrostatic charges (q) calculated via the Chelpg method (Charges from electrostatic potentials using a grid based method) [Frisch et al., 2009] are considered. If the reaction occurs via the polar mechanism, electrostatic charge of the NO_2 moiety will be close to those of isolated NO_2^+ ion, while it is close to those of NO_2 radical in SET mechanism. It was demonstrated that if most of the positive charge is located on the aromatic ring, this supports the formation of a SET complex rather than a π–complex. In the latter, the charge distribution is likely to be separated equally between the donor and acceptor [Esteves et al., 2003].

We have found that 1,3–CCW–Tautomer–C(5)–(R/S) and 1,5–CCW–Tautomer–C(5)–(R/S) nitrations occur via SET mechanisms while other nitrations occur via polar mechanisms. According to the charges presented in Table 5.10, no π–complex has been observed. This suggests that the SET mechanism based on radical states produces a more stable nitration pre–transition state than the polar process. We further note that 1,3–CCW–Tautomer–C(5)–(R/S) pre–transition states are more stable than 1,5–CCW–Tautomer–C(5)–(R/S) pre–transition states. In parallel with this situation, q(NO_2) of 1,3–CCW–Tautomer–C(5)–(R/S) pre–transition states are +0.10e while they are +0.17e and +0.16e in that of 1,5–CCW–Tautomer–C(5)–(R/S) pre–transition states, respectively (Table 5.10). We conclude that radicalic electron transfer takes place stronger in between C(5) position of 1,3–CCW–Tautomer and NO_2^+ couple compared to that of 1,5–CCW–Tautomer and NO_2^+ couple.

Table 5.10: Comparison of the NO_2 moiety of the pre–transition state of each nitration mechanism with isolated NO_2 radical and NO_2^+ ion in terms of electrostatic charges (q) calculated using Chelpg method at HF/6–311++G(d,p) level of theory.

	q (NO_2 moiety) (e)
Isolated NO_2 Radical	0.00
Isolated NO_2^+ ion	+ 1.00
PATO–N(2)–Pre–Transition State	+ 0.92
PATO–N(4)–Pre–Transition State	+ 0.91
PATO–C(5)–(R)–Pre–Transition State	+ 0.90
PATO–C(5)–(S)–Pre–Transition State	+ 0.93
1,3–CCW–Tautomer–N(1)–Pre–Transition State	+ 0.92
1,3–CCW–Tautomer–N(2)–Pre–Transition State	+ 0.92
1,3–CCW– Tautomer–C(5)–(R)–Pre–Transition State	+ 0.10
1,3–CCW– Tautomer–C(5)–(S)–Pre–Transition State	+ 0.10
1,5–CCW–Tautomer–N(1)–Pre–Transition State	+ 0.93
1,5–CCW–Tautomer–N(4)–Pre–Transition State	+ 0.92
1,5–CCW–Tautomer–C(5)–(R)–Pre–Transition State	+ 0.17
1,5–CCW– Tautomer–C(5)–(S)–Pre–Transition State	+ 0.16

5.3.7 Nitrations in Solution Phase

Solution phase single point calculations over the most favored mechanisms' (1,3–CCW–Tautomer–N(1)–Nitration) gas phase nitration states' fixed optimized structures have been performed at the same theoretical level (HF/6–311++G(d,p)) in order to compare the results. Gaussian 09 default SCRF method, the polarizable continuum model (PCM) using the integral equation formalism variant (IEFPCM), has been used in the calculations [Frisch et al., 2009]. Two different solvents of nonionized HNO_3 (I = 0.0; I: ionic strength of the solution) and ionized HNO_3 (I = 0.1) with dielectric constants (ε) of 50 [Addison, 1980], [McQuaid, 2003], [Zhang and Law, 2011] have been taken into account.

Gas and solution phase nitration energy diagrams are compiled in Figure 5.10. Pre–transition states, transition states and intermediates get stabilized from gas phase to ionized HNO_3 phase. The other point is that the activation energy of nitration reaction gets smaller in nonionized and ionized forms of HNO_3 (18 kJ/mol) compared to in gas phase (33 kJ/mol) (Figure 5.10). Nitration is more favored in ionized HNO_3 because of having well stabilized reaction states and lower activation energy.

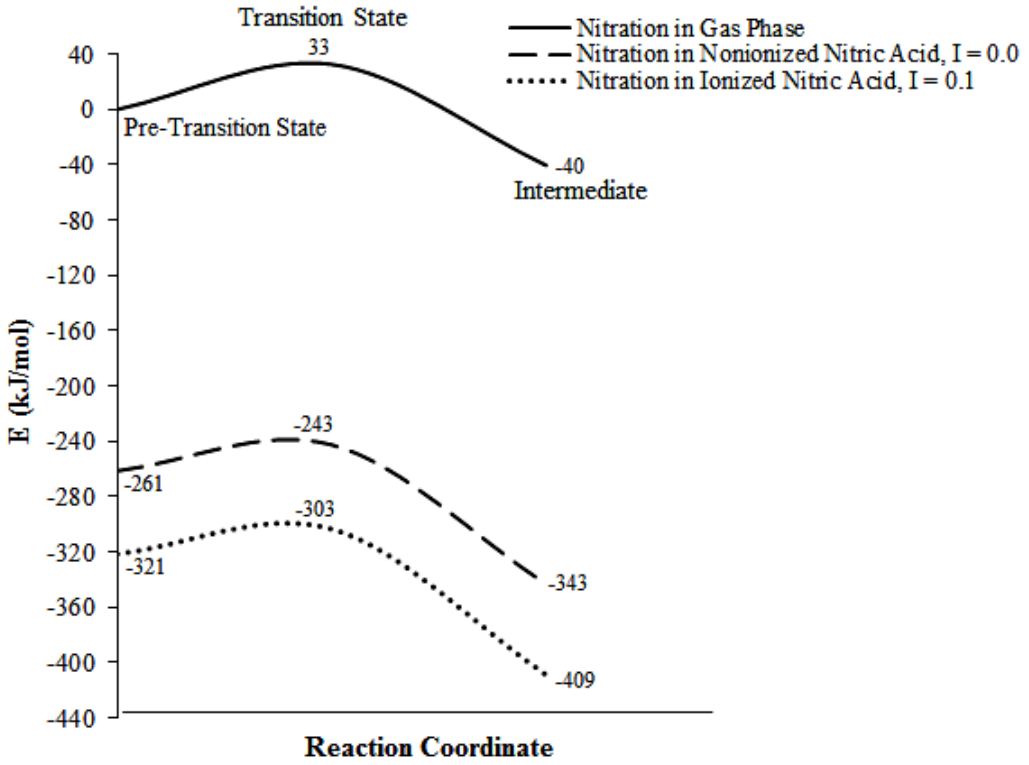

Figure 5.10: Solution phase single point energies performed over the most favored *1,3–CCW–Tautomer–N(1)–Nitration* mechanisms' gas phase nitration states' fixed optimized structures at the theoretical level of HF/6–311++G(d,p). The polarizable continuum model (PCM) using the integral equation formalism variant (IEFPCM) [Frisch et al., 2009] has been used in the calculations.

5.3.8 Nitrations using Protonated PATO Species as Substrates

In this part of the study, possible intermediates and nitration products have been detected in case of using protonated PATO species as substrates (conjugate acid forms of PATO but Lewis bases in nitration) in their gas phase. The chemical structures of the considered protonated PATO species are shown in Figure 5.11. Firstly, the relative total electronic energy orders of these protonated species have been calculated at the theoretical level of HF/6–311++G(d,p) to have an idea about which species are thermodynamically more stable (the Cartesian coordinates of the optimized protonated PATO species at HF/6–311++G(d,p) theoretical level are presented in APPENDIX D). The energy orders have shown that PATO–B and PATO–C species have been the most stable species considered of all (Table 5.11). Note that the energetic PATO–A structure is not aromatic and already out of scope.

Secondly, various nitration mechanisms for PATO–B and PATO–C have been drawn up (Figures 5.12 and 5.13). The relative total electronic energy orders of the intermediates of PATO–B and PATO–C species compiled in Figures 5.12 and 5.13 are shown in Table 5.12 (HF/6–311++G(d,p)). As PATO–B–C(5)–(R/S) and PATO–C–C(5)–(R/S) Wheland intermediates are high in energy (Table 5.12), it makes us think that C(5) nitrations of these protonated species may be unfavored with respect to their (N) nitrations as in the case of free base PATO and its tautomeric mechanisms discussed in the previous sections.

Lastly, the relative total electronic energy orders of nitration products of PATO–B and PATO–C species compiled in Figures 5.12 and 5.13 have been compared (HF/6–311++G(d,p)) (Table 5.13). According to the table C(5) products are the most stable ones (thermodynamic products) as in the case of free base mechanisms.

Finally, we can conclude that the trends of the energetics of the nitration reaction states show parallelisms both in the free base and protonated PATO species nitrations.

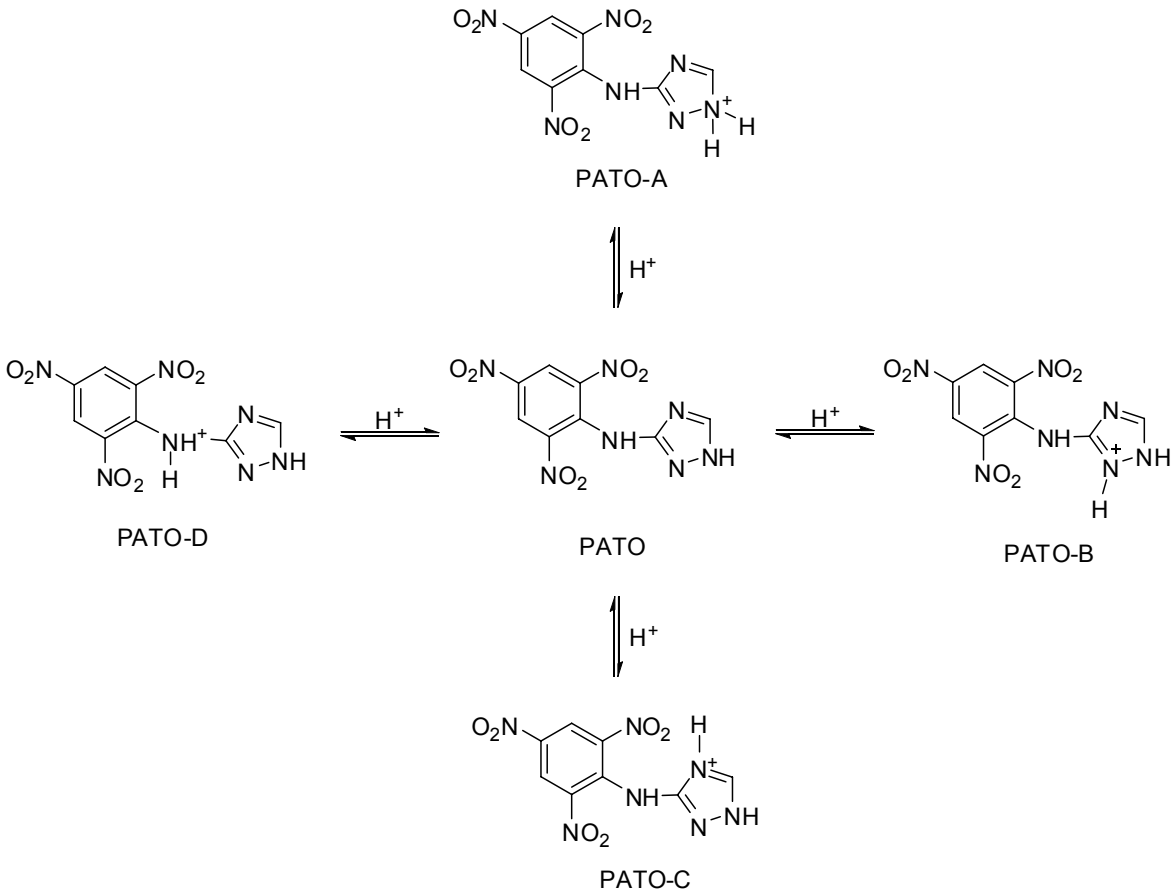

Figure 5.11: The chemical structures of the considered protonated PATO species.

Table 5.11: The relative total electronic energy orders of protonated PATO species at the theoretical level of HF/6–311++G(d,p).

	E_{rel} (kJ/mol)
PATO–C	0
PATO–B	20
PATO–D	99
PATO–A	147
The absolute total electronic energy of PATO–C is –1136.22077 au.	

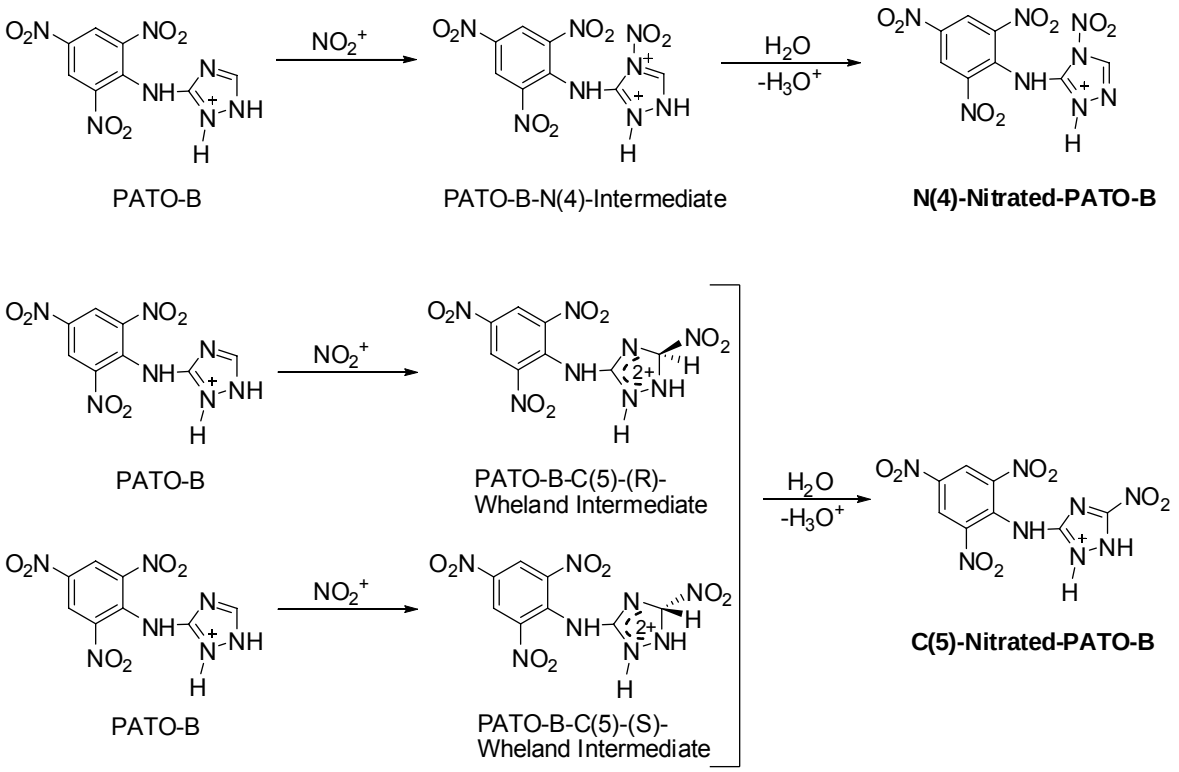

Figure 5.12: Various nitration mechanisms for PATO–B.

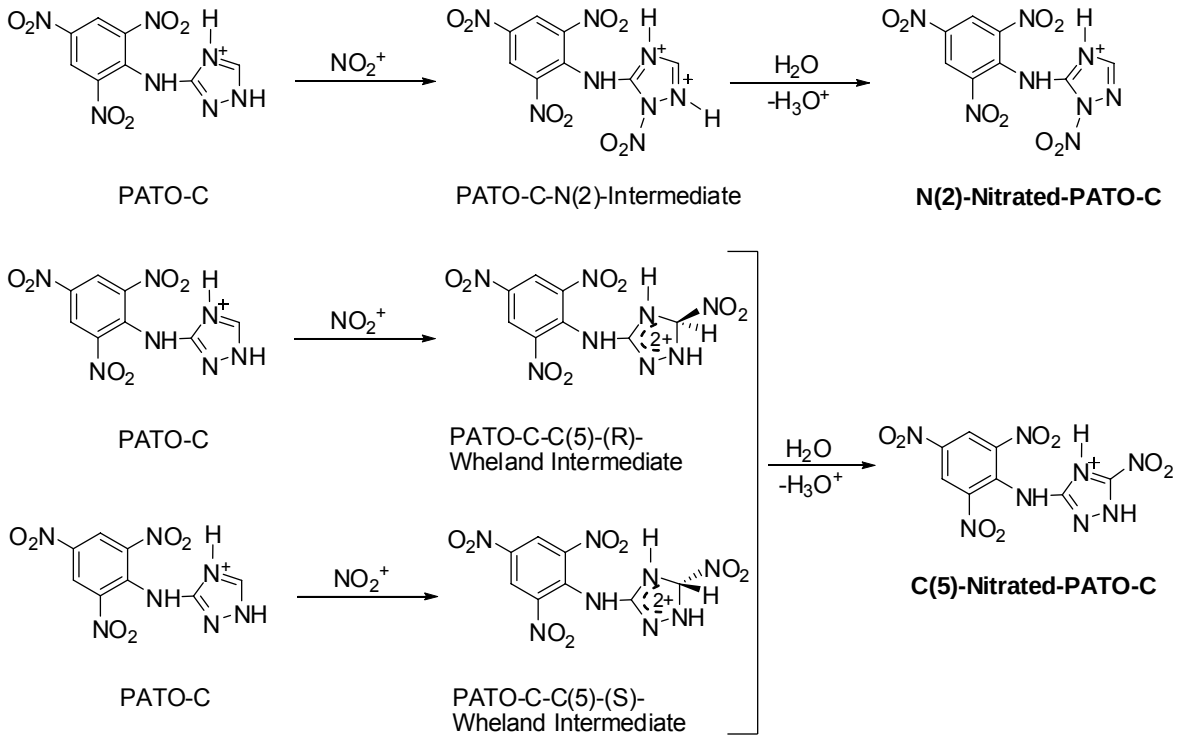

Figure 5.13: Various nitration mechanisms for PATO–C.

Table 5.12: The relative total electronic energy orders of intermediates of PATO–B and PATO–C species compiled in Figures 5.12 and 5.13 (HF/6–311++G(d,p)).

	E_{rel} (kJ/mol)
Isolated (PATO–C + NO_2^+)	0
Isolated (PATO–B + NO_2^+)	20
PATO–C–N(2)–Intermediate	297
PATO–C–C(5)–(R)–Wheland Intermediate	461
PATO–C–C(5)–(S)–Wheland Intermediate	467
PATO–B–N(4)–Intermediate	310
PATO–B–C(5)–(S)–Wheland Intermediate	445
PATO–B–C(5)–(R)–Wheland Intermediate	509
The absolute total electronic energy of isolated (PATO–C + NO_2^+) is –1339.94883 au.	

Table 5.13: The relative total electronic energy orders of nitration products of PATO–B and PATO–C species compiled in Figures 5.12 and 5.13 (HF/6–311++G(d,p)).

	E_{rel} (kJ/mol)
C(5)–Nitrated–PATO–C	0
N(2)–Nitrated–PATO–C	121
C(5)–Nitrated–PATO–B	5
N(4)–Nitrated–PATO–B	51
The absolute total electronic energy of C(5)–Nitrated–PATO–C is –1339.69448 au.	

5.3.9 Thermodynamic Stabilities and Detonation Performances of the Nitration Products

The relative total electronic energy orders of nitration products presented in Figure 5.5 are shown in Table 5.14. However C(5) nitrations have energetic transition states to Wheland intermediates and are kinetically difficult to perform (Figures 5.7–5.9), they produce less energetic (thermodynamic) products (Figure 5.5 and Table 5.14). On the other hand N(1), N(2) and N(4) nitrations have less energetic transition states to intermediates and are kinetically more favored. They produce more energetic (kinetic) products (Figure 5.5 and Table 5.14).

Table 5.14: The relative total electronic energy orders of nitration products presented in Figure 5.5 (HF/6–311++G(d,p)).

	E_{rel} (kJ/mol)
PATO–C(5)–Product	0
1,5–CCW–Tautomer–C(5)–Product	0.5
1,3–CCW–Tautomer–C(5)–Product	28
PATO–N(1)–Product	70
PATO–N(2)–Product	77
PATO–N(4)–Product	115
The absolute total electronic energy of PATO–C(5)–Product is –1339.38998 au.	

As DFT optimized structures and related molar volumes have been used in order to find out the detonation parameters of unnitrated PATO species in the previous chapter, the same methodology has been used for that of nitrated PATO species. This provides us to do comparison between their detonation properties. The other point is that detonation performances estimated with DFT method correlate well with the experimental data as mentioned in the previous chapters. The Cartesian coordinates

of the optimized nitrated PATO species at B3LYP/6–31G(d,p) theoretical level are presented in APPENDIX E.

According to the previous studies, ΔH^{o}_{f} in the gas phase calculated at the PM3 level can be used in lieu of the experimental data in evaluation of the detonation velocity (D) and the detonation pressure (P) of the energetic compounds because these quantities are sensitive to the density (ρ) but not to ΔH^{o}_{f} [Akutsu et al., 1991], [Dorsett and White, 2000], [Sikder et al., 2001] (see sections 2.3.5 and 4.3.5 for more details and discussions). Hence, PM3 single point calculations performed over B3LYP/6–31G(d,p) optimized structures have been used in the calculations. The predicted densities and Kamlet–Jacobs detonation properties of unnitrated and nitrated PATO species are compiled in Table 5.15. In the table, data in parentheses are the experimental values taken from [Coburn et al., 1986], [Türker and Çelik Bayar, 2012] for TATB and unnitrated PATO and from [Li et al., 1991] for PATO–C(5)–Product.

The oxygen balances (deficiencies) of PATO and its tautomeric species are reduced in their nitrated forms. Nitration increases the densities of some of the products a little bit (1.9 g/cm^3) while some of them stay unchanged (1.8 g/cm^3). The enhancement in the detonation performances (D and P) of nitrated products compared to their unnitrated forms mainly arise from the increase in their Q values. The detonation velocities (D) of all nitrated PATO species have been found to be between 8.1 – 8.3 km/s and higher than that of their unnitrated forms (7.4 – 7.6 km/s) and TATB (7.99 km/s). The detonation pressures (P) of nitrated species change between 28.9 – 31.1 GPa which are higher than that of their unnitrated forms (23.9 – 25.7 GPa), however lower than that of TATB (31.6 GPa). Overall, nitration reactions have provided enhanced detonation performances competing with TATB.

Table 5.15: The predicted densities and Kamlet–Jacobs detonation properties of unnitrated and nitrated PATO species.

Compound	Ω (%)	ΔH^{o}_{f} [a] (kJ/mol)	Q (cal/g)	V [b] (cm^3/mol)	ρ (g/cm^3)	D (km/s)	P (GPa)
UNNITRATED PATO SPECIES							
PATO	–68	350.3	1330.8	166.8	1.8 (1.82)	7.5 (7.44)	24.9 (24.7)
1,3–CCW–Tautomer	–68	349.3	1330.0	164.1	1.8	7.6	25.7
1,5–CCW–Tautomer	–68	391.0	1363.7	171.4	1.7	7.4	23.9
NITRATED PATO SPECIES							
PATO–N(1)–Product	–47	457.2	1490.5	188.6	1.8	8.1	28.9
PATO–N(2)–Product	–47	474.9	1502.9	182.2	1.9	8.3	31.1
PATO–N(4)–Product	–47	456.2	1489.8	184.7	1.8	8.2	30.1
PATO–C(5)–Product	–47	368.3	1428.1	185.6	1.8 (1.9)	8.1 (8.1)	29.2 (30.4)
1,3–CCW–Tautomer–C(5)–Product	–47	359.6	1421.9	183.1	1.9	8.1	29.9
1,5–CCW–Tautomer–C(5)–Product	–47	379.7	1436.0	183.7	1.9	8.1	29.9
TATB	–56				(1.94)	(7.99)	(31.6)

Ω (%): Oxygen Balance.

[a]Standard heats of formation obtained from the PM3 single point calculations [Akutsu et al., 1991], [Dorsett and White, 2000], [Sikder et al., 2001] over B3LYP/6–31G(d,p) optimized structures.

[b]Average molar volumes from 100 single point calculations at the B3LYP/6–31G(d,p) theoretical level over B3LYP/6–31G(d,p) optimized structures [Qiu et al., 2006].

Data in parentheses are the experimental values taken from [Coburn et al., 1986], [Türker and Çelik Bayar, 2012] for TATB and unnitrated PATO and from [Li et al., 1991] for PATO–C(5)–Product.

5.4 CONCLUSION

In general, it has been found that gas phase nitrogen nitrations of PATO and its 1,3–CCW– and 1,5–CCW– tautomers are kinetically more favored than their carbon nitrations. *1,3–CCW–Tautomer–N(1)–Nitration* mechanism is kinetically the most favored among all the reaction pathways we studied. The other competing nitration mechanism is *PATO–N(4)–Nitration*. The unfavored C(5)–(R/S) nitrations of all the considered species produce more energetic transition states to the intermediates with respect to that of favored nitrogen nitrations.

1,3–CCW–Tautomer– and 1,5–CCW–Tautomer–C(5)–(R/S) nitration processes show strong single electron transfer (SET) mechanistic character while those of other species proceed via polar mechanisms in terms of charge transfer between the nitratible substrate and nitrating NO_2^+ ion.

The solvation effect on the most favored gas phase mechanism, *1,3–CCW–Tautomer–N(1)–Nitration*, is also observed in the most common nitrating solvent, HNO_3. The results show that nitration is more favored in ionized HNO_3 with ionic strength (I) of 0.1 relative to gas phase and nonionized case because of having well stabilized reaction states and lower activation energy.

It is concluded that nitration reactions can be performed using protonated PATO species as well. The trend of their reaction state energies show parallelisms with that of free base PATO and its tautomeric nitration mechanisms.

Kamlet–Jacobs detonation performances of all the nitrated forms of PATO and its tautomeric species are found to be higher than that of their unnitrated forms and very close to that of TATB (1,3,5–triamino–2,4,6–trinitrobenzene).

P.S. This chapter has been constructed by the help of the collaborative study performed between the Middle East Technical University and Carnegie Mellon University (under the supervisions of Prof. Dr. Lemi Türker and Prof. Dr. Hyung J. Kim) and submitted as a journal article.

CHAPTER 6

CONCLUSIONS

Thirty six isomeric and tautomeric compounds derived from two NTO–picryl derivatives (5–nitro–4–picryl–2,4–dihydro–3*H*–1,2,4–triazol–3–one and 5–nitro–2–picryl–2,4–dihydro–3*H*–1,2,4–triazol–3–one) are all more sensitive than NTO and TNT whereas most of them are less sensitive than RDX and HMX. All of the structures have higher detonation performances than NTO and TNT. A1–enol–tautomer has the highest detonation performances competing with that of RDX and HMX.

Various tautomers of PATO are possible and our analyses indicate that the thermodynamic stabilities of PATO and its 1,3– and 1,5– tautomers mainly depend on the aromaticities of their triazole rings rather than that of their picryl rings. PATO tautomers which are not aromatic (1,3– and 1,5– CW Tautomers) were found to be kinetically more stable and less susceptible to oxidation than the others. Detonation performances of most of the PATO tautomers (1,5–CCW–Tautomer exception) lie between that of two thermally stable and insensitive explosives, PATO and TATB, the latter one is the best.

It has been found that gas phase nitrogen nitrations of PATO and its 1,3–CCW– and 1,5–CCW– tautomers are kinetically more favored than their carbon nitrations. *1,3–CCW–Tautomer–N(1)–Nitration* mechanism is kinetically the most favored among all the reaction pathways we studied. The other competing nitration mechanism is *PATO–N(4)–Nitration*. The unfavored C(5)–(R/S) nitrations of all the considered species produce more energetic transition states to the Wheland intermediates with respect to the intermediates of favored nitrogen nitrations.

1,3–CCW–Tautomer– and 1,5–CCW–Tautomer–C(5)–(R/S) nitration processes show strong single electron transfer (SET) mechanistic character while those of other species proceed via polar mechanisms in terms of charge transfer between the nitratible substrate and nitrating NO_2^+ ion.

The solvation effect on the most favored gas phase mechanism, *1,3–CCW–Tautomer–N(1)–Nitration*, is also observed in the most common nitrating solvent HNO_3. The results show that nitration is more favored in ionized HNO_3 with ionic strength (I) of 0.1 relative to gas phase and nonionized case because of having well stabilized reaction states and lower activation energy.

It is concluded that nitration reactions can be performed using protonated PATO species as well. The trend of their reaction state energies show parallelisms with that of free base PATO and its tautomeric mechanisms.

The detonation performances of all the nitrated forms of PATO and its tautomeric species are found to be higher than that of their unnitrated forms and very close to that of TATB (1,3,5–triamino–2,4,6–trinitrobenzene).

REFERENCES

[Addison, 1980] Addison, C. C. (1980). Dinitrogen tetroxide, nitric acid, and their mixtures as media for inorganic reactions. *Chemical Reviews*, 80:21–39.

[Agrawal, 2005] Agrawal, J. P. (2005). Some new high energy materials and their formulations for specialized applications. *Propellants, Explosives, Pyrotechniques*, 30:316–328.

[Agrawal and Hodgson, 2007] Agrawal, J. P. and Hodgson, R. D. (2007). *Organic chemistry of explosives, First Edition.* Wiley, West Sussex.

[Aihara et al., 1996] Aihara, J.–I., Oe, S., Yoshida, M., and Ōsawa, E. (1996). Further test of the isolated pentagon rule: Thermodynamic and kinetic stabilities of C_{84} fullerene isomers. *Journal of Computational Chemistry*, 17:1387–1394.

[Akhavan, 2004] Akhavan, J. (2004). *The chemistry of explosives, Second Edition*. The Royal Society of Chemistry, Cambridge, UK.

[Akutsu et al., 1991] Akutsu, Y., Tahara, S.–Y., Tamura, M., and Yoshida, T. (1991). Calculations of heats of formation for nitro compounds by semi–empirical MO methods and molecular mechanics. *Journal of Energetic Materials*, 9:161–171.

[Bader et al., 1987] Bader, R. F. W., Carroll, M. T., Cheeseman, J. R., and Chang, C. (1987). Properties of atoms in molecules: Atomic volumes. *Journal of the American Chemical Society*, 109:7968–7979.

[Balaban, 1980] Balaban, A. T. (1980). Is aromaticity outmoded? *Pure and Applied Chemistry*, 52:1409–1429.

[Becuwe, 1987] Becuwe, A. (1987). The use of 5–oxa–3–nitro–1,2,4–triazole as an explosive and explosives containing this substance. *French Patent FR 2584066*, Societe Nationale des Poudres et Explosifs, France.

[Bird, 1985] Bird, C. W. (1985). A new aromaticity index and its application to five–membered ring heterocycles. *Tetrahedron*, 41:1409–1414.

[Bolotina et al., 2003] Bolotina, N. B., Zhurova, E. A., and Pinkerton, A. A. (2003). Energetic materials: Variable–temperature crystal structure of β–NTO. *Journal of Applied Crystallography*, 36:280–285.

[Bolotina et al., 2005] Bolotina, N., Kirschbaum, K., and Pinkerton, A. A. (2005). Energetic materials: α–NTO crystallizes as a four–component triclinic twin. *Acta Crystallographica*, B61:577–584.

[Botcher et al., 1996] Botcher, T. R., Beardall, D. J., and Wight, C. A. (1996). Thermal decomposition mechanism of NTO. *Journal of Physical Chemistry*, 100:8802–8806.

[Boys and Bernardi, 1970] Boys, S. F. and Bernardi, F. (1970). The calculation of small molecular interaction by the differences of separate total energies: Some procedures with reduced errors. *Molecular Physics*, 19:553–566.

[Chase, Jr., 1998] Chase, Jr., M. W. (1998). *Journal of physical chemistry reference data, monograph no. 9, NIST–JANAF thermochemical tables, Part II, Cr–Zr, Fourth Edition.* American Chemical Society and the American Institute of Physics for the National Institute of Standards and Technology, USA.

[Chung et al., 2000] Chung, G., Schmidt, M. W., and Gordon, M. S. (2000). An ab initio study of potential energy surfaces for N_8 isomers. *Journal of Physical Chemistry A*, 104:5647–5650.

[Ciezak and Trevino, 2005] Ciezak, J. A. and Trevino, S. F. (2005). Theoretical and experimental study of the inelastic neutron scattering spectra of β–5–nitro–2,4–dihydro–3*H*–1,2,4–triazol–3–one. *Journal of Molecular Structure (THEOCHEM)*, 732:211–218.

[Coburn and Jackson, 1968] Coburn, M. D. and Jackson, T. E. (1968). Picrylamino–substituted heterocycles. III. 1,2,4–Triazoles. *Journal of Heterocyclic Chemistry*, 5:199–203.

[Coburn, 1969] Coburn, M. D. (1969). 3–Picrylamino–1,2,4–triazole and its preparation. *US Patent No. 3,483,211*.

[Coburn et al., 1986] Coburn, M. D., Harris, B. W., Lee, K.–Y., Stinecipher, M. M., and Hayden, H. H. (1986). Explosives synthesis at Los Alamos. *Industrial & Engineering Chemistry Product Research and Development*, 25:68–72.

[Coburn and Lee, 1990] Coburn, M. D. and Lee, K.–Y. (1990). Picryl derivatives of 5–nitro–2,4–dihydro–3*H*–1,2,4–triazol–3–one. *Journal of Heterocyclic Chemistry*, 27:575–577.

[Cramer, 2004] Cramer, C. J. (2004). *Essentials of computational chemistry: Theories and models, Second Edition.* Wiley, Chichester, West Sussex, England.

[de Queiroz et al., 2006] de Queiroz, J. F., de M. Carneiro, J. W., Sabino, A. A., Sparrapan, R., Eberlin, M. N., and Esteves, P. M. (2006). Electrophilic aromatic nitration: Understanding its mechanism and substituent effects. *The Journal of Organic Chemistry*, 71:6192–6203.

[Dong and Zhou, 1989] Dong, H. S. and Zhou, F. F. (1989). *Performance of high energetic explosive and related compounds.* Science Press, Beijing.

[Dorsett and White, 2000] Dorsett, H. and White, A. (2000). Overview of molecular modelling and ab initio molecular orbital methods suitable for use with energetic materials. *Report DSTO–GD–0253*, Defence Science & Technology Organisation (DSTO), Aeronautical and Maritime Research Laboratory, Melbourne, Australia.

[Esteves et al., 2003] Esteves, P. M., de M. Carneiro, J. W., Cardoso, S. P., Barbosa, A. G. H., Laali, K. K., Rasul, G., Prakash, G. K. S., and Olah, G. A. (2003). Unified mechanistic concept of electrophilic aromatic nitration: Convergence of computational results and experimental data. *Journal of the American Chemical Society*, 125:4836–4849.

[Fan et al., 1996] Fan, L., Dass, C., and Burkey, T. J. (1996). Synthesis and thermal decomposition of ^{15}N–labelled NTO. *Journal of Labelled Compounds and Radiopharmaceuticals*, 38:87–94.

[Fletcher, 1987] Fletcher, R. (1987). *Practical methods of optimization, Second Edition.* Wiley, Chichester, West Sussex, England.

[Foresman and Frisch, 1996] Foresman, J. B. and Frisch, Æ. (1996). *Exploring chemistry with electronic structure methods: A guide to using Gaussian, Second Edition.* Gaussian, Inc., Pittsburgh, PA.

[Frisch et al., 2004] Frisch, M. J., et al. (2004). Gaussian 03, Revision C. 02. Gaussian, Inc., Wallingford CT.

[Frisch et al., 2009] Frisch, M. J., et al. (2009). Gaussian 09, Revision A. 02. Gaussian, Inc., Wallingford CT.

[Gordy, 1947] Gordy, W. (1947). Dependence of bond order and of bond energy upon bond length. *Journal of Chemical Physics*, 15:305–310.

[Gwaltney et al., 2003] Gwaltney, S. R., Rosokha, S. V., Head–Gordon, M., and Kochi, J. K. (2003). Charge–transfer mechanism for electrophilic aromatic nitration and nitrosation via the convergence of (ab initio) molecular–orbital and Marcus–Hush theories with experiments. *Journal of the American Chemical Society*, 125:3273–3283.

[Haddon and Fukunaga, 1980] Haddon, R. C. and Fukunaga, T. (1980). Unified theory of the thermodynamic and kinetic criteria of aromatic character in the [4n+2] annulenes. *Tetrahedron Letters*, 21:1191–1192.

[Harris and Lammertsma, 1996] Harris, N. J. and Lammertsma, K. (1996). Tautomerism, ionization, and bond dissociations of 5–nitro–2,4–dihydro–3*H*–1,2,4–triazolone. *Journal of the American Chemical Society*, 118:8048–8055.

[Harris and Lammertsma, 1997] Harris, N. J. and Lammertsma, K. (1997). Ab initio density functional computations of conformations and bond dissociation energies for hexahydro–1,3,5–trinitro–1,3,5–triazine. *Journal of the American Chemical Society*, 119:6583–6589.

[Hess and Schaad, 1971] Hess, B. A. Jr. and Schaad, L. J. (1971). Hückel molecular orbital π resonance energies. The benzenoid hydrocarbons. *Journal of the American Chemical Society*, 93:2413–2416.

[Hou et al., 2012] Hou, C., Shi, W., Ren, F., Wang, Y., and Wang, J. (2012). A B3LYP and MP2(full) theoretical investigation into explosive sensitivity upon the formation of the molecule–cation interaction between the nitro group of RNO_2 (R = $–CH_3$, $–NH_2$, $–OCH_3$) and Na^+, Mg^{2+} or Al^{3+}. *Computational and Theoretical Chemistry*, 991:107–115.

[Jensen, 2007] Jensen, F. (2007). *Introduction to computational chemistry, Second Edition*. Wiley, Chichester, West Sussex, England.

[Jimenez et al., 1989] Jimenez, P., Roux, M. V., and Turrion, C. (1989). Thermochemical properties of N–heterocyclic compounds II. Enthalpies of combustion, vapour pressures, enthalpies of sublimation, and enthalpies of formation of 1,2,4–triazole and benzotriazole. *Journal of Chemical Thermodynamics*, 21:759−764.

[Ju et al., 2005] Ju, X.–H., Li, Y.–M., and Xiao, H.–M. (2005). Theoretical studies on the heats of formation and the interactions among the difluoroamino groups in polydifluoroaminocubanes. *Journal of Physical Chemistry A*, 109:934−938.

[Kamlet and Jacobs, 1968] Kamlet, M. J. and Jacobs, S. J. (1968). Chemistry of detonations. 1. Simple method for calculating detonation properties of C–H–N–O explosives. *Journal of Chemical Physics*, 48:23–35.

[Kohn and Sham, 1965] Kohn, W. and Sham, L. J. (1965). Self–consistent equations including exchange and correlation effects. *Physical Review*, 140:A1133–A1138.

[Kohno et al., 2001] Kohno, Y., Takahashi, O., and Saito, K. (2001). Theoretical study of initial decomposition process of NTO dimer. *Physical Chemistry Chemical Physics*, 3:2742–2746.

[Koopmans, 1934] Koopmans, T. (1934). Über die zuordnung von wellenfunktionen und eigenwerten zu den einzelnen elektronen eines atoms. *Physica*, 1:104–113.

[Kulkarni et al., 2005] Kulkarni, P. B., Purandare, G. N., Nair, J. K., Talawar, M. B., Mukundan, T., and Asthana, S. N. (2005). Synthesis, characterization, thermolysis and performance evaluation studies on alkali metal salts of TABA and NTO. *Journal of Hazardous Materials*, A119:53–61.

[Langlet, 1990] Langlet, A. (1990). 3–Nitro–1,2,4–triazole–5–one (NTO), a new explosive with high performance and low sensitivity. *Report FAO–29787–23*, Department of Weapons and Technology, Foersvarets Forskningsanst., Stockholm, Sweden.

[Lazzara et al. 1979] Lazzara, M. G., Harrison, J. J., Rule, M., and Berson, J. A. (1979). Mechanisms of dimerization and rearrangement of a bicyclo[3.1.0]hex–l–ene. *Journal of the American Chemical Society*, 101:7094–7095.

[Le Campion et al., 1997] Le Campion, L., Adeline, M. T., and Ouazzani, J. (1997). Separation of NTO related 1,2,4–triazole–3–one derivatives by a high performance liquid chromatography and capillary electrophoresis. *Propellants, Explosives, Pyrotechniques*, 22:233–237.

[Leach, 2001] Leach, A. R. (2001). *Molecular modelling: Principles and applications, Second Edition.* Prentice Hall, Harlow, England.

[Lee and Coburn, 1985] Lee, K.–Y. and Coburn, M. D. (1985). 3–Nitro–1,2,4–triazol–5–one, a less sensitive explosive. *Report LA–10302–MS*, Los Alamos National Laboratory, New Mexico, USA.

[Lee et al., 1987] Lee, K.–Y., Chapman, L. B., and Coburn, M. D. (1987). 3–Nitro–1,2,4–triazol–5–one, a less sensitive explosive. *Journal of Energetic Materials*, 5:27–33.

[Li et al., 1991] Li, J., Chen, B., and Ou, Y. (1991). Modified preparation and nitration of 3–picrylamino–1,2,4–triazole. In *Proceedings of the 17th International Pyrotechnics Seminar (Combined with 2nd Beijing International Symposium on Pyrotechnics and Explosives)*, Beijing, China.

[Li et al., 1999] Li, J., Chen, B., and Ou, Y. (1999). Modified preparation and purification of 3–(2',4',6'–trinitrobenzenyl)amino–1,2,4–triazole. *Propellants, Explosives, Pyrotechnics*, 24:95.

[Li, 2010] Li, J. (2010). A quantitative relationship for the shock sensitivities of energetic compounds based on X–NO_2 (X = C, N, O) bond dissociation energy. *Journal of Hazardous Materials*, 180:768–772.

[Liu et al., 1992] Liu, X., Schmalz, T. G., and Klein, D. J. (1992). Favorable structures for higher fullerenes. *Chemical Physics Letters*, 188:550–554.

[Long et al., 2002] Long, G. T., Brems, B. A., and Wight, C. A. (2002). Thermal activation of the high explosive NTO: Sublimation, decomposition, and autocatalysis. *Journal of Physical Chemistry B*, 106:4022–4026.

[Lowe–Ma, 1990] Lowe–Ma, C. K. (1990). Structure of 2,4,8,10–tetranitro–2,4,8,10–tetraazaspiro[5.5]undecane (TNSU), an energetic spiro bicyclic nitramine. *Acta Crystallographica*, C46:1029–1033.

[Luo, 2003] Luo, Y.–R. (2003). *Handbook of bond dissociation energies in organic compounds, First Edition.* CRC Press, USA.

[Mader, 1998] Mader, C. L. (1998). *Numerical modeling of explosives and propellants, Second Edition.* CRC Press, Boca Raton, Florida, USA.

[Manolopoulos et al., 1991] Manolopoulos, D. E., May, J. C., and Down, S. E. (1991). Theoretical studies of the fullerenes: C_{34} to C_{70}. *Chemical Physics Letters*, 181:105–111.

[McKee, 1995] McKee, M. L. (1995). Ab initio study of the N_2O_4 potential energy surface. Computational evidence for a new N_2O_4 isomer. *Journal of the American Chemical Society*, 117:1629–1637.

[McQuaid, 2003] McQuaid, M. J. (2003). Computationally based measures of amine azide basicity and their correlation with hypergolic ignition delays. *Report ARL–TR–3122*, U.S. Army Research Laboratory Aberdeen Proving Ground MD, USA.

[Meredith et al., 1998] Meredith, C., Russell, T. P., Mowrey, R. C., and McDonald, J. R. (1998). Decomposition of 5–nitro–2,4–dihydro–3*H*–1,2,4–triazol–3–one (NTO): Energetics associated with several proposed initiation routes. *Journal of Physical Chemistry A*, 102:471–477.

[Meyer et al., 2007] Meyer, R., Köhler, J., and Homburg, A. (2007). *Explosives, Sixth Edition.* Wiley–VCH, Weinheim.

[Murray et al., 2009] Murray, J. S., Concha, M. C., and Politzer, P. (2009). Links between surface electrostatic potentials of energetic molecules, impact sensitivities and C–NO_2/N–NO_2 bond dissociation energies. *Molecular Physics*, 107:89–97.

[Osmont et al., 2007] Osmont, A., Catoire, L., Gökalp, I., and Yang, V. (2007). Ab initio quantum chemical predictions of enthalpies of formation, heat capacities, and entropies of gas–phase energetic compounds. *Combustion and Flame*, 151:262–273.

[Owens, 1996] Owens, F. J. (1996). Calculation of energy barriers for bond rupture in some energetic molecules. *Journal of Molecular Structure (THEOCHEM)*, 370:11–16.

[Owens, 1999] Owens, F. J. (1999). Molecular orbital calculation of decomposition pathways of nitrocubanes and nitroazacubanes. *Journal of Molecular Structure (THEOCHEM)*, 460:137–140.

[Oxley et al., 1995] Oxley, J. C., Smith, J. L., Yeager, K. E., Coburn, M. D., and Ott, D. G. (1995). Synthesis of ^{15}N–labeled isomers of 5–nitro–2,4–dihydro–3*H*–1,2,4–triazol–3–one (NTO). *Journal of Energetic Materials*, 13:93–105.

[Oxley et al., 1997] Oxley, J. C., Smith, J. L., Rogers, E., and Dong, X. X. (1997). NTO decomposition products tracked with ^{15}N labels. *Journal of Physical Chemistry A*, 101:3531–3536.

[Parr and Yang, 1989] Parr, R. G. and Yang, W. (1989). *Density functional theory of atoms and molecules, First Edition.* Oxford University Press, New York.

[Parr and Zhou, 1993] Parr, R. G. and Zhou, Z. (1993). Absolute hardness: Unifying concept for identifying shells and subshells in nuclei, atoms, molecules, and metallic clusters. *Accounts of Chemical Research*, 26:256–258.

[Pearson, 1973] Pearson, R. G. (1973). *Hard and soft acids and bases, First Edition.* Dowden, Hutchinson and Ross, Stroudsburg, Pennsylvania.

[Pearson, 1997] Pearson, R. G. (1997). *Chemical hardness, First Edition.* Wiley–VCH, Weinheim, Germany.

[Politzer and Lane, 1996] Politzer, P. and Lane, P. (1996). Comparison of density functional calculations of C–NO_2, N–NO_2 and C–NF_2 dissociation energies. *Journal of Molecular Structure (THEOCHEM)*, 388:51–55.

[Politzer and Murray, 1996] Politzer, P. and Murray, J. S. (1996). Relationships between dissociation energies and electrostatic potentials of C–NO_2 bonds: Applications to impact sensitivities. *Journal of Molecular Structure*, 376:419–424.

[Politzer et al., 1997] Politzer, P., Murray, J. S., Grice, M. E., Desalvo, M., and Miller, E. (1997). Calculation of heats of sublimation and solid phase heats of formation. *Molecular Physics*, 91:923–928.

[Pospisil et al., 2010] Pospisil, M., Vavra, P., Concha, M. C., Murray, J. S., and Politzer, P. (2010). A possible crystal volume factor in the impact sensitivities of some energetic compounds. *Journal of Molecular Modeling*, 16:895–901.

[Qiu et al., 2006] Qiu, L., Xiao, H., Gong, X., Ju, X., and Zhu, W. (2006). Theoretical studies on the structures, thermodynamic properties, detonation properties and pyrolysis mechanisms of spiro nitramines. *Journal of Physical Chemistry A*, 110:3797–3807.

[Rice et al., 2002] Rice, B. M., Sahu, S., and Owens, F. J. (2002). Density functional calculations of bond dissociation energies for NO_2 scission in some nitroaromatic molecules. *Journal of Molecular Structure (THEOCHEM)*, 583:69–72.

[Rosokha and Kochi, 2002] Rosokha, S. V. and Kochi, J. K. (2002). The preorganization step in organic reaction mechanisms. Charge–transfer complexes as precursors to electrophilic aromatic substitutions. *The Journal of Organic Chemistry*, 67:1727–1737.

[Rule et al., 1982] Rule, M., Mondo, J. A., and Berson, J. A. (1982). Synthesis and thermolysis of 5–alkylidenebicyclo[2.1.0]pentanes. Generation and dimerization of trimethylenemethane triplet biradicals by bond rupture of strained hydrocarbons. *Journal of the American Chemical Society*, 104:2209–2216.

[Schleyer et al., 1996] Schleyer, P. v. R., Maerker, C., Dransfeld, A., Jiao, H., and Hommes, N. J. R. v. E. (1996). Nucleus–independent chemical shifts: A simple and efficient aromaticity probe. *Journal of the American Chemical Society*, 118:6317–6318.

[Schmalz et al., 1988] Schmalz, T. G., Seitz, W. A., Klein, D. J., and Hite, G. E. (1988). Elemental carbon cages. *Journal of the American Chemical Society*, 110:1113–1127.

[Shao et al., 2005] Shao, J., Cheng, X., and Yang, X. (2005). Density functional calculations of bond dissociation energies for removal of the nitrogen dioxide moiety in some nitroaromatic molecules. *Journal of Molecular Structure (THEOCHEM)*, 755:127–130.

[Sikder et al., 2001] Sikder, A. K., Maddala, G., Agrawal, J. P., and Singh, H. (2001). Important aspects of behaviour of organic energetic compounds: A review. *Journal of Hazardous Materials*, A84:1–26.

[Silbey and Alberty, 2001] Silbey, R. J. and Alberty, R. A. (2001). *Physical Chemistry, Third Edition.* Wiley, USA.

[Singh et al., 2001] Singh, G., Kapoor, I. P. S., Tiwari, S. K., and Felix, P. S. (2001). Studies on energetic compounds: Part 16. Chemistry and decomposition mechanisms of 5–nitro–2,4–dihydro–3*H*–1,2,4–triazole–3–one (NTO). *Journal of Hazardous Materials*, B81:67–82.

[Singh and Felix, 2002] Singh, G. and Felix, S. P. (2002). Studies on energetic compounds: 25. An overview of preparation, thermolysis and applications of the salts of 5–nitro–2,4–dihydro–3*H*–1,2,4–triazol–3–one (NTO). *Journal of Hazardous Materials*, A90:1–17.

[Singh and Felix, 2003] Singh, G. and Felix, S. P. (2003). Studies on energetic compounds part 36. Evaluation of transition metal salts of NTO as burning rate modifiers for HTPB–AN composite solid propellants. *Combustion and Flame*, 135:145–150.

[Sokolov, 2004] Sokolov, A. V. (2004). New aspects of electrophilic aromatic substitution mechanism: Computational model of nitration reaction. *International Journal of Quantum Chemistry*, 100:1–12.

[Solomons and Fryhle, 2000] Solomons, T. W. G. and Fryhle, C. B. (2000). *Organic chemistry, Seventh Edition.* Wiley, New York.

[Sorescu et al., 1996] Sorescu, D. C., Sutton, T. R. L., Thompson, D. L., Beardall, D., and Wight, C. A. (1996). Theoretical and experimental studies of the structure and vibrational spectra of NTO. *Journal of Molecular Structure*, 384:87–99.

[Sorescu and Thompson, 1997] Sorescu, D. C. and Thompson, D. L. (1997). Crystal packing and molecular dynamics studies of the 5–nitro–2,4–dihydro–3*H*–1,2,4–triazol–3–one crystal. *Journal of Physical Chemistry B*, 101:3605–3613.

[Spear et al., 1989] Spear, R. J., Louey, C. N., and Wolfson, M. G. (1989). A preliminary assessment of NTO as an insensitive high explosive. *Report MRL–TR–89–18*, Materials Research Laboratory, Victoria, Australia.

[Stewart, 1989a] Stewart, J. J. P. (1989). Optimization of parameters for semiempirical methods. I. Method. *Journal of Computational Chemistry*, 10:209–220.

[Stewart, 1989b] Stewart, J. J. P. 1989. Optimization of parameters for semiempirical methods. II. Applications. *Journal of Computational Chemistry*, 10:221–264.

[Tanaka et al., 2000] Tanaka, M., Muro, E., Ando, H., Xu, Q., Fujiwara, M., Souma, Y., and Yamaguchi, Y. (2000). NO_2^+ nitration mechanism of aromatic compounds: Electrophilic vs. charge–transfer process. *The Journal of Organic Chemistry*, 65:2972–2978.

[Türker and Atalar, 2006] Türker, L. and Atalar, T. (2006). Quantum chemical study on 5–nitro–2,4–dihydro–3*H*–1,2,4–triazol–3–one (NTO) and some of its constitutional isomers. *Journal of Hazardous Materials*, A137:1333–1344.

[Türker and Çelik Bayar, 2012] Türker, L. and Çelik Bayar, Ç. (2012). A computational view of PATO and its tautomers. *Zeitschrift für Anorganische und Allgemeine Chemie (ZAAC) (Journal of Inorganic and General Chemistry)*, 638:1316–1322.

[Wang et al., 2009] Wang, G. X., Gong, X. D., and Xiao, H. M. (2009). Theoretical investigation on density, detonation properties, and pyrolysis mechanism of nitro derivatives of benzene and aminobenzenes. *International Journal of Quantum Chemistry*, 109:1522–1530.

[Wang et al., 2012] Wang, H., Shi, W., Ren, F., Yang, L., and Wang, J.–l. (2012). A B3LYP and MP2(full) theoretical investigation into explosive sensitivity upon the formation of the intermolecular hydrogen–bonding interaction between the nitro group of RNO_2 (R = $–CH_3$, $–NH_2$, $–OCH_3$) and HF, HCl or HBr. *Computational and Theoretical Chemistry*, 994:73–80.

[Wei et al., 2013] Wei, Q., Shi, W., Ren, F., Wang, Y., and Ren, J. (2013). A B3LYP and MP2(full) theoretical investigation into the strength of the C–NO_2 bond upon the formation of the molecule–cation interaction between Na^+ and the nitro group of nitrotriazole or its methyl derivatives. *Journal of Molecular Modeling*, 19:453–463.

[Yim and Liu, 2001] Yim, W.–L. and Liu, Z.–f. (2001). Application of ab initio molecular dynamics for a priori elucidation of the mechanism in unimolecular decomposition: The case of 5–nitro–2,4–dihydro–3*H*–1,2,4–triazol–3–one (NTO). *Journal of the American Chemical Society*, 123:2243–2250.

[Zhang et al., 2002] Zhang, J., Xiao, J., and Xiao, H. (2002). Theoretical studies on heats of formation for cubylnitrates using density functional theory B3LYP method and semiempirical MO methods. *International Journal of Quantum Chemistry*, 86:305−312.

[Zhang and Law, 2011] Zhang, P. and Law, C. K. (2011). Density functional theory study of the ignition mechanism of 2–azido–*N*,*N*–dimethylethanamine (DMAZ). In *Fall Technical Meeting of the Eastern States Section of the Combustion Institute Hosted by the University of Connecticut*, Storrs, Connecticut.

[Zhou et al., 1988] Zhou, Z., Parr, R. G., and Garst, J. F. (1988). Absolute hardness as a measure of aromaticity. *Tetrahedron Letters*, 29:4843–4846.

[Zhou and Parr, 1989] Zhou, Z. and Parr, R. G. (1989). New measures of aromaticity: Absolute hardness and relative hardness. *Journal of the American Chemical Society*, 111:7371–7379.

[Zhou and Parr, 1990] Zhou, Z. and Parr, R. G. (1990). Activation hardness: New index for describing the orientation of electrophilic aromatic substitution. *Journal of the American Chemical Society*, 112:5720–5724.

[Zhurova and Pinkerton, 2001] Zhurova, E. A. and Pinkerton, A. A. (2001). Chemical bonding in energetic materials: β–NTO. *Acta Crystallographica*, B57:359–365.

[Zhurova et al., 2004] Zhurova, E. A., Tsirelson, V. G., Stash, A. I., Yakovlev, M. V., and Pinkerton, A. A. (2004). Electronic energy distributions in energetic materials: NTO and the biguanidinium dinitramides. *Journal of Physical Chemistry B*, 108:20173–20179.

APPENDIX A

The Cartesian coordinates of the optimized structures presented in Chapters 2 and 3 (B3LYP/6–31G(d,p)). For all structures total charge = 0, multiplicity = 1 and number of imaginary frequencies = 0.

A1 ZPE = 399.15 kJ/mol			
Coordinates (Å)			
Atom	X	Y	Z
C	–2.34755	0.95494	0.31039
C	–1.57826	2.01403	0.67371
C	–1.73458	–0.29441	–0.07429
C	–0.29756	–0.28672	–0.34707
C	0.48633	0.82208	0.16504
C	–0.15204	1.92451	0.65574
N	–3.79753	1.15507	0.18814
O	–4.36502	0.52718	–0.70088
O	–4.31989	1.96988	0.94570
N	0.23431	–1.25864	–1.07442
O	1.37831	–1.52161	–1.42406
O	–0.83006	–2.20241	–1.54244
H	–2.06533	2.93734	0.96256
N	1.89531	0.85194	0.03317
C	2.87473	–0.05523	0.40013
C	2.56849	1.89860	–0.67381
N	3.87734	1.45210	–0.64418
N	4.06310	0.28430	0.02437
O	2.10014	2.90330	–1.15616
N	2.63971	–1.22837	1.22086
O	1.49603	–1.34476	1.67157
O	3.58141	–1.97734	1.41822
H	4.66762	1.94601	–1.03109
N	–2.38119	–1.45534	0.02420
O	–1.52042	–2.60699	–0.39226
O	–3.47961	–1.76312	0.43223
H	0.43596	2.76969	0.98906

A1–enol–tautomer ZPE = 397.28 kJ/mol			
Coordinates (Å)			
Atom	X	Y	Z
C	–2.31491	0.94162	0.37827
C	–1.52676	1.96649	0.79360
C	–1.72964	–0.29299	–0.09116
C	–0.29814	–0.28983	–0.38847
C	0.50430	0.78649	0.15467
C	–0.10109	1.86199	0.73268
N	–3.76496	1.17043	0.29355
O	–4.35222	0.61791	–0.63136
O	–4.26356	1.93487	1.11605
N	0.21916	–1.24063	–1.15512
O	1.35311	–1.50369	–1.52387
O	–0.86826	–2.14764	–1.65638
H	–1.99636	2.87470	1.15103
N	1.91926	0.78943	–0.00875
C	2.92008	–0.03481	0.49628
C	2.63847	1.64758	–0.79995
N	3.92576	1.38828	–0.77002
N	4.09641	0.31339	0.06602
N	2.66357	–1.11761	1.41150
O	1.47762	–1.29100	1.72452
O	3.61792	–1.76406	1.81036
N	–2.39423	–1.44653	–0.04240
O	–1.55545	–2.59044	–0.51894
O	–3.49474	–1.75461	0.36039
H	0.50919	2.67185	1.11385
O	2.03112	2.60785	–1.49013
H	2.71422	3.06321	–2.00897

A1–aci–tautomer ZPE = 393.63 kJ/mol			
Coordinates (Å)			
Atom	X	Y	Z
C	2.37915	0.93456	–0.33117
C	1.62273	2.00676	–0.68589
C	1.74872	–0.30358	0.06309
C	0.31602	–0.26697	0.36122
C	–0.45682	0.85367	–0.14484
C	0.19673	1.94258	–0.65140
N	3.83273	1.10776	–0.22924
O	4.40347	0.46077	0.64434
O	4.35884	1.92015	–0.98763
N	–0.21818	–1.21890	1.11474
O	–1.35364	–1.44980	1.50757
O	0.83564	–2.18544	1.56071
H	2.12283	2.92027	–0.98373
N	–1.85901	0.90433	0.00061
C	–2.84787	0.02130	–0.37413
C	–2.54956	1.94986	0.69416
N	–3.94185	1.56910	0.67967
N	–4.08081	0.46572	0.05235
O	–2.06412	2.94159	1.17006
N	–2.68387	–1.06645	–1.10946
O	–1.61151	–1.49883	–1.55651
O	–3.84476	–1.76976	–1.39370
N	2.37038	–1.47622	–0.04287
O	1.48926	–2.60856	0.39612
O	3.45569	–1.81077	–0.46629
H	–0.38089	2.79572	–0.98296
H	–3.48317	–2.53727	–1.87758

B1 ZPE = 398.56 kJ/mol			
Coordinates (Å)			
Atom	X	Y	Z
C	2.72551	0.88871	–0.25855
C	1.99894	2.03294	–0.37460
C	2.06338	–0.38477	–0.09149
C	0.64277	–0.35300	0.26408
C	–0.10158	0.85672	–0.03853
C	0.57099	2.00761	–0.34091
N	4.18631	0.99862	–0.16732
O	4.75439	0.18433	0.55498
O	4.72276	1.92283	–0.77589
N	0.12139	–1.35472	0.96703
O	–0.95201	–1.54194	1.50690
O	1.12945	–2.45275	1.13894
H	2.52629	2.97005	–0.50536
N	–1.50573	0.83605	0.00333
C	–2.34428	1.85032	0.53997
N	–3.60461	1.29277	0.33460
O	–2.03249	2.91095	1.02873
H	–4.48847	1.71366	0.58206
N	2.63720	–1.54435	–0.39506
O	1.68582	–2.68601	–0.12356
O	3.71014	–1.86082	–0.86003
H	0.01413	2.91634	–0.52775
N	–2.20613	–0.22679	–0.50937
C	–3.43950	0.08823	–0.28652
N	–4.57503	–0.72693	–0.66428
O	–4.36071	–1.78875	–1.22655
O	–5.67274	–0.24324	–0.37005

B1–enol–tautomer ZPE = 398.46 kJ/mol			
Coordinates (Å)			
Atom	X	Y	Z
C	2.70584	0.88164	–0.33204
C	1.97083	2.00692	–0.53371
C	2.05945	–0.38616	–0.07784
C	0.63801	–0.34850	0.26843
C	–0.11277	0.83703	–0.09105
C	0.54100	1.96579	–0.48758
N	4.16764	1.01370	–0.24646
O	4.73772	0.27116	0.54688
O	4.69618	1.88674	–0.93106
N	0.10716	–1.33089	0.99194
O	–0.98198	–1.51305	1.49890
O	1.12973	–2.40237	1.24290
H	2.48838	2.93702	–0.73448
N	–1.52462	0.80753	–0.01946
C	–2.38840	1.60524	0.67988
N	–3.62982	1.21527	0.51431
O	–1.94164	2.62543	1.40704
N	2.65017	–1.55362	–0.31269
O	1.71419	–2.69226	0.00491
O	3.73088	–1.87684	–0.75431
H	–0.02911	2.84804	–0.75206
N	–2.24373	–0.16209	–0.66942
C	–3.46799	0.14623	–0.30727
N	–4.60683	–0.63879	–0.78830
O	–4.35669	–1.55920	–1.55805
O	–5.71196	–0.30384	–0.37846
H	–2.70632	3.02184	1.85411

B1–1,3–tautomer ZPE = 400.13 kJ/mol			
Coordinates (Å)			
Atom	X	Y	Z
C	2.73489	0.85812	–0.14945
C	2.03205	2.05261	–0.27977
C	2.04540	–0.34102	0.01944
C	0.65612	–0.32822	0.09306
C	–0.06975	0.86395	–0.08402
C	0.64602	2.06014	–0.26776
N	4.20630	0.91543	–0.12003
O	4.78888	0.01840	0.47977
O	4.73186	1.87815	–0.67007
N	–0.05400	–1.60313	0.36035
O	–0.47303	–1.76738	1.49211
O	–0.18953	–2.36202	–0.59862
H	2.59236	2.97018	–0.40935
N	–1.46838	0.91527	–0.12870
C	–2.32123	1.97482	0.37484
N	–3.62841	1.45902	0.38095
O	–1.92854	3.06488	0.70755
N	2.73296	–1.65577	0.05069
O	3.37131	–1.94817	–0.94751
O	2.55264	–2.34009	1.04849
H	0.09800	2.98517	–0.38001
N	–2.27649	–0.20136	–0.32225
C	–3.52417	0.25839	–0.06564
N	–4.64758	–0.65760	–0.33881
O	–4.34176	–1.66031	–0.98603
O	–5.74453	–0.34292	0.07775
H	–2.07554	–0.87540	–1.05778

A2 ZPE = 402.87 kJ/mol			
Coordinates (Å)			
Atom	X	Y	Z
C	2.61421	–0.05019	0.12640
C	2.05782	–1.32181	0.10305
C	1.76553	1.03737	–0.02852
C	0.39229	0.85670	–0.20606
C	–0.14717	–0.43487	–0.19331
C	0.69492	–1.53572	–0.05315
N	–0.51783	1.98439	–0.50216
O	–1.40525	2.20523	0.31226
O	–0.33784	2.54994	–1.56906
N	–1.53612	–0.64308	–0.41400
C	–2.62155	–0.48123	0.42988
C	–2.06019	–1.00867	–1.68898
N	–3.42188	–1.01291	–1.42779
N	–3.75545	–0.70480	–0.14633
O	–1.45234	–1.24572	–2.70536
N	–2.51147	–0.18735	1.84793
O	–1.37401	–0.25679	2.31764
O	–3.53945	0.07811	2.44785
H	–4.14210	–1.23726	–2.09811
N	2.35937	2.38891	0.05744
O	1.60708	3.30597	0.36664
O	3.56186	2.47855	–0.15928
H	3.67790	0.09678	0.25935
N	2.94887	–2.49211	0.26177
O	2.42378	–3.60074	0.23243
O	4.14508	–2.26671	0.41014
H	0.29937	–2.54301	–0.06126

A2–enol–tautomer ZPE = 400.79 kJ/mol			
Coordinates (Å)			
Atom	X	Y	Z
C	–2.60111	–0.11498	–0.10699
C	–2.00698	–1.35841	0.05435
C	–1.78860	1.01222	–0.07718
C	–0.41038	0.89307	0.10870
C	0.16198	–0.37466	0.25412
C	–0.63815	–1.51231	0.23598
N	0.50790	2.05172	0.19718
O	1.16906	2.29422	–0.80018
O	0.57252	2.59734	1.28873
N	1.56790	–0.49167	0.47538
C	2.63991	–0.59005	–0.40877
C	2.20269	–0.47624	1.69114
N	3.50693	–0.56693	1.56605
N	3.77581	–0.63938	0.22107
N	2.47506	–0.66393	–1.84149
O	1.30762	–0.70823	–2.24712
O	3.48456	–0.68662	–2.52557
N	–2.42951	2.33149	–0.26795
O	–1.68510	3.29266	–0.42562
O	–3.65423	2.35941	–0.26277
H	–3.66907	–0.01571	–0.24982
N	–2.86182	–2.56573	0.03354
O	–2.30341	–3.64558	0.20114
O	–4.06269	–2.39651	–0.14592
H	–0.21050	–2.49998	0.35233
O	1.49717	–0.38314	2.81122
H	2.12342	–0.33350	3.55169

A2–aci–tautomer ZPE = 397.50 kJ/mol			
Coordinates (Å)			
Atom	X	Y	Z
C	2.63208	–0.06423	0.16650
C	2.07192	–1.33380	0.13116
C	1.79075	1.02570	–0.01164
C	0.42182	0.85002	–0.22394
C	–0.12526	–0.44010	–0.22415
C	0.71249	–1.54296	–0.05976
N	–0.47140	1.98335	–0.55202
O	–1.36847	2.23006	0.24359
O	–0.26319	2.53061	–1.62311
N	–1.50504	–0.64628	–0.47130
C	–2.60015	–0.47035	0.34846
C	–2.04085	–1.04271	–1.73313
N	–3.47353	–1.06573	–1.54659
N	–3.75985	–0.73599	–0.34519
O	–1.41455	–1.30361	–2.72573
N	–2.55878	–0.18643	1.64120
O	–1.53995	–0.01946	2.32348
O	–3.79545	–0.06289	2.25772
N	2.38736	2.37512	0.08745
O	1.63013	3.29635	0.37232
O	3.59598	2.46002	–0.09386
H	3.69255	0.07953	0.32599
N	2.95404	–2.50647	0.31956
O	2.42473	–3.61306	0.28954
O	4.14765	–2.28483	0.49334
H	0.31412	–2.54921	–0.07909
H	–3.52826	0.19172	3.16201

B2 ZPE = 403.33 kJ/mol			
Coordinates (Å)			
Atom	X	Y	Z
C	2.80341	0.86815	–0.01765
C	1.81076	1.83086	0.11491
C	2.40643	–0.45601	–0.12464
C	1.05825	–0.82669	–0.07548
C	0.07996	0.16664	0.09255
C	0.46488	1.50839	0.17711
N	0.67743	–2.25267	–0.20381
O	–0.16353	–2.50719	–1.05774
O	1.22916	–3.03652	0.54874
N	–1.29521	–0.13529	0.18264
C	–1.89372	–1.13810	0.98727
N	–3.24737	–0.90044	0.75159
O	–1.35302	–1.95113	1.69645
H	–4.01877	–1.42293	1.14169
N	3.47350	–1.44454	–0.40320
O	3.22513	–2.30567	–1.23748
O	4.53504	–1.28041	0.18533
H	3.84993	1.14023	–0.05174
N	2.20670	3.25344	0.21259
O	1.30718	4.07635	0.35022
O	3.40589	3.50365	0.14959
H	–0.27858	2.28602	0.29333
C	–3.34856	0.17828	–0.07602
N	–2.21163	0.67886	–0.43554
N	–4.63762	0.69477	–0.49406
O	–5.60647	0.07624	–0.04565
O	–4.65459	1.66828	–1.22984

B2–enol–tautomer ZPE = 403.10 kJ/mol			
Coordinates (Å)			
Atom	X	Y	Z
C	2.79604	0.86131	–0.04354
C	1.81047	1.82518	0.12808
C	2.39376	–0.46037	–0.15726
C	1.04499	–0.82562	–0.08247
C	0.07503	0.16745	0.11753
C	0.46467	1.50697	0.21257
N	0.65206	–2.25007	–0.18546
O	–0.18600	–2.52063	–1.03510
O	1.17727	–3.01656	0.60680
N	–1.31061	–0.11528	0.21220
C	–2.00172	–1.03926	0.94987
N	–3.29586	–0.89912	0.79253
O	–1.35555	–1.90279	1.72173
N	3.44704	–1.45453	–0.46457
O	3.15112	–2.34993	–1.24605
O	4.54131	–1.26752	0.05270
H	3.84253	1.13044	–0.09954
N	2.21541	3.24522	0.23842
O	1.32373	4.06734	0.41851
O	3.41354	3.48997	0.14372
H	–0.27743	2.28301	0.34794
C	–3.35052	0.15742	–0.05663
N	–2.21188	0.68880	–0.44025
N	–4.62367	0.70309	–0.53503
O	–5.63689	0.11921	–0.17172
O	–4.56178	1.69460	–1.25298
H	–2.00275	–2.50823	2.11676

B2–1,3–tautomer ZPE = 401.16 kJ/mol			
Coordinates (Å)			
Atom	X	Y	Z
C	2.94888	0.27157	–0.21911
C	2.33581	1.49259	0.02310
C	2.15236	–0.86560	–0.23345
C	0.77725	–0.79360	0.00191
C	0.17752	0.45429	0.24466
C	0.97215	1.60098	0.26236
N	–0.04227	–2.02487	0.06507
O	–1.03944	–2.04623	–0.64787
O	0.33350	–2.88719	0.83960
N	–1.21068	0.60389	0.52018
C	–1.90983	–0.15680	1.52090
N	–3.26971	–0.17991	1.13582
O	–1.37352	–0.65841	2.47531
N	2.81212	–2.14039	–0.59920
O	2.15891	–2.92416	–1.27656
O	3.97285	–2.27896	–0.23462
H	4.01465	0.20264	–0.39453
N	3.16351	2.71854	0.03571
O	2.58313	3.78022	0.24152
O	4.36545	2.58203	–0.16347
H	0.53556	2.56756	0.48026
C	–3.29625	0.40487	–0.00523
N	–2.11319	0.80996	–0.54020
N	–4.51640	0.69704	–0.78542
O	–5.54638	0.14483	–0.45554
O	–4.35348	1.50136	–1.70593
H	–2.06933	1.68225	–1.05994

A3 ZPE = 402.92 kJ/mol			
Coordinates (Å)			
Atom	X	Y	Z
C	2.42604	1.74084	–0.40152
C	1.23580	2.45818	–0.40246
C	2.40269	0.37756	–0.13376
C	1.20036	–0.27485	0.13747
C	–0.00973	0.42472	0.10789
C	0.03481	1.80213	–0.15708
N	–1.19733	2.62102	–0.20442
O	–2.25485	2.05456	–0.46392
O	–1.06336	3.82240	–0.00144
N	1.15378	–1.70101	0.53596
O	0.55992	–2.46203	–0.21592
O	1.66787	–1.97361	1.60981
H	1.21991	3.52327	–0.59412
N	–1.20296	–0.24802	0.46642
C	–2.10506	–0.95036	–0.30928
C	–1.74898	–0.18790	1.77964
N	–2.90652	–0.93315	1.62110
N	–3.12709	–1.37513	0.35473
O	–1.29636	0.37240	2.74966
N	–1.95582	–1.14873	–1.73699
O	–1.02318	–0.53758	–2.26386
O	–2.75955	–1.87952	–2.29205
H	–3.58943	–1.10677	2.34338
N	3.68239	–0.36095	–0.19524
O	3.62078	–1.56208	–0.42951
O	4.70522	0.29616	–0.03810
H	3.37691	2.21775	–0.60291

A3–enol–tautomer ZPE = 400.88 kJ/mol			
Coordinates (Å)			
Atom	X	Y	Z
C	2.40629	1.77364	–0.30588
C	1.21685	2.48561	–0.21768
C	2.39287	0.39154	–0.15165
C	1.19621	–0.28351	0.08497
C	–0.01232	0.41630	0.15051
C	0.02141	1.81056	0.00502
N	–1.20969	2.63023	0.07270
O	–2.27820	2.08452	–0.17905
O	–1.06121	3.81174	0.36695
N	1.12141	–1.74784	0.31347
O	0.72040	–2.42163	–0.62196
O	1.39953	–2.12553	1.44221
H	1.19639	3.56307	–0.31767
N	–1.19786	–0.31189	0.44589
C	–2.15109	–0.89037	–0.38441
C	–1.68860	–0.60239	1.69216
N	–2.80537	–1.28901	1.63073
N	–3.09251	–1.46752	0.29861
N	–2.08246	–0.80754	–1.82171
O	–1.13720	–0.15185	–2.27744
O	–2.94803	–1.37694	–2.46520
N	3.67782	–0.33342	–0.26570
O	3.62420	–1.55437	–0.35550
O	4.69758	0.34681	–0.27364
H	3.35229	2.26737	–0.48792
O	–1.04196	–0.19017	2.77597
H	–1.51849	–0.53033	3.55056

A3–aci–tautomer ZPE = 397.46 kJ/mol			
Coordinates (Å)			
Atom	X	Y	Z
C	2.46965	1.69714	–0.48002
C	1.29211	2.43500	–0.48562
C	2.42635	0.34281	–0.17055
C	1.21869	–0.27849	0.14580
C	0.01879	0.44145	0.12116
C	0.08468	1.80703	–0.20088
N	–1.13614	2.63884	–0.27470
O	–2.19181	2.07905	–0.55731
O	–0.99436	3.84013	–0.07830
N	1.15722	–1.69044	0.59059
O	0.53441	–2.46394	–0.12457
O	1.69552	–1.93983	1.65774
H	1.29096	3.49325	–0.71348
N	–1.17387	–0.19043	0.53142
C	–2.10119	–0.89671	–0.20129
C	–1.73727	–0.06727	1.83502
N	–2.97977	–0.80141	1.77861
N	–3.16182	–1.25564	0.59789
O	–1.26389	0.53155	2.76417
N	–2.02037	–1.15361	–1.49587
O	–1.11176	–0.79946	–2.25883
O	–3.07039	–1.89468	–2.01808
N	3.69033	–0.42144	–0.23936
O	3.60134	–1.62530	–0.45086
O	4.72846	0.21777	–0.11193
H	3.42529	2.14988	–0.71246
H	–2.79647	–1.97222	–2.95217

B3 ZPE = 403.15 kJ/mol			
Coordinates (Å)			
Atom	X	Y	Z
C	2.88167	1.69084	–0.18051
C	1.72951	2.45380	–0.03303
C	2.78292	0.30517	–0.20076
C	1.54836	–0.33507	–0.07833
C	0.37955	0.42122	0.08734
C	0.50286	1.82032	0.12542
N	–0.66036	2.69172	0.40999
O	–0.65955	3.79388	–0.12608
O	–1.50377	2.27217	1.19455
N	1.46712	–1.81656	–0.08803
O	0.69963	–2.31546	–0.90104
O	2.16319	–2.39835	0.72732
H	1.76640	3.53589	–0.02375
N	–0.87556	–0.20740	0.18412
C	–1.26461	–1.12188	1.19198
N	–2.60657	–1.31581	0.87030
O	–0.58789	–1.58858	2.07598
H	–3.25342	–1.92107	1.35506
N	4.02587	–0.45253	–0.46723
O	3.93513	–1.42771	–1.20210
O	5.05273	–0.00565	0.03044
H	3.85675	2.15054	–0.28324
N	–1.89867	0.15151	–0.65591
C	–2.89815	–0.53708	–0.21169
N	–4.22673	–0.51491	–0.79125
O	–5.04621	–1.24044	–0.22119
O	–4.41801	0.19747	–1.76344

B3–enol–tautomer ZPE = 402.28 kJ/mol			
Coordinates (Å)			
Atom	X	Y	Z
C	2.99497	1.46412	–0.33869
C	1.91917	2.34045	–0.24753
C	2.77871	0.09699	–0.21880
C	1.49395	–0.40876	–0.01244
C	0.40668	0.46141	0.11449
C	0.64513	1.83896	–0.00923
N	–0.45204	2.82706	0.11739
O	–0.31972	3.86720	–0.51693
O	–1.38368	2.55149	0.86439
N	1.21975	–1.86634	–0.02609
O	0.80184	–2.35721	1.01196
O	1.39874	–2.42628	–1.09625
H	2.05218	3.40951	–0.35466
N	–0.89966	–0.06469	0.27482
C	–1.56980	–0.40165	1.41679
N	–2.80829	–0.74033	1.14709
O	–0.96583	–0.34928	2.59377
N	3.95722	–0.79572	–0.27093
O	4.95316	–0.36008	–0.83685
O	3.85410	–1.88358	0.28338
H	4.00402	1.81971	–0.50601
N	–1.75722	–0.15034	–0.79607
C	–2.85217	–0.56337	–0.19702
N	–4.06910	–0.81893	–0.97270
O	–5.04433	–1.21154	–0.34423
O	–4.00614	–0.61602	–2.18003
H	–1.59585	–0.65067	3.26696

B3–1,3–tautomer ZPE = 401.99 kJ/mol			
Coordinates (Å)			
Atom	X	Y	Z
C	3.04467	1.32182	–0.48563
C	1.98379	2.22107	–0.51005
C	2.79764	–0.01625	–0.20879
C	1.50405	–0.45670	0.07548
C	0.41736	0.42619	0.03651
C	0.68963	1.76964	–0.28111
N	–0.39563	2.76340	–0.44729
O	–0.12016	3.92775	–0.19296
O	–1.46533	2.35124	–0.88566
N	1.24533	–1.84549	0.51891
O	1.77530	–2.19196	1.55879
O	0.49241	–2.51998	–0.18105
H	2.14046	3.27081	–0.72472
N	–0.85766	–0.04813	0.42381
C	–1.72661	0.66708	1.32171
N	–3.03699	0.22980	1.04264
O	–1.33739	1.47601	2.12554
N	3.93436	–0.95886	–0.27742
O	3.67126	–2.12373	–0.55500
O	5.05048	–0.49115	–0.08715
H	4.06123	1.63597	–0.68691
N	–1.67672	–0.71502	–0.50429
C	–2.91354	–0.55623	0.03461
N	–4.01909	–1.31655	–0.58564
O	–5.15414	–1.02898	–0.25983
O	–3.66104	–2.18713	–1.37992
H	–1.35012	–1.62708	–0.82197

A4 ZPE = 403.43 kJ/mol			
Coordinates (Å)			
Atom	X	Y	Z
C	–2.30755	0.57387	–0.10122
C	–1.30759	1.47731	–0.42328
C	–1.97402	–0.74508	0.20946
C	–0.65030	–1.15609	0.18651
C	0.37323	–0.25877	–0.13626
C	0.02014	1.06437	–0.45927
N	–3.70415	1.03930	–0.21145
O	–4.51546	0.24098	–0.66317
O	–3.92188	2.20189	0.10998
N	1.00256	2.07929	–0.89701
O	2.11618	1.68651	–1.24166
O	0.62867	3.24439	–0.92099
H	–1.55676	2.50295	–0.66170
N	1.68763	–0.78418	–0.15141
C	2.87213	–0.35615	0.42223
C	2.02547	–1.89989	–0.97954
N	3.39320	–1.98274	–0.78460
N	3.89591	–1.06482	0.07846
O	1.29046	–2.57642	–1.65913
N	2.97671	0.69857	1.41362
O	1.90570	1.17241	1.80451
O	4.09352	1.01246	1.78710
H	3.99735	–2.68107	–1.19205
N	–2.96936	–1.72542	0.69577
O	–3.78348	–1.31610	1.51241
O	–2.85291	–2.87313	0.28436
H	–0.41351	–2.18311	0.43121

A4–enol–tautomer ZPE = 401.40 kJ/mol			
Coordinates (Å)			
Atom	X	Y	Z
C	–2.29980	0.53447	–0.09498
C	–1.32948	1.46893	–0.42703
C	–1.92809	–0.77301	0.21655
C	–0.59183	–1.14705	0.17578
C	0.39368	–0.22394	–0.17459
C	0.00645	1.09077	–0.48071
N	–3.71159	0.96049	–0.19025
O	–4.49739	0.14901	–0.66263
O	–3.96217	2.10667	0.16157
N	0.97255	2.13491	–0.89028
O	2.08022	1.76726	–1.27108
O	0.58320	3.29486	–0.84522
H	–1.60931	2.49008	–0.65168
N	1.73631	–0.69692	–0.22426
C	2.87069	–0.40197	0.52529
C	2.23395	–1.56997	–1.15520
N	3.51614	–1.79886	–0.98350
N	3.91161	–1.05283	0.09666
N	2.86476	0.49363	1.65392
O	1.78174	1.04249	1.90138
O	3.90600	0.63741	2.27165
N	–2.89077	–1.78438	0.70385
O	–3.72934	–1.40088	1.50680
O	–2.72561	–2.93030	0.30134
H	–0.31951	–2.16375	0.43023
O	1.44055	–2.08284	–2.08888
H	1.98472	–2.65764	–2.65166

A4–aci–tautomer ZPE = 398.30 kJ/mol			
Coordinates (Å)			
Atom	X	Y	Z
C	2.31918	–0.59867	–0.08747
C	1.30029	–1.47969	–0.40762
C	2.01525	0.73407	0.20195
C	0.70415	1.17796	0.16699
C	–0.34282	0.30149	–0.15227
C	–0.01714	–1.03367	–0.46140
N	3.70410	–1.09825	–0.18029
O	4.54234	–0.31969	–0.61753
O	3.88915	–2.26711	0.14085
N	–1.01399	–2.01878	–0.92400
O	–2.07896	–1.58520	–1.36360
O	–0.69660	–3.20133	–0.88409
H	1.52568	–2.51303	–0.63635
N	–1.64267	0.84505	–0.14963
C	–2.83239	0.38496	0.36756
C	–2.00405	2.00031	–0.91848
N	–3.43415	2.13229	–0.77028
N	–3.87646	1.19768	–0.02367
O	–1.25850	2.70718	–1.54132
N	–2.97306	–0.61066	1.22755
O	–2.06264	–1.32795	1.66967
O	–4.27017	–0.85937	1.64363
N	3.03091	1.69280	0.68996
O	3.81334	1.27406	1.53287
O	2.96017	2.83498	0.25447
H	0.49082	2.21190	0.40412
H	–4.13919	–1.64481	2.20955

B4 ZPE = 403.17 kJ/mol			
Coordinates (Å)			
Atom	X	Y	Z
C	2.66491	0.56836	–0.06313
C	1.70614	1.55552	0.10721
C	2.27421	–0.77141	–0.13913
C	0.93711	–1.12516	–0.05640
C	–0.04169	–0.13720	0.11725
C	0.36694	1.20240	0.22796
N	4.07933	0.98492	–0.03666
O	4.86735	0.22920	0.51843
O	4.33859	2.07776	–0.52909
N	–0.56306	2.29226	0.59224
O	–0.35652	3.38787	0.08441
O	–1.42565	2.02825	1.42276
H	2.00212	2.59474	0.17604
N	–1.39345	–0.51643	0.11238
C	–1.92951	–1.69288	0.70287
N	–3.28839	–1.52884	0.44251
O	–1.34478	–2.58819	1.26518
H	–4.02586	–2.16692	0.70602
N	3.22792	–1.85838	–0.45333
O	4.02735	–1.63837	–1.35337
O	3.09263	–2.90247	0.17207
H	0.65452	–2.16696	–0.13195
N	–2.34928	0.27611	–0.47232
C	–3.44881	–0.36293	–0.24817
N	–4.75732	0.07470	–0.69764
O	–5.68252	–0.67896	–0.38343
O	–4.82857	1.11599	–1.32834

B4–enol–tautomer ZPE = 402.97 kJ/mol			
Coordinates (Å)			
Atom	X	Y	Z
C	2.65729	0.54846	–0.06678
C	1.71223	1.54358	0.13845
C	2.25279	–0.78251	–0.19160
C	0.90932	–1.11956	–0.11339
C	–0.04963	–0.12978	0.11481
C	0.37046	1.20039	0.25633
N	4.07876	0.94858	–0.02999
O	4.84505	0.19665	0.55844
O	4.35670	2.02552	–0.54388
N	–0.56100	2.28665	0.63205
O	–0.33037	3.39387	0.16256
O	–1.44836	2.00153	1.42729
H	2.01983	2.57769	0.23134
N	–1.41535	–0.48747	0.12815
C	–2.05701	–1.46533	0.83995
N	–3.34740	–1.44437	0.61097
O	–1.37403	–2.28555	1.63142
N	3.19148	–1.86969	–0.54520
O	4.04239	–1.60903	–1.38406
O	2.99645	–2.95364	–0.00708
H	0.61369	–2.15253	–0.24614
N	–2.34283	0.21262	–0.59958
C	–3.44895	–0.40984	–0.26342
N	–4.73642	0.00118	–0.83017
O	–5.72417	–0.60187	–0.42920
O	–4.71058	0.90865	–1.65301
H	–2.00770	–2.87901	2.06536

B4–1,3–tautomer ZPE = 401.62 kJ/mol			
Coordinates (Å)			
Atom	X	Y	Z
C	–2.67018	0.55798	0.09914
C	–1.73090	1.56508	0.00963
C	–2.24462	–0.77154	0.01423
C	–0.91061	–1.08568	–0.14576
C	0.07611	–0.07732	–0.22558
C	–0.37952	1.26767	–0.17703
N	–4.08945	0.94240	0.15908
O	–4.89497	0.16261	–0.33604
O	–4.34606	2.03073	0.66437
N	0.46173	2.44866	–0.41977
O	0.09132	3.51912	0.03741
O	1.46810	2.30811	–1.13499
H	–2.04764	2.59880	0.05361
N	1.41250	–0.48306	–0.30304
C	1.91869	–1.84634	–0.41977
N	3.28275	–1.79795	–0.09653
O	1.25820	–2.80720	–0.72668
N	–3.16629	–1.91259	0.22265
O	–3.83088	–1.88352	1.24928
O	–3.13324	–2.80304	–0.61456
H	–0.61314	–2.12376	–0.20079
N	2.47011	0.29484	0.17175
C	3.51832	–0.56623	0.17672
N	4.84857	–0.00750	0.49421
O	5.74991	–0.79504	0.70605
O	4.90062	1.22215	0.50306
H	2.55360	1.23832	–0.22391

A5 ZPE = 403.70 kJ/mol			
Coordinates (Å)			
Atom	X	Y	Z
C	2.73996	–0.05070	0.09988
C	2.05352	–1.21901	–0.19484
C	2.09408	1.16854	0.23430
C	0.71168	1.19973	0.09911
C	–0.04144	0.04340	–0.17039
C	0.67292	–1.15793	–0.33502
N	4.20954	–0.10449	0.25963
O	4.78144	0.95145	0.50919
O	4.74402	–1.20073	0.12965
N	–0.00228	–2.42990	–0.67752
O	–1.18217	–2.56250	–0.36722
O	0.68205	–3.27356	–1.24584
N	0.06903	2.52311	0.28588
O	–1.08539	2.54853	0.70244
O	0.76086	3.50343	0.04039
H	2.57857	–2.15528	–0.32923
H	2.64826	2.07539	0.43684
N	–1.42894	0.13342	–0.42061
C	–2.51175	–0.17528	0.37645
C	–1.94710	0.74259	–1.59676
N	–3.30978	0.65497	–1.36652
N	–3.64593	0.12402	–0.16106
O	–1.33074	1.19952	–2.53127
N	–2.39244	–0.72599	1.70983
O	–1.24224	–0.80152	2.15159
O	–3.41864	–1.04909	2.28408
H	–4.02611	1.02165	–1.97546

A5–enol–tautomer ZPE = 401.70 kJ/mol			
Coordinates (Å)			
Atom	X	Y	Z
C	–2.72744	–0.00039	0.11417
C	–2.06145	1.21308	0.03255
C	–2.06115	–1.21348	0.02952
C	–0.67966	–1.19907	–0.11615
C	0.05091	0.00031	–0.17588
C	–0.67994	1.19937	–0.11316
N	–4.19787	–0.00076	0.27942
O	–4.75042	–1.09390	0.33964
O	–4.75069	1.09210	0.34229
N	–0.01742	2.52244	–0.18972
O	1.14429	2.60636	0.19283
O	–0.70013	3.44685	–0.61759
N	–0.01684	–2.52177	–0.19618
O	1.14466	–2.60657	0.18680
O	–0.69913	–3.44504	–0.62718
H	–2.60113	2.15002	0.07220
H	–2.60062	–2.15064	0.06679
N	1.44869	0.00083	–0.42795
C	2.53326	–0.00105	0.43604
C	2.05750	0.00424	–1.65252
N	3.36616	0.00425	–1.54930
N	3.66054	0.00088	–0.20762
O	1.32686	0.00708	–2.76398
N	2.37233	–0.00446	1.86532
O	1.20162	–0.00487	2.27120
O	3.37797	–0.00656	2.55504
H	1.94039	0.00935	–3.51668

A5–aci–tautomer ZPE = 399.51 kJ/mol			
Coordinates (Å)			
Atom	X	Y	Z
C	–2.77672	–0.07003	–0.13487
C	–2.08313	–1.22717	0.18412
C	–2.14135	1.15518	–0.27100
C	–0.76260	1.20057	–0.11305
C	0.00009	0.05784	0.19594
C	–0.70625	–1.15126	0.35763
N	–4.24190	–0.14235	–0.32411
O	–4.82016	0.90497	–0.59469
O	–4.76636	–1.24369	–0.19695
N	–0.03272	–2.41151	0.74839
O	1.17186	–2.51627	0.53998
O	–0.74165	–3.27400	1.25472
N	–0.12605	2.52136	–0.33554
O	1.01111	2.53561	–0.79851
O	–0.80791	3.50524	–0.08035
H	–2.60074	–2.16772	0.31711
H	–2.70065	2.05305	–0.49875
N	1.37582	0.17533	0.46221
C	2.45995	–0.17257	–0.29836
C	1.92015	0.89358	1.57596
N	3.34601	0.84607	1.40099
N	3.61054	0.23751	0.30160
O	1.28843	1.41978	2.45460
N	2.48215	–0.77541	–1.48599
O	1.50923	–1.15312	–2.12279
O	3.72733	–0.99558	–2.05164
H	4.36863	–0.62271	–1.40434

B5 ZPE = 403.80 kJ/mol			
Coordinates (Å)			
Atom	X	Y	Z
C	–3.08192	–0.31080	–0.13099
C	–2.25016	–1.40875	0.04080
C	–2.58599	0.98262	–0.21098
C	–1.21056	1.17051	–0.15534
C	–0.32207	0.09791	0.04509
C	–0.88575	–1.18569	0.16633
N	–4.54028	–0.52628	–0.22936
O	–5.24256	0.46832	–0.38040
O	–4.93905	–1.68423	–0.15288
N	–0.06374	–2.36566	0.52344
O	–0.39482	–3.43347	0.02325
O	0.84216	–2.19439	1.33152
N	–0.73592	2.55393	–0.40041
O	0.31628	2.68985	–1.01491
O	–1.46828	3.45624	–0.01685
H	–2.65448	–2.41037	0.10709
H	–3.25032	1.82656	–0.34235
N	1.06222	0.29420	0.13115
C	1.70730	1.18598	1.02497
N	3.04490	0.90177	0.76333
O	1.20030	1.96297	1.79691
H	3.84327	1.34633	1.19335
N	1.93227	–0.47905	–0.59331
C	3.09115	–0.07514	–0.18854
N	4.35375	–0.58498	–0.68716
O	4.32436	–1.45072	–1.54634
O	5.35126	–0.07205	–0.17280

B5–enol–tautomer ZPE = 403.44 kJ/mol			
Coordinates (Å)			
Atom	X	Y	Z
C	–3.06662	–0.31404	–0.15946
C	–2.23773	–1.40630	0.05804
C	–2.57283	0.97829	–0.25584
C	–1.19878	1.17194	–0.16921
C	–0.31528	0.10519	0.07146
C	–0.87724	–1.17578	0.20722
N	–4.52359	–0.53463	–0.28696
O	–5.22211	0.45499	–0.47979
O	–4.92157	–1.69064	–0.18930
N	–0.05263	–2.34428	0.59811
O	–0.35523	–3.41700	0.09228
O	0.81974	–2.15331	1.43674
N	–0.72283	2.55940	–0.39100
O	0.37406	2.70928	–0.91604
O	–1.49069	3.45493	–0.05940
H	–2.64092	–2.40784	0.13421
H	–3.23649	1.81717	–0.41875
N	1.07994	0.27776	0.15571
C	1.82003	1.05892	0.99813
N	3.10187	0.87882	0.80063
O	1.21847	1.85701	1.87170
N	1.92632	–0.46342	–0.62765
C	3.09368	–0.04769	–0.19252
N	4.33234	–0.57296	–0.77226
O	4.21311	–1.38195	–1.68509
O	5.37837	–0.15590	–0.29065
H	1.90288	2.34327	2.35815

B5–1,3–tautomer ZPE = 401.84 kJ/mol			
Coordinates (Å)			
Atom	X	Y	Z
C	–3.05959	–0.40202	–0.10872
C	–2.15979	–1.45166	0.01906
C	–2.64232	0.91951	–0.18456
C	–1.27865	1.18343	–0.18678
C	–0.31915	0.16320	–0.04831
C	–0.80630	–1.15115	0.09434
N	–4.50544	–0.70160	–0.15522
O	–5.26956	0.25193	–0.26343
O	–4.83232	–1.88232	–0.08467
N	0.09254	–2.27666	0.43141
O	–0.16501	–3.36055	–0.07973
O	0.99127	–2.05027	1.23448
N	–0.88962	2.59847	–0.40595
O	0.09987	2.81363	–1.09630
O	–1.63062	3.44333	0.07894
H	–2.50518	–2.47444	0.09758
H	–3.35941	1.72588	–0.26633
N	1.04365	0.48954	–0.02171
C	1.68382	1.13958	1.09304
N	3.05360	0.80042	1.00999
O	1.10196	1.81306	1.90088
N	1.99438	–0.30761	–0.66274
C	3.14751	0.03737	–0.01423
N	4.40874	–0.47838	–0.58092
O	4.30641	–0.93082	–1.72306
O	5.40950	–0.40373	0.10325
H	1.99436	–0.30441	–1.68127

A6 ZPE = 402.80 kJ/mol			
Coordinates (Å)			
Atom	X	Y	Z
C	–1.99762	–0.08569	–0.02223
C	–1.42947	1.15934	0.25444
C	–1.13282	–1.13128	–0.35929
C	0.24156	–0.94523	–0.43549
C	0.78388	0.29878	–0.12017
C	–0.05302	1.35796	0.22281
N	–3.46896	–0.29232	0.03431
O	–4.03479	–0.38220	–1.04178
O	–3.95502	–0.35077	1.15066
N	2.18240	0.53714	–0.21216
C	3.27823	–0.20957	0.18848
C	2.70340	1.64085	–0.95431
N	4.06455	1.38956	–0.90733
N	4.40910	0.28431	–0.20271
O	2.09541	2.54365	–1.48044
N	3.23445	–1.36534	1.07248
O	2.15686	–1.57615	1.63276
O	4.26200	–2.01213	1.19403
H	4.77930	1.98124	–1.30520
N	–1.63419	–2.49737	–0.63515
O	–0.89584	–3.23541	–1.27974
O	–2.73286	–2.79288	–0.18364
H	0.33648	2.33991	0.45311
N	–2.26463	2.34043	0.57257
O	–3.43248	2.31601	0.20498
O	–1.71255	3.26214	1.16391
H	0.85431	–1.78509	–0.73337

A6–enol–tautomer ZPE = 400.88 kJ/mol			
Coordinates (Å)			
Atom	X	Y	Z
C	–1.98386	–0.05679	–0.00616
C	–1.36854	1.16006	0.29404
C	–1.16536	–1.11987	–0.40327
C	0.21166	–0.97786	–0.51166
C	0.79931	0.24043	–0.18048
C	0.01357	1.31229	0.22566
N	–3.46004	–0.21814	0.08395
O	–4.05521	–0.23552	–0.97989
O	–3.91664	–0.31623	1.20899
N	2.21142	0.42296	–0.30956
C	3.30596	–0.21571	0.27134
C	2.82486	1.31608	–1.14964
N	4.13506	1.23575	–1.09136
N	4.43238	0.25839	–0.17753
O	2.10323	2.13294	–1.90999
N	3.20391	–1.23362	1.29239
O	2.06058	–1.51011	1.67532
O	4.24254	–1.73065	1.69514
N	–1.72260	–2.45869	–0.70982
O	–1.02571	–3.19926	–1.39524
O	–2.82099	–2.72821	–0.24229
H	0.44388	2.26985	0.48866
N	–2.15173	2.36020	0.66985
O	–3.33980	2.36965	0.37527
O	–1.53894	3.26420	1.22868
H	0.79706	–1.82581	–0.84127
H	2.72217	2.66188	–2.43973

A6–aci–tautomer ZPE = 398.77 kJ/mol			
Coordinates (Å)			
Atom	X	Y	Z
C	–2.03331	–0.12061	–0.01567
C	–1.51062	1.15105	0.23081
C	–1.12885	–1.14236	–0.31468
C	0.23945	–0.91085	–0.38657
C	0.73703	0.36149	–0.10411
C	–0.14347	1.39949	0.20566
N	–3.49635	–0.37741	0.03787
O	–4.04929	–0.53509	–1.03717
O	–3.99073	–0.40412	1.15216
N	2.12346	0.64086	–0.17392
C	3.21675	–0.13838	0.12094
C	2.67259	1.79123	–0.83626
N	4.09703	1.59105	–0.86293
N	4.36665	0.47348	–0.29788
O	2.05410	2.72752	–1.27099
N	3.30490	–1.25129	0.85883
O	2.38244	–1.85861	1.38331
O	4.57282	–1.78563	1.02361
N	–1.57875	–2.53347	–0.55139
O	–0.81698	–3.25931	–1.18242
O	–2.66155	–2.85909	–0.08236
H	0.20831	2.40046	0.41312
N	–2.39178	2.30877	0.51040
O	–3.54696	2.24113	0.10955
O	–1.88650	3.25467	1.10469
H	0.88162	–1.73980	–0.64930
H	5.17778	–1.14270	0.58556

B6 ZPE = 403.31 kJ/mol			
Coordinates (Å)			
Atom	X	Y	Z
C	–2.34248	0.18728	–0.00074
C	–1.81573	–1.10548	–0.00206
C	–1.43366	1.24869	–0.00070
C	–0.06171	1.04089	0.01130
C	0.43475	–0.26532	–0.00071
C	–0.44753	–1.35005	–0.01424
N	–3.80813	0.42545	0.00175
O	–4.27787	0.85127	1.04383
O	–4.39230	0.17112	–1.03843
N	1.83057	–0.46824	–0.00018
C	2.52314	–1.70710	0.02382
N	3.85124	–1.28071	0.02018
O	2.07974	–2.83257	0.04286
H	4.66557	–1.87857	0.03225
N	–1.89028	2.65681	–0.06123
O	–1.11362	3.50767	0.35868
O	–2.99456	2.86460	–0.54871
H	–0.09113	–2.37098	–0.02857
N	–2.69799	–2.29487	0.05478
O	–3.80474	–2.14402	0.55814
O	–2.24015	–3.34359	–0.38440
H	0.60182	1.89498	0.02508
N	2.67747	0.61119	–0.01504
C	3.85561	0.08087	–0.00285
N	5.09435	0.83630	–0.01357
O	6.11494	0.14333	0.00118
O	5.02218	2.05399	–0.03548

B6–enol–tautomer ZPE = 403.25 kJ/mol			
Coordinates (Å)			
Atom	X	Y	Z
C	–2.33197	0.19443	0.00226
C	–1.81252	–1.10102	0.00121
C	–1.41697	1.25108	–0.00424
C	–0.04615	1.03626	–0.01937
C	0.44286	–0.27255	–0.00472
C	–0.44423	–1.34908	0.01018
N	–3.79713	0.44152	0.00942
O	–4.36981	0.21711	1.06215
O	–4.27398	0.84283	–1.03865
N	1.84606	–0.46765	–0.00455
C	2.61450	–1.60538	–0.02323
N	3.89416	–1.31715	–0.01724
O	2.07026	–2.81841	–0.04570
N	–1.86734	2.66292	0.04677
O	–1.08473	3.50618	–0.37475
O	–2.97362	2.87689	0.52690
H	–0.11080	–2.37650	0.02633
N	–2.69529	–2.29031	–0.05236
O	–3.82511	–2.12886	–0.49512
O	–2.21441	–3.35266	0.32924
H	0.62721	1.88288	–0.03747
N	2.68648	0.61586	0.01414
C	3.86430	0.03788	0.00552
N	5.08964	0.84216	0.02096
O	6.14597	0.22288	0.00765
O	4.94735	2.05897	0.04570
H	2.79309	–3.46692	–0.05380

B6–1,3–tautomer ZPE = 401.61 kJ/mol			
Coordinates (Å)			
Atom	X	Y	Z
C	2.33399	0.19567	–0.00731
C	1.82427	–1.10175	–0.11601
C	1.41055	1.23985	0.05803
C	0.04068	1.01301	0.00249
C	–0.44106	–0.29307	–0.11221
C	0.46229	–1.36393	–0.16420
N	3.79627	0.45297	0.03475
O	4.27788	0.95522	–0.96706
O	4.36421	0.13705	1.06656
N	–1.81989	–0.54264	–0.20446
C	–2.52622	–1.70050	0.27852
N	–3.88445	–1.32320	0.39536
O	–2.01551	–2.76358	0.52493
N	1.83715	2.64603	0.24579
O	1.03416	3.51394	–0.08508
O	2.94188	2.83655	0.73625
H	0.11882	–2.38735	–0.22841
N	2.72654	–2.27197	–0.24831
O	3.84362	–2.06287	–0.70591
O	2.27227	–3.35926	0.08572
H	–0.61714	1.86877	0.07549
N	–2.73174	0.51455	–0.24855
C	–3.91999	–0.09437	0.03550
N	–5.14007	0.72219	–0.11327
O	–6.17300	0.28558	0.35297
O	–4.97194	1.78190	–0.72053
H	–2.68377	1.16740	–1.02796

APPENDIX B

The Cartesian coordinates of the optimized PATO and its possible clockwise (CW) and counterclockwise (CCW) 1,3– and 1,5– tautomers presented in Chapter 4 (B3LYP/6–31G(d,p)). For all structures total charge = 0, multiplicity = 1 and number of imaginary frequencies = 0.

PATO ZPE = 433.65 kJ/mol			
Coordinates (Å)			
Atom	X	Y	Z
H	0.49300	1.13200	–3.49000
C	0.43500	1.08600	–2.41100
C	0.33300	0.96300	0.36600
C	0.43500	–0.14900	–1.77300
C	0.33800	2.24300	–1.65900
C	0.29800	2.19000	–0.26900
C	0.32900	–0.27800	–0.34500
H	0.27700	3.09900	0.31800
N	0.51800	–1.31300	–2.66000
O	0.42400	–1.12700	–3.86700
O	0.69500	–2.43600	–2.15800
N	0.54400	1.02600	1.82300
O	1.29600	0.18700	2.31200
O	0.01400	1.94900	2.43200
N	0.31400	3.54300	–2.33300
O	0.22600	4.54400	–1.62300
O	0.38000	3.54500	–3.56100
N	0.20800	–1.50000	0.23300
H	0.42500	–2.27700	–0.39100
C	–0.41800	–1.85300	1.42200
N	–0.23700	–3.10100	1.93300
N	–1.26300	–1.07200	2.08100
C	–1.01600	–3.08200	3.00000
H	–1.16100	–3.89200	3.70100
N	–1.62700	–1.88400	3.10600
H	–2.26000	–1.54200	3.81300

1,3–CW–Tautomer ZPE = 427.57 kJ/mol			
Coordinates (Å)			
Atom	X	Y	Z
H	0.08300	1.03300	–3.35600
C	0.16500	1.03400	–2.27700
C	0.43200	1.03500	0.49000
C	0.27100	–0.17100	–1.59600
C	0.14500	2.22400	–1.57200
C	0.28500	2.23200	–0.18900
C	0.36100	–0.24300	–0.15600
H	0.31100	3.16500	0.35800
N	0.24900	–1.36700	–2.44400
O	0.15500	–1.21500	–3.65600
O	0.33300	–2.48900	–1.91100
N	0.79100	1.17700	1.90500
O	1.61900	0.37600	2.35300
O	0.31600	2.11800	2.52800
N	0.01100	3.49200	–2.29200
O	0.00600	4.52300	–1.62100
O	–0.08900	3.43800	–3.51700
N	0.33400	–1.44400	0.46300
H	0.31500	–2.23000	–0.19000
C	0.00800	–1.77200	1.82700
N	–0.28900	–3.18200	1.94200
N	–1.20400	–1.03900	2.31700
C	–1.42900	–3.20700	2.50800
H	–1.97200	–4.09700	2.80400
N	–2.01600	–1.88500	2.74800
H	0.81000	–1.50700	2.53200

1,5–CW–Tautomer ZPE = 427.81 kJ/mol			
Coordinates (Å)			
Atom	X	Y	Z
H	0.35100	1.18900	–3.47100
C	0.33200	1.13600	–2.39100
C	0.31900	0.99800	0.39000
C	0.37800	–0.09900	–1.75600
C	0.24200	2.28700	–1.62900
C	0.24500	2.22900	–0.24100
C	0.32600	–0.23400	–0.33000
H	0.22200	3.13400	0.35100
N	0.45600	–1.26100	–2.65200
O	0.26000	–1.07700	–3.84600
O	0.73500	–2.37000	–2.16900
N	0.54100	1.06200	1.84900
O	1.19000	0.15000	2.36000
O	0.12900	2.05200	2.43800
N	0.17800	3.59300	–2.29700
O	0.10000	4.58800	–1.58000
O	0.20600	3.59800	–3.52600
N	0.27700	–1.47500	0.24000
H	0.55600	–2.23100	–0.38600
C	–0.31700	–1.86000	1.42400
N	–0.16500	–3.00600	1.97200
N	–1.30200	–1.00300	2.06400
C	–1.08200	–2.95700	3.07800
N	–1.75700	–1.64200	3.04000
H	–0.57000	–3.06000	4.04500
H	–1.84900	–3.74100	3.02400

1,3–CCW–Tautomer ZPE = 431.33 kJ/mol			
Coordinates (Å)			
Atom	X	Y	Z
H	0.36800	1.30600	–3.40600
C	0.32400	1.20900	–2.33000
C	0.24200	0.95500	0.44100
C	0.31500	–0.05500	–1.74800
C	0.25700	2.32900	–1.52200
C	0.21900	2.21100	–0.13500
C	0.23700	–0.24800	–0.32900
H	0.20100	3.09200	0.49200
N	0.35900	–1.17700	–2.68900
O	0.27500	–0.93300	–3.88500
O	0.49500	–2.33200	–2.24200
N	0.40400	0.94400	1.90700
O	1.08300	0.03800	2.38900
O	–0.08600	1.87300	2.53600
N	0.25500	3.66200	–2.13300
O	0.19700	4.62800	–1.37500
O	0.31100	3.72000	–3.36000
N	0.16000	–1.50100	0.20400
H	0.25700	–2.23000	–0.50700
C	–0.54200	–1.81900	1.36700
N	–1.66000	–1.27100	1.77500
C	–1.11300	–2.82700	3.18600
N	–2.01800	–1.91200	2.94700
N	–0.15200	–2.82100	2.20800
H	0.72100	–3.32700	2.18900
H	–1.11000	–3.51200	4.02100

1,5–CCW–Tautomer ZPE = 432.66 kJ/mol			
Coordinates (Å)			
Atom	X	Y	Z
H	0.62800	1.15200	–3.39900
C	0.52400	1.08500	–2.32400
C	0.30800	0.91100	0.43500
C	0.44800	–0.16100	–1.71700
C	0.44300	2.23300	–1.55200
C	0.34200	2.15500	–0.16800
C	0.28500	–0.31400	–0.29700
H	0.32900	3.05400	0.43600
N	0.52300	–1.31200	–2.62400
O	0.49800	–1.09700	–3.82900
O	0.62200	–2.44900	–2.13500
N	0.44100	0.91800	1.90100
O	1.22200	0.11200	2.39600
O	–0.22200	1.75000	2.52100
N	0.49700	3.54700	–2.19900
O	0.41700	4.53400	–1.47100
O	0.61400	3.56900	–3.42200
N	0.08400	–1.53900	0.25100
H	0.30800	–2.31300	–0.37600
C	–0.50400	–1.93400	1.44700
N	–0.32500	–3.14400	1.94300
N	–1.42400	–1.25600	2.17900
C	–1.16200	–3.15000	3.01800
N	–1.84600	–2.03500	3.21500
H	–1.78000	–0.31500	2.09700
H	–1.26800	–4.00200	3.67400

APPENDIX C

The Cartesian coordinates of the optimized structures presented in section 5.3.3 (HF/6–311++G(d,p)).

Isolated PATO

charge = 0, multiplicity = 1
number of imaginary frequencies = 0
ZPE = 471.68 kJ/mol

Coordinates (Å)			
Atom	X	Y	Z
H	0.36286	1.11202	–3.44369
C	0.37654	1.06769	–2.37440
C	0.41945	0.93342	0.37562
C	0.42584	–0.15377	–1.73566
C	0.32392	2.21368	–1.62201
C	0.34594	2.15503	–0.24369
C	0.41762	–0.29040	–0.32874
H	0.33397	3.05095	0.34279
N	0.45369	–1.31838	–2.62003
O	0.02679	–1.18104	–3.71400
O	0.92126	–2.33185	–2.20045
N	0.62396	0.99760	1.82705
O	1.39180	0.23139	2.30180
O	0.05701	1.85691	2.41291
N	0.26878	3.50900	–2.28596
O	0.21035	4.47102	–1.59456
O	0.28408	3.51356	–3.47208
N	0.38311	–1.50834	0.27537
H	0.68745	–2.28561	–0.26584
C	–0.36801	–1.83987	1.39044
N	–0.19409	–3.03378	1.98918
N	–1.28429	–1.08901	1.89811
C	–1.06757	–2.98726	2.95126
H	–1.24657	–3.75639	3.67445
N	–1.72384	–1.83912	2.92672
H	–2.42905	–1.49843	3.53640

Isolated Nitronium Ion

charge = 1, multiplicity = 1
number of imaginary frequencies = 0
ZPE = 34.66 kJ/mol

Coordinates (Å)			
Atom	X	Y	Z
N	0.00000	0.00000	0.00000
O	0.00000	0.00000	–1.08067
O	0.00000	0.00000	1.08067

PATO–N(2)–Pre–Transition State

charge = 1, multiplicity = 1
number of imaginary frequencies = 0
ZPE = 508.26 kJ/mol

Coordinates (Å)			
Atom	X	Y	Z
H	2.78434	–0.44260	1.84476
C	2.22155	–0.10913	0.99435
C	0.79391	0.79392	–1.19189
C	0.92107	0.32792	1.10761
C	2.77259	–0.11840	–0.26725
C	2.07565	0.31669	–1.37252
C	0.16667	0.81269	0.05106
H	2.52199	0.30118	–2.34702
N	0.31087	0.25854	2.44083
O	0.74942	0.93442	3.28371
O	–0.58482	–0.53472	2.58260
N	0.11310	1.30591	–2.38648
O	0.32137	0.73310	–3.39845
O	–0.57779	2.25837	–2.24780
N	4.14663	–0.60956	–0.43485
O	4.60431	–0.55212	–1.52183
O	4.68062	–1.02916	0.53484
N	–1.12041	1.33806	0.31686
H	–1.16263	2.33160	0.20500
C	–2.25388	0.75380	–0.21653
N	–3.31723	1.51606	–0.51962
C	–4.16557	0.65463	–0.99223
H	–5.14125	0.87981	–1.37393
N	–3.66464	–0.57052	–0.94647
H	–4.00990	–1.39058	–1.38953
N	–2.39860	–0.52065	–0.43884
N	–2.04480	–2.26254	1.60935
O	–1.24172	–2.76435	1.09001
O	–2.87243	–1.83079	2.15055

PATO–N(2)–Transition State

charge = 1, multiplicity = 1
number of imaginary frequencies = 1
ZPE = 504.36 kJ/mol

Coordinates (Å)			
Atom	X	Y	Z
H	2.93302	–0.44027	2.00861
C	2.40425	–0.16957	1.11542
C	1.05926	0.57214	–1.18500
C	1.09052	0.24274	1.15228
C	3.01629	–0.22345	–0.11682
C	2.37221	0.15365	–1.27332
C	0.37645	0.62903	0.02607
H	2.87926	0.13455	–2.21763
N	0.43335	0.25706	2.46366
O	0.98069	0.81241	3.33708
O	–0.60527	–0.33433	2.54965
N	0.41551	0.97855	–2.44203
O	1.10889	1.48769	–3.24710
O	–0.74294	0.74588	–2.55839
N	4.40980	–0.68660	–0.19546
O	4.90671	–0.69345	–1.26667
O	4.91363	–1.01847	0.82153
N	–0.90330	1.21092	0.17570
H	–0.93583	2.20971	0.16021
C	–2.10228	0.64951	–0.07743
N	–3.17344	1.44254	–0.20453
C	–4.14752	0.61130	–0.41638
H	–5.16724	0.88289	–0.60692
N	–3.73121	–0.64521	–0.38110
H	–4.19013	–1.43615	–0.77637
N	–2.37390	–0.64330	–0.20220
N	–1.78604	–2.10178	1.02091
O	–0.80436	–2.41380	0.61951
O	–2.63638	–2.21621	1.71673

PATO–N(2)–Intermediate charge = 1, multiplicity = 1 number of imaginary frequencies = 0 ZPE = 509.35 kJ/mol			
Coordinates (Å)			
Atom	X	Y	Z
H	0.21856	0.99365	–3.50479
C	0.45824	1.06619	–2.46211
C	1.06885	1.26154	0.22297
C	0.35333	–0.02909	–1.63029
C	0.87684	2.25624	–1.90978
C	1.18725	2.38116	–0.57390
C	0.66915	0.03577	–0.28323
H	1.50791	3.31930	–0.16530
N	–0.16403	–1.27250	–2.21184
O	0.13720	–1.51056	–3.32177
O	–0.87606	–1.93354	–1.51848
N	1.32992	1.42217	1.65753
O	2.17905	2.17235	1.96667
O	0.63767	0.79688	2.40219
N	0.98401	3.44047	–2.77587
O	1.34215	4.44121	–2.26014
O	0.70376	3.28972	–3.91360
N	0.75434	–1.14436	0.50573
H	1.63935	–1.61269	0.49006
C	–0.10720	–1.77378	1.27669
N	0.25490	–2.88452	1.91034
C	–0.78620	–3.28147	2.58876
H	–0.82139	–4.15488	3.21056
N	–1.81925	–2.48808	2.43513
H	–2.75053	–2.49514	2.79979
N	–1.40233	–1.50075	1.58668
N	–2.30786	–0.49749	1.23741
O	–1.90305	0.31987	0.51184
O	–3.36257	–0.61966	1.72972

PATO–N(4)–Pre–Transition State charge = 1, multiplicity = 1 number of imaginary frequencies = 0 ZPE = 510.65 kJ/mol			
Coordinates (Å)			
Atom	X	Y	Z
H	3.57207	–1.48358	–0.10037
C	2.73122	–0.82485	–0.01562
C	0.56985	0.85226	0.20508
C	1.44573	–1.32998	–0.07079
C	2.91281	0.52819	0.12958
C	1.83876	1.38273	0.23518
C	0.30483	–0.51525	0.01423
H	1.99059	2.43599	0.36367
N	1.34146	–2.78122	–0.24983
O	2.27611	–3.33961	–0.69248
O	0.32088	–3.31066	0.08165
N	–0.51031	1.81221	0.44330
O	–1.43994	1.45642	1.12228
O	–0.39448	2.89044	0.00192
N	4.26848	1.07325	0.18988
O	4.36527	2.24712	0.31462
O	5.16002	0.30090	0.10961
N	–0.98211	–1.00507	–0.08291
H	–1.03296	–2.00141	–0.03521
C	–1.90457	–0.43674	–0.96758
N	–1.58931	0.05793	–2.11202
C	–3.73613	0.15042	–1.75097
H	–4.77235	0.35089	–1.93354
N	–2.77483	0.44277	–2.60374
H	–2.83870	0.85672	–3.50703
N	–3.22748	–0.39611	–0.67654
N	–3.54100	0.23788	1.89658
O	–2.97373	–0.62474	2.20807
O	–4.14148	1.10129	1.64961

PATO–N(4)–Transition State

charge = 1, multiplicity = 1
number of imaginary frequencies = 1
ZPE = 508.06 kJ/mol

Coordinates (Å)			
Atom	X	Y	Z
H	3.70243	–1.54067	0.14648
C	2.88174	–0.85334	0.19130
C	0.76765	0.90315	0.30904
C	1.58179	–1.32013	0.15358
C	3.10351	0.49913	0.26926
C	2.05673	1.38946	0.32171
C	0.46679	–0.46500	0.19832
H	2.23916	2.44302	0.39401
N	1.43646	–2.77605	0.04548
O	2.36290	–3.38363	–0.34291
O	0.39048	–3.26065	0.37230
N	–0.28037	1.91514	0.47044
O	–1.27312	1.60253	1.06369
O	–0.07307	2.98525	0.03116
N	4.47637	1.00379	0.31015
O	4.60989	2.17828	0.37262
O	5.34215	0.19912	0.27656
N	–0.82714	–0.95000	0.14398
H	–0.89466	–1.94079	0.25909
C	–1.80548	–0.37474	–0.64283
N	–1.62963	0.09409	–1.82191
C	–3.71620	0.33492	–1.22004
H	–4.75076	0.61081	–1.26022
N	–2.84712	0.55078	–2.16832
H	–2.99374	0.96603	–3.06365
N	–3.10006	–0.26097	–0.22035
N	–3.68159	–0.19076	1.63050
O	–2.93257	–0.77471	2.18954
O	–4.60853	0.41794	1.59002

PATO–N(4)–Intermediate

charge = 1, multiplicity = 1
number of imaginary frequencies = 0
ZPE = 513.23 kJ/mol

Coordinates (Å)			
Atom	X	Y	Z
H	0.12812	1.71451	–3.60648
C	0.19921	1.61152	–2.54192
C	0.38212	1.33634	0.19754
C	0.19786	0.36087	–1.95757
C	0.28097	2.71531	–1.72816
C	0.36676	2.59784	–0.36093
C	0.27788	0.17626	–0.57492
H	0.43784	3.46823	0.26032
N	0.10967	–0.78056	–2.87583
O	–0.43197	–0.60043	–3.90218
O	0.60895	–1.80815	–2.52561
N	0.55144	1.29053	1.65575
O	1.12755	0.35380	2.11929
O	0.11837	2.19437	2.27143
N	0.28509	4.05233	–2.33184
O	0.34212	4.96960	–1.58775
O	0.22884	4.10183	–3.51126
N	0.25628	–1.11390	–0.02851
H	0.70373	–1.83100	–0.56109
C	–0.49418	–1.46241	1.02082
N	–1.50892	–0.83740	1.49242
C	–1.15179	–2.55925	2.81717
H	–1.23041	–3.27736	3.60831
N	–1.87192	–1.52338	2.60429
H	–2.64555	–1.20097	3.15174
N	–0.25191	–2.58331	1.81737
N	0.76664	–3.56205	1.71438
O	1.37785	–3.53009	0.72279
O	0.83835	–4.27207	2.63745

PATO–C(5)–(R)–Pre–Transition State

charge = 1, multiplicity = 1
number of imaginary frequencies = 0
ZPE = 511.44 kJ/mol

Coordinates (Å)			
Atom	X	Y	Z
H	3.57399	–1.28705	–0.19267
C	2.74179	–0.63477	–0.01754
C	0.59904	1.03024	0.40235
C	1.48458	–1.14945	0.22368
C	2.90153	0.73191	–0.02806
C	1.84687	1.58289	0.20003
C	0.35987	–0.34560	0.41718
H	1.99359	2.64430	0.22139
N	1.38463	–2.61389	0.25754
O	2.13577	–3.21522	–0.41919
O	0.57119	–3.09247	0.98635
N	–0.47718	1.97902	0.68876
O	–0.20693	2.92307	1.33158
O	–1.57368	1.75096	0.25103
N	4.23209	1.29730	–0.27286
O	4.31223	2.47806	–0.29391
O	5.11669	0.52974	–0.43095
N	–0.93607	–0.84958	0.65807
H	–0.88381	–1.69840	1.18613
C	–1.73333	–1.04956	–0.48654
N	–3.08021	–0.90323	–0.45418
N	–1.26222	–1.41826	–1.62432
C	–3.42999	–1.22807	–1.67230
N	–2.36057	–1.52240	–2.38328
H	–2.29624	–1.81230	–3.33341
H	–4.42684	–1.25343	–2.06335
N	–3.85196	1.04700	1.13057
O	–3.44015	0.55912	2.00027
O	–4.31556	1.57380	0.30987

PATO–C(5)–(R)–Transition State

charge = 1, multiplicity = 1
number of imaginary frequencies = 1
ZPE = 502.90 kJ/mol

Coordinates (Å)			
Atom	X	Y	Z
H	3.66284	–1.26852	–0.44082
C	2.90318	–0.57946	–0.12947
C	0.93942	1.19038	0.65084
C	1.64300	–1.02362	0.21339
C	3.15681	0.77023	–0.05291
C	2.19797	1.66975	0.35017
C	0.61621	–0.16108	0.59505
H	2.42116	2.71508	0.42996
N	1.42887	–2.47534	0.15958
O	2.00669	–3.06500	–0.68115
O	0.70122	–2.95284	0.97115
N	–0.04796	2.19062	1.06836
O	0.34412	3.06300	1.75530
O	–1.16080	2.06344	0.66902
N	4.49567	1.26469	–0.40137
O	4.65903	2.43436	–0.34900
O	5.29769	0.45265	–0.70840
N	–0.66128	–0.63802	0.97438
H	–0.65176	–1.35062	1.67480
C	–1.69649	–0.75925	0.11568
N	–2.78804	–1.43294	0.37494
N	–1.69918	–0.20414	–1.13307
C	–3.54510	–1.27033	–0.70078
N	–2.80423	–0.57561	–1.62666
H	–3.04672	–0.32582	–2.56760
H	–4.39743	–1.86247	–0.96882
N	–4.55181	0.53456	–0.15187
O	–3.77364	1.22508	0.25891
O	–5.65044	0.37022	–0.34959

PATO–C(5)–(R)–Wheland Intermediate

charge = 1, multiplicity = 1
number of imaginary frequencies = 0
ZPE = 512.02 kJ/mol

Coordinates (Å)			
Atom	X	Y	Z
H	0.00426	1.42851	–3.83256
C	0.18511	1.41042	–2.77568
C	0.63742	1.35372	–0.05360
C	0.33333	0.21304	–2.10757
C	0.27619	2.57582	–2.05087
C	0.51787	2.56983	–0.69851
C	0.53654	0.13572	–0.72969
H	0.61712	3.48882	–0.15554
N	0.27776	–1.00125	–2.93070
O	–0.45756	–0.98571	–3.84853
O	0.99194	–1.90206	–2.61918
N	0.92470	1.42146	1.38286
O	1.53054	2.34552	1.76521
O	0.51006	0.53273	2.07565
N	0.12432	3.86290	–2.74252
O	0.18202	4.83332	–2.07051
O	–0.04610	3.81740	–3.91043
N	0.69994	–1.11952	–0.11048
H	1.34512	–1.75098	–0.54245
C	–0.01076	–1.62889	0.89550
N	0.22078	–2.64897	1.58391
N	–1.29873	–0.99325	1.23970
C	–0.85529	–2.83487	2.45006
N	–1.73519	–1.67123	2.12834
H	–2.60596	–1.44224	2.58995
H	–1.41356	–3.75166	2.30117
N	–0.54178	–2.76027	3.92122
O	0.51151	–3.11110	4.26770
O	–1.46258	–2.38722	4.57556

PATO–C(5)–(S)–Pre–Transition State

charge = 1, multiplicity = 1
number of imaginary frequencies = 0
ZPE = 508.94 kJ/mol

Coordinates (Å)			
Atom	X	Y	Z
H	1.66780	–1.67633	–1.52200
C	1.63675	–0.84247	–0.85108
C	1.57250	1.26918	0.92114
C	0.48199	–0.53583	–0.15882
C	2.75841	–0.08437	–0.63321
C	2.74267	0.96203	0.26301
C	0.36677	0.56535	0.71412
H	3.62311	1.54861	0.43441
N	–0.57728	–1.51998	–0.28668
O	–0.66290	–2.13878	–1.30560
O	–1.28146	–1.74615	0.64681
N	1.64286	2.41329	1.83534
O	0.85186	2.45691	2.72576
O	2.49346	3.20492	1.64135
N	3.99161	–0.41469	–1.34284
O	4.93847	0.25368	–1.11234
O	3.94527	–1.32891	–2.09690
N	–0.81262	0.95363	1.28005
H	–0.73490	1.55051	2.07552
C	–2.00616	1.11783	0.59497
N	–3.01601	1.77327	1.19669
N	–2.23225	0.73456	–0.61756
C	–3.92258	1.80461	0.26617
N	–3.49297	1.18229	–0.82081
H	–3.91732	1.11867	–1.71656
H	–4.88762	2.26284	0.34510
N	–2.68224	–3.65764	–0.50694
O	–3.39534	–2.93926	–0.88245
O	–2.01138	–4.41808	–0.13614

PATO–C(5)–(S)–Transition State

charge = 1, multiplicity = 1
number of imaginary frequencies = 1
ZPE = 501.80 kJ/mol

Coordinates (Å)			
Atom	X	Y	Z
H	2.82144	–2.34861	–0.34043
C	2.42906	–1.37449	–0.12593
C	1.40448	1.13418	0.40014
C	1.15887	–1.21964	0.38870
C	3.17655	–0.24219	–0.35121
C	2.69167	1.01700	–0.08359
C	0.59751	0.02808	0.65284
H	3.29845	1.88614	–0.24236
N	0.39902	–2.44972	0.63776
O	0.56628	–3.33845	–0.11881
O	–0.32434	–2.46849	1.58272
N	0.93843	2.50024	0.66989
O	–0.20127	2.75109	0.43956
O	1.74235	3.25643	1.07971
N	4.53668	–0.38270	–0.88834
O	5.13086	0.61761	–1.09633
O	4.92316	–1.48489	–1.07103
N	–0.69481	0.15442	1.20208
H	–0.86960	–0.33515	2.05407
C	–1.78692	0.49253	0.50033
N	–2.98711	0.62514	1.02884
N	–1.76719	0.71040	–0.84250
C	–3.75905	0.91455	0.00756
N	–2.97015	1.02330	–1.11162
H	–3.22844	1.30862	–2.03764
H	–4.77026	1.26802	0.04807
N	–4.11297	–1.14111	–0.74894
O	–3.12815	–1.66831	–0.66479
O	–5.21457	–1.23399	–0.96775

PATO–C(5)–(S)–Wheland Intermediate charge = 1, multiplicity = 1 number of imaginary frequencies = 0 ZPE = 512.02 kJ/mol			
Coordinates (Å)			
Atom	X	Y	Z
H	0.34744	1.51765	–3.62390
C	0.45703	1.51122	–2.55712
C	0.72689	1.48356	0.18906
C	0.55598	0.32060	–1.86799
C	0.50270	2.68465	–1.84104
C	0.65414	2.69268	–0.47588
C	0.66582	0.25743	–0.47846
H	0.72035	3.61756	0.06201
N	0.55353	–0.90163	–2.68158
O	–0.11039	–0.89060	–3.65191
O	1.23729	–1.80316	–2.30910
N	0.92277	1.56887	1.63964
O	0.46673	0.68770	2.31764
O	1.50234	2.49782	2.04940
N	0.40126	3.96440	–2.55476
O	0.41616	4.94185	–1.89036
O	0.31003	3.90698	–3.73084
N	0.78074	–0.99044	0.16389
H	1.43040	–1.63989	–0.23423
C	0.00773	–1.47864	1.13478
N	0.18777	–2.49242	1.84799
N	–1.29578	–0.83527	1.38360
C	–0.90266	–2.60425	2.71056
N	–1.78956	–1.49297	2.25745
H	–2.71956	–1.29882	2.60567
H	–0.65822	–2.47211	3.75858
N	–1.70703	–3.87218	2.60936
O	–1.13354	–4.85054	2.34900
O	–2.85997	–3.72464	2.86403

Isolated 1,3–CCW–Tautomer charge = 0, multiplicity = 1 number of imaginary frequencies = 0 ZPE = 469.91 kJ/mol			
Coordinates (Å)			
Atom	X	Y	Z
H	0.28877	1.27770	–3.37207
C	0.29155	1.18623	–2.30586
C	0.30335	0.93464	0.43550
C	0.32892	–0.06483	–1.72000
C	0.24045	2.29785	–1.50691
C	0.24190	2.18118	–0.13137
C	0.31519	–0.25734	–0.32136
H	0.21787	3.05157	0.49197
N	0.35270	–1.18834	–2.65738
O	0.01452	–0.97885	–3.76818
O	0.72811	–2.25139	–2.25899
N	0.44509	0.93081	1.89582
O	1.14632	0.09990	2.37544
O	–0.10030	1.79265	2.49097
N	0.20457	3.62126	–2.11640
O	0.16139	4.55311	–1.38459
O	0.22139	3.67435	–3.30110
N	0.30699	–1.50117	0.24378
H	0.46486	–2.24615	–0.39849
C	–0.50410	–1.81376	1.33111
N	–1.64120	–1.30384	1.59802
C	–1.21321	–2.74979	3.10668
H	–1.27442	–3.38755	3.96308
N	–2.09008	–1.89625	2.74583
N	–0.16653	–2.75695	2.23410
H	0.71394	–3.20604	2.33240

1,3–CCW–Tautomer–N(1)–Pre–Transition State

charge = 1, multiplicity = 1
number of imaginary frequencies = 0
ZPE = 508.98 kJ/mol

Coordinates (Å)			
Atom	X	Y	Z
H	3.74803	–1.00426	–0.65035
C	2.84648	–0.51945	–0.33386
C	0.53181	0.71174	0.48370
C	1.78221	–1.26606	0.13040
C	2.72126	0.84668	–0.40616
C	1.56627	1.47636	–0.00809
C	0.56988	–0.68702	0.54925
H	1.48151	2.54389	–0.05328
N	1.98979	–2.71962	0.14037
O	2.82130	–3.14933	–0.56899
O	1.31256	–3.37651	0.87715
N	–0.59846	1.47360	1.01346
O	–1.03051	1.16992	2.06094
O	–0.99336	2.39186	0.34789
N	3.83696	1.64960	–0.90814
O	3.66023	2.81863	–0.98025
O	4.82244	1.06894	–1.20501
N	–0.49418	–1.46771	0.96812
H	–0.22831	–2.39155	1.23374
C	–1.79341	–1.30911	0.56239
N	–2.29489	–0.34171	–0.11079
C	–3.88440	–1.71647	0.29489
H	–4.83532	–2.20410	0.34588
N	–3.63593	–0.60426	–0.27341
N	–2.74729	–2.22260	0.84941
H	–2.65198	–3.07228	1.35970
N	–3.41889	2.06660	–0.67047
O	–3.83298	2.22609	0.31343
O	–3.03842	1.95155	–1.67361

1,3–CCW–Tautomer–N(1)–Transition State

charge = 1, multiplicity = 1
number of imaginary frequencies = 1
ZPE = 506.93 kJ/mol

Coordinates (Å)			
Atom	X	Y	Z
H	3.87594	–0.85406	–0.97597
C	3.01013	–0.37958	–0.56016
C	0.78287	0.82827	0.51232
C	1.90044	–1.13060	–0.22239
C	2.97684	0.97920	–0.37155
C	1.86649	1.59801	0.15568
C	0.73651	–0.56074	0.32135
H	1.85089	2.65885	0.30738
N	2.00883	–2.57037	–0.48285
O	2.82669	–2.92007	–1.24954
O	1.26881	–3.30479	0.10731
N	–0.31473	1.55564	1.15645
O	–0.87223	1.02360	2.06205
O	–0.55786	2.63591	0.74527
N	4.14390	1.78555	–0.73071
O	4.05421	2.95457	–0.56642
O	5.08223	1.20715	–1.15896
N	–0.36735	–1.33442	0.63691
H	–0.18686	–2.31652	0.67692
C	–1.65718	–0.95111	0.39362
N	–2.07254	–0.11006	–0.47666
C	–3.78836	–0.82388	0.62492
H	–4.78872	–0.97813	0.97365
N	–3.41206	–0.02359	–0.30826
N	–2.70356	–1.45046	1.10525
H	–2.65959	–2.06309	1.89125
N	–4.26947	1.40240	–1.43362
O	–5.34153	1.33889	–1.17660
O	–3.39374	1.80445	–1.95663

1,3–CCW–Tautomer–N(1)–Intermediate charge = 1, multiplicity = 1 number of imaginary frequencies = 0 ZPE = 512.17 kJ/mol			
Coordinates (Å)			
Atom	X	Y	Z
H	1.41199	–0.32879	–3.80891
C	1.34498	–0.41597	–2.74292
C	1.16451	–0.64215	0.00039
C	0.11174	–0.46197	–2.12205
C	2.47784	–0.47040	–1.96949
C	2.40518	–0.57688	–0.60153
C	–0.02954	–0.57077	–0.73060
H	3.29703	–0.62666	–0.00951
N	–1.05114	–0.38469	–3.01611
O	–0.88051	0.07119	–4.08207
O	–2.09928	–0.80412	–2.60992
N	1.18463	–0.83175	1.45601
O	0.24322	–1.36899	1.96253
O	2.13590	–0.45622	2.03348
N	3.79245	–0.42452	–2.61615
O	4.73541	–0.46781	–1.90396
O	3.80107	–0.34664	–3.79559
N	–1.29536	–0.61874	–0.14594
H	–2.03358	–0.83932	–0.78747
C	–1.63554	0.08538	0.96158
N	–1.15515	1.19706	1.36696
C	–2.68208	0.50346	2.81410
H	–3.31914	0.47724	3.67554
N	–1.79935	1.42307	2.52841
N	–2.61104	–0.36483	1.82877
H	–3.09339	–1.24072	1.77848
N	–1.52536	2.57909	3.32902
O	–2.20640	2.64028	4.28100
O	–0.69011	3.26416	2.92495

1,3–CCW–Tautomer–N(2)–Pre–Transition State charge = 1, multiplicity = 1 number of imaginary frequencies = 0 ZPE = 508.95 kJ/mol			
Coordinates (Å)			
Atom	X	Y	Z
H	2.66693	–0.82371	–1.29311
C	2.14974	–0.37939	–0.46566
C	0.79775	0.80413	1.62434
C	0.92332	–0.84508	–0.04999
C	2.70094	0.67402	0.23044
C	2.04904	1.27522	1.28328
C	0.20043	–0.27902	0.99773
H	2.49657	2.09135	1.81600
N	0.34970	–1.97143	–0.78858
O	0.32801	–1.88032	–1.98148
O	–0.06385	–2.88564	–0.17327
N	0.09509	1.50793	2.70136
O	–1.03805	1.80771	2.50003
O	0.71832	1.75003	3.67058
N	4.02033	1.17538	–0.17398
O	4.45687	2.08341	0.44259
O	4.53768	0.62967	–1.08800
N	–1.06157	–0.75896	1.43021
H	–1.04883	–1.74650	1.58739
C	–2.16327	–0.37862	0.65081
C	–4.05358	0.44017	0.07898
H	–4.99770	0.94125	0.12414
N	–3.54178	–0.10686	–0.96341
N	–3.22193	0.29387	1.13399
H	–3.29842	0.68575	2.04756
N	–2.33781	–0.62848	–0.59430
N	–2.16817	–1.49381	–3.04168
O	–2.52369	–2.46985	–2.74806
O	–1.82567	–0.53430	–3.39751

1,3–CCW–Tautomer–N(2)–Transition State charge = 1, multiplicity = 1 number of imaginary frequencies = 1 ZPE = 506.29 kJ/mol			
Coordinates (Å)			
Atom	X	Y	Z
H	3.18537	–1.49751	–0.90492
C	2.51994	–0.81518	–0.41400
C	0.79588	0.93699	0.83606
C	1.24570	–1.20746	–0.05698
C	2.91169	0.46989	–0.12467
C	2.07196	1.35233	0.51415
C	0.32778	–0.35189	0.56058
H	2.40311	2.33967	0.76840
N	0.89112	–2.59541	–0.37636
O	1.35244	–3.04839	–1.36032
O	0.17285	–3.17151	0.38146
N	–0.03241	1.91510	1.54773
O	–1.20552	1.89561	1.34183
O	0.52729	2.66180	2.26393
N	4.26323	0.90655	–0.49304
O	4.54091	2.03046	–0.25382
O	4.95994	0.09992	–1.00442
N	–0.93884	–0.80116	0.96237
H	–0.94439	–1.76778	1.21965
C	–2.12836	–0.38031	0.41320
C	–4.23693	0.03156	0.27528
H	–5.26745	0.12529	0.54584
N	–3.73411	0.31316	–0.85795
N	–3.26418	–0.42120	1.11752
H	–3.34332	–0.62281	2.09064
N	–2.40770	0.03739	–0.78386
N	–1.61419	0.48621	–2.59176
O	–0.53440	0.25912	–2.50436
O	–2.51642	0.82158	–3.11117

1,3–CCW–Tautomer–N(2)–Intermediate charge = 1, multiplicity = 1 number of imaginary frequencies = 0 ZPE = 512.15 kJ/mol			
Coordinates (Å)			
Atom	X	Y	Z
H	0.60981	1.21080	–3.49188
C	0.61483	1.22211	–2.41971
C	0.61783	1.24458	0.33789
C	0.56517	0.04375	–1.70363
C	0.67608	2.40679	–1.72494
C	0.69412	2.43855	–0.35170
C	0.52995	0.01448	–0.31027
H	0.76662	3.36879	0.17627
N	0.55933	–1.19375	–2.49386
O	0.05888	–1.15191	–3.55192
O	1.08935	–2.15465	–2.01174
N	0.64080	1.33938	1.79692
O	0.08868	0.46773	2.40742
O	1.18905	2.25837	2.27154
N	0.73810	3.67080	–2.47018
O	0.77474	4.66141	–1.82722
O	0.74558	3.58871	–3.64873
N	0.53717	–1.23270	0.36140
H	1.14862	–1.89509	–0.07741
C	–0.28713	–1.78521	1.25097
C	–0.97105	–3.19630	2.78498
H	–0.93224	–4.00435	3.48556
N	–1.97404	–2.46213	2.57420
N	0.09202	–2.82587	1.98891
H	1.02062	–3.19215	2.02678
N	–1.56692	–1.60384	1.60100
N	–2.47287	–0.63580	1.12904
O	–2.11447	–0.09369	0.14232
O	–3.43863	–0.50784	1.74599

1,3–CCW–Tautomer–C(5)–(R)–Pre Transition State

charge = 1, multiplicity = 1
number of imaginary frequencies = 0
ZPE = 503.37 kJ/mol

Coordinates (Å)			
Atom	X	Y	Z
H	0.25708	–0.56720	–0.19905
C	1.29438	–0.30261	–0.15941
C	3.95047	0.39522	–0.06028
C	1.89622	0.29756	–1.24689
C	2.03372	–0.53579	0.97441
C	3.36052	–0.18907	1.04144
C	3.25143	0.65822	–1.25187
H	3.93332	–0.37597	1.92746
N	1.00186	0.57653	–2.37573
O	0.02122	–0.06670	–2.45979
O	1.31154	1.45821	–3.11835
N	5.37488	0.71690	0.08883
O	5.82372	1.60378	–0.58014
O	5.98839	0.09080	0.87004
N	1.39362	–1.15819	2.13502
O	2.06832	–1.31641	3.09362
O	0.25513	–1.45745	2.01867
N	3.91480	1.25400	–2.31908
H	4.74412	1.75214	–2.06259
C	3.76941	0.97737	–3.63740
N	3.50064	–0.15523	–4.21136
N	3.43746	–0.04100	–5.55352
N	3.94091	1.85943	–4.63108
H	4.05666	2.84350	–4.51952
C	3.71666	1.18019	–5.79082
H	3.77550	1.62293	–6.76233
N	4.02717	–2.79762	–4.38952
O	3.21368	–1.27695	–3.60286
O	3.47359	–3.61871	–4.03071

1,3–CCW–Tautomer–C(5)–(R)– Transition State

charge = 1, multiplicity = 1
number of imaginary frequencies = 1
ZPE = 501.04 kJ/mol

Coordinates (Å)			
Atom	X	Y	Z
H	2.79247	–2.09313	–0.49387
C	2.37556	–1.13208	–0.25927
C	1.28464	1.36766	0.37622
C	1.04867	–0.99142	0.16355
C	3.12067	–0.00131	–0.35602
C	2.58821	1.24911	–0.03945
C	0.44332	0.24282	0.47373
H	3.19768	2.12872	–0.12631
N	0.28796	–2.15298	0.34831
O	0.68684	–3.22082	0.23747
O	–0.95318	–2.03306	0.75550
N	0.79829	2.71382	0.69034
O	–0.28872	2.79335	1.17283
O	1.51763	3.61075	0.45792
N	4.51446	–0.09717	–0.79694
O	5.11874	0.91443	–0.85736
O	4.91082	–1.18183	–1.05196
N	–0.85624	0.26141	0.84486
H	–1.28900	1.16476	0.87092
C	–1.65246	–0.80268	0.40131
N	–1.91423	–0.94626	–1.03630
N	–3.06967	–1.44620	–1.19929
N	–2.94414	–0.91040	0.94679
H	–3.20195	–0.73778	1.89522
C	–3.73872	–1.26789	–0.05181
H	–4.78317	–1.48290	0.06495
N	–3.56332	1.02612	–1.06479
O	–2.31879	0.98226	–1.15661
O	–4.11238	2.04573	–1.20894

1,3–CCW–Tautomer–C(5)–(R)–Wheland Intermediate

charge = 1, multiplicity = 1
number of imaginary frequencies = 0
ZPE = 513.32 kJ/mol

Coordinates (Å)			
Atom	X	Y	Z
H	–0.37982	1.29163	–3.36577
C	–0.01346	1.38489	–2.36109
C	0.96672	1.61334	0.25040
C	0.05862	0.28190	–1.50349
C	0.40924	2.58177	–1.87802
C	0.90659	2.70461	–0.58053
C	0.51675	0.34326	–0.17092
H	1.24087	3.66013	–0.22321
N	–0.27776	–0.97753	–2.02269
O	–0.58215	–1.16692	–3.11121
O	–0.16137	–2.03261	–1.25868
N	1.49290	1.82634	1.60002
O	1.53984	0.87459	2.31704
O	1.83378	2.91417	1.87863
N	0.34966	3.76449	–2.73908
O	0.73497	4.77729	–2.27138
O	–0.07939	3.60019	–3.82894
N	0.50969	–0.77811	0.56999
H	0.74086	–0.70962	1.54428
C	–0.31594	–1.85698	0.17656
N	–1.74426	–1.59320	0.39417
N	–2.22493	–2.40057	1.14745
N	–0.09260	–3.07855	0.78268
H	0.82736	–3.32965	1.07404
C	–1.21498	–3.36759	1.59307
H	–1.58417	–4.37854	1.56177
N	–0.96972	–3.03378	3.05523
O	–0.28505	–2.08119	3.25870
O	–1.48731	–3.72657	3.84193

1,3–CCW–Tautomer–C(5)–(S)–Pre–Transition State

charge = 1, multiplicity = 1
number of imaginary frequencies = 0
ZPE = 503.37 kJ/mol

Coordinates (Å)			
Atom	X	Y	Z
H	2.95062	–2.16339	0.40658
C	2.35510	–1.27696	0.31918
C	0.81088	1.00017	0.10086
C	1.08011	–1.23853	0.84475
C	2.83754	–0.16518	–0.32601
C	2.07832	0.97326	–0.44488
C	0.25033	–0.10671	0.75462
H	2.46692	1.83953	–0.94099
N	0.63562	–2.47413	1.50076
O	1.14273	–3.47653	1.15911
O	–0.20320	–2.38804	2.35196
N	0.11524	2.28709	–0.00824
O	–0.73576	2.52246	0.79497
O	0.46132	3.01759	–0.86208
N	4.18836	–0.19096	–0.89059
O	4.54837	0.78413	–1.45527
O	4.80865	–1.18698	–0.74110
N	–1.02275	–0.14341	1.31304
H	–1.14266	–0.84153	2.02012
C	–2.15881	0.39733	0.81054
N	–2.51760	0.54341	–0.42817
N	–3.72918	1.12483	–0.53984
N	–3.18520	0.84794	1.54424
H	–3.18193	0.96820	2.53408
C	–4.12307	1.29209	0.66117
H	–5.06087	1.71666	0.95030
N	–2.74699	–0.56989	–2.87732
O	–1.78561	0.27322	–1.47797
O	–2.15486	–0.43026	–3.73712

1,3–CCW–Tautomer–C(5)–(S)–Transition State charge = 1, multiplicity = 1 number of imaginary frequencies = 1 ZPE = 501.04 kJ/mol			
Coordinates (Å)			
Atom	X	Y	Z
H	3.09181	–2.06557	–0.03374
C	2.48275	–1.18551	0.05151
C	0.94428	1.05612	0.25039
C	1.17945	–1.30256	0.46840
C	3.01549	0.06395	–0.26837
C	2.27092	1.19525	–0.17372
C	0.33865	–0.17714	0.56389
H	2.68805	2.15558	–0.41087
N	0.69277	–2.64778	0.78601
O	1.41157	–3.54554	0.55514
O	–0.39392	–2.72573	1.26949
N	0.18417	2.21842	0.43298
O	–1.05672	2.09996	0.84136
O	0.58341	3.28583	0.31937
N	4.40901	0.15821	–0.71053
O	4.80562	1.24211	–0.96836
O	5.01282	–0.85378	–0.76902
N	–0.96064	–0.19434	0.93600
H	–1.39375	–1.09745	0.96449
C	–1.75675	0.86903	0.49054
N	–2.01951	1.00936	–0.94721
N	–3.17486	1.50939	–1.11053
N	–3.04799	0.97855	1.03670
H	–3.30519	0.80826	1.98572
C	–3.84315	1.33404	0.03785
H	–4.88743	1.54974	0.15486
N	–3.66942	–0.96241	–0.96989
O	–2.42494	–0.91927	–1.06272
O	–4.21899	–1.98213	–1.11127

1,3–CCW–Tautomer–C(5)–(S)–Wheland Intermediate charge = 1, multiplicity = 1 number of imaginary frequencies = 0 ZPE = 513.31 kJ/mol			
Coordinates (Å)			
Atom	X	Y	Z
H	0.36004	1.40675	–3.58863
C	0.42235	1.40029	–2.51696
C	0.58690	1.39879	0.20582
C	0.39278	0.20333	–1.84524
C	0.52504	2.60346	–1.81841
C	0.61380	2.62712	–0.46342
C	0.44921	0.15016	–0.43552
H	0.70959	3.55430	0.06898
N	0.27460	–1.01440	–2.64967
O	0.22023	–0.88586	–3.81488
O	0.24638	–2.05019	–2.05931
N	0.78102	1.40297	1.59548
O	0.82002	0.26329	2.23603
O	0.98722	2.34420	2.21596
N	0.54623	3.86523	–2.56099
O	0.63629	4.85297	–1.91667
O	0.47225	3.78677	–3.73632
N	0.40233	–0.96345	0.31544
H	0.20420	–1.83757	–0.13626
C	0.07090	–0.85508	1.68618
N	–1.34500	–0.53423	1.90854
N	–1.88872	–1.39374	2.55350
N	0.30544	–1.95924	2.48322
H	1.06454	–2.57173	2.27614
C	–0.94896	–2.46926	2.89084
H	–1.03481	–2.77068	3.92093
N	–1.38931	–3.65444	2.04755
O	–1.07818	–3.61378	0.89900
O	–2.00536	–4.48353	2.59520

Isolated 1,5–CCW–Tautomer charge = 0, multiplicity = 1 number of imaginary frequencies = 0 ZPE = 471.33 kJ/mol			
Coordinates (Å)			
Atom	X	Y	Z
H	0.84908	0.81104	–3.37250
C	0.66790	0.86565	–2.31910
C	0.21054	0.99033	0.39402
C	0.69956	–0.28170	–1.55091
C	0.38366	2.06325	–1.71624
C	0.15063	2.13596	–0.35824
C	0.45034	–0.28171	–0.16271
H	–0.05229	3.07557	0.11371
N	0.98497	–1.51549	–2.28489
O	0.80297	–1.51008	–3.45041
O	1.40296	–2.45325	–1.67273
N	0.10291	1.19876	1.84273
O	–0.61209	2.06622	2.20790
O	0.78627	0.52684	2.54157
N	0.34797	3.28102	–2.51813
O	0.09244	4.29216	–1.95484
O	0.57623	3.17431	–3.67684
N	0.43162	–1.43690	0.57146
H	0.83226	–2.22808	0.11925
C	–0.53341	–1.70621	1.52679
N	–1.67846	–1.12276	1.65224
N	–0.38761	–2.66774	2.42832
C	–2.22633	–1.78252	2.70956
N	–1.49455	–2.71939	3.19993
H	0.40697	–3.22692	2.63243
H	–3.19551	–1.54937	3.09764

1,5–CCW–Tautomer–N(1)–Pre–Transition State charge = 1, multiplicity = 1 number of imaginary frequencies = 0 ZPE = 507.86 kJ/mol			
Coordinates (Å)			
Atom	X	Y	Z
H	2.66100	–2.35964	0.08035
C	2.43515	–1.31239	0.08844
C	1.85019	1.37643	0.12756
C	1.15879	–0.87986	0.36989
C	3.41673	–0.37874	–0.15496
C	3.14265	0.96584	–0.13237
C	0.80208	0.47556	0.37424
H	3.91109	1.68671	–0.32527
N	0.20580	–1.93631	0.73058
O	0.34252	–2.98304	0.20522
O	–0.61333	–1.68068	1.55490
N	1.63127	2.82606	0.11649
O	2.39420	3.48329	–0.48973
O	0.70177	3.25693	0.73648
N	4.78162	–0.82881	–0.43056
O	5.59509	0.01057	–0.61503
O	4.96518	–1.99801	–0.44945
N	–0.49171	0.91852	0.59617
H	–0.56633	1.86377	0.90477
C	–1.58776	0.36026	0.00932
N	–1.60174	–0.43917	–1.01884
N	–2.82256	0.60093	0.43315
C	–2.90594	–0.69269	–1.18535
H	–3.10679	1.07744	1.25724
H	–3.26975	–1.33252	–1.96451
N	–3.69583	–0.09566	–0.34585
N	–6.18223	–0.42512	–0.18350
O	–6.28767	0.20882	0.68525
O	–6.18100	–1.07440	–1.04667

1,5–CCW–Tautomer–N(1)–Transition State

charge = 1, multiplicity = 1
number of imaginary frequencies = 1
ZPE = 505.34 kJ/mol

Coordinates (Å)			
Atom	X	Y	Z
H	2.70496	–2.35898	0.07423
C	2.43345	–1.32244	0.08095
C	1.73387	1.33911	0.11458
C	1.14427	–0.94209	0.38654
C	3.36613	–0.34837	–0.19001
C	3.03668	0.98470	–0.17213
C	0.73639	0.39510	0.38968
H	3.76961	1.73619	–0.38677
N	0.23722	–2.03325	0.76466
O	0.41576	–3.07787	0.25109
O	–0.59290	–1.79889	1.58556
N	1.44619	2.77742	0.11078
O	2.13916	3.46377	–0.54341
O	0.53678	3.16431	0.78661
N	4.74474	–0.74175	–0.49323
O	5.51446	0.13174	–0.70177
O	4.97670	–1.90164	–0.50699
N	–0.57615	0.79318	0.63903
H	–0.67857	1.70245	1.03734
C	–1.65826	0.21910	0.07739
N	–1.66678	–0.60608	–0.94068
N	–2.89819	0.46228	0.50598
C	–2.95353	–0.90081	–1.09308
H	–3.15838	0.78655	1.41132
H	–3.31995	–1.55090	–1.86310
N	–3.74207	–0.31161	–0.23819
N	–5.74205	–0.03867	–0.35631
O	–5.91364	0.79339	0.34329
O	–6.03589	–0.81694	–1.07437

1,5–CCW–Tautomer–N(1)–Intermediate

charge = 1, multiplicity = 1
number of imaginary frequencies = 0
ZPE = 511.20 kJ/mol

Coordinates (Å)			
Atom	X	Y	Z
H	–0.06309	0.62777	–3.53148
C	0.20803	0.98595	–2.55834
C	0.92049	1.90619	–0.06245
C	0.30915	0.11230	–1.49355
C	0.47902	2.31712	–2.34869
C	0.84059	2.79754	–1.11262
C	0.64463	0.54702	–0.21264
H	1.05002	3.83832	–0.96330
N	0.07844	–1.30592	–1.80369
O	–0.62896	–1.54367	–2.71023
O	0.63773	–2.11528	–1.12790
N	1.33127	2.46079	1.23349
O	1.07305	3.58539	1.44081
O	1.91879	1.73161	1.97842
N	0.39105	3.25002	–3.47994
O	0.65070	4.38013	–3.25359
O	0.06611	2.79109	–4.51920
N	0.71259	–0.31126	0.90744
H	1.47614	–0.14285	1.53274
C	–0.21097	–1.18091	1.24808
N	–1.44520	–1.25883	0.71186
N	–0.04506	–2.08714	2.21253
C	–2.01691	–2.24595	1.30480
H	0.81527	–2.49677	2.51992
H	–3.02883	–2.57526	1.17034
N	–1.17584	–2.86200	2.16868
N	–1.57559	–3.56360	3.32660
O	–0.73595	–3.68681	4.12768
O	–2.67467	–3.95498	3.29224

1,5–CCW–Tautomer–N(4)–Pre–Transition State

charge = 1, multiplicity = 1
number of imaginary frequencies = 0
ZPE = 509.80 kJ/mol

Coordinates (Å)			
Atom	X	Y	Z
H	2.90354	–2.18488	0.15009
C	2.31258	–1.29525	0.24034
C	0.81017	0.97658	0.47816
C	1.00826	–1.35609	0.68675
C	2.83843	–0.06360	–0.08052
C	2.10610	1.09625	0.03198
C	0.20277	–0.22204	0.80215
H	2.53901	2.04710	–0.21296
N	0.50573	–2.68451	1.05706
O	0.98162	–3.61015	0.51394
O	–0.34397	–2.73102	1.89636
N	0.02255	2.20664	0.62962
O	–0.03557	2.69760	1.68655
O	–0.50346	2.62791	–0.36714
N	4.22785	0.02002	–0.55077
O	4.62683	1.09838	–0.83055
O	4.83012	–0.99358	–0.61365
N	–1.15439	–0.19733	1.23307
H	–1.24887	–0.61849	2.13435
C	–2.13931	–0.65531	0.34757
N	–2.73264	–1.83453	0.44993
C	–3.56138	–0.86861	–1.16149
N	–3.65336	–1.97194	–0.51206
H	–2.54651	–2.57244	1.09397
H	–4.16863	–0.66115	–2.01861
N	–2.64020	0.00553	–0.66011
N	–2.81453	2.57840	–1.27201
O	–3.26723	2.80660	–0.31855
O	–2.41075	2.40936	–2.25837

1,5–CCW–Tautomer–N(4)–Transition State

charge = 1, multiplicity = 1
number of imaginary frequencies = 1
ZPE = 507.21 kJ/mol

Coordinates (Å)			
Atom	X	Y	Z
H	2.98061	–1.82854	–0.53984
C	2.39294	–0.99411	–0.21158
C	0.88427	1.14827	0.61287
C	1.10087	–1.17300	0.24208
C	2.91204	0.28065	–0.21157
C	2.18373	1.36969	0.21244
C	0.30265	–0.10921	0.65565
H	2.61355	2.35278	0.22226
N	0.60728	–2.55681	0.28919
O	1.03181	–3.29748	–0.51887
O	–0.17567	–2.82875	1.14559
N	0.09386	2.32161	0.99553
O	0.53228	3.02246	1.82422
O	–0.93112	2.48819	0.39944
N	4.29334	0.48747	–0.67210
O	4.67755	1.60516	–0.69927
O	4.89909	–0.47822	–0.97974
N	–0.99249	–0.26769	1.21895
H	–0.96116	–0.84632	2.03231
C	–2.12344	–0.48198	0.48477
N	–3.11011	–1.24111	0.91822
C	–3.74847	–0.47792	–0.88798
N	–4.14609	–1.23619	0.05078
H	–3.14649	–1.80632	1.73833
H	–4.33690	–0.25156	–1.75301
N	–2.48308	0.02374	–0.68099
N	–1.83431	1.46319	–1.84350
O	–2.69393	2.15350	–1.88061
O	–0.81963	1.15648	–2.16357

1,5–CCW–Tautomer–N(4)–Intermediate charge = 1, multiplicity = 1 number of imaginary frequencies = 0 ZPE = 512.59 kJ/mol			
Coordinates (Å)			
Atom	X	Y	Z
H	0.68461	0.74165	–3.61396
C	0.69305	0.87351	–2.54987
C	0.70258	1.20350	0.18632
C	0.59813	–0.21524	–1.70710
C	0.80185	2.12573	–1.99395
C	0.82249	2.30878	–0.63306
C	0.56963	–0.09102	–0.31678
H	0.93070	3.28874	–0.21185
N	0.53625	–1.52879	–2.36121
O	0.03541	–1.57704	–3.41896
O	1.02271	–2.45672	–1.77926
N	0.72915	1.46468	1.62341
O	1.29715	2.41692	1.99526
O	0.15345	0.68048	2.32716
N	0.91078	3.29467	–2.87538
O	0.98499	4.34905	–2.34701
O	0.91367	3.08109	–4.03730
N	0.53498	–1.25767	0.47918
H	1.06300	–2.00975	0.07598
C	–0.24586	–1.64421	1.49603
N	0.14249	–2.53655	2.36941
C	–1.81881	–2.17191	2.97064
N	–0.81484	–2.86644	3.27634
H	1.06054	–2.91996	2.45773
H	–2.76538	–2.14854	3.46673
N	–1.53739	–1.40557	1.83989
N	–2.45208	–0.53309	1.23880
O	–3.44625	–0.39344	1.82713
O	–2.10701	–0.07288	0.21567

1,5–CCW–Tautomer–C(5)–(R)–Pre–Transition State charge = 1, multiplicity = 1 number of imaginary frequencies = 0 ZPE = 511.20 kJ/mol			
Coordinates (Å)			
Atom	X	Y	Z
H	3.63712	–1.73249	–0.33599
C	2.91772	–0.96710	–0.12144
C	1.06098	1.00161	0.43964
C	1.61429	–1.29436	0.19105
C	3.26460	0.36248	–0.15746
C	2.35564	1.35674	0.11564
C	0.64574	–0.32849	0.46484
H	2.64674	2.38802	0.09202
N	1.29539	–2.72684	0.23864
O	1.92870	–3.43937	–0.44370
O	0.42536	–3.06843	0.98574
N	0.16138	2.10959	0.79192
O	0.39527	3.15666	0.31479
O	–0.73035	1.87518	1.54988
N	4.64821	0.73108	–0.48561
O	4.89460	1.88639	–0.51430
O	5.39617	–0.15917	–0.69498
N	–0.68064	–0.72444	0.74731
H	–0.77335	–1.53421	1.32874
C	–1.75504	–0.21015	0.19378
N	–1.76405	0.62574	–0.86369
N	–2.99450	–0.48954	0.59956
C	–3.00169	0.90414	–1.07233
N	–3.80389	0.33003	–0.14489
H	–3.28647	–0.75921	1.51853
H	–3.39817	1.50522	–1.86732
N	–5.15039	–0.03808	–0.35534
O	–5.67667	0.54818	–1.21656
O	–5.55108	–0.84136	0.39036

1,5–CCW–Tautomer–C(5)–(R)–Transition State

charge = 1, multiplicity = 1
number of imaginary frequencies = 1
ZPE = 504.79 kJ/mol

Coordinates (Å)			
Atom	X	Y	Z
H	4.74953	–2.22238	–1.14285
C	4.11133	–1.39866	–0.89168
C	2.46701	0.72161	–0.23506
C	2.84373	–1.61757	–0.39274
C	4.52820	–0.10081	–1.06795
C	3.72364	0.96789	–0.75075
C	1.97803	–0.57162	–0.06305
H	4.06796	1.97418	–0.88428
N	2.44793	–3.02039	–0.21645
O	2.96878	–3.81584	–0.90192
O	1.63277	–3.26084	0.62812
N	1.69807	1.90655	0.17000
O	1.87758	2.89164	–0.44712
O	0.97224	1.79212	1.10650
N	5.87399	0.15091	–1.59846
O	6.18354	1.28250	–1.74109
O	6.53353	–0.79947	–1.84048
N	0.67907	–0.84760	0.40521
H	0.60187	–1.66037	0.98288
C	–0.42057	–0.29395	–0.08057
N	–0.57433	0.51520	–1.07129
N	–1.67115	–0.54506	0.49601
C	–1.89860	0.72012	–1.13645
N	–2.57197	0.09941	–0.10778
H	–1.90336	–1.14932	1.26314
H	–2.36660	1.51314	–1.68411
N	–2.72264	–0.79886	–2.09796
O	–3.63033	–0.44148	–2.68797
O	–2.07414	–1.73886	–2.01126

1,5–CCW–Tautomer–C(5)–(R)–Wheland Intermediate

charge = 1, multiplicity = 1
number of imaginary frequencies = 0
ZPE = 511.16 kJ/mol

Coordinates (Å)			
Atom	X	Y	Z
H	1.17048	0.91146	–3.71830
C	1.06542	0.99225	–2.65454
C	0.80313	1.19546	0.08703
C	0.87171	–0.13541	–1.88093
C	1.10972	2.21594	–2.03202
C	0.97748	2.33757	–0.66924
C	0.72364	–0.07329	–0.49220
H	1.02475	3.29935	–0.19838
N	0.83958	–1.41517	–2.60122
O	0.57099	–1.38490	–3.73981
O	1.10843	–2.40689	–1.98056
N	0.74495	1.39885	1.54148
O	0.35362	2.43906	1.91888
O	1.11367	0.50433	2.24451
N	1.31678	3.42354	–2.84043
O	1.34234	4.45144	–2.25769
O	1.43861	3.26547	–4.00493
N	0.51722	–1.24288	0.25844
H	0.85848	–2.07964	–0.17943
C	–0.43540	–1.35168	1.18714
N	–1.46310	–0.70934	1.45518
N	–0.27459	–2.42274	2.19667
C	–2.00788	–1.24908	2.63964
N	–1.14693	–2.39706	3.02184
H	0.46996	–3.10652	2.25662
H	–2.05892	–0.56698	3.47739
N	–3.37606	–1.82948	2.38732
O	–4.26659	–1.31872	2.94611
O	–3.38948	–2.74294	1.63542

1,5–CCW–Tautomer–C(5)–(S)–Pre–Transition State

charge = 1, multiplicity = 1
number of imaginary frequencies = 0
ZPE = 511.20 kJ/mol

Coordinates (Å)			
Atom	X	Y	Z
H	3.79209	–1.51024	–0.34549
C	3.02365	–0.78651	–0.15816
C	1.04077	1.07501	0.33286
C	1.74609	–1.18709	0.17514
C	3.28042	0.56068	–0.25058
C	2.30767	1.50232	–0.01302
C	0.71579	–0.27773	0.41491
H	2.52885	2.54890	–0.08051
N	1.52416	–2.63453	0.28313
O	2.20167	–3.33060	–0.37324
O	0.68137	–3.00247	1.04874
N	0.06995	2.13388	0.64485
O	0.23158	3.17373	0.12396
O	–0.80169	1.87170	1.41694
N	4.63516	1.00720	–0.60168
O	4.80339	2.17424	–0.67901
O	5.44047	0.16110	–0.77892
N	–0.58014	–0.74957	0.72115
H	–0.61649	–1.53901	1.33584
C	–1.68835	–0.33162	0.15335
N	–1.75673	0.45748	–0.93737
N	–2.90500	–0.67635	0.57751
C	–3.01091	0.64357	–1.14997
N	–3.76989	0.05582	–0.19510
H	–3.17533	–0.92673	1.50848
H	–3.44931	1.18348	–1.96655
N	–5.08929	–0.41003	–0.38248
O	–5.43287	–1.20691	0.39779
O	–5.65640	0.10367	–1.26388

1,5–CCW–Tautomer–C(5)–(S)–Transition State

charge = 1, multiplicity = 1
number of imaginary frequencies = 1
ZPE = 504.39 kJ/mol

Coordinates (Å)			
Atom	X	Y	Z
H	3.54674	–1.30487	–0.73683
C	2.81967	–0.61823	–0.35124
C	0.94187	1.15342	0.62967
C	1.58435	–1.06016	0.07442
C	3.09237	0.72727	–0.26112
C	2.17983	1.62551	0.23826
C	0.60580	–0.19188	0.55700
H	2.42072	2.66633	0.32540
N	1.34635	–2.50827	–0.00249
O	1.92606	–3.09992	–0.83420
O	0.59166	–2.98639	0.79207
N	0.00593	2.15220	1.16012
O	0.48214	3.04591	1.76196
O	–1.14996	1.99706	0.93605
N	4.40740	1.21682	–0.69989
O	4.59023	2.38160	–0.62437
O	5.16973	0.40389	–1.09299
N	–0.65462	–0.67345	1.00576
H	–0.58967	–1.41528	1.67173
C	–1.70548	–0.71760	0.18353
N	–1.84103	–0.28691	–1.01631
N	–2.89936	–1.33899	0.57947
C	–3.11833	–0.58372	–1.33985
N	–3.74201	–1.31613	–0.35795
H	–3.13979	–1.73029	1.47176
H	–3.48906	–0.60683	–2.34442
N	–4.31611	0.81401	–0.64462
O	–3.89168	1.29209	0.29703
O	–5.17475	0.96281	–1.37993

1,5–CCW–Tautomer–C(5)–(S)–Wheland Intermediate

charge = 1, multiplicity = 1
number of imaginary frequencies = 0
ZPE = 512.07 kJ/mol

Coordinates (Å)			
Atom	X	Y	Z
H	0.29356	0.87964	–3.73043
C	0.48958	0.95061	–2.67890
C	0.98238	1.13120	0.02657
C	0.54430	–0.18644	–1.89592
C	0.68703	2.17156	–2.07967
C	0.94671	2.28299	–0.73498
C	0.77510	–0.13723	–0.51927
H	1.12475	3.24073	–0.28759
N	0.34584	–1.46153	–2.59986
O	–0.26045	–1.42973	–3.60207
O	0.82737	–2.44475	–2.11343
N	1.30262	1.30846	1.44467
O	1.92111	2.25549	1.74367
O	0.90715	0.47526	2.21325
N	0.63407	3.38832	–2.90002
O	0.80436	4.41305	–2.33647
O	0.42453	3.23949	–4.05316
N	0.85723	–1.31033	0.27118
H	1.10181	–2.10894	–0.28987
C	–0.17150	–1.58421	1.13455
N	–1.40043	–1.64149	1.00652
N	0.16323	–1.95815	2.52822
C	–1.94639	–2.05421	2.24909
N	–0.81017	–2.20227	3.18451
H	1.08916	–1.94129	2.93812
H	–2.48712	–2.98891	2.19750
N	–2.85192	–1.00159	2.83142
O	–2.34071	0.04700	3.01158
O	–3.95520	–1.33374	3.03879

PATO–N(1)–Product

charge = 0, multiplicity = 1
number of imaginary frequencies = 0
ZPE = 436.69 kJ/mol

Coordinates (Å)			
Atom	X	Y	Z
H	–0.70134	3.81379	–1.20432
C	–0.65810	2.73386	–1.16519
C	–0.58357	–0.04597	–1.05947
C	–0.64846	2.08496	0.06402
C	–0.58866	1.98571	–2.32728
C	–0.55944	0.59653	–2.28517
C	–0.56411	0.65941	0.17936
H	–0.55186	0.01515	–3.19796
N	–0.70394	2.96361	1.23982
O	–0.54702	4.16510	1.06647
O	–0.92350	2.45683	2.35236
N	–0.79243	–1.50589	–1.12771
O	–1.50381	–2.00778	–0.26106
O	–0.30122	–2.09991	–2.07962
N	–0.57974	2.66917	–3.62646
O	–0.51655	1.96400	–4.63105
O	–0.63431	3.89695	–3.61752
N	–0.45469	0.06786	1.40552
H	–0.69616	0.67830	2.18610
C	0.21423	–1.09071	1.74784
N	1.06439	–1.72900	0.96262
N	1.45522	–2.73194	1.78366
N	0.05943	–1.60297	3.01416
C	0.85483	–2.64430	3.00772
H	1.03946	–3.34476	3.80688
N	2.38626	–3.74015	1.34865
O	2.63729	–4.57493	2.20079
O	2.79779	–3.63189	0.21985

PATO–N(2)–Product

charge = 0, multiplicity = 1
number of imaginary frequencies = 0
ZPE = 477.88 kJ/mol

Coordinates (Å)			
Atom	X	Y	Z
H	0.22425	0.44761	–3.38303
C	0.40741	0.76566	–2.37703
C	0.85203	1.58534	0.20770
C	–0.25219	0.16311	–1.33130
C	1.28275	1.79458	–2.10886
C	1.51189	2.21947	–0.82373
C	–0.03832	0.52151	0.00621
H	2.19752	3.01585	–0.61845
N	–1.26311	–0.82800	–1.72223
O	–1.02754	–1.48095	–2.67865
O	–2.26420	–0.86346	–1.08852
N	1.14959	2.08480	1.55233
O	2.22231	2.54689	1.72906
O	0.28863	2.01609	2.37082
N	1.97176	2.45618	–3.21564
O	2.69719	3.35197	–2.94114
O	1.75545	2.04833	–4.30655
N	–0.63103	–0.12913	1.07610
H	–0.86481	0.41025	1.88074
C	–0.65009	–1.47852	1.19247
N	–0.07065	–2.32175	0.41597
C	–0.39514	–3.53622	0.95174
H	–0.05906	–4.45788	0.52497
N	–1.11815	–3.50412	2.00397
N	–1.30270	–2.16671	2.17793
N	–2.02910	–1.68751	3.23800
O	–2.02259	–0.50287	3.35803
O	–2.57210	–2.47052	3.90807

PATO–N(4)–Product

charge = 0, multiplicity = 1
number of imaginary frequencies = 0
ZPE = 476.77 kJ/mol

Coordinates (Å)			
Atom	X	Y	Z
H	0.04640	1.65918	–3.47495
C	0.11945	1.56059	–2.41148
C	0.30503	1.28739	0.32467
C	0.18214	0.30921	–1.83254
C	0.13434	2.66538	–1.59902
C	0.22269	2.54194	–0.22884
C	0.25684	0.11218	–0.44396
H	0.24820	3.40851	0.39970
N	0.14442	–0.81887	–2.76571
O	–0.38055	–0.64012	–3.80792
O	0.66205	–1.83889	–2.42982
N	0.53339	1.26347	1.77555
O	1.23915	0.41046	2.20448
O	0.04320	2.13196	2.40715
N	0.07191	3.99648	–2.19710
O	0.08059	4.92175	–1.45716
O	0.01708	4.05569	–3.37964
N	0.26772	–1.15193	0.10568
H	0.62799	–1.88858	–0.45916
C	–0.52483	–1.49352	1.16463
N	–1.50366	–0.83076	1.62554
C	–1.33150	–2.54267	2.90807
H	–1.46392	–3.28681	3.66169
N	–2.00182	–1.48992	2.72754
N	–0.34711	–2.62891	1.93024
N	0.55882	–3.64549	1.78870
O	1.20679	–3.63673	0.80198
O	0.58719	–4.42996	2.66367

PATO–C(5)–Product

charge = 0, multiplicity = 1
number of imaginary frequencies = 0
ZPE = 480.12 kJ/mol

Coordinates (Å)			
Atom	X	Y	Z
H	4.02019	–1.50459	0.37543
C	3.21106	–0.81099	0.27486
C	1.11730	0.95993	0.02586
C	1.91930	–1.21298	0.54292
C	3.43559	0.47779	–0.13982
C	2.39411	1.37115	–0.26913
C	0.80363	–0.35941	0.40813
H	2.57396	2.38299	–0.57051
N	1.77275	–2.60952	0.95643
O	2.62086	–3.36357	0.62909
O	0.82209	–2.90285	1.61399
N	0.11264	2.02918	0.01710
O	0.22947	2.86872	–0.80905
O	–0.70963	2.01071	0.86994
N	4.79700	0.91399	–0.42842
O	4.94003	2.03136	–0.79779
O	5.66439	0.12048	–0.27502
N	–0.47099	–0.80705	0.61366
H	–0.57292	–1.61955	1.17982
C	–1.56908	–0.49420	–0.15892
N	–2.80538	–0.85203	0.24488
N	–1.51628	0.10616	–1.30416
C	–3.52016	–0.41023	–0.72693
N	–2.80358	0.17393	–1.66196
H	–3.10480	0.61210	–2.50314
N	–4.96484	–0.51273	–0.84627
O	–5.42422	–0.01482	–1.82557
O	–5.54404	–1.06636	0.01017

1,3–CCW–Tautomer–C(5)–Product

charge = 0, multiplicity = 1
number of imaginary frequencies = 0
ZPE = 478.50 kJ/mol

Coordinates (Å)			
Atom	X	Y	Z
H	4.12137	–1.36713	–0.54726
C	3.29738	–0.75120	–0.25173
C	1.16888	0.82048	0.51346
C	2.09242	–1.32827	0.09968
C	3.41294	0.61431	–0.23200
C	2.35239	1.41081	0.14462
C	0.96574	–0.57296	0.48171
H	2.45011	2.47692	0.17171
N	2.05633	–2.79066	0.02434
O	2.87607	–3.32084	–0.63587
O	1.21417	–3.36815	0.64677
N	0.14977	1.74662	1.02180
O	–0.55316	1.36063	1.89903
O	0.13348	2.83176	0.55846
N	4.68275	1.23369	–0.59831
O	4.73407	2.41707	–0.56885
O	5.57130	0.50885	–0.89852
N	–0.23371	–1.16569	0.79211
H	–0.18712	–2.15260	0.92534
C	–1.44177	–0.67653	0.33446
N	–1.62649	0.02688	–0.72516
N	–2.95466	0.29508	–0.80822
N	–2.60292	–0.92045	0.96493
H	–2.76897	–1.34444	1.85029
C	–3.49867	–0.27086	0.18415
N	–4.90649	–0.28184	0.50436
O	–5.19034	–0.88884	1.49190
O	–5.64133	0.29153	–0.20854

1,5–CCW–Tautomer–C(5)–Product charge = 0, multiplicity = 1 number of imaginary frequencies = 0 ZPE = 480.04 kJ/mol			
Coordinates (Å)			
Atom	X	Y	Z
H	4.16477	–1.15026	–0.68792
C	3.26663	–0.66567	–0.36497
C	0.95081	0.56833	0.47456
C	2.19702	–1.41477	0.08402
C	3.15094	0.69993	–0.40560
C	1.99610	1.32826	0.00776
C	0.98354	–0.83740	0.50507
H	1.91520	2.39599	–0.01137
N	2.40056	–2.86537	0.07282
O	3.24676	–3.28953	–0.62881
O	1.71457	–3.53666	0.78641
N	–0.17602	1.33476	1.02058
O	–0.39880	2.38354	0.52771
O	–0.75036	0.87339	1.95257
N	4.27694	1.50189	–0.87614
O	4.13171	2.67733	–0.89367
O	5.25484	0.91880	–1.20580
N	–0.08500	–1.60748	0.90242
H	0.13758	–2.55576	1.11251
C	–1.37475	–1.36359	0.48555
N	–1.74034	–0.65830	–0.53416
N	–2.43626	–1.88628	1.09837
C	–3.07761	–0.78390	–0.48039
N	–3.55022	–1.50810	0.46040
H	–2.48766	–2.40984	1.94218
N	–3.95046	–0.14297	–1.45658
O	–3.41973	0.51704	–2.28095
O	–5.11101	–0.33724	–1.34465

APPENDIX D

The Cartesian coordinates of the optimized protonated PATO species presented in section 5.3.8 (HF/6–311++G(d,p)).

PATO–A

charge = 1, multiplicity = 1
number of imaginary frequencies = 0
ZPE = 507.26 kJ/mol

Coordinates (Å)			
Atom	X	Y	Z
H	–0.59622	0.59650	–2.90290
C	–0.18104	0.76538	–1.92934
C	0.89348	1.19500	0.56882
C	–0.06954	–0.27150	–1.02585
C	0.26939	2.01105	–1.56147
C	0.81141	2.24644	–0.32044
C	0.44840	–0.09091	0.25647
H	1.15409	3.22337	–0.04291
N	–0.49414	–1.58921	–1.51564
O	–1.40440	–1.61012	–2.26376
O	0.11830	–2.53831	–1.14263
N	1.48414	1.49764	1.87784
O	2.06985	0.61692	2.43044
O	1.35357	2.59339	2.28212
N	0.17352	3.11679	–2.52188
O	0.58964	4.16455	–2.16740
O	–0.31438	2.86784	–3.56975
N	0.51576	–1.11966	1.21190
H	1.33804	–1.15760	1.77921
C	–0.46678	–1.94601	1.52878
N	–0.17297	–2.99480	2.42838
N	–1.67702	–1.90052	1.10202
C	–1.21923	–3.65164	2.51634
H	–1.41368	–4.53725	3.09260
N	–2.27196	–3.05419	1.67879
H	–2.57519	–3.68597	0.94388
H	–3.09328	–2.79315	2.21293

PATO–B

charge = 1, multiplicity = 1
number of imaginary frequencies = 0
ZPE = 505.05 kJ/mol

Coordinates (Å)			
Atom	X	Y	Z
H	–0.82283	1.07909	–2.92882
C	–0.35670	1.04094	–1.96352
C	0.80303	0.99156	0.53722
C	–0.86333	0.24219	–0.95971
C	0.76779	1.78396	–1.69042
C	1.36592	1.77219	–0.45159
C	–0.31516	0.18910	0.31704
H	2.24029	2.36054	–0.25420
N	–2.03525	–0.56509	–1.30361
O	–2.90566	–0.03596	–1.87877
O	–1.99885	–1.72207	–0.99357
N	1.43728	1.06305	1.86048
O	0.72136	1.01640	2.80892
O	2.60865	1.17774	1.87789
N	1.34145	2.62270	–2.75291
O	2.28706	3.26829	–2.46385
O	0.80833	2.57620	–3.80674
N	–0.91477	–0.55071	1.37029
H	–1.11207	–0.01229	2.19118
C	–0.70614	–1.83907	1.66234
N	–0.95337	–2.33708	2.86681
N	–0.23676	–2.77449	0.82913
C	–0.68552	–3.61202	2.75816
H	–0.75034	–4.32566	3.55616
N	–0.30477	–3.93928	1.54175
H	0.13617	–4.77380	1.21803
H	–0.46057	–2.78555	–0.14763

PATO–C

charge = 1, multiplicity = 1
number of imaginary frequencies = 0
ZPE = 507.18 kJ/mol

Coordinates (Å)			
Atom	X	Y	Z
H	0.25280	1.06422	–3.26560
C	0.27875	0.98421	–2.19740
C	0.34789	0.76884	0.54902
C	0.25921	–0.25683	–1.59061
C	0.31672	2.10749	–1.40943
C	0.34399	2.01674	–0.03804
C	0.28716	–0.41720	–0.19617
H	0.38119	2.89982	0.56797
N	0.19898	–1.40603	–2.50247
O	–0.18815	–1.20933	–3.59187
O	0.55990	–2.47130	–2.08674
N	0.46346	0.76642	2.01161
O	1.02344	–0.15563	2.52353
O	0.01052	1.68705	2.58721
N	0.33785	3.42900	–2.04112
O	0.36073	4.36366	–1.31636
O	0.32841	3.45391	–3.22309
N	0.26525	–1.68366	0.37889
H	0.48348	–2.42635	–0.25624
C	–0.49171	–2.00674	1.46267
N	–0.11779	–3.00223	2.32903
N	–1.59650	–1.48279	1.83500
C	–1.03994	–3.03871	3.27929
H	–1.06083	–3.69428	4.12618
N	–1.90695	–2.12722	2.98194
H	–2.73658	–1.88365	3.48256
H	0.73891	–3.51640	2.31095

PATO–D

charge = 1, multiplicity = 1
number of imaginary frequencies = 0
ZPE = 508.09 kJ/mol

Coordinates (Å)			
Atom	X	Y	Z
H	–0.49173	0.46153	–2.96118
C	–0.14636	0.64021	–1.96152
C	0.78341	1.12254	0.60590
C	0.16523	–0.39255	–1.09631
C	0.02765	1.92256	–1.50434
C	0.49510	2.18254	–0.23470
C	0.60679	–0.20240	0.21872
H	0.62543	3.19220	0.10402
N	0.05717	–1.73080	–1.66430
O	–0.59649	–1.94214	–2.57368
O	0.80188	–2.68161	–1.22398
N	1.27790	1.46429	1.94632
O	1.96228	0.65772	2.49175
O	0.97600	2.51845	2.36853
N	–0.27784	3.04158	–2.40402
O	–0.10071	4.12643	–1.97609
O	–0.67760	2.75614	–3.48004
C	–0.37351	–1.92488	1.55064
N	–1.41685	–2.19489	0.74973
N	–0.49342	–2.27947	2.77638
C	–2.25193	–2.77080	1.57665
H	–3.22538	–3.14461	1.33392
N	–1.71627	–2.83454	2.78084
H	–2.09505	–3.21337	3.62023
N	0.80998	–1.32576	1.04317
H	1.45770	–1.13767	1.78541
H	1.14130	–2.43257	–0.34737

PATO–B–N(4)–Intermediate

charge = 2, multiplicity = 1
number of imaginary frequencies = 0
ZPE = 543.23 kJ/mol

Coordinates (Å)			
Atom	X	Y	Z
H	–0.23064	0.84709	–3.50914
C	0.06950	1.08673	–2.50490
C	0.95633	1.69887	0.03391
C	0.09114	0.11530	–1.50490
C	0.49230	2.35358	–2.21150
C	0.97897	2.66251	–0.95807
C	0.42725	0.38177	–0.14382
H	1.35699	3.65011	–0.76693
N	–0.12402	–1.20795	–1.99256
O	–0.77882	–1.46373	–2.89611
O	0.57761	–2.12498	–1.40880
N	1.47576	2.13643	1.31837
O	1.57473	1.31909	2.29285
O	1.83835	3.21058	1.47465
N	0.49377	3.37444	–3.26254
O	0.89584	4.43854	–2.95329
O	0.08584	3.03368	–4.31701
N	0.29830	–0.38895	0.93655
H	1.15040	0.46462	2.04040
C	–0.63924	–1.30776	1.11996
N	–1.59897	–1.69299	0.34608
N	–2.33367	–2.57949	1.06826
H	–3.15944	–2.98687	0.67310
H	0.40872	–2.96237	–1.84610
N	–0.77267	–2.00221	2.33813
C	–1.86504	–2.77904	2.24307
H	–2.24848	–3.42458	3.00947
N	0.01841	–1.95804	3.52506
O	0.87283	–1.16588	3.52429
O	–0.31004	–2.72848	4.33253

N(4)–Nitrated–PATO–B

charge = 1, multiplicity = 1
number of imaginary frequencies = 0
ZPE = 513.25 kJ/mol

Coordinates (Å)			
Atom	X	Y	Z
H	0.23263	0.90596	–3.72780
C	0.28627	1.05662	–2.66683
C	0.44057	1.44784	0.06577
C	0.27469	–0.01092	–1.79241
C	0.36735	2.32107	–2.13062
C	0.44814	2.54287	–0.77331
C	0.36731	0.14496	–0.41959
H	0.51800	3.53817	–0.38041
N	0.12039	–1.35005	–2.36417
O	0.76402	–1.61452	–3.30702
O	–0.68278	–2.05460	–1.82945
N	0.49926	1.71611	1.51024
O	–0.05795	0.93943	2.22862
O	1.06835	2.68228	1.85061
N	0.36488	3.47883	–3.03974
O	0.44999	4.54351	–2.53647
O	0.27745	3.24089	–4.19322
N	0.54267	–0.98245	0.43955
H	1.43896	–1.05930	0.87666
C	–0.45589	–1.53358	1.12302
N	–1.71651	–1.60950	0.79897
N	–2.47218	–2.24244	1.74120
H	–2.11069	–1.38552	–0.09052
N	–0.38098	–2.16397	2.32360
C	–1.67701	–2.56634	2.65959
H	–1.90896	–3.08002	3.56789
N	0.73527	–2.27280	3.16208
O	1.75617	–1.93072	2.68560
O	0.51059	–2.70381	4.21717

PATO–B–C(5)–(R)–Wheland Intermediate

charge = 2, multiplicity = 1
number of imaginary frequencies = 0
ZPE = 547.22 kJ/mol

Coordinates (Å)			
Atom	X	Y	Z
H	1.55779	0.54377	–2.88048
C	1.15377	1.01181	–2.00015
C	0.07985	2.25751	0.21707
C	0.25247	0.32982	–1.16588
C	1.49868	2.29393	–1.70343
C	0.94771	2.94264	–0.61348
C	–0.28300	0.88994	0.03763
H	1.21192	3.96763	–0.42387
N	–0.18485	–0.91267	–1.69330
O	0.12620	–1.36097	–2.68855
O	–1.16579	–1.55542	–1.02931
N	–0.42478	3.04965	1.33848
O	–1.28551	2.56665	2.15084
O	–0.08186	4.12685	1.49519
N	2.43930	3.01362	–2.57267
O	2.68354	4.12248	–2.25784
O	2.85551	2.40763	–3.49386
N	–1.03106	0.32027	1.00883
H	–1.42422	1.62193	1.93000
C	–1.11973	–0.97101	1.17275
N	–0.71740	–1.88027	0.21716
N	–1.51743	–1.63778	2.20545
N	–1.68933	–3.01240	1.92036
H	–1.30305	–3.57620	2.65932
H	–1.90766	–1.25853	3.04545
C	–1.00165	–3.22543	0.67411
H	–1.56711	–3.80443	–0.04154
N	0.33568	–3.92959	0.81232
O	1.02690	–3.83811	–0.13905
O	0.53313	–4.50131	1.81846

PATO–B–C(5)–(S)–Wheland Intermediate

charge = 2, multiplicity = 1
number of imaginary frequencies = 0
ZPE = 539.97 kJ/mol

Coordinates (Å)			
Atom	X	Y	Z
H	–0.47218	1.13641	–3.46993
C	–0.12172	1.34198	–2.47501
C	0.71492	1.96531	0.08774
C	–0.58861	0.58360	–1.37470
C	0.74755	2.35828	–2.27047
C	1.14145	2.71352	–0.98136
C	–0.09454	0.77339	–0.03094
H	1.78274	3.56602	–0.84658
N	–1.67736	–0.22962	–1.68059
O	–2.11787	–0.37222	–2.73743
O	–2.26458	–0.82334	–0.67426
N	1.19140	2.43176	1.38389
O	0.79222	1.88243	2.46549
O	1.90184	3.32402	1.46290
N	1.23129	3.14450	–3.40961
O	1.95616	4.03763	–3.14910
O	0.85416	2.80350	–4.47379
N	–0.27866	0.07289	1.06162
H	0.26488	1.08553	2.23324
C	–0.49003	–1.22274	1.27161
N	–0.93475	–1.77876	2.30330
N	0.01066	–2.22918	0.29071
N	–0.11857	–3.28650	0.84205
H	0.19126	–4.14205	0.39346
H	–3.10561	–1.16277	–0.98990
C	–0.71521	–3.15538	2.21209
H	–1.58061	–3.79206	2.32847
N	0.35548	–3.58884	3.19504
O	1.44053	–3.17952	2.95489
O	–0.01222	–4.25677	4.07619

C(5)–Nitrated–PATO–B charge = 1, multiplicity = 1 number of imaginary frequencies = 0 ZPE = 512.82 kJ/mol			
Coordinates (Å)			
Atom	X	Y	Z
H	–1.27082	2.83760	–2.29519
C	–0.49523	2.22510	–1.87898
C	1.48802	0.65965	–0.78877
C	–0.77786	0.96596	–1.38904
C	0.80696	2.66559	–1.83053
C	1.81792	1.89536	–1.30515
C	0.19468	0.14924	–0.81484
H	2.83134	2.24708	–1.29381
N	–2.17027	0.51456	–1.52218
O	–2.34762	–0.64142	–1.74219
O	–3.00307	1.33779	–1.41421
N	2.58295	–0.10970	–0.19615
O	2.36678	–0.60724	0.87403
O	3.59034	–0.16207	–0.78581
N	1.13130	3.99743	–2.36358
O	2.25827	4.34047	–2.27130
O	0.23778	4.60887	–2.83413
N	–0.11221	–1.17367	–0.39127
H	–0.58409	–1.72642	–1.08128
C	–0.39137	–1.58067	0.84527
N	–1.05537	–2.71683	1.07866
N	–0.08053	–0.96198	1.98778
N	–0.48681	–1.80212	2.97972
H	–0.51985	–1.54814	3.94769
H	0.74257	–0.40254	2.11254
C	–1.08813	–2.78875	2.36421
N	–1.74321	–3.84231	3.14587
O	–1.75241	–3.63372	4.31352
O	–2.17006	–4.74812	2.54811

PATO–C–N(2)–Intermediate charge = 2, multiplicity = 1 number of imaginary frequencies = 0 ZPE = 545.70 kJ/mol			
Coordinates (Å)			
Atom	X	Y	Z
H	0.73131	1.28953	–3.64759
C	0.59146	1.24431	–2.58229
C	0.23925	1.14830	0.11890
C	0.38386	0.02547	–1.97114
C	0.61726	2.41797	–1.82958
C	0.43620	2.40116	–0.48446
C	0.19315	–0.06558	–0.58435
H	0.45149	3.31100	0.08780
N	0.35083	–1.16544	–2.82659
O	0.55477	–1.01656	–3.96426
O	0.11260	–2.20982	–2.28378
N	0.05872	1.10297	1.49852
O	–0.04345	–0.08431	2.10691
O	0.04467	1.99713	2.20392
N	0.83549	3.70288	–2.50830
O	0.84312	4.65790	–1.81459
O	0.98256	3.65396	–3.67576
N	–0.00492	–1.22997	0.08784
H	–0.11843	–2.05333	–0.48074
C	–0.40333	–1.28034	1.42214
N	0.20722	–2.34208	2.17242
N	–1.81599	–1.63733	1.65184
C	–0.66630	–2.97011	2.93409
H	–0.42761	–3.75833	3.62758
N	–1.85713	–2.53091	2.71753
H	–2.73452	–2.91788	3.02015
H	1.20086	–2.46531	2.21918
N	–2.77636	–0.61450	1.71101
O	–2.50837	0.31719	1.03652
O	–3.71241	–0.83399	2.35904

N(2)–Nitrated–PATO–C

charge = 1, multiplicity = 1
number of imaginary frequencies = 0
ZPE = 510.99 kJ/mol

Coordinates (Å)			
Atom	X	Y	Z
H	0.83125	1.24646	–3.61809
C	0.73148	1.19827	–2.55069
C	0.48310	1.08750	0.16188
C	0.53288	–0.01809	–1.94225
C	0.79935	2.36300	–1.79359
C	0.66888	2.33143	–0.43921
C	0.38259	–0.12445	–0.54125
H	0.71602	3.23243	0.14200
N	0.45951	–1.19193	–2.81336
O	0.56547	–1.01632	–3.96747
O	0.30000	–2.25419	–2.28665
N	0.35910	1.04212	1.55943
O	0.31114	–0.11557	2.15165
O	0.37370	1.96722	2.23520
N	1.00913	3.64610	–2.46511
O	1.06340	4.60167	–1.77003
O	1.10857	3.61731	–3.64128
N	0.18063	–1.27646	0.11974
H	0.07787	–2.10896	–0.42719
C	–0.19601	–1.36625	1.47750
N	0.36148	–2.43640	2.16301
N	–1.56828	–1.59264	1.79432
C	–0.58417	–2.95154	3.02870
H	–0.35106	–3.70443	3.75385
N	–1.73028	–2.47229	2.85595
H	1.34589	–2.56968	2.23405
N	–2.52014	–0.63076	1.59910
O	–2.14218	0.28883	0.92184
O	–3.56833	–0.79436	2.05893

PATO–C–C(5)–(R)–Wheland Intermediate

charge = 2, multiplicity = 1
number of imaginary frequencies = 0
ZPE = 548.60 kJ/mol

Coordinates (Å)			
Atom	X	Y	Z
H	0.64007	1.47514	–3.91279
C	0.49823	1.43441	–2.84772
C	0.17363	1.37192	–0.10851
C	0.51282	0.23248	–2.15900
C	0.29060	2.60314	–2.14589
C	0.14928	2.59429	–0.78798
C	0.30683	0.11979	–0.76199
H	0.03160	3.52465	–0.26137
N	0.75178	–0.94208	–3.00185
O	0.76288	–0.85080	–4.13858
O	0.99812	–2.08663	–2.48570
N	0.19277	1.49780	1.32045
O	0.15125	0.40949	2.06996
O	0.35705	2.48163	1.86639
N	0.25541	3.88300	–2.86863
O	0.07983	4.84227	–2.20667
O	0.40173	3.81796	–4.03568
N	0.27969	–1.13883	–0.23170
H	0.85351	–2.03309	–1.52044
C	–0.33585	–1.41701	0.86010
N	–0.57115	–2.58387	1.40380
N	–0.92432	–0.42040	1.67124
N	–1.44058	–1.03898	2.78208
H	–2.41927	–0.85955	2.88152
H	–0.21820	–3.44707	1.03967
C	–1.04769	–2.41988	2.75492
H	–1.83330	–3.09821	3.04384
N	0.10829	–2.61891	3.71437
O	1.12781	–2.10655	3.38386
O	–0.12881	–3.22412	4.68531

PATO–C–C(5)–(S)–Wheland Intermediate charge = 2, multiplicity = 1 number of imaginary frequencies = 0 ZPE = 548.25 kJ/mol			
Coordinates (Å)			
Atom	X	Y	Z
H	0.57508	1.66584	–3.78066
C	0.50779	1.59696	–2.70965
C	0.36454	1.46573	0.04124
C	0.67722	0.39148	–2.04822
C	0.24062	2.73215	–1.97290
C	0.18560	2.69115	–0.60957
C	0.57202	0.24110	–0.64356
H	0.01435	3.59840	–0.05775
N	0.96432	–0.74435	–2.92791
O	0.89865	–0.63492	–4.06103
O	1.33782	–1.87181	–2.45119
N	0.45651	1.56651	1.46758
O	0.52163	0.46552	2.19552
O	0.58355	2.54959	2.02573
N	0.04297	4.01327	–2.66673
O	–0.17771	4.94259	–1.97619
O	0.12197	3.97857	–3.84148
N	0.69925	–1.01826	–0.13197
H	1.25192	–1.84647	–1.47859
C	0.15680	–1.36742	0.98073
N	0.11150	–2.54455	1.53864
N	–0.51129	–0.44252	1.81635
N	–0.89350	–1.11437	2.95639
H	–1.84383	–0.90919	3.20556
H	0.45435	–3.39464	1.13347
C	–0.63182	–2.51798	2.77060
H	–0.11479	–2.98904	3.59332
N	–1.90923	–3.31365	2.58204
O	–1.74733	–4.37643	2.10246
O	–2.90895	–2.81130	2.94777

C(5)–Nitrated–PATO–C charge = 1, multiplicity = 1 number of imaginary frequencies = 0 ZPE = 514.31 kJ/mol			
Coordinates (Å)			
Atom	X	Y	Z
H	0.25072	1.39132	–3.93397
C	0.27454	1.38663	–2.86255
C	0.33994	1.36640	–0.10552
C	0.38134	0.19515	–2.17185
C	0.18660	2.55822	–2.15209
C	0.21132	2.56487	–0.77836
C	0.41252	0.13507	–0.77065
H	0.15053	3.48675	–0.23523
N	0.45761	–1.01462	–3.00146
O	0.05412	–0.93996	–4.09919
O	0.93900	–1.99866	–2.51299
N	0.43579	1.47541	1.35500
O	1.03915	0.62413	1.93910
O	–0.07702	2.40478	1.85879
N	0.07352	3.82944	–2.87305
O	–0.01045	4.80720	–2.21325
O	0.07371	3.77163	–4.05356
N	0.52463	–1.09096	–0.11493
H	0.85985	–1.83805	–0.69315
C	–0.19613	–1.43181	0.97928
N	0.28027	–2.32140	1.90780
N	–1.36495	–1.01434	1.31725
N	–1.61613	–1.60793	2.49860
H	–2.47166	–1.44531	2.99736
H	1.18421	–2.75432	1.94791
C	–0.65053	–2.38451	2.83679
N	–0.59413	–3.19980	4.03919
O	0.38206	–3.84536	4.15188
O	–1.53044	–3.10795	4.74381

APPENDIX E

The Cartesian coordinates of the optimized nitrated PATO species presented in section 5.3.9 (B3LYP/6–31G(d,p)). For all structures total charge = 0, multiplicity = 1 and number of imaginary frequencies = 0. See Appendix B for the Cartesian coordinates of the unnitrated PATO species optimized at the same theoretical level.

PATO–N(1)–Product ZPE = 436.69 kJ/mol			
Coordinates (Å)			
Atom	X	Y	Z
H	–0.70134	3.81379	–1.20432
C	–0.65810	2.73386	–1.16519
C	–0.58357	–0.04597	–1.05947
C	–0.64846	2.08496	0.06402
C	–0.58866	1.98571	–2.32728
C	–0.55944	0.59653	–2.28517
C	–0.56411	0.65941	0.17936
H	–0.55186	0.01515	–3.19796
N	–0.70394	2.96361	1.23982
O	–0.54702	4.16510	1.06647
O	–0.92350	2.45683	2.35236
N	–0.79243	–1.50589	–1.12771
O	–1.50381	–2.00778	–0.26106
O	–0.30122	–2.09991	–2.07962
N	–0.57974	2.66917	–3.62646
O	–0.51655	1.96400	–4.63105
O	–0.63431	3.89695	–3.61752
N	–0.45469	0.06786	1.40552
H	–0.69616	0.67830	2.18610
C	0.21423	–1.09071	1.74784
N	1.06439	–1.72900	0.96262
N	1.45522	–2.73194	1.78366
N	0.05943	–1.60297	3.01416
C	0.85483	–2.64430	3.00772
H	1.03946	–3.34476	3.80688
N	2.38626	–3.74015	1.34865
O	2.63729	–4.57493	2.20079
O	2.79779	–3.63189	0.21985

PATO–N(2)–Product ZPE = 436.48 kJ/mol			
Coordinates (Å)			
Atom	X	Y	Z
H	0.32858	0.40021	–3.40737
C	0.48572	0.73776	–2.39122
C	0.84187	1.63593	0.21648
C	–0.16308	0.10488	–1.34409
C	1.30426	1.82791	–2.12219
C	1.47236	2.29724	–0.83127
C	0.02535	0.48376	0.01286
H	2.09984	3.15487	–0.62972
N	–1.17938	–0.88902	–1.75001
O	–0.95297	–1.53877	–2.76245
O	–2.20917	–0.93591	–1.08313
N	1.09027	2.19099	1.55612
O	2.01481	2.98286	1.68261
O	0.34319	1.84760	2.48320
N	1.98267	2.51240	–3.23278
O	2.67242	3.48958	–2.95307
O	1.81124	2.05561	–4.36015
N	–0.50842	–0.19506	1.08536
H	–0.57344	0.33482	1.95529
C	–0.66201	–1.55287	1.16308
N	–0.19819	–2.45928	0.33520
C	–0.61587	–3.64235	0.88927
H	–0.39497	–4.60074	0.44181
N	–1.29625	–3.55033	2.00975
N	–1.33396	–2.19841	2.18835
N	–1.97610	–1.64445	3.33862
O	–1.82752	–0.43467	3.46806
O	–2.58122	–2.41455	4.04037

PATO–N(4)–Product ZPE = 434.69 kJ/mol			
Coordinates (Å)			
Atom	X	Y	Z
H	0.17790	1.65374	–3.51552
C	0.18145	1.56382	–2.43771
C	0.21676	1.32648	0.33561
C	0.20532	0.30574	–1.84542
C	0.14005	2.68771	–1.63250
C	0.16247	2.58093	–0.24646
C	0.18626	0.12616	–0.42854
H	0.16683	3.46554	0.37690
N	0.22738	–0.83043	–2.77686
O	–0.01938	–0.61004	–3.95495
O	0.51167	–1.95454	–2.33363
N	0.45453	1.32481	1.79441
O	1.16845	0.43061	2.24293
O	–0.01408	2.25333	2.43873
N	0.10063	4.01892	–2.25351
O	0.06325	4.98816	–1.49945
O	0.10738	4.06708	–3.48124
N	0.13509	–1.13417	0.11481
H	0.39056	–1.88539	–0.52755
C	–0.55093	–1.46992	1.25721
N	–1.47313	–0.77307	1.85997
C	–1.22562	–2.59663	3.03247
H	–1.31171	–3.38844	3.75906
N	–1.89209	–1.48593	2.98256
N	–0.34773	–2.65792	1.95613
N	0.53204	–3.73434	1.66744
O	1.10026	–3.68355	0.58959
O	0.60841	–4.58767	2.52754

PATO–C(5)–Product ZPE = 439.09 kJ/mol			
Coordinates (Å)			
Atom	X	Y	Z
H	4.07865	–1.49111	0.50997
C	3.25755	–0.80857	0.33789
C	1.14413	0.95469	–0.06637
C	1.95115	–1.22931	0.55676
C	3.49026	0.47621	–0.12087
C	2.44098	1.36638	–0.31883
C	0.81980	–0.37948	0.32239
H	2.63170	2.38398	–0.63412
N	1.80695	–2.61548	1.02016
O	2.79668	–3.33531	0.99497
O	0.69748	–2.99500	1.43068
N	0.13784	2.03225	–0.07919
O	0.29494	2.94041	–0.88749
O	–0.75184	1.97505	0.76595
N	4.86753	0.91560	–0.37137
O	5.02448	2.06282	–0.78410
O	5.76602	0.10591	–0.15333
N	–0.44737	–0.86487	0.45412
H	–0.49973	–1.75609	0.94823
C	–1.59812	–0.48738	–0.21588
N	–2.80766	–0.93484	0.20993
N	–1.61240	0.24964	–1.32963
C	–3.60614	–0.41878	–0.69665
N	–2.92809	0.29277	–1.61374
H	–3.29667	0.80784	–2.40231
N	–5.04853	–0.55162	–0.77755
O	–5.57086	0.04450	–1.72524
O	–5.61028	–1.22257	0.07122

1,3–CCW–Tautomer–C(5)–Product ZPE = 436.84 kJ/mol			
Coordinates (Å)			
Atom	X	Y	Z
H	4.18790	–1.40075	–0.44397
C	3.34369	–0.76784	–0.20624
C	1.17575	0.85835	0.43401
C	2.11296	–1.33782	0.10481
C	3.46477	0.60916	–0.22608
C	2.38927	1.43014	0.09503
C	0.95829	–0.54967	0.40912
H	2.49968	2.50670	0.10760
N	2.07400	–2.80512	0.07565
O	3.05095	–3.39915	–0.35595
O	1.05897	–3.38723	0.50285
N	0.15960	1.80098	0.94324
O	–0.60817	1.38447	1.81000
O	0.19410	2.94744	0.51785
N	4.75946	1.21488	–0.56685
O	4.81938	2.44180	–0.57198
O	5.68734	0.45111	–0.82188
N	–0.24936	–1.15086	0.65171
H	–0.16694	–2.16968	0.71530
C	–1.47904	–0.62148	0.29866
N	–1.71751	0.20331	–0.70801
N	–3.06504	0.44317	–0.73077
N	–2.63292	–0.95593	0.93310
H	–2.79163	–1.50118	1.76997
C	–3.58207	–0.25582	0.24413
N	–4.97449	–0.35122	0.61177
O	–5.20713	–1.09108	1.57666
O	–5.78826	0.28749	–0.03501

1,5–CCW–Tautomer–C(5)–Product ZPE = 438.61 kJ/mol			
Coordinates (Å)			
Atom	X	Y	Z
H	4.28402	–1.15275	–0.54264
C	3.34835	–0.66962	–0.29583
C	0.94765	0.57479	0.36955
C	2.25476	–1.43253	0.10127
C	3.21579	0.70359	–0.38914
C	2.02315	1.33533	–0.05564
C	0.98854	–0.84804	0.42130
H	1.93669	2.41331	–0.09910
N	2.48177	–2.88237	0.14708
O	3.53478	–3.31533	–0.29675
O	1.60420	–3.61168	0.64689
N	–0.19856	1.34608	0.89034
O	–0.38970	2.45773	0.41661
O	–0.83974	0.84317	1.81236
N	4.36533	1.51120	–0.82137
O	4.20268	2.72688	–0.88560
O	5.40443	0.91199	–1.08672
N	–0.08212	–1.64158	0.74098
H	0.18533	–2.62361	0.85066
C	–1.40199	–1.36268	0.42553
N	–1.84814	–0.61515	–0.56551
N	–2.44161	–1.92209	1.09515
C	–3.18708	–0.75531	–0.43030
N	–3.61463	–1.53783	0.54274
H	–2.43752	–2.49323	1.92928
N	–4.13315	–0.09058	–1.32816
O	–3.65001	0.62696	–2.19560
O	–5.32347	–0.31052	–1.13547

CURRICULUM VITAE

Çağlar Çelik Bayar
Middle East Technical University
Chemistry Department
Ankara, Turkey
e–mail: caglarbayar@gmail.com

EDUCATION

Doctor of Philosophy, Chemistry Department, Middle East Technical University, Ankara, Turkey (2005–2012).
Thesis Title: Theoretical Investigation of Tautomeric Equilibria in Certain Explosive Materials.

Master of Science, Chemistry Department, Middle East Technical University, Ankara, Turkey (2002–2005).
Thesis Title: Carbon Supported and Surfactant Stabilized Metal Nanoparticle Catalysts for Direct Methanol Fuel Cells.

Bachelor of Science, Chemistry Education Department, Dokuz Eylül University, İzmir, Turkey (1997–2001).

RESEARCH INTERESTS

High energy density materials
Energetic fuels and their oxidation products
Polycyclic aromatic compounds
Fuel cells and their applications

ACADEMIC AND PROFESSIONAL EXPERIENCE

Research–Teaching Assistant, Chemistry Department, Middle East Technical University, Ankara, Turkey (2002–2010; 2012).

Researcher, Carnegie Mellon University, Mellon Institute, Chemistry Department, Pittsburgh, PA, USA, *Computational Studies of Aromatic Nitration Mechanisms of 3–Picrylamino–1,2,4–Triazole (PATO) and its Tautomers* (2011–2012; 15 months).

Laboratory training assistant for *International Chemistry Olympiads (ICHO)*, Middle East Technical Univesity, Ankara, Turkey (2008–2010).

Researcher, SANTEZ Project, the collaboration of Middle East Technical University and Mechanical and Chemical Industries Corporation (Makina ve Kimya Endüstrisi Kurumu (MKE)), *Hexanitrostilbene (HNS) Synthesis*, Ankara, Turkey (2008–2010).

LIST OF PUBLICATIONS

Book Chapters

1. Lemi Türker and Çağlar Çelik Bayar. (2010). Tetraazapentalenes and Benzofuroxanes as Explosive Materials, Chapter 6, in *Explosive Materials: Classification, Composition and Properties*. Nova Science Publishers, USA.

2. Lemi Türker and Çağlar Çelik Bayar. (2011). Endohedrally Hydrogen Doped Fullerenes, Chapter 39, in *Handbook of Nanophysics: Functional Nanomaterials*. CRC Press, Boca Raton.

Journal Articles

1. Lemi Türker and Çağlar Çelik Bayar. (2010). A DFT Study on Disubstituted R–Hexahelicenes Having Donor/Acceptor Groups. *Procedia Computer Science 1*, 1149–1158.

2. Lemi Türker, Çağlar Çelik Bayar and Alexandru T. Balaban. (2010). A DFT Study on Push–Pull (Amino–Nitro) Fulminenes and Hexahelicenes. *Polycyclic Aromatic Compounds*, 30:91–111.

3. Lemi Türker and Çağlar Çelik Bayar. (2012). NTO–Picryl Constitutional Isomers – A DFT Study. *Journal of Energetic Materials*, 30:72–96.

4. Lemi Türker and Çağlar Çelik Bayar. (2012). A Computational View of PATO and its Tautomers. *Zeitschrift für Anorganische und Allgemeine Chemie (ZAAC) (Journal of Inorganic and General Chemistry)*, 638:1316–1322.

5. Lemi Türker and Çağlar Çelik Bayar. (2012). Novel RDX Based Cage and Cage–Like Nitramines. *Journal of Energetic Materials*, in press.

6. Lemi Türker, Serhat Varış and Çağlar Çelik Bayar. (2013). A Theoretical Study of JP–10 Hydroperoxidation. *Fuel*, 104:128–132.

7. Lemi Türker, Çağlar Çelik Bayar and Hyung J. Kim. Computational Studies of Aromatic Nitration Mechanisms of 3–Picrylamino–1,2,4–Triazole (PATO) and its Tautomers. Submitted.

8. Lemi Türker and Çağlar Çelik Bayar. A Computational View of Estrone and TNT Interaction: A π–Complex Formation. Submitted.

National and International Congress

1. Gülsün Gökağaç and Çağlar Çelik. (2005). Carbon Supported and Surfactant Stabilized Metal Nanoparticles for Direct Methanol Fuel Cells. *International Hydrogen Energy Congress (ICHEC' 2005)*, July 13–15, İstanbul, Turkey.

2. Lemi Türker, Selçuk Gümüş, Taner Atalar, Yakup Çamur and Çağlar Çelik Bayar. (2008). Theoretical Treatment of Some Novel Nitropyrimidines. *New Trends in Research of Energetic Materials (NTREM)*, April 09–11, Pardubice, Czech Republic (also published as a conference proceeding).

3. Lemi Türker and Çağlar Çelik Bayar. (2009). NTO–Pikril Yapı İzomerlerine Ait Patlayıcı Performans Değerlerinin Teorik Olarak İncelenmesi. *Makina Kimya Endüstrisi Kurumu (MKE), Patlayıcı Maddeler ve Bileşenleri*, November 06–09, Ankara, Turkey.

4. Lemi Türker, Çağlar Çelik Bayar. (2009). Potansiyel Yeni Bir Patlayıcı Türü: RDX Dimer Molekülü. *Makina Kimya Endüstrisi Kurumu (MKE), Patlayıcı Maddeler ve Bileşenleri*, November 06–09, Ankara, Turkey.

5. Lemi Türker and Çağlar Çelik Bayar. (2010). A DFT Study on Disubstituted R–Hexahelicenes Having Donor/Acceptor Groups. *International Conference on Computational Science (ICCS 2010)*, May 31–June 2, Amsterdam, Netherlands.

6. Lemi Türker and Çağlar Çelik Bayar. (2010). İtme–Çekme (Push–Pull) Tipi Amino–Nitro Hegzahelisen/Fulminen Yapılarının DFT Yöntemi ile Teorik Olarak İncelenmesi. *XXIV. Ulusal Kimya Kongresi*, June 29–July 2, Zonguldak, Turkey.